

DISSERTATION

THE FRESH GROUNDWATER LENSES IN THE ARABIAN PENINSULA: FORMATIVE,
STABILITY AND MANAGEMENT ASSESSMENTS

Submitted by

Mosaed Alrashidi

Department of Civil and Environmental Engineering

In partial fulfillment of the requirements

For the Degree of Doctor of Philosophy

Colorado State University

Fort Collins, Colorado

Fall 2019

Doctoral Committee:

Advisor: Ryan Bailey

Neil Grigg

Thomas Sale

William Sanford

Copyright by Mosaed Alrashidi 2019

All Rights Reserved

ABSTRACT

THE FRESH GROUNDWATER LENSES IN THE ARABIAN PENINSULA: FORMATIVE, STABILITY AND MANAGEMENT ASSESSMENTS

The formation of fresh groundwater lenses (FGLs) overlying denser, saline or brackish groundwater is a fascinating hydrologic phenomenon that creates groundwater supplies of great potential value for humans and ecosystems in several formation settings, such as coastal areas, atoll islands, riverine floodplains, and subterranean oases in arid regions. In particular, FGLs in subterranean oases are a critical source of freshwater supply in arid regions, due to a general lack of perennial rivers and lakes. These FGLs are in danger of salinization due to natural events and anthropogenic stresses. Although extensive research has been conducted on FGLs in general, the FGLs in subterranean oases in arid regions have received less attention. Key knowledge gaps include the quantity and frequency of natural recharge to these FGLs; reliable estimates of environmental aquifer dispersivity at the scale of subterranean FGLs; the timing of lens development; and the impact of anthropogenic activities on lens dynamics.

This dissertation focuses on the FGLs of subterranean oases in the Arabian Peninsula (AP), using the Rawdatain FGL in Kuwait as a case study. Among the FGLs in the AP, the Rawdatain FGL in Kuwait is perhaps a unique candidate because of its size and the availability of extensive subsurface data for the pre-development period. The main objectives of this study are as follows: (1) estimate long-term average annual recharge for the Rawdatain FGL and investigate the timing of lens depletion due to climate change; (2) provide a realistic range of longitudinal (α_L), horizontal transverse (α_h), and vertical transverse (α_v) dispersivity values for

the aquifer; and (3) assess the impacts of historical and future anthropogenic activities and evaluate artificial recharge alternatives for lens recovery storage (LSR).

In this study, a 3D density-dependent groundwater flow and solute transport model using the SEAWAT modeling code is developed using the following pre-development period calibration targets: (1) groundwater head, (2) spatially-variable total dissolved solids (TDS) groundwater concentration, (3-5) three groundwater volume targets, (6-8) three vertical thickness targets of stored groundwater of three different water quality TDS ranges (0–700, 700–1000, and 1000–2000 mg/L), and (9) geometrical shape features of the lens along cross-sections. In addition, groundwater age data of the Rawdatain FGL was used as an independent factor to constrain the dispersivity and recharge rate during the simulated period of lens development. Moreover, a sensitivity analysis was performed to explore the effects of the hydraulic conductivity, boundary conditions, and vertical transverse dispersivity on lens geometry.

Based on a comparison of twelve annual recharge amount scenarios using a constant recharge mechanism (CRM) (R1 to R12: 0.2 to 5.0 million m³/year) with data targets, the R5 (0.5 million m³/year) recharge scenario is selected to represent the long-term average annual recharge. These results demonstrated that the annual natural replenishment of the Rawdatain FGL is minimal compared with its size. A macro-scale stability assessment shows that a 50% reduction in annual recharge within a 100-year time frame would reduce the lens volumes by 21%, 17% and 9% for the three water quality categories. A multi-criteria score-based method was performed to rank the best performance of 28 dispersivity sets (D1 to D28: 1 to 500 m) among all of the targets with an equal weight, on a scale of 0 to 300 x 10⁶ m³. The results illustrated that the D16 dispersivity set ($\alpha_L = 50$ m: $\alpha_h = 5$ m: $\alpha_v = 0.1$ m) represents the best

large-scale environmental dispersivity values for the Rawdatain FGL and can be used for analyzing the natural mixing between the ambient brackish water and fresh water.

A new baseline model for the predevelopment period using a pulse recharge mechanism (PRM) was established to assess the recharge frequency along with the longitudinal dispersivity. The results revealed that the 50 m longitudinal dispersivity set and one pulse recharge every two years had the best performance, and they were selected to simulate the effects of the infrequent rainfall events and anthropogenic impacts simultaneously. During the groundwater abstraction from 1963 to 2018, the reduction in the stored volumes was 28%, 17% and 12% for the three quality categories. The future pumping scenarios (2019-2100) suggested that the 0.16×10^6 m³/year is a suitable alternative for long-term use, 0.5×10^6 m³/year is an appropriate option for short-term use, and extraction scenarios greater than 1.0×10^6 m³/year will cause a remarkable degeneration of the Rawdatain FGL. Artificial recharge scenarios (2019-2028) imply that a successful LSR for the Rawdatain FGL depends on selecting appropriate well locations and amounts of injected water. For instance, the I2 alternative could achieve a 100% storage recovery within 7.5, 8 and 9 years for the three water quality categories.

This study provides a first attempt to model the formation of a FGL, assess the historical anthropogenic stresses, and evaluate future management scenarios in subterranean oases in arid regions. Implementing multiple data targets and water age is a unique process of calibration that was helpful in eliminating several non-unique calibration parameters and in decreasing the uncertainty of the calibrated parameters. The methodology presented herein provides a general approach that can be extrapolated to other FGLs with similar climatic and environmental circumstances. The outputs of this dissertation enhance the understanding of the formation, stability, and management of these lenses and will be very valuable to water managers for

establishing appropriate water supply plans for these valuable water reserves, leading to preferable future water security in the AP.

ACKNOWLEDGEMENTS

First and Foremost, I am thankful to ALLAH who made this dissertation possible. I would like to express my sincerest gratitude to my advisor, Dr. Ryan Bailey, for all of his valuable guidance and generous assistance throughout my doctoral program. I am grateful to my advisory committee, Dr. Neil Grigg, Dr. Thomas Sale, and Dr. William Sanford, for their insightful comments and encouragements. I would also like to express my gratitude to my parents, Salamah and Batla Alrashidi, for their continuous, unquestioned, and invaluable guidance and support at every stage of my life. Also, I thank my wife, Nawal Alrashidi, for providing unbounded support throughout this academic journey. Also, I would express appreciation to my colleagues at our research group and all of my friends in Fort Collins and Kuwait. My gratitude is also extended to Kuwait University for its support and sponsorship.

DEDICATION

To

My parents Salamah and Batla

My brothers Bader and Mutlaq

My sisters Amana and Falhah

My wife Nawal

My son Sulaiman

My daughter Hadeel

TABLE OF CONTENTS

ABSTRACT.....	ii
ACKNOWLEDGEMENTS.....	vi
DEDICATION.....	vii
LIST OF TABLES.....	xii
LIST OF FIGURES.....	xiii
CHAPTER 1. INTRODUCTION.....	1
1.1 Problem Statement.....	1
1.2 Dissertation Objectives.....	2
1.3 Research Importance.....	4
1.4 The Numerical Model.....	4
1.4.1 Simulation Code Selection.....	4
1.4.2 SEWAT Assumptions and Governing Equations.....	5
1.4.3 Graphical User Interfaces.....	7
1.5 Previous Data Survey and Availability.....	7
1.6 Dissertation Outline and Outputs.....	10
REFERENCES.....	11
CHAPTER 2. LITERATURE REVIEW.....	12
2.1 Arabian Peninsula.....	12
2.1.1 Climate, water and challenges in the Arabian Peninsula.....	12
2.1.2 Fresh groundwater lenses in the Arabian Peninsula.....	17
2.2 State of Kuwait.....	19
2.2.1 Population and Climate.....	19
2.2.2 Water Resources in Kuwait.....	22
2.3 Approaches to Estimating Groundwater Recharge.....	24
REFERENCES.....	30
CHAPTER 3. ESTIMATING GROUNDWATER RECHARGE FOR A FRESH GROUNDWATER LENS IN AN ARID REGION: FORMATIVE AND STABILITY ASSESSMENT.....	38

3.1. Introduction	40
3.2. The Rawdatain Basin	46
3.2.1 Physical Description and Climate.....	46
3.2.2 Previous Studies of Recharge Mechanisms.....	48
3.2.3 Previous Studies of Recharge Quantity	49
3.3. Methods.....	51
3.3.1 Approaches to Estimating Groundwater Recharge	51
3.3.2 Model Code	52
3.3.3 Model Construction	52
3.3.4 Multi-Target Calibration Approach.....	57
3.3.5 Groundwater Age Constraint.....	58
3.3.6 Scenarios.....	59
3.4. Results	60
3.4.1 Simulations of Lens Formation as a Function of Recharge.....	60
3.4.2 Simulation of Lens Stability under Changes in Recharge.....	67
3.4.3 Sensitivity Analysis	69
3.5. Discussion	76
3.5.1 Lens Formation and Stability	76
3.5.2. A Tool for Future Work.....	77
3.6. Summary and Conclusions.....	78
REFERENCES	81
CHAPTER 4. DETERMINING VALUES OF LARGE-SCALE DISPERSIVITY FOR A FRESH GROUNDWATER LENS IN AN ARID REGION	88
4.1. Introduction	89
4.2. Research Objective.....	94
4.3. Background	95
4.3.1. Study Area	95
4.3.2. Previous Studies	98
4.3.2.1. Dispersivity Data from Field Studies.....	98
4.3.2.2. Dispersivity Data from FGLs Studies.....	103
4.3.2.3. Dispersivity Data from Studies in Kuwait	105

4.4. Methods	108
4.4.1. Dispersivity Value Sets	108
4.4.2. Model Code	111
4.4.3. Model Construction	113
4.4.3.1 Model Grid and Boundary Conditions.....	113
4.4.3.2. Aquifer Parameters and Recharge Rates.....	113
4.4.4. Testing Processes.....	115
4.5. Results and Discussion.....	117
4.5.1. Dispersivity Sets Simulation	117
4.5.2. Sensitivity Analysis	125
4.6. Summary and Conclusions.....	127
REFERENCES	130
CHAPTER 5. ASSESSMENT OF THE NATURAL AND ANTHROPOGENIC IMPACTS ON A FRESH GROUNDWATER LENS IN A SUBTERRANEAN OASIS IN KUWAIT	142
5.1. Introduction	143
5.2. Background	146
5.2.1 The State of Kuwait.....	146
5.2.2 The Rawdatain Freshwater Lens	147
5.2.3 Comparison with Other Freshwater Lenses.....	149
5.3. Methods.....	151
5.3.1 Pulse Recharge Mechanism (PRM).....	151
5.3.2 Historical Abstraction (1963-2018).....	154
5.3.3 Future Pumping Scenarios (2019-2100).....	160
5.3.4 Lens Storage Recovery (LSR).....	161
5.4. Results and Discussion.....	162
5.4.1 Aquifer Properties for Baseline Model.....	162
5.4.2 Historical Period (1963-2018)	168
5.4.3 Future Period (2019-2100)	172
5.5. Summary and Conclusion	179
REFERENCES	183
CHAPTER 6. SUMMARY, CONCLUSIONS, AND FUTURE WORK	188

6.1 Summary for Problem Statement and Research Objectives	188
6.2 Conclusion for Estimating Groundwater Recharge for a Freshwater Lens in an Arid Region: Formative and Stability Assessment	189
6.3 Conclusion for Determining Values of Large-Scale Dispersivity for a Fresh Groundwater Lens in an Arid Region	191
6.4 Conclusion for Assessment of the Natural and Anthropogenic Impacts on a Fresh Groundwater Lens in a Subterranean Oasis in Kuwait	192
6.5 Future Work	194
APPENDIX A.....	196

LIST OF TABLES

TABLE 2.1. MAIN AND SECONDARY AQUIFERS IN THE ARABIAN PENINSULA.	14
TABLE 2.2. AVERAGE DAILY EVAPORATION AND MONTHLY PRECIPITATION DATA FROM KUWAIT INTERNATIONAL AIRPORT	21
TABLE 3.1. SUMMARY OF RECHARGE ESTIMATE STUDIES FOR THE RAWDATAIN BASIN	44
TABLE 3.2. VOLUMES OF STORED WATER IN THE RAWDATAIN BASIN (SENAY, 1977).....	48
TABLE 3.3. MODEL LAYER DETAILS AND HYDRAULIC CONDUCTIVITY VALUES (SENAY, 1988)	54
TABLE 3.4. MODEL RECHARGE ZONES	55
TABLE 3.5. ANNUAL VOLUME RECHARGE SCENARIOS	59
TABLE 3.6. SENSITIVITY OF LENS DEVELOPMENT TO BOUNDARY CONDITIONS .	73
TABLE 4.1.A. ENVIRONMENTAL LONGITUDINAL DISPERSIVITY DATA FROM FIELD STUDIES (GELHER ET AL., 1992)	101
TABLE 4.1.B. VERTICAL DISPERSIVITY DATA FROM FIELD STUDIES (GELHER ET AL., 1992).....	102
TABLE 4.1.C. DISPERSIVITY DATA FROM FGLS STUDIES	104
TABLE 4.1.D. DISPERSIVITY DATA FROM STUDIES IN KUWAIT.....	107
TABLE 4.2. DISPERSIVITY SET IDS AND VALUES, GRID PECKET NUMBERS, AND NUMERICAL METHODS	109
TABLE 4.3. MULTI-CRITERIA SCORE-BASED METHOD RESULTS.....	123
TABLE 5.2. MODEL RECHARGE ZONES AND ANNUAL VOLUME RECHARGE SCENARIOS	154
TABLE 5.3. WELL DATA (PARSONS CORPORATION, 1964).....	158
TABLE 5.4. PRODUCTION WELLS TIME SERIES (1963-2018).....	159
TABLE 5.5. EXTRACTION SCENARIOS	160
TABLE 5.6. INJECTION SCENARIOS	161
TABLE 5.7. RESULTS OF THE SIMULATED VOLUMES OF STORED WATER USING CONSTANT RECHARGE AND PULSE RECHARGE SCENARIOS WITH DIFFERENT LONGITUDINAL DISPERSIVITY VALUES AT 2000 YEARS.....	167
TABLE 5.8. PREDICTION OF VOLUMES OF STORED WATER WITH DIFFERENT PUMPING AND RECHARGE SCENARIOS FROM 2019 TO 2100.....	173

LIST OF FIGURES

FIGURE 1.1. THREE-DIMENSIONAL DEPICTIONS OF SALINITY DATA IN THE RAWDATAIN BASIN.....	9
FIGURE 2.1. POPULATION AND GROWTH RATES IN KUWAIT.....	20
FIGURE 2.2. STRATIGRAPHY OF THE AQUIFER SYSTEMS IN KUWAIT.....	23
FIGURE 3.1. STATE OF KUWAIT AND THE RAWDATAIN MODEL DOMAIN	48
FIGURE 3.2. MODEL DOMAIN SET UP (*BC STAND FOR BOUNDARY CONDITIONS WHERE THE SOUTH AND WEST BOUNDARIES REPRESENT SPECIFIED-HEAD CONDITIONS AND THE NORTH AND EAST BOUNDARIES REPRESENT HEAD-DEPENDENT FLUX CONDITIONS)	53
FIGURE 3.3. SCENARIOS OF RAWDATAIN FGL DEVELOPMENT: A) 700 MG/L, B) 1000 MG/L, AND C) 2000 MG/L WATER QUALITY CATEGORIES.....	61
FIGURE 3.4. VOLUMES PREDICTED FOR DIFFERENT RECHARGE SCENARIOS AT 2000 YEARS COMPARED WITH TARGET VOLUMES (RED LINES).	63
FIGURE 3.5. OBSERVED VS. MODELED TDS CONCENTRATIONS FOR THE R1, R5, AND R10 RECHARGE SCENARIOS.	64
FIGURE 3.6. S-RMSE FOR TDS AND HEAD WITH DIFFERENT RECHARGE SCENARIOS	64
FIGURE 3.7. OBSERVED VS. MODELED HEAD FOR THE R1, R5, AND R10 RECHARGE SCENARIOS.....	65
FIGURE 3.8. MAXIMUM LENS THICKNESS PREDICTED FOR DIFFERENT RECHARGE SCENARIOS AT 2000 YEARS COMPARED WITH TARGET VALUES (BLACK LINES).....	66
FIGURE 3.9. (A) & (B) RAWDATAIN CROSS-SECTIONS A-A' AND B-B', RESPECTIVELY (MODIFIED AFTER SENAY, 1977). (C) & (D) MODELED CROSS SECTIONS A-A' AND B-B', RESPECTIVELY (NOT TO SCALE) USING THE R5 RECHARGE SCENARIO.....	67
FIGURE 3.10. DEVELOPMENT PERIOD AND SHRINKAGE SCENARIOS FOR THE A) 700 MG/L, B) 1000 MG/L, AND C) 2000 MG/L WATER QUALITY CATEGORIES.....	69
FIGURE 3.11. SENSITIVITY OF LENS VOLUME AND THICKNESS TO HYDRAULIC CONDUCTIVITY WITH THE R5 RECHARGE SCENARIO: A) 700 MG/L, B) 1000 MG/L, AND C) 2000 MG/L WATER QUALITY CATEGORIES. (MAX Z STANDS FOR MAXIMUM LENS THICKNESS) (RED LINES REPRESENT THE TARGETS OF THE VOLUMES OF STORED WATER AT EACH WATER QUALITY CATEGORY AND THE CORRESPONDING LENS THICKNESS).....	71
FIGURE 4.1. THE ARABIAN PENINSULA (LEFT) AND THE MODEL DOMAIN AT THE RAWDATAIN BASIN IN KUWAIT (RIGHT)	96

FIGURE 4.2. (A) RECHARGE ZONES, DATA TARGET POINTS, AND BOUNDARY CONDITIONS (*BC WHERE THE SOUTH AND WEST BOUNDARIES REPRESENT SPECIFIED-HEAD CONDITIONS AND THE NORTH AND EAST BOUNDARIES REPRESENT HEAD-DEPENDENT FLUX CONDITIONS). (B) VERTICAL CROSS-SECTION OF MODEL GRID.	110
FIGURE 4.3. (A) & (B) RAWDATAIN CROSS-SECTIONS A-A' AND B-B', RESPECTIVELY (MODIFIED AFTER SENAY, 1977).....	116
FIGURE 4.4. VOLUMES PREDICTED FOR DIFFERENT DISPERSIVITY SETS AT 2000 YEARS COMPARED WITH TARGET VOLUMES (RED LINES).	118
FIGURE 4.5. MAXIMUM LENS THICKNESS PREDICTED FOR DIFFERENT DISPERSIVITY SETS AT 2000 YEARS COMPARED WITH TARGET VALUES (RED LINES).....	119
FIGURE 4.6. S-RMSE FOR TDS AND MAE FOR HEAD WITH DIFFERENT DISPERSIVITY SETS	120
FIGURE 4.7. MODELED CROSS SECTIONS B-B' (NOT TO SCALE) FOR THE D1, D8, AND D16 DISPERSIVITY SETS	124
FIGURE 4.8. SENSITIVITY OF LENS VOLUME TO VERTICAL TRANSVERSE DISPERSIVITY: A) 700 MG/L, B) 1000 MG/L, AND C) 2000 MG/L WATER QUALITY CATEGORIES. (D REPRESENTS FIXED A_v AND EQUAL TO 0.1 M, WHEREAS D' REPRESENTS VARIABLE A_v AS A FUNCTION OF $1/100A_L$) (VERTICAL LINES SHOW THE REDUCTION PERCENTAGE OF SIMULATED VOLUMES OF STORED WATER FROM USING D' COMPARED WITH D).....	126
FIGURE 5.1. STATE OF KUWAIT AND THE RAWDATAIN MODEL DOMAIN	148
FIGURE 5.2. MODEL DOMAIN, BOUNDARY CONDITIONS, AND PRODUCTION WELLS (GHB STAND FOR GENERAL HEAD BOUNDARY)	155
FIGURE 5.3. WELLS OPERATIONS: A) WELLS STARTED FROM 1963. B) WELLS STARTED FROM 1964.....	156
FIGURE 5.4. TOTAL ANNUAL PRODUCTION AND AVERAGE TDS FROM 1963 TO 1985 (A) AND FROM 1986 TO 2015 (B) FOR THE RAWDATAIN BASIN.....	157
FIGURE 5.5. PULSE RECHARGE SCENARIO WITH ONE PULSE PER YEAR AND DIFFERENT LONGITUDINAL DISPERSIVITY VALUES.....	163
FIGURE 5.6. PULSE RECHARGE SCENARIO WITH ONE PULSE EVERY TWO YEARS AND DIFFERENT LONGITUDINAL DISPERSIVITY VALUES	164
FIGURE 5.7. PULSE RECHARGE SCENARIO WITH ONE PULSE EVERY FOUR YEARS AND DIFFERENT LONGITUDINAL DISPERSIVITY VALUES.	165
FIGURE 5.8. SIMULATED VOLUMES OF STORED WATER AND THE REDUCTION IN VOLUMES DURING THE PUMPING PERIOD 1963-2018: A) 700 MG/L, B) 1000 MG/L, AND C) 2000 MG/L WATER QUALITY CATEGORIES.....	170

FIGURE 5.9. SIMULATED VOLUMES OF STORED WATER AND THE REDUCTION IN VOLUMES VS. TOTAL ABSTRACTION VOLUME: A) 700 MG/L, B) 1000 MG/L, AND C) 2000 MG/L WATER QUALITY CATEGORIES. 171

FIGURE 5.10. SIMULATED VOLUMES OF STORED WATER FOR HISTORICAL CONDITIONS (INITIAL CONDITION IN 1963; INTENSIVE PUMPING PERIOD 1963-1978; LOW PUMPING RATE PERIOD 1979-2018) AND FUTURE SCENARIOS (S0 TO S6 FOR 2019-2100): A) 700 MG/L, B) 1000 MG/L, AND C) 2000 MG/L WATER QUALITY CATEGORIES..... 174

FIGURE 5.11. SIMULATED TDS OF THE PUMPED WATER FOR A RANGE OF ANNUAL VOLUME EXTRACTION SCENARIOS FOR 2019-2100. 175

FIGURE 5.12. SENSITIVITY OF CHANGE IN STORED WATER VOLUMES WITH THREE ANNUAL VOLUME EXTRACTION SCENARIOS (S0, S1 AND S2) ASSOCIATED WITH THREE LONG-TERM ANNUAL RECHARGE SCENARIOS (R = 500,000 M³/YEAR, +20%R = 600,000 M³/YEAR AND -20%R = 400,000 M³/YEAR) AT THE YEAR 2100..... 177

FIGURE 5.13. SIMULATED VOLUMES OF STORED WATER FOR THREE ANNUAL VOLUME INJECTION SCENARIOS (I1, I2 AND I3) FOR THE PERIOD 2019-2028: A) 700 MG/L, B) 1000 MG/L, AND C) 2000 MG/L WATER QUALITY CATEGORIES. (HORIZONTAL SOLID LINES REPRESENT THE PRE-DEVELOPMENT VOLUMES IN 1963)..... 178

CHAPTER 1. INTRODUCTION

In this chapter, the problem statement and the main dissertation objectives are presented. The modeling tool and previous data survey and availability to conduct this study are briefly listed. The dissertation organization and outputs are outlined.

1.1 Problem Statement

Freshwater supplies are extremely scarce across the Arabian Peninsula (AP). According to the global distribution of climatic zones, the aridity index for the region is classified as hyper-arid to arid (UNESCO, 1979). Desalination provides much of the region's water. More than 65% of the world's desalination capacity was concentrated in the Gulf Cooperation Council (GCC) countries in 2003 (Dawoud, 2005). There are no perennial rivers or lakes, and the climate and landforms make it difficult to harvest and store precipitation (Alrashid and Sherif 2000). Therefore, groundwater is the main source of freshwater supply (Alrashed & Sherif, 2000). FAO (1979) conducted a comprehensive investigation of the region, which classified the regional groundwater into two main aquifer systems with various potentialities: Systems A and B. System A represents the deep, non-renewable (fossil) groundwater aquifers, and System B represents the shallow, renewable groundwater aquifers. System B mainly includes discontinuous fresh groundwater lenses (FGLs) that extend over the eastern part of the AP and over deeper brackish groundwater.

Understanding the formation and hydrogeology of these FGLs in subterranean oases in the desert has long been of scientific interest (e.g., Senay, 1973, 1977, 1988; Omar et al., 1981; Macumber 1995; Kwarteng 2000; and others) and is also of great practical importance for their protection and for their best potential use. Recharge and in-situ mixing are two key factors that

affect freshwater lens formation and flow dynamics. Information on the recharge quantity and mechanism of these lenses is both scarce and uncertain (SMEC, 2002).

An assessment of the creation and sustainability FGLs in the AP is crucial to help water managers in analyzing future water security for the region and establishing appropriate short-term emergency water supply plans. This dissertation focuses on the Rawdatain FGL in Kuwait. Among the fresh groundwater lenses in the AP, the Rawdatain basin is perhaps the most notable example because it is very large, and an extensive subsurface data set was collected in 1960-1962 by the Parsons Corporation before significant groundwater extraction from the lens began. The existence of that pre-development data, as well as the quality and quantity of that data, makes Rawdatain an ideal and potentially unique candidate to use for evaluating the formative and potentially changing dynamics of lenses in arid regions.

1.2 Dissertation Objectives

The overall objective of this dissertation is to provide accurate long-term estimates of recharge for the Rawdatain FGL and to investigate the timing of lens depletion under scenarios of decreased recharge. Also a primarily goal is to quantify the current volumes of the stored water for different water quality categories that can be used during emergency conditions such as desalination plant breakdown or damage to surface storage. The assessment will be fulfilled by applying the public domain, three-dimensional, variable-density, transient ground-water flow numerical model SEAWAT (Langevin et al. 2007), to one of the largest fresh groundwater lenses in the AP, the Rawdatain basin in Kuwait, for simulating the development and stability of the freshwater source. The following tasks were carried out to accomplish these objectives:

- (1) Develop a 3D density-dependent groundwater flow model for the Rawdatain FGL in Kuwait that is capable of simulating the interaction between the stored freshwater and the surrounding brackish water
- (2) Establish a baseline model using constant recharge mechanism (CRM) for the lens using the pre-development data from 1962
- (3) Test the model against multiple data targets and water age to estimate long-term diffuse and focused groundwater recharge
- (4) Assess the impact of reduced recharge scenarios that may occur due to changes in land-use or climate
- (5) Provide a realistic range of longitudinal (α_L), horizontal transverse (α_h), and vertical transverse (α_v) dispersivity values for the Rawdatain FGL
- (6) Evaluate the original baseline model using a pulse recharge mechanism (PRM) for different recharge frequency scenarios and a range of different dispersivity sets
- (7) Establish a new baseline model using PRM for the predevelopment period to assess the natural recharge and anthropogenic impacts simultaneously
- (8) Assess the effect of 18 years of heavy anthropogenic activities for the period 1963-1978, evaluate the impact of low pumping rates for the period 1979-2018, and determine the current quantity and quality of the stored water at different thresholds
- (9) Consider six hypothetical future pumping scenarios to evaluate the impact of a wide range of total annual volume extraction
- (10) Use the new baseline model for implementing three artificial injection scenarios to measure the Rawdatain Lens Storage Recovery (LSR)

1.3 Research Importance

This research establishes a baseline for a fresh groundwater lens using a 3D density-dependent groundwater flow model tested against multiple raw data targets and water age. This model is capable of evaluating conceptual models and model assumptions, assessing the sensitivity of recharge estimates to model parameters, and predicting the effect of future climate and land use changes on recharge rates. The output of this model provides a reliable assessment and results that enhance the understanding of the formation and stability of these lenses, and thus it will lead to better planning and management for these valuable water reserves in the AP.

1.4 The Numerical Model

1.4.1 Simulation Code Selection

To analyze the mixing between the freshwater and brackish groundwater of the Rawdatain basin, the SEAWAT code (Langevin et al. 2007) was used to simulate the formation and behavior of the Rawdatain lens. SEAWAT is a three-dimensional finite-difference code developed by the U.S. Geological Survey. It is capable of simulating transient flow and advection and dispersion of density-dependent solute transport. Essentially, SEAWAT combines the established codes MODFLOW and MT3DMS, using the former to simulate groundwater flow and the latter to simulate solute transport. It uses those two codes iteratively to update the head solution based on the changes in density caused by changing salinity concentration. The original SEAWAT code generates a binary salt concentration file for each time step. In this research, the code was adapted to generate a text file that reports the salt concentrations for the entire grid model cells at specified time steps. Then, a short code written in MATLAB was used to read the salt concentration text file and report the volume and thickness of the lens at specific concentration thresholds.

When selecting an appropriate model for this research, the model must be able to match the desired hydrological target based on the mass balance principle. The hydrological target includes the volumes of available fresh groundwater in certain water quality zones at the appropriate spatial scale. The SEAWAT model was selected for several reasons. First, it can simulate freshwater lenses on top of brackish groundwater by coupling the USGS groundwater flow (MODFLOW) and solute transport (MT3DMS) models. Second, it can simulate the mixing between freshwater and brackish groundwater based on the transition zone approach, rather than at a sharp interface. In this approach, the interaction between fresh water and brackish water is represented by a transition zone in which water fluid density changes gradually rather than at a narrow zone with a sharp change in density. Finally, SEAWAT is in the public domain, and it has been implemented and verified in many applications involving different fluid densities.

1.4.2 SEWAT Assumptions and Governing Equations

SEAWAT is based on a number of assumptions that are common in groundwater flow and solute transport modeling (USGS, 2002):

- Darcy's equation is valid (laminar flow).
- The standard expression for specific storage in a confined aquifer is applicable.
- Fick's law can be applied, i.e. Fickian processes can be used to model the dispersion.
- Isothermal conditions prevail.
- The porous medium is assumed to be fully saturated with water
- The fluid consists of a single, fully miscible liquid phase of very small compressibility.

In MODFLOW, the equation for flow of water in saturated media is modified to solve for variable density flow as follows:

$$\begin{aligned} & \frac{\partial}{\partial x} \left[\rho K_{fx} \left(\frac{\partial h_f}{\partial x} + \frac{\rho - \rho_f}{\rho} \cdot \frac{\partial Z}{\partial x} \right) \right] + \frac{\partial}{\partial y} \left[\rho K_{fy} \left(\frac{\partial h_f}{\partial y} + \frac{\rho - \rho_f}{\rho} \cdot \frac{\partial Z}{\partial y} \right) \right] + \frac{\partial}{\partial z} \left[\rho K_{fz} \left(\frac{\partial h_f}{\partial z} + \frac{\rho - \rho_f}{\rho} \cdot \frac{\partial Z}{\partial z} \right) \right] \\ & = \rho S_f \cdot \frac{\partial h_f}{\partial t} + \theta \cdot \frac{\partial \rho}{\partial C} \cdot \frac{\partial C}{\partial t} - \rho_s q_s \end{aligned} \quad (1.1)$$

where

x, y, z are the orthogonal coordinate axes

K_f is the freshwater hydraulic conductivity (L/T)

h_f is the freshwater equivalent head (L)

ρ is the density of the water at a specific concentration C (M/L³)

ρ_f is the freshwater density (M/L³)

Z is the elevation above a datum (L)

S_f is the specific storage in term of freshwater head (1/L)

t is time (T)

θ is the effective porosity

C is solute concentration (M/L)

q_s is the volumetric flow rate per unit volume of aquifer representing sources and sinks (1/T)

MODFLOW solves Equation (1.1) for the velocity field, and then MT3DMS solves for concentration in the following transport equation:

$$\frac{\partial C}{\partial t} = \nabla \cdot (D \nabla C) - \nabla \cdot (\vec{v} C) - \frac{q_s}{\theta} \cdot C_s + \sum_{k=1}^N R_k \quad (1.2)$$

where

D is the coefficient of the hydrodynamic dispersion (L^2/T)

\vec{v} is the fluid velocity (L/T)

C_s is the solute concentration of water entering from sources or sinks (M/L^3)

R_k is the rate of solute production or decay in reaction k of N different reactions ($M/L^3/T$)

After solving Equations (1.1) and (1.2), the code updates the density in each grid cell as follows:

$$\rho = \rho_f + E.C \quad (1.3)$$

where

E is dimensionless number equal to 0.7143

1.4.3 Graphical User Interfaces

Several commercial and non-commercial graphical user interfaces are currently available for SEAWAT, which aid in the creation of input files and in visualizing results. In this research, Groundwater Vistas (Rumbaugh & Rumbaugh, 2011), which runs on Microsoft Windows and is developed by Environmental Simulations Inc., is used for preparing input files and for running SEAWAT. Model Viewer, a program for 3D visualization of groundwater model results developed by the U.S. Geological Survey (USGS), is used for processing output after running SEAWAT.

1.5 Previous Data Survey and Availability

Fresh water was discovered accidentally in a well (Well ID: R8) that was drilled in the Rawdatain basin in 1960 for a brackish water supply for the construction of a road between Kuwait city and Basra city in Iraq. After the well had continued to produce fresh water with total dissolved solids (TDS) of 600 mg/L for several months, an investigation of the basin became an

interest. The Ministry of Electricity and Water (M.E.W) in Kuwait summoned the Parsons Corporation, Los Angeles (USA), to conduct an extensive hydrological survey for evaluating the groundwater potential of the area in 1961. The investigation was carried out by drilling 197 wells and test holes for the northern part of Kuwait, aggregating more than 18,000 m of drilling, and several pumping tests. The pre-development data for Rawdatain was collected in 1961-1962 and consists of TDS at 47 locations (including various depths) and water table data at 42 locations (Parson corporation, 1964). The volumes of stored water with less than 1000 and 2000 mg/L TDS in Rawdatain basin were 68.1 and 136.3 million cubic meters, respectively. The volumes of the stored water were determined from an isopach map and multiplied by an estimated porosity. A 3D visualization of the 1962 and 1964 TDS data is presented in Figure 1.1. The TDS samples were taken over approximately 80 km² with well screen depths ranging from roughly 30 meters below the ground surface (near the water table) to approximately 85 meters deep.

Later in 1964, the Parsons Corporation study was reevaluated by experts from the United Arab Republic (U.A.R, 1964) on the invitation by M.E.W. Their work consisted of a reinterpretation of Parsons' data, water quality analysis, and some short-term pumping tests. Their overall results were the same as those of the Parsons study. They estimated that the volumes of the stored water with less than 700, 1000, and 2000 mg/L TDS were 32.6, 60.6 and 161.6 million cubic meters, respectively.

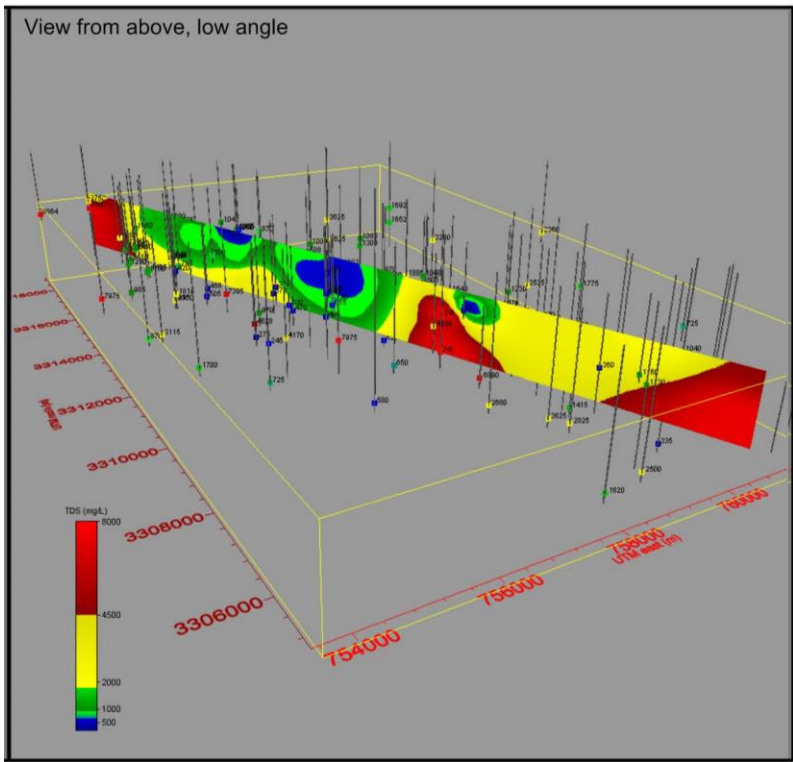
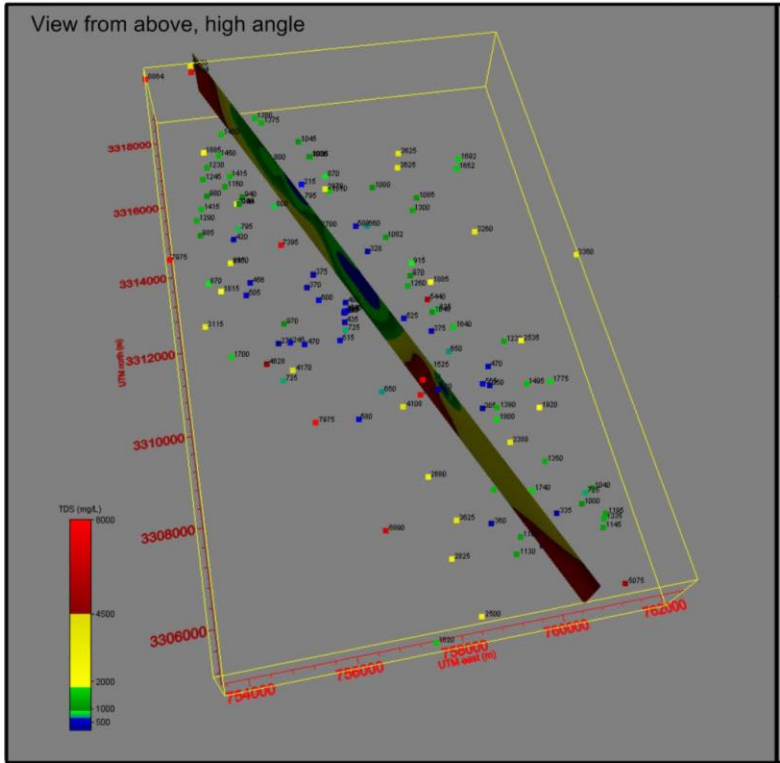


Figure 1.1. Three-dimensional depictions of salinity data in the Rawdatain basin.

1.6 Dissertation Outline and Outputs

Three manuscripts for high-impact journal were written from the dissertation, and each manuscript is separately addressed in Chapters 3, 4 and 5. The dissertation is organized as follows:

Chapter (1): introducing the problem statement, dissertation objectives, numerical code, data availability, and dissertation organization

Chapter (2): providing a brief overview and investigation of the literature regarding the climate, water resources, and challenges in the Arabian Peninsula, and approaches to estimating groundwater recharge

Chapter (3): demonstrating the development of the SEAWAT model for the Rawdatain FGL, testing the model against multiple data targets, estimating the long-term annual recharge rate, and investigating the timing of lens depletion under scenarios of decreased recharge

Chapter (4): assessing the longitudinal, transverse horizontal, and transverse vertical dispersivities simultaneously with recharge rate against the multiple data targets, evaluating the model with three major transport solution techniques based on the grid Peclet number, and then providing a range of 3D large-scale environmental dispersivity for the Rawdatain basin

Chapter (5): evaluating the model with PRM scenarios, assessing the impact of past anthropogenic stresses, estimating the current volumes of stored water, and then evaluating future pumping and artificial injection scenarios

Chapter (6): presenting a summary of the three journal manuscripts and discussing potential future research challenges and requirements

REFERENCES

- Al-Rashed, M. F., & Sherif, M. M. (2000). Water resources in the GCC countries: an overview. *Water resources management*, 14(1), 59-75.
- Dawoud, M. A. (2005). The role of desalination in augmentation of water supply in GCC countries. *Desalination*, 186(1-3), 187-198.
- FAO. 1979. Survey and evaluation of available data on shared water resources in the Gulf States and Arabian Peninsula, Three Volumes, FAO, Rome.
- Kwarteng, A. Y., Viswanathan, M. N., Al-Senafy, M. N., & Rashid, T. (2000). Formation of fresh ground-water lenses in northern Kuwait. *Journal of arid environments*, 46(2), 137-155.
- Langevin, C., Thorne, D. J., Dausman, A., Sukop, M., & Guo, W. (2007). User's Guide to SEAWAT: A Computer Program for Simulation of Three-Dimensional Variable-Density Ground-Water Flow. United States Geological Survey.
- Macumber, P. G., Barghash, B. G. S., Kew, G. A., & Tennakoon, T. B. (1995). Hydrogeologic implications of a cyclonic rainfall event in central Oman. *Groundwater quality. Chapman and Hall, London*, 87-97.
- Omar, S. A., Al-Yaqubi, A., & Senay, Y. (1981). Geology and groundwater hydrology of the State of Kuwait. *Journal of the Gulf and Arabian Peninsula Studies*, 1, 5-67.
- Parsons Corporation. 1964. Groundwater Resources of Kuwait, vols I, II and III. Ministry of Electricity and Water, Kuwait.
- Senay, Y. (1973). Geohydrology of Al-Rawdhatain Field. *Report to the Ministry of Electricity and Water, Kuwait*, 24-43.
- Senay, Y. (1977). Groundwater resources and artificial recharge in Rawdhatain water field. *Ministry of Electricity and Water, Kuwait*, 35.
- Senay, Y. (1989). Artificial recharge and reproduction of fresh water at Rawdhatain for emergency use. *Report to the Ministry of Electricity and Water, Kuwait*.
- SMEC (Snowy Mountains Engineering Corporation). (2002). Characteristics of groundwater quality in Kuwait before August 1990. Report No. 4, GD1.1.
- U.A.R (United Arab Republic) Experts. 1964. Ministry of Electricity and Water, Kuwait.
- UNESCO. (1979). Map of the world distribution of arid regions. Man and Biosphere Tech Notes, no. 7, UNESCO: Paris; 54.

CHAPTER 2. LITERATURE REVIEW

In this chapter, a brief overview and investigation of the literature regarding the climate, water resources, and challenges in the Arabian Peninsula and State of Kuwait, as well as approaches to estimating groundwater recharge, are presented.

2.1 Arabian Peninsula

2.1.1 Climate, water and challenges in the Arabian Peninsula

The Arabian Peninsula (AP), located in southwest Asia, includes seven countries: Kuwait, Saudi Arabia (SA), Bahrain, Qatar, Oman, the United Arab Emirates (UAE), and the Yemen Arab Republic (YAR). The first six political units formed the Gulf Cooperation Council (GCC), and the YAR will not be discussed in this paper due to a lack of information. According to the global distribution of climatic zones, the aridity index for the region is classified mostly as hyperarid, with some mountainous areas in SA and Oman and the northern east side of the AP being classified as arid (UNESCO, 1979). The region has a harsh climate, and its landforms make it difficult to harvest and store precipitation (Alrashid & Sherif, 2000).

The AP is located within one of the great desert belts of the world. The majority of the AP is characterized by high average temperature, erratic sparse rainfall, and high evapotranspiration rates. In the central part of the AP, shade temperatures frequently exceed 48°C during the summer months. The annual average precipitation received by the region is very low, typically less than 150 mm/year and ranging from as low as 50 mm in the northern and central parts to as high as 300 mm/year in the south. The average annual volume of precipitation over the AP is estimated at 205.93 billion cubic meters (ACSAD, 1997). The annual potential

evaporation ranges from 2500 mm/year in the coastal areas to approximately 4500 mm in the central areas (Alsharhan et al., 2001).

Fresh water is extremely scarce over the entire AP. There are no perennial rivers or lakes, and surface water does not exist with the exception of some mountainous areas in SA, UAE, Oman, and Yemen. Therefore, groundwater is the main source of freshwater supply. FAO (1979) conducted a comprehensive investigation of the region, which classified the regional groundwater into two main aquifer systems with various potentialities: Systems A and B. System A represents the deep, non-renewable (fossil) groundwater aquifers, and System B represents the shallow, renewable groundwater aquifers. Authman (1983), BAAC (1980) and MAW (1984) classified the deep aquifers into more than 20 principal and secondary aquifers based on various parameters such as specific yield, aquifer thickness, areal extent, and the volume and quality of stored water. Table 2.1 summarizes several studies that discussed the deep aquifers in the region (MAW, 1984; Khouri, et al., 1986; De Jong, 1989; Lloyd and Pim, 1990; Edgel, 1990; Danish et al., 1992; Abdulrazzak, 1994, 1995; Alrashed & Sherif, 2000, FAO 1998; UN-ESCWA & BGR, 2013).

The groundwater reserves in the deep aquifers are estimated at 2330 billion cubic meters (BCM), with a wide range of total dissolved solids. The reserves represent groundwater exploitable by lowering the water level to 300 m below the ground surface (the maximum depth currently possible with modern pumping technology). The total annual recharge of these aquifers is approximately 0.1% of the total reserved volume, or 2692 million cubic meters per year. Therefore, the natural recharge of these aquifers is negligible. The main aquifers generally have higher volumes of stored water with better water quality compared with the secondary aquifers, except for the Um Er Radhuma, Damman and Minjur-Dhurma aquifers. These three aquifers

Table 2.1. Main and secondary aquifers in the Arabian Peninsula.

Aquifer Name	Sharing Countries	Formation	Thickness (m)	Total Reserve; Annual Recharge (mcm)	Water Quality (Use)
Main Aquifers					
Saq	Saudi Arabia, Jordan*	Medium to coarse grained, brown to tan, friable, quartzose sandstone	400-928	277000 ; 310	TDS: 300-1500 mg/L (Mainly agricultural)
Tabuk	Saudi Arabia, Jordan*, Iraq*	Marine to continental sequences of cross and inter bedded sandstone, shale and siltstone	Approximately 1070	205000 ; 455	TDS: 200-4000 mg/L (Mainly agricultural)
Wajid	Saudi Arabia, Yemen	Fine to coarse-grained sandstone. Homogeneous, poorly cemented porous rocks	200-900	255000 ; 104	TDS: 500-1200 mg/L (Predominantly agricultural; limited municipal and industrial)
Minjur-Dhruma	Saudi Arabia	Continental sandstone. Coarse quartzitic sandstone with thin layers of limestone, shale, conglomerate and gypsum	300-400	182000 ; 80	TDS: 1100-20000 mg/L (Heavy agricultural activities)
Wasia-Biyadh	Saudi Arabia, Kuwait, Bahrain, Qatar, UAE, Oman, *Iraq	Sandstone and shale	50-1000	740000 ;480	TDS: 900-10000 mg/L (Domestic and irrigation)
Um Er Radhuma-Dammam	<u>Northern Part:</u> Kuwait, Saudi Arabia, Iraq* <u>Central Part:</u> SA, UAE, Bahrain, Qatar <u>Southern Part:</u> UAE, Oman, Yemen	Light colored, dense limestone, dolomitic limestone and dolomites	Um Er Radhuma: 245-700 Dammam: 5-250	Um Er Radhuma: 188,000 ; 406 Dammam: 25,000 ; 200	Um Er Radhuma : TDS: 2500-15000 mg/L Dammam: TDS: 2600-60000 mg/L (Agricultural, industrial and domestic use)
Neogene	<u>South-East Part:</u> Kuwait, Saudi Arabia, Iraq* <u>North-West Part:</u> Saudi Arabia, Iraq*, Syria*	<u>South-East Part:</u> Predominantly sands and gravel <u>North-West Part:</u> Sandstones	<u>South-East Part:</u> 20-200 <u>North-West Part:</u> 500-550	130000 ; 290	TDS: 3700-4000 mg/L (Agriculture and domestic)
Secondary Aquifers					
Khuff and Tuwail	Saudi Arabia	Limestone and dolomites, with some anhydrite aquicludes	250-600	30000 ; 132	TDS: 3800-6000 mg/L
Aruma	Saudi Arabia, Iraq*	Fine-grained to chalky or calcarenite limestone, with some shale and dolomite towards the top	60-140	85000 ; 80	TDS: 1600-2000 mg/L
Jauf and Sakaka	Saudi Arabia, Jordan*, Iraq*	Sandstone and sandy shale	100-300	100000 ;95	TDS: 400-5000 mg/L (Domestic and irrigation)
Jilh	Saudi Arabia	Thin-bedded limestone, with minor shale and gypsum	100-400	113000 ; 60	TDS: 3800-5000 mg/L

(*) indicates that the country is outside the AP

have high TDS because they are located at the eastern side of the AP and thus interact with the Persian Gulf. The Wasia-Biyahd aquifer alone holds approximately 32% of the groundwater reserves in the region.

Significant withdrawals have been reported from these aquifers. For instance, 141.4 BCM of the reserved amount in the principal aquifers was used in SA between 1984 and 1996 (FAO, 1998). As a result, the water level declined dramatically. For example, the water tables of the Minjur-Dhruma and Wasis-Biyahd aquifers dropped from 45 to 170 m below the surface between 1956 and 1980 (MAW, 1982 & 1984). A noteworthy increase in salinity was observed in the Dammam aquifer in Kuwait and Bahrain (Fadlelmawla & Al-Otaibi, 2005; Zubari, 1999). These aquifers cover two-thirds of SA, and some of them extend into other countries within the AP or even outside of the AP, as shown in Table 1. At present, this situation has led to another problem, which is conflict over transboundary aquifers in the region (Puri & Aureli, 2005; Fallatah et al., 2017; Lee et al., 2018). System B will be discussed in detail in the next section.

With the lack of natural freshwater sources in the region, desalinated seawater supplies most of the drinking water for the region. Desalination becomes the most feasible alternative for meeting the current and future water supply requirements, even if it is vulnerable to power interruptions and various other risks. More than 65% of the world's desalination capacity was concentrated in the GCC in 2003 (Dawoud, 2005). SA, Kuwait and UAE ranked within the top five countries in the world in terms of desalination capacity, which are SA (17.4%), USA (16.2%), UAE (14.7%), Spain (6.4%), and Kuwait (5.8%) (IDA Desalting Inventory Report, 2004). The desalination capacity of the region is expected to increase exponentially to meet increasing demand (Saif et al., 2014).

Treated wastewater in the region is generally used for the irrigation of gardens, highways, landscaping and limited farming activities, but this resource is not fully utilized. Treated wastewater that is not reused is discharged into the Arabian Gulf or into wadis to recharge shallow aquifers (AFED, 2011). Kuwait has the highest rate of wastewater treatment in the region (62%), and 70% of treated wastewater is reused. In contrast, SA treats only 23% of its wastewater and reuses only 40% of that treated water (World Bank, 2005).

Water availability is an obstacle to the sustainable development of the region (Shiklomanov, 1990&1998), and drinking water security is clearly of grave importance in populated areas in the AP. Abdulrazzah (1995) reported an imbalance between the available water resources and demand in the region as a result of rapid economic development. The demand for water increased from 5.95 billion to 22.6 billion cubic meters in the period from 1980 to 1990. The population in the GCC increased rapidly from 7.6 million in 1970 to 48.9 million in 2012, which has resulted in a major increase in the demand for water for municipal, agricultural, and industrial uses (GCC, 2015). According to the GCC plan, the amount of renewable water available to the average citizen in the GCC countries is less than 100 cubic meters per year, which is one of the lowest values worldwide.

Climate change is expected to result in an increase in the severity and frequency of droughts in the region (Feitelson & Tubi, 2017; Döll et al., 2015). Climate change projections in the SA show increasing temperature and greater variability in rainfall, which may increase uncertainty related to the development of sustainable water resource management strategies (Tarawneh & Chowdhury, 2018). In addition to a scarcity of water resources, the region also suffers from large-scale water management problems, including over-exploitation of aquifers, decreasing water quality, and inadequate water availability for optimal irrigation (World

Bank, 2007). These issues related to water supply and quality affect the potential for social and economic development in the region (Tropp & Jagerskog, 2006). Future tensions will likely arise that are related to the management of water resources and food security (Allan, 2001).

2.1.2 Fresh groundwater lenses in the Arabian Peninsula

System B represents discontinuous fresh groundwater lenses (FGLs) that extend over the eastern part of the AP. The potentiality of these lenses is relatively small, and it depends on surface runoff from rainfall events, and thus it may vary considerably from one year to the other. Unlike the System A aquifers, the System B aquifers have a small areal extent. As a result, the potential for transboundary conflicts is negligible because each known lens falls within the boundary of one political unit. The groundwater isotopic data provide evidence of recent recharge and a general dissimilarity with respect to the deeper main aquifers (FAO, 1979). As of the mid-1950s, several studies have discussed the existence of these FGLs, which are flooded and surrounded by brackish or saline water. Italcounsel (1969) and BRGM (1977) reported the existence of FGLs along the eastern coast of SA that are separated by semi-confining beds from deeper aquifers. This fresh water has been used for a long time for various purposes such as domestic and municipal uses for Dhahran and Al-Khober cities or agricultural activities in the Eastern Province (Abderrahman et al., 1995). Since the earliest groundwater studies in Qatar, a survey of the freshwater resources was conducted by Le Grand ADSCO Ltd., et al (1959), which recognized the existence of a lens-type aquifer (the Ghyben-Herzberg type). This freshwater aquifer resides in the Dammam and Rus Formations, and it floats on the Umm Er Radhuma (high TDS) aquifer. Detailed investigation revealed the existence of a major 40 m thick FGL in Qatar with a volume of 17.6 million cubic meters and TDS less than 1000 mg/L (FAO, 1979). Lloyd et al. (1987) studied the hydrogeology of the complex FGLs in Qatar. The authors showed the

presence of two-layered complex freshwater lenses in the northern and central parts of Qatar. Extensive historical dissolution of the limestone of the Umm Er Rhadhuma has led to a wide area of surface collapse, which has provided a mechanism for recharge from storm runoff. Due to an increase in the extraction rate from 1971 to 1985, the total volume of the freshwater lenses decreased to almost half of its original size (Lloyd, 1994). The FGLs in the Liwa area in UAE were also documented and proposed as appropriate locations for artificial aquifer storage recovery (FAO, 1979; Rizk & Alsharhan, 2003; Al-Katheeri, 2008). In the Wusta region of central Oman, thin locally derived freshwater lenses were found overlying the saline regional groundwater (Macumber et al., 1995; 1998; 2003). These lenses were formed beneath the Rawanb Wadi as a result of rapid infiltration and insignificant evaporation during infrequent cyclonic rainfall events. The lenses are up to tens of kilometers long, 10-100 meters thick, and several kilometers wide, with average TDS values as low as 200 mg/L and as high as 1750 mg/L. The same phenomenon occurs on the Al Khawd fan at the eastern edge of the Batinah coastal plain of northern Oman, but with poorer water quality due to seawater intrusion.

In Kuwait, the FGLs were the subject of comprehensive investigations from the 1960s to the present because they are the only source of fresh water in Kuwait. Early in the 1960s, the Parsons Corporation named two large FGLs in the northern part (the Rawdatain and Umm Al-Aish basins) and several small lenses in the Al-Qashaniya, Mutla and Al-Abdali areas (Parsons Corporation, 1964). The volumes of stored water with less than 2000 mg/L TDS in these lenses in the Rawdatain and Umm Al-Aish areas were 136.3 and 71.9 million cubic meters, respectively. In 1964, the Parsons studies were reevaluated by experts from the United Arab Republic (U.A.R, 1964) at the invitation of the Ministry of Electricity and Water in Kuwait. These two studies have provided an enormous amount of information and data associated with

these lenses. The Umm-Aish FGL was affected by hydrocarbon pollution after the 1991 Gulf War (Mukhopadhyay et al., 2008). Because of that, this area has been of interest to many studies, such as Bergstrom and Aten (1964), Robinson & Al-Ruwaih (1985), Al-Sulaimi et al. (1997), Din et al. (2007), Kwarteng et al. (2000), Al-Dousari et al. (2010), Al-Senafy et al. (2013), Mukhopadhyay et al. (2016), Al-Weshah & Yihdego (2016), and Yihdego & Al-Weshah (2017)).

2.2 State of Kuwait

2.2.1 Population and Climate

The state of Kuwait is one of the smallest countries in the Middle East, and it is one of the Gulf Cooperation Council (GCC) countries. It is located in the northwestern portion of the Arabian Peninsula, where it covers an area of 17,818 km² and has a total coastline of 195 km. Its geographic coordinates are between latitudes 28.4° and 30.2° N and longitudes 46.4° and 48.5° E. It shares borders with Iraq to the north and northwest and the Kingdom of Saudi Arabia to the south and southwest, and the Arabian Gulf bounds Kuwait to the east. Kuwait is divided into six governorates and has nine islands. The total population of Kuwait was 4,777,433 in mid-2019, of which only 1,414,297 were Kuwaitis and the rest were foreign, according to the official website of the Public Authority for Civil Information. The population growth rate has fluctuated rapidly because approximately 70% of the population are non-citizens. Figure 2.1 shows the total population and relative growth rate from 2000 to 2016. Based on this figure, the maximum and minimum growth rates were 8.6% and 1.25%, respectively. Kuwait depends mainly on crude oil reserves of approximately 104 billion barrels - about 8% of world reserves. The Gross Domestic Product (GDP) purchasing power is \$141.0 billion, and the GDP per capita is \$ 45,130. People in

Kuwait have access to improved water sources and sanitation facilities (99% and 100%, respectively) (source: World Bank, World Development Indicators, 2015).

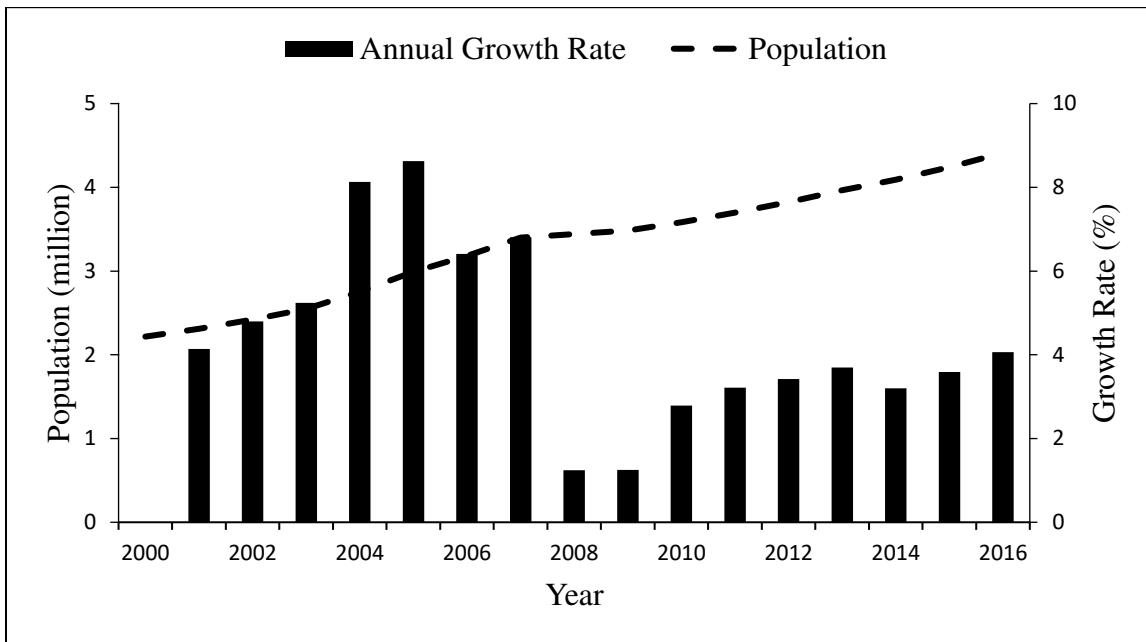


Figure 2.1. Population and growth rates in Kuwait

Like most parts of the Arabian Shield, Kuwait is characterized by a desert-type environment with scanty rainfall, and a dry, hot climate. Summer is very hot, especially in July and August, with a mean temperature of 37.4°C and a mean maximum temperature of 45°C. The average total yearly potential precipitation recorded between 1962 and 2014 was 115 mm, as shown in Table 2.2. The onset of appreciable rainfall occurs in November and subsides by April. Although detectable rainfall usually begins in November and ends in April, Almedej (2012) described rare occasions in which rainfall occurs in October and May. The maximum and minimum annual potential precipitation for the same period was 260 mm in 1975 to 1976, and 28 mm in 1963 to 1964. From the number of years of rainfall data available, there appears to be no conspicuous pattern of highs and lows. In sharp contrast, extreme rainfall events, such as the one that occurred in Kuwait City on 11 November 1997, can cause excessive rainfall (greater than

100 mm) in just hours, resulting in large surface runoff and property damage (Al-Rashed and Sherif 2000).

Table 2.2. Average daily evaporation and monthly precipitation data from Kuwait International Airport

Month	Average Pan A Evaporation (mm/day) (1968-2002)	Average Precipitation (mm/month) (1962-2014)
January	3.2	27.9
February	4.7	14.2
March	6.9	15.5
April	10.2	12.5
May	14.9	3.8
June	20.6	0.0
July	21.0	0.0
August	18.8	0.0
September	14.5	0.0
October	9.1	2.2
November	5.4	16.8
December	3.3	22.2
Annual Total (mm/year)	4039.8	115.2

Table 2.2 shows the average rainfall and average Pan A evaporation for the period between 1968 and 2002. The average monthly potential evaporation exceeds rainfall many times over. The annual total potential evaporation, as measured using a Pan A evaporimeter, is approximately 4040 mm, corresponding to a potential evaporation rate of 11.1 mm/day. This high evaporation results in the concentration of salts near the land surface, thus enriching the upper surface of the soil with gypsum, common salt, and calcium carbonate. However, there are periods during which high intensity rainfall far exceeds evaporation rates, resulting in the formation of water in wadis and, in extreme cases, severe flooding. For example, the highest daily total rainfall of 65 mm and the highest intensity of 38.4 mm in 20 min were recorded on 4 April 1976.

2.2.2 Water Resources in Kuwait

As a country where surface water resources such as rivers or lakes do not exist, Kuwait has very limited natural water resources. The only naturally occurring body of water in Kuwait is the Arabian Gulf (AG), which is undrinkable due to its high salinity, which exceeds 40,000 mg/L near the Kingdom of Bahrain (Burashid & Hussian, 2004). The AG, which extends from Shatt Al-Arab to the Strait of Hormuz, has an area of 240,000 square kilometers (Al Barwani & Purnama, 2008) and a mean depth of 36 m (Reynolds, 1993). The shallowness and high evaporation rate of the AG, as well as the low river discharges entering the sea, are the main factors contributing to its high surface salinity.

Two regional aquifer systems, the Kuwait Group and Dammam aquifers, make up most of the groundwater resources in Kuwait. These aquifers produce brackish water, with TDS contents of 2,500-7,500 mg/L, which is mainly used as raw water for desalination and also for irrigation, watering of gardens, and blending with distilled water to raise TDS. These waters become more saline as they flow from recharge zones in Saudi Arabia and southern Iraq to the discharge zone along the coast of the Arabian Gulf (Alsharhan et al., 2001). The stratigraphy of the aquifer systems in Kuwait is shown in Figure 2.2.

The Kuwait Group, which ranges in thickness from 150 to 400 m, mainly consists of clastic sediments with minor amounts of gypsum and calcareous limestone. It is divided into three formations: the Dibdibba, Lower Fars, and Ghar Formations, from youngest to oldest. The Dibdibba Formation consists mainly of sand and gravel and is only present in the north of Kuwait (Al-Senafy & Al-Fahad, 2000), and it is host to the freshwater lenses at Rawdatain and Umm-Al Aish.


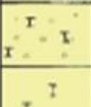
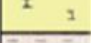
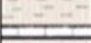
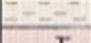
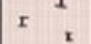
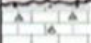




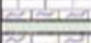

GENERALIZED STRATIGRAPHY				HYDROGEOLOGICAL UNITS	
Kuwait Group – Quaternary	Quaternary sediments <30 m <i>Unconformity</i>		Unconsolidated sands and gravels, gypsiferous and calcareous silt and clay	Localized aquifers	
	Kuwait Group Mio-Pliocene sediments of Hadruk, Dam and Hafuf Formations in Saudi Arabia; Ghar, Lower Fars and Dibdibba formations in Kuwait and southern Iraq 150-210 m		Gravely sands, sandy gravel, calcareous and gypsiferous sand, calcareous silty sandstone, sandy limestone, marl and shale; locally cherty	Dibdibba Aquifer	
				Upper Aquifer	
				Aquitard	
				Lower Aquifer	
<i>Unconformity</i>		Localized shale, clay and calcareous silty limestone	Aquitard		
Hasa Group – Eocene	Dammam Formation 60-200 m		Cherty limestone		
			Chalky, marly, dolomitic and calcarenitic limestone	Aquifer	Upper Middle Lower
	Rus Formation 20-200 m		Nummulitic limestone with lignites and shales	Aquitard; locally aquiclude where Rus Formation is predominantly anhydritic	
			anhydrite and limestone		
	Umm Er-Radhuma Formation 300-600 m		Limestone and dolomite (calcareenitic in the middle) with localized anhydrite layers	Aquifer	
		<i>Disconformity</i>		Shales and marls	Aquitard
Aruma Group 400-600 m		limestone and shaly limestone	Aquifer		

Figure 2.2. Stratigraphy of the aquifer systems in Kuwait

In the Eocene aquifer system, the Rus anhydrite Formation forms an aquitard that separates the Dammam and Umm Al-Radhuma Formations. The Dammam Formation is one of the most important aquifers of the Arabian Peninsula. The aquifer is exploited in the southwestern and central parts of Kuwait, where it produces brackish water with salinity ranging

from 2500 to 5000 mg/L (Mukhopadhyay, 1995). In Kuwait, the Dammam Formation has a thickness that ranges from 120 m in the southwest to 280 m in the north and a transmissivity that ranges from 1000 to 100,000 m²/d (Alsharhan et al., 2001).

2.3 Approaches to Estimating Groundwater Recharge

Groundwater recharge is a hydrologic process where water moves (primarily downward, but movement can be in any direction) to reach the water table of an aquifer and adds to groundwater storage (Meinzer, 1923; Freeze and cherry, 1979; Lerner et al., 1990). Recharge occurs through two types of mechanisms: diffuse and focused (Healy, 2010). Diffuse recharge (sometimes referred to as direct recharge) is recharge through processes that occur relatively uniformly over large areas, such as precipitation and irrigation (Simmers, 1997). Focused recharge is concentrated at topographic lows such as depressions, rivers, and lakes. Lerner et al. (1990) proposed a distinction between two different types of focused recharge: localized recharge and indirect recharge. Localized recharge occurs at small depressions, joints, or cracks, and indirect recharge occurs at larger-scale mappable features such as rivers, canals, and lakes. Rushton (1997) distinguished actual recharge from potential recharge. Actual recharge, which is estimated from groundwater studies, is water that is known to reach the water table. In potential recharge, which is estimated from surface-water and unsaturated-zone studies, the water has infiltrated but may not actually reach the water table because of unsaturated-zone processes, such as bank storage and evapotranspiration, or the inability of the saturated zone to accept recharge due to factors such as low transmissivity or a shallow water table.

Scanlon et al. (2002) discussed various techniques for estimating recharge, ranging from carrying out a water budget/balance to other, more complicated, techniques involving modeling or assessing the behavior of surface or groundwater formations. They noted that the simple water

balance has the advantage of being generally applicable, but it is limited in its eventual usefulness by the accuracy and precision of the input parameters. In arid regions in particular, parameter values can be dramatically affected by environmental conditions.

Beyond the water balance approach, Scanlon and coauthors discussed other techniques that have been used to quantify recharge. For each technique, they discussed its applicable space and time scales, the range of recharge fluxes that have been estimated, the reliability of the recharge estimates, and important factors that promote or limit the use of a particular technique. In their paper, techniques for estimating recharge are subdivided into three types according to the hydrologic zones from which the data are obtained: surface water, the unsaturated zone, and the saturated zone. Each of these zones provides recharge estimates over different space and time scales, and techniques within each zone include physical, tracer, or numerical modeling approaches.

Additional methods for estimating groundwater recharge have been reported elsewhere in the literature (e.g., Kumar, 1997; Lerner et al., 1990; de Vries and Simmers, 2002; Healy, 2010), but it is often difficult to determine which of a wide variety of techniques is likely to provide reliable recharge estimates. When choosing a technique, important considerations include the space/time scales and the range and reliability of recharge estimates associated with the technique. The goal of the recharge study may also dictate the required space/time scales of the recharge estimates. For example, some studies concentrate on recharge quantification to assess water resources (Kumar & Seethapathi, 2002; Manna et al., 2016), and others focus on estimates used for predicting the fate and transport of contaminants or assessing the vulnerability of the aquifer to contamination (Böhlke, 2002; Almasri, 2008).

The techniques for recharge estimation vary depending on the climatic conditions of the system, which in turn govern the location of recharge. In humid regions, for example, recharge is generally considered to occur at topographic highs, whereas recharge in arid regions usually occurs at topographic lows such as stream channels (Tóth, 1963; Scanlon et al., 2002). Additionally, diffuse recharge tends to dominate in wet climates due to shallow water tables and gaining streams, whereas focused recharge dominates in arid climates where there are deep water tables and losing streams. This means that surface-water and saturated-zone techniques are more widely used for assessments in wet climates, and unsaturated-zone techniques are used more often for arid and semiarid climates. This also means that watershed-modeling approaches may be more accurate for wet climates, where perennial surface-water flow may be used for calibrating models.

The required space and time scales of the different techniques also affect their usefulness in particular situations. For example, surface-water and groundwater approaches tend to provide regional estimates of recharge, whereas unsaturated zone methods are typically used for point or small-scale estimates. Similarly, surface-water approaches provide recharge estimates on the time scale of rainfall events, whereas unsaturated-zone and saturated zone tracer techniques are good for long-term recharge estimation.

The accuracy and precision that is required for the recharge estimate is also a consideration. Saturated-zone techniques generally provide more reliable estimates because they estimate actual recharge, in contrast with surface-water and unsaturated-zone techniques that estimate potential recharge. Techniques using Darcy's Law methods and direct groundwater modeling of the unsaturated and saturated zones have limited accuracy because estimates of hydraulic conductivity can vary over several orders of magnitude. In addition, hydraulic

conductivities in unsaturated systems are highly nonlinear with respect to water content, thereby making their determination more difficult.

In the past, groundwater recharge estimation was carried out by graphically analyzing flow nets for unconfined and confined aquifers (Cedegren, 1997). This technique has now largely been supplanted by numerical groundwater flow models. Such models can be used to predict recharge rates based on information concerning hydraulic head, hydraulic conductivity, and other parameters (Sanford, 2002). Because recharge is typically highly correlated with hydraulic conductivity, model inversion using only hydraulic head is limited to estimating the ratio of recharge to hydraulic conductivity. Errors in modeling may be minimized using a wide range of recharge and hydraulic conductivity values if the ratio between those parameters is constant (Luckey et al., 1986). However, because the hydraulic conductivity may range over several orders of magnitude, the resulting estimate of recharge may not be particularly accurate. To complicate matters further, the same values of the hydraulic head may be obtained for a range of recharge rates as long as the ratio of recharge to hydraulic conductivity is constant.

To constrain recharge in inversion groundwater models, recent studies have combined hydraulic heads and groundwater ages (Böhlke & Denver, 1995; Atkinson et al., 2014). These studies have employed manual trial and error or automated procedures with nonlinear regression between measured and simulated data. Whereas hydraulic head is sensitive to the ratio of recharge to hydraulic conductivity, groundwater age is sensitive to the ratio of recharge to porosity (Portniaguine and Solomon, 1998). The combination of head and age data provides the needed constraints on recharge, hydraulic conductivity, and porosity. However, a unique solution requires some information on one of these three parameters, as they are typically correlated.

The uncertainties associated with the various approaches for estimating recharge suggest the use of many approaches to constraining the recharge estimates. Often, different approaches can be complementary and thus help refine the conceptual model of the recharge processes. For example, various tracers (such as Cl, ^{36}Cl , and ^3H) have been used in combination to estimate recharge in unsaturated zones (Scanlon, 1992; Allison et al., 1994; Harrington et al., 2002; Wang et al., 2008; Li et al., 2017; Huang et al., 2017), and other tracers (such as chlorofluorocarbons (CFCs), $^3\text{H}/^3\text{He}$, and ^{85}Kr) have been used in saturated zones (Cook & Solomon, 1997; Raiber et al., 2015). Also, the combination of multiple environmental tracers and numerical modeling has been used for estimating recharge (Reilly et al., 1994; Liu et al., 2014).

To estimate recharge, it is advantageous to use as many different approaches as possible, and it is especially useful to combine surface water, unsaturated zone, and saturated zone techniques. For example, Sophocleous (1991) combined unsaturated-zone water-balance monitoring with water-table fluctuations to improve the reliability of recharge estimates. Other studies have used estimates of recharge from catchment-scale surface-water models as input to groundwater models (Burns et al., 2011; Kahle et al., 2011), and surface water and groundwater models such as SWAT and MODFLOW have been integrated (Kim et al., 2008; Bailey et al., 2016). Such integrated approaches provide models for the overall system that can be used to constrain model parameters and check the continuity of mass balance.

For the reasons discussed above, it is advantageous to use multiple numerical models, which can be used to evaluate conceptual models and model assumptions, assess the sensitivity of recharge estimates to model parameters, and predict the effect of future climate and land use changes on recharge rates. Estimation of recharge using multiple models is carried out iteratively, as estimates are refined as additional data and results are obtained. Furthermore,

modeling is the only technique that can be used to predict future recharge rates, and it is also invaluable for isolating the impacts of different controls on groundwater recharge (Scanlon et al., 2005; Bailey et al., 2009). Models can also be adapted for large spaces and long time periods, used over multiple recharge zones, and made more reliable by their use in saturated zones (so that estimated recharge is based on actual recharge).

REFERENCES

- Abderrahman, W. A., Rasheeduddin, M., Al-Harazin, I. M., Esuflebbe, M., & Eqnaibi, B. S. (1995). Impacts of management practices on groundwater conditions in the eastern province, Saudi Arabia. *Hydrogeology Journal*, 3(4), 32-41.
- Abdulrazzak, M. J. (1994). Review and assessment of water resources in Gulf Cooperation Council countries. *International Journal of Water Resources Development*, 10(1), 23-37.
- Abdulrazzak, M. J. (1995). Water supplies versus demand in countries of Arabian Peninsula. *Journal of Water Resources Planning and Management*, 121(3), 227-234.
- ACSAD (The Arab Center for the Studies of Arid Zones and Dry Lands). (1997). Water resources in the Arab World and their utilization, *Proc. 2nd Arab Workshop on Water Resources in the Arab World*, March 8–10, Kuwait (in Arabic).
- AFED. (2011). Report of the Arab Forum for Environment & Development: Water Sustainable Management of a Scarce Resource. Beirut, Lebanon.
<http://www.afedonline.org/Report2011/main2011.html>.
- Al Barwani, H. H., & Purnama, A. (2008). Evaluating the effect of producing desalinated seawater on hypersaline Arabian Gulf. *European Journal of Scientific Research*, 22(2), 279-285.
- Al-Dousari, A., Milewski, A., Din, S. U., & Ahmed, M. (2010). Remote sensing inputs to SWAT model for groundwater recharge estimates in Kuwait. *Advances in Natural and Applied Sciences*, 4(1), 71-77.
- Al-Katheeri, E. S. (2008). Towards the establishment of water management in Abu Dhabi Emirate. *Water resources management*, 22(2), 205.
- Allan, J. A. (2001). *The Middle East water questions. Hydropolitics and the global economy*. London: I.B. Tauris.
- Allison, G. B., Gee, G. W., & Tyler, S. W. (1994). Vadose-zone techniques for estimating groundwater recharge in arid and semiarid regions. *Soil Science Society of America Journal*, 58(1), 6-14.
- Almasri, M. N. (2008). Assessment of intrinsic vulnerability to contamination for Gaza coastal aquifer, Palestine. *Journal of Environmental Management*, 88(4), 577-593.
- Almedeij, J. (2012). Modeling rainfall variability over urban areas: a case study for Kuwait. *The Scientific World Journal*, 2012.
- Al-Rashed, M. F., & Sherif, M. M. (2000). Water resources in the GCC countries: an overview. *Water resources management*, 14(1), 59-75.

Al-Senafy, M., & Al-Fahad, K. (2000). *Petrography of calcretes and their effects on the hydrology of Kuwait Group aquifer*. Paper presented at the Proceedings of the First International Conference on Geotechnical Geo-Environmental Engineering and Management in Arid Lands.

Al-Senafy, M., Fadlelmawla, A., Bhandary, H., Al-Khalid, A., Rashid, T., Al-Fahad, K., & Al-Salman, B. (2013). Assessment of Usable Groundwater Reserve in Northern Kuwait. *International Journal of Scientific & Engineering Research*, 4(6), 2427-2436.

Alsharhan, A. S., Rizk, Z. A., Nairn, A. E. M., Bakhit, D. W., & Alhajari, S. A. (Eds.). (2001). *Hydrogeology of an arid region: the Arabian Gulf and adjoining areas*. Elsevier.

Al-Sulaimi, J., Khalaf, F. J., & Mukhopadhyay, A. (1997). Geomorphological analysis of paleo drainage systems and their environmental implications in the desert of Kuwait. *Environmental geology*, 29(1-2), 94-111.

Al-Weshah, R. A., & Yihdego, Y. (2016). Flow modelling of strategically vital freshwater aquifers in Kuwait. *Environmental Earth Sciences*, 75(19), 1315.

Atkinson, A. P., Cartwright, I., Gilfedder, B. S., Cendón, D. I., Unland, N. P., & Hofmann, H. (2014). Using ^{14}C and ^3H to understand groundwater flow and recharge in an aquifer window. *Hydrology and Earth System Sciences*, 18(12), 4951-4964.

Authman, M. N. (1983). *Water and development processes in Saudi Arabia*, Tihama Press, Jeddah, Saudi Arabia.

BAAC (British Arabian Advisory Company). 1980. *Water demand and re-use*. Ministry of Agriculture and Water, Riyadh, Saudi Arabia. 246 pp.

Bailey, R. T., Jenson, J. W., & Olsen, A. E. (2009). Numerical modeling of atoll island hydrogeology. *Groundwater*, 47(2), 184-196.

Bailey, R. T., Wible, T. C., Arabi, M., Records, R. M., & Ditty, J. (2016). Assessing regional-scale spatio-temporal patterns of groundwater–surface water interactions using a coupled SWAT-MODFLOW model. *Hydrological processes*, 30(23), 4420-4433.

Bergstrom, R. E., & Aten, R. E. (1965). Natural recharge and localization of fresh ground water in Kuwait. *Journal of Hydrology*, 2(3), 213-231.

Böhlke, J. K. (2002). Groundwater recharge and agricultural contamination. *Hydrogeology Journal*, 10(1), 153-179.

Böhlke, J. K., & Denver, J. M. (1995). Combined use of groundwater dating, chemical, and isotopic analyses to resolve the history and fate of nitrate contamination in two agricultural watersheds, Atlantic coastal plain, Maryland. *Water Resources Research*, 31(9), 2319-2339.

Burashid, K., & Hussain, A. R. (2004). Seawater RO plant operation and maintenance experience: Addur desalination plant operation assessment. *Desalination*, 165, 11-22.

- Bureau De Recherche Geologiques et Minereres (BRGM). 1977. Al-Hassa development project: groundwater resources study and management program, unpublished report to Ministry of Agriculture and Water, Riyadh, 4 vols.
- Burns, E. R., Morgan, D. S., Rachael, S. P., Rachael, S., & Kahle, S. C. (2011). *Three-Dimensional Model of the geologic framework for the Columbia Plateau regional aquifer system, Idaho, Oregon, and Washington*. U. S. Geological Survey.
- Cedergren, H. R. (1997). *Seepage, drainage, and flow nets* (Vol. 16). John Wiley & Sons.
- Cook, P. G., & Solomon, D. K. (1997). Recent advances in dating young groundwater: chlorofluorocarbons, ^3H and ^85Kr . *Journal of hydrology*, 191(1-4), 245-265.
- Danish, S., Khater, A., & Al-Ansari, M. (1992, October). Options in water reuse in Bahrain. In *Proc. 1st Gulf Water Conference*.
- Dawoud, M. A. (2005). The role of desalination in augmentation of water supply in GCC countries. *Desalination*, 186(1-3), 187-198.
- De Jong, R. L. (1989). Water resources of GCC: international aspects. *Journal of Water Resources Planning and Management*, 115(4), 503-510.
- De Vries, J. J., & Simmers, I. (2002). Groundwater recharge: an overview of processes and challenges. *Hydrogeology Journal*, 10(1), 5-17.
- Din, S. U., Al Dousari, A., & Al Ghadban, A. N. (2007). Sustainable fresh water resources management in Northern Kuwait—a remote sensing view from Raudatain basin. *International journal of applied earth observation and geoinformation*, 9(1), 21-31.
- Döll, P., Jiménez-Cisneros, B., Oki, T., Arnell, N. W., Benito, G., Cogley, J. G., ... & Nishijima, A. (2015). Integrating risks of climate change into water management. *Hydrological Sciences Journal*, 60(1), 4-13.
- Edgell, H. S. (1990). Geological framework of Saudi Arabia groundwater resources. *Journal of King Abdulaziz University, Earth Sciences*, 3, 267-286.
- Fadlelmawla, A., & Al-Otaibi, M. (2005). Analysis of the water resources status in Kuwait. *Water resources management*, 19(5), 555-570.
- Fallatah, O. A., Ahmed, M., Save, H., & Akanda, A. S. (2017). Quantifying temporal variations in water resources of a vulnerable middle eastern transboundary aquifer system. *Hydrological Processes*, 31(23), 4081-4091.
- FAO (Food and Agriculture Organization), 1998. Proceedings of the Second Expert Consultation on National Water Policy Reform in the Near East, Cairo, Egypt, 24–25 November 1997.
- FAO. 1979. Survey and evaluation of available data on shared water resources in the Gulf States and Arabian Peninsula, Three Volumes, FAO, Rome.

Feitelson, E., & Tubi, A. (2017). A main driver or an intermediate variable? Climate change, water and security in the Middle East. *Global Environmental Change*, 44, 39-48.

Freeze, R. A., & Cherry, J. A. (1974). A. 1979. Groundwater. *Prentice—Hall, Inc Englewood cliffs, New Jersey*, 604, 215-227.

Gulf Cooperation Council, GCC (2015). Development of United Water Sector Strategy and Implementation Plan for the Gulf Cooperation Council of Arab member States for the Year 2015-2035.

Harrington, G. A., Cook, P. G., & Herczeg, A. L. (2002). Spatial and temporal variability of ground water recharge in central Australia: a tracer approach. *Groundwater*, 40(5), 518-527.

Healy, R. W. (2010). *Estimating groundwater recharge*. Cambridge University Press.

Huang, T., Pang, Z., Liu, J., Yin, L., & Edmunds, W. M. (2017). Groundwater recharge in an arid grassland as indicated by soil chloride profile and multiple tracers. *Hydrological processes*, 31(5), 1047-1057.

Italconsult. 1969. Water and Agricultural Development Studies for Area IV. Eastern Province. Saudi Arabia: Riyadh, Saudi Arabia: Unpublished report to Ministry of Agriculture and Water.

Kahle, S. C., Morgan, D. S., Welch, W. B., Ely, S. R., Vaccaro, J. J., & Orzol, L. L. (2011). *Hydrogeologic framework and hydrologic budget components of the Columbia Plateau Regional Aquifer System, Washington, Oregon, and Idaho*. U. S. Geological Survey.

Khoury, J., Agha, W., & Al-Deroubi, A. (1986). Water resources in the Arab World and future perspectives. In *Proc. Symposium on Water Resources and Uses in the Arab World, Kuwait Google Scholar*.

Kim, N. W., Chung, I. M., Won, Y. S., & Arnold, J. G. (2008). Development and application of the integrated SWAT–MODFLOW model. *Journal of Hydrology*, 356(1-2), 1-16.

Kumar, C. P., & Seethapathi, P. V. (2002). Assessment of natural groundwater recharge in Upper Ganga Canal command area. *Journal of Applied Hydrology*, 15(4), 13-20.

Kumar, C. P., & Seethapathi, P. V. (2002). Assessment of natural groundwater recharge in Upper Ganga Canal command area. *Journal of Applied Hydrology*, 15(4), 13-20.

Kwarteng, A. Y., Viswanathan, M. N., Al-Senafy, M. N., & Rashid, T. (2000). Formation of fresh ground-water lenses in northern Kuwait. *Journal of arid environments*, 46(2), 137-155.

Le Grand ADSCO Ltd., Messrs, J.D., & Watson, D.M. 1959. A Survey of the Freshwater Resources of the Northern Qatar.

Lee, E., Jayakumar, R., Shrestha, S., & Han, Z. (2018). Assessment of transboundary aquifer resources in Asia: Status and progress towards sustainable groundwater management. *Journal of Hydrology: Regional Studies*.

- Lerner, D. N., Issar, A. S., & Simmers, I. (1990). *Groundwater recharge: a guide to understanding and estimating natural recharge* (Vol. 8, pp. 99-228). Hannover: Heise.
- Li, Z., Chen, X., Liu, W., & Si, B. (2017). Determination of groundwater recharge mechanism in the deep loessial unsaturated zone by environmental tracers. *Science of the Total Environment*, 586, 827-835.
- Liu, Y., Yamanaka, T., Zhou, X., Tian, F., & Ma, W. (2014). Combined use of tracer approach and numerical simulation to estimate groundwater recharge in an alluvial aquifer system: A case study of Nasunogahara area, central Japan. *Journal of hydrology*, 519, 833-847.
- Lloyd, J. W. (1994). Groundwater-management problems in the developing world. *Applied Hydrogeology*, 2(4), 35-48.
- Lloyd, J. W., & Pim, R. H. (1990). The hydrogeology and groundwater resources development of the Cambro-Ordovician sandstone aquifer in Saudi Arabia and Jordan. *Journal of Hydrology*, 121(1-4), 1-20.
- Lloyd, J. W., Pike, J. G., Eccleston, B. L., & Chidley, T. R. E. (1987). The hydrogeology of complex lens conditions in Qatar. *Journal of hydrology*, 89(3-4), 239-258.
- Luckey, R. R., Gutentag, E. D., Heimes, F. J., & Weeks, J. B. (1986). Digital simulation of ground-water flow in the High Plains aquifer in parts of Colorado, Kansas, Nebraska, New Mexico, Oklahoma, South Dakota, Texas, and Wyoming. US Geol Surv Prof Pap 1400-D: 57.
- Macumber, P. G. (2003). Lenses, plumes and wedges in the Sultanate of Oman: a challenge for groundwater management. In *Developments in Water Science* (Vol. 50, pp. 349-370). Elsevier.
- Macumber, P. G., Al Abri, R., & Al Akhzami, S. (1998). Hydrochemical facies in the groundwater of central and southern Oman. In *Quaternary Deserts and Climatic Change* (pp. 511-520). Balkema Rottendam.
- Macumber, P. G., Barghash, B. G. S., Kew, G. A., & Tennakoon, T. B. (1995). Hydrogeologic implications of a cyclonic rainfall event in central Oman. *Groundwater quality*. Chapman and Hall, London, 87-97.
- Manna, F., Cherry, J. A., McWhorter, D. B., & Parker, B. L. (2016). Groundwater recharge assessment in an upland sandstone aquifer of southern California. *Journal of Hydrology*, 541, 787-799.
- MAW (Ministry of Agriculture and Water), 1982. Census of agriculture according to farm size, 1981-82. MAW, Riyadh.
- MAW (Ministry of Agriculture and Water), 1984. Water Atlas of Saudi Arabia. Riyadh, MAW.
- Meinzer, O. E. (1923). Outline of ground-water hydrology. *US Geological Survey Water Supply Paper*, 494(5).

Mukhopadhyay, A. (1995). Distribution of transmissivity in the Dammam limestone formation, Kuwait. *Groundwater*, 33(5), 801-805.

Mukhopadhyay, A., Akber, A., Rashed, T., Kotwicki, V., Uddin, S., & Bushehri, A. (2016). Establishing a baseline to evaluate future impacts to groundwater resources in North Kuwait. *Environmental Earth Sciences*, 75(4), 324.

Mukhopadhyay, A., Al-Awadi, E., Quinn, M., Akber, A., Al-Senafy, M., & Rashid, T. (2008). Ground water contamination in Kuwait resulting from the 1991 Gulf War: a preliminary assessment. *Groundwater Monitoring & Remediation*, 28(2), 81-93.

Parsons Corporation. 1964. Groundwater Resources of Kuwait, vols I, II and III. Ministry of Electricity and Water, Kuwait.

Portniaguine, O., & Solomon, D. K. (1998). Parameter estimation using groundwater age and head data, Cape Cod, Massachusetts. *Water Resources Research*, 34(4), 637-645.

Puri, S., & Aureli, A. (2005). Transboundary aquifers: a global program to assess, evaluate, and develop policy. *Groundwater*, 43(5), 661-668.

Raiber, M., Webb, J. A., Cendón, D. I., White, P. A., & Jacobsen, G. E. (2015). Environmental isotopes meet 3D geological modelling: conceptualising recharge and structurally-controlled aquifer connectivity in the basalt plains of south-western Victoria, Australia. *Journal of Hydrology*, 527, 262-280.

Reilly, T. E., Plummer, L. N., Phillips, P. J., & Busenberg, E. (1994). The use of simulation and multiple environmental tracers to quantify groundwater flow in a shallow aquifer. *Water Resources Research*, 30(2), 421-433.

Reynolds, R. M. (1993). Physical oceanography of the Gulf, Strait of Hormuz, and the Gulf of Oman—Results from the Mt Mitchell expedition. *Marine Pollution Bulletin*, 27, 35-59.

Rizk, Z. S., & Alsharhan, A. S. (2003). Water resources in the United Arab Emirates. In *Developments in Water Science* (Vol. 50, pp. 245-264). Elsevier.

Robinson, B. W., & Al Ruwaih, F. (1985). The stable-isotopic composition of water and sulfate from the raudhatain and Umm Al Aish freshwater fields, Kuwait. *Chemical Geology: Isotope Geoscience section*, 58(1-2), 129-136.

Rushton, K. (1997). Recharge from permanent water bodies. In: Simmers I (ed) Recharge of phreatic aquifers in (semi)arid areas. AA Balkema, Rotterdam, pp 215–255.

Saif, O., Mezher, T., & Arafat, H. A. (2014). Water security in the GCC countries: challenges and opportunities. *Journal of Environmental Studies and Sciences*, 4(4), 329-346.

Sanford, W. (2002). Recharge and groundwater models: an overview. *Hydrogeology journal*, 10(1), 110-120.

- Scanlon, B. R. (1992). Evaluation of liquid and vapor water flow in desert soils based on chlorine 36 and tritium tracers and nonisothermal flow simulations. *Water Resources Research*, 28(1), 285-297.
- Scanlon, B. R., Reedy, R. C., Stonestrom, D. A., Prudic, D. E., & Dennehy, K. F. (2005). Impact of land use and land cover change on groundwater recharge and quality in the southwestern US. *Global Change Biology*, 11(10), 1577-1593.
- Senay, Y. (1977). Groundwater resources and artificial recharge in Rawdhatain water field. *Ministry of Electricity and Water, Kuwait*, 35.
- Shiklomanov, I. A. (1990). Global water resources. *Nature and resources*, 26(3), 34-43.
- Shiklomanov, I. A. (1998). *World water resources: a new appraisal and assessment for the 21st century: a summary of the monograph World water resources*. UNESCO.
- Simmers, I. (ed) (1997). Recharge of phreatic aquifers in (semi-)arid areas. AA Balkema, Rotterdam, 277 pp.
- Sophocleous, M. A. (1991). Combining the soilwater balance and water-level fluctuation methods to estimate natural groundwater recharge: practical aspects. *Journal of hydrology*, 124(3-4), 229-241.
- Tarawneh, Q. Y., & Chowdhury, S. (2018). Trends of Climate Change in Saudi Arabia: Implications on Water Resources. *Climate*, 6(1), 8.
- Toth, J. (1963). A theoretical analysis of groundwater flow in small drainage basins. *Journal of geophysical research*, 68(16), 4795-4812.
- Tropp, H., & Jagerskog, A. (2006). Water scarcity challenges in the Middle East and North Africa (MENA). *Human Development Paper. UNDP*. http://hdr.undp.org/hdr2006/pdfs/background-docs/Thematic_Papers/SIWI.pdf.
- U.A.R (United Arabic Republic) Experts. 1964. Ministry of Electricity and Water, Kuwait.
- UNESCO. (1979). Map of the world distribution of arid regions. Man and Biosphere Tech Notes, no. 7, UNESCO: Paris; 54.
- UN-ESCWA and BGR (United Nations Economic and Social Commission for Western Asia; Bundesanstalt für Geowissenschaften und Rohstoffe). 2013. Inventory of Shared Water Resources in Western Asia. Beirut.
- Wang, B., Jin, M., Nimmo, J. R., Yang, L., & Wang, W. (2008). Estimating groundwater recharge in Hebei Plain, China under varying land use practices using tritium and bromide tracers. *Journal of Hydrology*, 356(1-2), 209-222.

World Bank. 2005. A Water Sector Assessment Report on the Countries of the Cooperation Council of the Arab States of the Gulf. Washington, DC. © World Bank.
<https://openknowledge.worldbank.org/handle/10986/8719> License: CC BY 3.0 IGO.

World Bank. 2007. Making the Most of Scarcity: Accountability for Better Water Management Results in the Middle East and North Africa. MENA Development Report. Washington, DC. © World Bank. <https://openknowledge.worldbank.org/handle/10986/6845> License: CC BY 3.0 IGO.

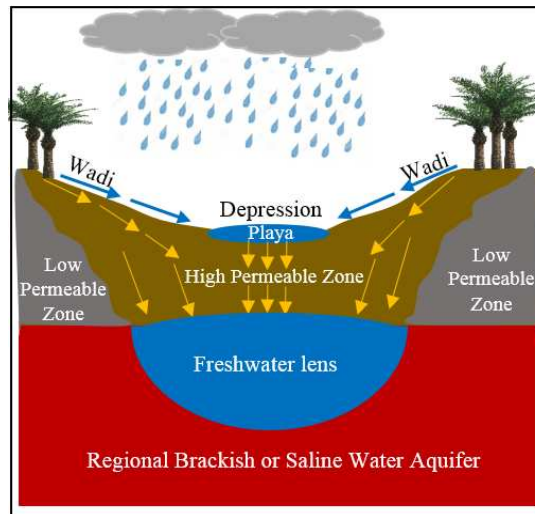
Yihdego, Y., & Al-Weshah, R. A. (2017). Assessment and prediction of saline sea water transport in groundwater using 3-D numerical modelling. *Environmental Processes*, 4(1), 49-73.

Zubari, W. K. (1999). The Dammam aquifer in Bahrain—Hydrochemical characterization and alternatives for management of groundwater quality. *Hydrogeology Journal*, 7(2), 197-208.

**CHAPTER 3. ESTIMATING GROUNDWATER RECHARGE FOR A FRESH
GROUNDWATER LENS IN AN ARID REGION: FORMATIVE AND STABILITY
ASSESSMENT**

Overview Summary

- The formation of focused rainfall recharge fresh groundwater lenses floating above denser, saline or brackish groundwater are a crucial source of freshwater supplies in arid regions.
- A baseline for an example of these lenses is established by using a 3D density-dependent groundwater flow model tested against multiple data targets and water age.
- This study assesses the natural dynamic of these lenses and therefore enhances the understanding of their formation and stability.



A conceptual model of a focused rainfall recharge fresh groundwater lens in subterranean oases
in arid regions

Highlights

The formation of subsurface fresh groundwater lenses (FGLs) on top of brackish groundwater is a fascinating hydrologic phenomenon that creates groundwater supplies of great potential value in arid regions. Information on the recharge quantity and mechanism of these lenses is both scarce and uncertain. This study examines the formation and macroscale stability of the Rawdatain FGL in Kuwait, for which significant pre-development data are available. The Rawdatain is a large (150 million m³) subsurface freshwater lens overlying brackish groundwater. In this study, a 3D density-dependent groundwater flow model is tested against the following data targets to estimate long-term diffuse and focused groundwater recharge: (1) groundwater head, (2) total dissolved solids (TDS) groundwater concentration, (3) volume and vertical thickness of stored groundwater of three different water quality TDS ranges (0-700 mg/L, 700-1,000 mg/L, 1,000-2,000 mg/L), and (4) geometrical shape features of the lens along cross-sections. To better represent the spatial variation in TDS, six different recharge zones were assigned to allocate diffuse and focused recharge conditions. Twelve recharge rate scenarios, encompassing a wide range of feasible long-term average annual recharge values (200,000 - 5,000,000 m³/year), were tested against the multiple targets and compared with the groundwater age of the Rawdatain lens. Based on comparison with data targets, the long-term average annual recharge is estimated to be 500,000 m³/year. Scenarios of reduced recharge, which may occur due to changes in land-use or climate, demonstrate the extremely slow response of the lens, which is in agreement with the slow development and formation of the lens (> 2,000 years). Within a 100-year time frame, a 50% reduction in annual recharge reduces the lens volumes by 21%, 17% and 9% for the three water quality categories, respectively. This study demonstrates

the stability of FGLs in arid regions and also provides methodology for similar focused rainfall recharge FGLs.

3.1. Introduction

Most of the Arabian Peninsula (AP) has a harsh climate characterized by high average temperature, erratic sparse rainfall, and high evapotranspiration rates, and its landforms make it difficult to harvest and store precipitation (Al-Rashed & Sherif, 2000). The lack of water availability is an obstacle to sustainable development in the AP (Shiklomanov, 1990&1998), and drinking water security is clearly of strong importance in urban and rural areas. The population in the Gulf Cooperation Council (GCC) countries increased rapidly from 7.6 million in 1970 to 48.9 million in 2012, resulting in a major increase in water demand for municipal, agricultural, and industrial uses (GCC, 2015). With the lack of natural freshwater sources in the region, desalinated seawater supplies most of the drinking water (Al-Rashed & Sherif, 2000). In addition to a scarcity of water resources, the region also suffers from large-scale water management problems, including over-exploitation of aquifers, decreasing water quality, and inadequate water availability for optimal irrigation (World Bank, 2007). Challenges of balancing between water scarcity and food production will likely arise in the future worldwide according to climate change projections and global population growth, and the AP located within the most critical areas (Mancosu et al., 2015).

Fresh water is extremely scarce over the entire AP. There are no perennial rivers or lakes, and surface water does not exist with the exception of some mountainous areas in the southern and western regions. Therefore, groundwater is the main source of freshwater supply (Al-Rashed & Sherif, 2000). FAO (1979) conducted a comprehensive investigation of the region, which classified the regional groundwater into two main aquifer systems with various potentialities:

Systems A and B. System A represents the deep, non-renewable (fossil) groundwater aquifers, and System B represents the shallow, renewable groundwater aquifers. System B represents discontinuous fresh groundwater lenses (FGLs) that extend over the eastern part of the AP and over deeper brackish groundwater. The longevity and likelihood of creation of these lenses are both relatively small, as recharge of these lenses depends on surface runoff from rainfall events that may vary considerably from year to year (FAO, 1979).

Italconsult (1969) and BRGM (1977) reported the existence of FGLs along the eastern coast of Saudi Arabia (SA) that are separated by semi-confining beds from deeper aquifers. Since the earliest groundwater studies in Qatar, a survey of the freshwater resources was conducted by Le Grand ADSCO et al., (1959), which recognized the existence of a lens-type aquifer (the Ghyben-Herzberg type). Detailed investigation revealed the existence of a major 40 m thick FGL in Qatar with a volume of 17.6 million cubic meters and total dissolved solids (TDS) concentrations of less than 1000 mg/L (FAO, 1979). The FGLs in the Liwa area in United Arab Emirates (UAE) were also documented and proposed as appropriate locations for artificial aquifer storage and recovery (FAO, 1979; Rizk & Alsharhan, 2003; Al-Katheeri, 2008). In the Wusta region of central Oman, thin locally derived FGLs were found overlying the saline regional groundwater (Macumber et al., 1995; 1998; 2003). The lenses are up to tens of kilometers long, 10-100 meters thick, and several kilometers wide, with average TDS values as low as 200 mg/L and as high as 1750 mg/L.

In Kuwait, the FGLs have been the subject of comprehensive investigations from the 1960s to the present, as they are the only source of fresh water in Kuwait. Early in the 1960s, the Parsons Corporation identified two large FGLs in the northern part, the Rawdatain and Umm Al-Aish basins, and several small lenses in the Al-Qashaniya, Mutla and Al-Abdali areas of Kuwait

(Parsons Corporation, 1964). The volumes of stored fresh groundwater with less than 2,000 mg/L TDS in the Rawdatain and Umm Al-Aish areas were estimated as 136.3 and 71.9 million m³, respectively.

Among the FGLs in the AP, the Rawdatain basin in Kuwait is perhaps the most notable example because it is very large and because an extensive subsurface data set was collected in 1960-1962 by the Parsons Corporation before significant groundwater extraction from the lens began. The existence of that pre-development data, as well as the quality and quantity of that data, makes Rawdatain an ideal and potentially unique candidate to use for evaluating the formative and potentially changing dynamics of lenses in arid regions. A number of studies have been dedicated to the hydrogeological aspects of the depressions in the Rawdatain FGL and the general hydrogeology of the area (Parsons Corporation, 1964; Bergstrom and Aten, 1964; Robinson & Al-Ruwaih, 1985; Ebrahim et al., 1993; Viswanathan et al., 1997; Grealish et al., 1998; Kwarteng et al., 2000; Din et al., 2007; Al-Dousari et al., 2010; Al-Senafy et al., 2013; Milewski et al., 2014). These studies are discussed in detail in sections 3.2.2 and 3.2.3.

However, estimates of recharge for the lens vary widely (Table 3.1), from 1 million m³/year to approximately 47 million m³/year, with average annual areal recharge (mm/yr) ranging from 4.9 mm/yr to 33.9 m/yr, which is likely because the studies were performed over short time periods. Also, none of the studies listed in Table 3.1 quantified the spatially focused recharge beneath the wadis, the center of the depression (playa), and the edges of the depression. The annual average rate of recharge must be quantified more accurately to assist with water management strategies in the region. Milewski et al. (2014) discussed the challenges of estimating the recharge of the freshwater lenses in the deserts due to the unique hydrological processes such as, infrequent-intensive rainfall events, losses through the wadis, infiltration

capacity, and salinity of the hosting aquifers. Inclusion of dispersion to allow for mixing of recharge water with ambient groundwater yields a better representation of the recharge mechanism, with the former remaining an open question in the literature (Garabedian et al., 1991; LeBlanc et al., 1991; Gelhar et al., 1992; Schulze-Makuch, 2005).

In general, estimating recharge rates for groundwater in arid regions has been known to be difficult through the decades (Lloyd, 1986; Gee, 1988; Lerner et al., 1990; de Vries and Simmers, 2002; Healy, 2010). Recently, several studies have provided new approaches to constrain the uncertainties associated with groundwater recharge estimations. Integrating different approaches of estimating recharge can be complementary and thus help refine the conceptual model of the recharge processes. For example, various tracers (such as Cl, ^{36}Cl , and ^3H) have been used in combination to estimate recharge in unsaturated zones (Wang et al., 2008; Li et al., 2017; Huang et al., 2017), and other tracers (such as chlorofluorocarbons (CFCs)) have been used in saturated zones (Raiber et al., 2015). Also, the combination of multiple environmental tracers and numerical modeling has been used for estimating recharge (Liu et al., 2014). Atkinson et al. (2014) used an inversion groundwater model that combines hydraulic heads and groundwater ages.

Other studies have used estimates of recharge from catchment-scale surface-water models as input to groundwater models (Burns et al., 2011; Kahle et al., 2011), and surface water and groundwater models such as SWAT and MODFLOW have been integrated (Kim et al., 2008; Bailey et al., 2016). Jeong et al. (2017) combined a water-table fluctuation model with unsaturated-zone gravitational flow to demonstrate the effect of the unsaturated zone drainage and a delayed recharge flux in the water-table fluctuation.

Table 3.1. Summary of recharge estimate studies for the Rawdatain basin

Reference	Space Scale (km ²)	Time Scale	Recharge Estimation Method	Estimated Recharge Volume (million m ³ /year)	Average Areal Recharge (mm/year)
Bergstrom and Aten (1964)	75	1 year (1961)	Saturated Zone-Darcy's Law	1	13.3
Kwarteng et al. (2000)	75	17 years (1962-1978)	Saturated Zone-Water Budget Equation	2	26.7
Ud Din et al. (2007)	2879	1 year (2003)	Surface Water-Physical Techniques	22.38	7.8
Al-Dousari et al. (2010)	3696	9 years (1998-2006)	Surface Water-Numerical Modeling (SWAT)	46.8	12.7
Al-Senafy et al. (2013)	3696	10 years (2000-2009)	Surface Water-Numerical Modeling (SWAT)	18	4.9
Al-Senafy et al. (2013)	75	6 months (Oct. 2010-Apr.2011)	Saturated Zone-Water Table Fluctuation	NA	25
Milewski et al. (2014)	241	12 years (1998-2009)	Surface Water-Numerical Modeling (SWAT)	8.17	33.9

Such integrated approaches provide models for the overall system that can be used to constrain model parameters and check the continuity of mass balance.

Different formation settings and recharge mechanisms of the FGLs have reported from fifteen locations worldwide (Laattoe et al., 2017). The recharge mechanisms found to vary between surface and subsurface water interactions, topographic mounding, focused rainfall recharge, and recharge from anthropogenic activities. Within the AP, Laattoe et al. (2017) classified the Rawdatain and Umm-Al-Aish FGLs in Kuwait and FGLs in the Wusta region of central Oman as focused rainfall recharge type. Similar recharge mechanisms were found on the Eyre Peninsula and Stockyard Plain in South Australia (Laattoe et al., 2017).

The objective of this study is to provide accurate long-term estimates of recharge for the Rawdatain FGL and to investigate the timing of lens depletion under scenarios of decreased recharge. Such information is valuable for formulating water management strategies for the region. A primary focus is to establish a reliable, well-constrained estimate of the balance between the main formative factor (i.e., recharge rate) and the major pre-development loss factor (i.e., natural dispersive mixing). The recharge rate estimate is based on multi-target calibration of a three-dimensional (3D) density-dependent groundwater flow and solute transport model using the following pre-development period calibration targets: (1) spatially-variable groundwater head, (2) spatially-variable TDS concentration, (3) volumes and thicknesses of stored groundwater at three different water quality categories (TDS of 0-700 mg/L, 700-1,000 mg/L, 1,000-2,000 mg/L), and (4) the geometrical shape of the lens along aquifer cross sections.

The methodology presented herein is a general approach to estimating recharge rates for focused rainfall recharge freshwater lenses in arid regions. Furthermore, dispersion parameters at

the relevant scales have not been quantified for Rawdatain, and these may not be well-quantified in many similar basins. This additional factor must be considered when using lens observations to estimate recharge rates.

3.2. The Rawdatain Basin

3.2.1 Physical Description and Climate

The Rawdatain basin is a closed topographical depression located approximately 60 km north-northwest of Kuwait City. Fresh water was discovered accidentally in a well (Well ID: R8) that was drilled in the Rawdatain basin in 1960 for a brackish water supply for the construction of a road between Kuwait city and Basra city in Iraq. After the well had continued to produce fresh water with TDS of 600 mg/L for several months, an investigation of the basin became an interest. The Ministry of Electricity and Water (M.E.W) in Kuwait summoned the Parsons Corporation, Los Angeles (USA), to conduct an extensive hydrological survey for evaluating the groundwater potential of the area in 1961. Later, the project objectives expanded beyond the data survey to develop and construct the Rawdatain freshwater production field. On September 19th, 1962, the officially opening of the Rawdatain facilities was held, and the significant pumping was begun at a rate of 9,000 m³/day in October 1962 (Parsons Corporation 1964). In this study, the volumes of the stored water, groundwater head measurements, and TDS data points that was collected in 1961-1962 prior to the sustained pumping is considered to represent the pre-development period.

Summers in the study area are long, hot, and dry, and winters are short, which is typical for the AP. Temperatures reach daytime highs averaging 44°C and 15°C and nighttime lows averaging 23°C and 3°C in summer and winter, respectively (Almedeij, 2012). Most of the annual precipitation falls between November and April, and the average total annual

precipitation is 115 mm for the period 1962 to 2016. For this period, the highest annual precipitation was 260 mm in 1975-1976, and the lowest was 28 mm in 1963-1964. The average daily potential evaporation varies from as low as 3.2 mm/day in January to as high as 21.0 mm/day in July, with an annual total of approximately 4040 mm. Although the average climate is very dry, high-intensity rainfall can occur, resulting in flowing water in wadis and sometimes severe flooding. For example, the highest recorded intensity of rainfall of 38.4 mm in 20 min occurred on 4 April 1976.

The depression has an area of approximately 75 km², but its catchment area is approximately 3696 km². Numerous wadis converge and terminate in the basin (Figure 3.1). Based on the lower permeability of shallow soils in the center of the basin, researchers have suggested that recharge occurs primarily in the wadis and along the margins of the basin, with the recharged water then flowing toward the center of the basin through the subsurface (Grealish et al., 1998; Fadlilmawla et al., 2008). Even so, surface runoff through the wadis does occasionally result in water being ponded relatively deep across the lower depression, forming a lake that may last several days before infiltrating or evaporating (Senay, 1977).

The Rawdatain FGL, as mapped to date, is roughly 10 km long and 5 km wide, with an average thickness of approximately 25 m and a maximum thickness of 35 m. The freshwater volume based on pre-development data (Parsons Corporation 1964, UAR 1964) has been estimated at 33 million m³ of groundwater below 700 mg/L TDS, 64 million m³ below 1000 mg/L, and 149 million m³ below 2000 mg/L (Table 3.2). Pumping from the lens was as high as 4 million m³/year in 1967, but has been limited to approximately 0.2 million m³/year in recent years (MEW, 2015).

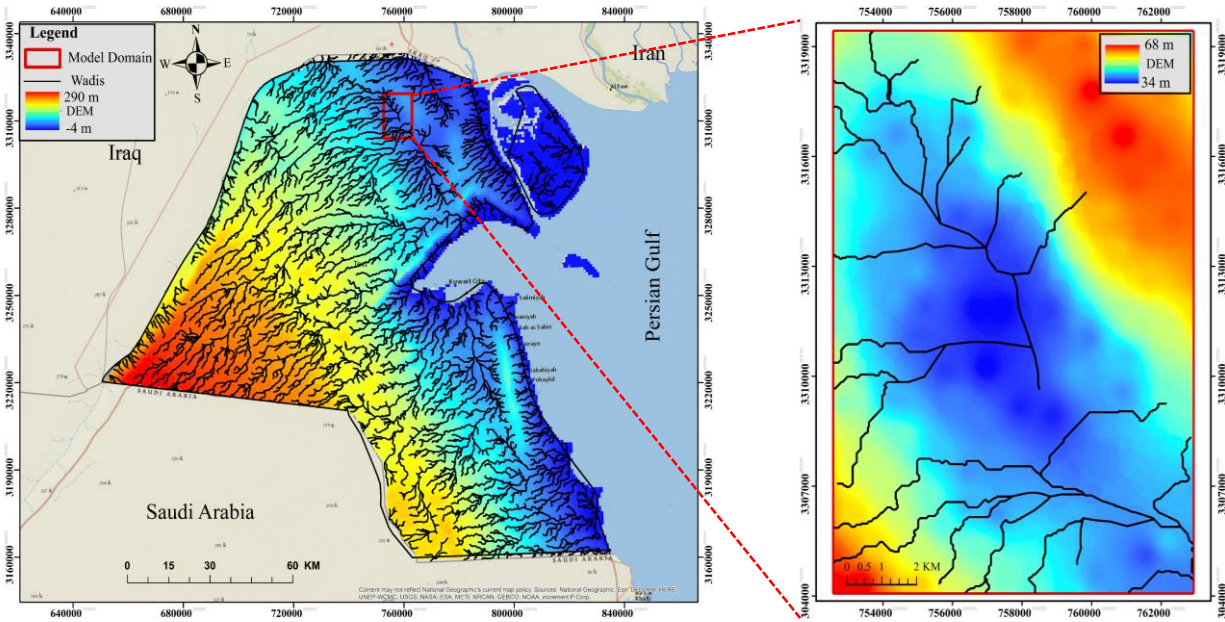


Figure 3.1. State of Kuwait and the Rawdatain model domain

Table 3.2. Volumes of stored water in the Rawdatain basin (Senay, 1977)

Data Source	Volumes of Stored Water (million m ³) with TDS equal or less than		
	700 ppm	1000 ppm	2000 ppm
Parsons Corporation (1964)	----	68.1	136.3
U.A.R Experts (1964)	32.6	60.6	161.6
Average	32.6	64.4	149.0

3.2.2 Previous Studies of Recharge Mechanisms

The topic of recharge mechanism and phenomena has been of interest to many studies because of the uniqueness of FGLs hydrology in deserts. Bergstrom and Aten (1964) used piezometric water levels to identify possible recharge locations in the area. Based on a contour map of the heads, the local water flow was identified as flowing northward from the central area of the lens and fanning outward to the west, north and east. Based on this observation, the authors concluded that recharge generally occurs at the central area of the lens, and they further

identified three localities as the specific recharge areas within the central area of the lens based on surface water accumulations attributed to direct rainfall.

However, the soil infiltration rates within the depression were low (Parsons Corporation, 1964; Grealish et al., 1998), so the mechanism of recharge was unclear. Robinson & Al-Ruwaih (1985) and Ebrahim et al. (1993) used stable isotope ratios of groundwater at Al-Rawdatain to constrain the age of recharge associated with recent rainfall events. Because the $\delta^{18}\text{O}$ and $\delta^2\text{H}$ values showed no sign of evaporation, they concluded that infiltration of rainwater was fast. Grealish et al. (1998) reported that the wadi beds in the area had vertical infiltration rates of up to 60 cm/h, which were much larger than those of the inter-wadi soils at Al-Rawdatain (2 cm/h), and higher infiltration rates were found near the periphery of the main depression. Viswanathan et al. (1997) developed a conceptual model for recharge to the freshwater aquifers in the area, in which water in the main depression migrates laterally along low-permeability calcrete horizons to the center of the depression, where it then infiltrates vertically to the freshwater lens through discontinuities in the cemented horizon.

3.2.3 Previous Studies of Recharge Quantity

Several studies have quantified the recharge rate in the Rawdatain basin, as shown in Table 3.1. These studies used a wide range of spatial and time scales and different methods of recharge estimation. Bergstrom & Aten (1964), Kwarteng et al. (2000), and Al-Senafy et al. (2013) used techniques based on the saturated zone to estimate the actual recharge to the Rawdatain depression (approximately 75 km²). Actual recharge, which is estimated from groundwater studies, is water that is known to reach the water table (Rushton, 1997). Their estimates ranged from 1 to 2 million m³/year (13.3 to 26.7 mm). These authors used different techniques: Darcy's law, Water Budget Equation, and Water Table Fluctuation, respectively.

Saturated zone techniques are applicable for arid regions, where focused recharge tends to dominate, to provide actual regional estimates of recharge based on long-term recharge estimation (Scanlon et al., 2002).

Potential recharge, which is estimated from surface-water and unsaturated-zone studies, is water that has infiltrated but may not actually reach the water table because of unsaturated-zone processes, such as bank storage and evapotranspiration, or the inability of the saturated zone to accept recharge due to factors such as low transmissivity or a shallow water table (Rushton, 1997). Compared with actual recharge, potential recharge estimates based on the surface zone were higher and had a wider range of values, ranging from 4.9 to 33.9 mm/year for the entire Rawdatain watershed (8.2 to 46.8 million m³/year) (Din et al., 2007; Al-Dousari et al., 2010; Al-Senafy et al., 2013; Milewski et al., 2014). Their studies used SWAT model simulations and modern precipitation records to estimate the potential recharge, with the exception of Din et al. (2007), who used physical techniques. Their approaches (watershed modeling) may be more accurate in humid regions, where perennial surface-water flow can be used for model calibration. Unsaturated zone methods are typically used for point or small-scale estimates of potential recharge in arid and semiarid climates (Scanlon et al., 2002).

Senay (1973) found that estimated recharge by Bergstrom & Aten (1964) was high based on the rapid increase in the TDS of produced water from 1963 to 1973, when the average annual water extraction was approximately 3.6 million m³. Thus, the published recharge estimates in Table 3.1 are highly uncertain and likely substantially overestimate recharge, and relying on them for water resources planning is risky. Moreover, it has been directly observed that over-pumping (i.e., when pumping rates likely exceeded recharge rates) can damage the groundwater quality of the Rawdatain basin (Senay, 1977; Mukhopadhyay, 2016). However, the water quality

degradation could also occur from accelerated mixing between freshwater and brackish groundwater due to pumping.

3.3. Methods

3.3.1 Approaches to Estimating Groundwater Recharge

In this study, numerical modeling of the saturated zone was used to estimate long-term recharge over a large area, including both diffuse and focused actual recharge. Diffuse recharge (sometimes referred to as direct recharge) is recharge through processes that occur relatively uniformly over large areas, such as precipitation and irrigation (Simmers, 1997), and focused recharge is concentrated at topographic lows such as depressions, rivers, and lakes. To constrain the uncertainty of numerical modeling, multiple calibration targets and groundwater age data were used to constrain the uncertainty in the groundwater recharge models (discussed in sections 3.4 and 3.5). This method was selected because of the wealth of data available in the saturated zone and the capability of such models to evaluate conceptual models and model assumptions, assess the sensitivity of recharge estimates to model parameters, and predict the effect of future climate and land use changes on recharge rates.

The recharge estimation techniques based on surface water or unsaturated zone models were eliminated from consideration because of their limited capability in our study area and the limited availability of relevant data. The surface water approaches may be less accurate for the Rawdatain basin, where perennial surface-water flow data are not available for calibrating models. In our case, the unsaturated approaches are not appropriate because of the thick unsaturated zone, ranging between approximately 25 and 40 m in depth. In addition, hydraulic conductivities in unsaturated systems are highly nonlinear with respect to water content, thereby making determination more difficult (Scanlon et al., 2002).

3.3.2 Model Code

The SEAWAT code (Langevin et al. 2007) was used to simulate the formation and behavior of the Rawdatain lens. SEAWAT is a 3D finite difference code developed by the U.S. Geological Survey, capable of simulating transient density-dependent flow and advection and dispersion of solutes by combining MODFLOW (McDonald & Harbaugh, 1988) and MT3DMS (Zheng & Wang, 1999), using the former to simulate groundwater flow and the latter to simulate solute transport. The two codes are run iteratively to update the head solution based on changes in fluid density caused by changing solute concentration. Numerous applications of SEAWAT have been published, including the simulation of coastal seawater intrusions (Qahman & Larabi, 2006; Goswami & Clement, 2007) and the behavior of freshwater lenses that form on islands (Comte et al., 2014; Holding and Allen, 2015; Wallace and Bailey, 2017; Alsumaiei & Bailey, 2018).

3.3.3 Model Construction

The model domain is depicted in Figures 3.1 and 3.2. It has a uniform 100 m x 100 m grid spacing with 155 rows and 105 columns (total number of cells is 553,350), aligned with true north and centered on the surface depression. The model uses 34 computational layers to represent three aquifer zones (Upper A, Upper B, and Lower) and two aquitards that separate them (Table 3.3). Horizontally, each layer has homogenous hydraulic conductivity values (Table 3.3). The hydraulic conductivity values were obtained from Parsons Corporation (1964) and

Senay (1988), which were based on results from 14 pumping tests. The authors also estimated the specific yield and porosity to be 0.12 and 0.22, respectively.

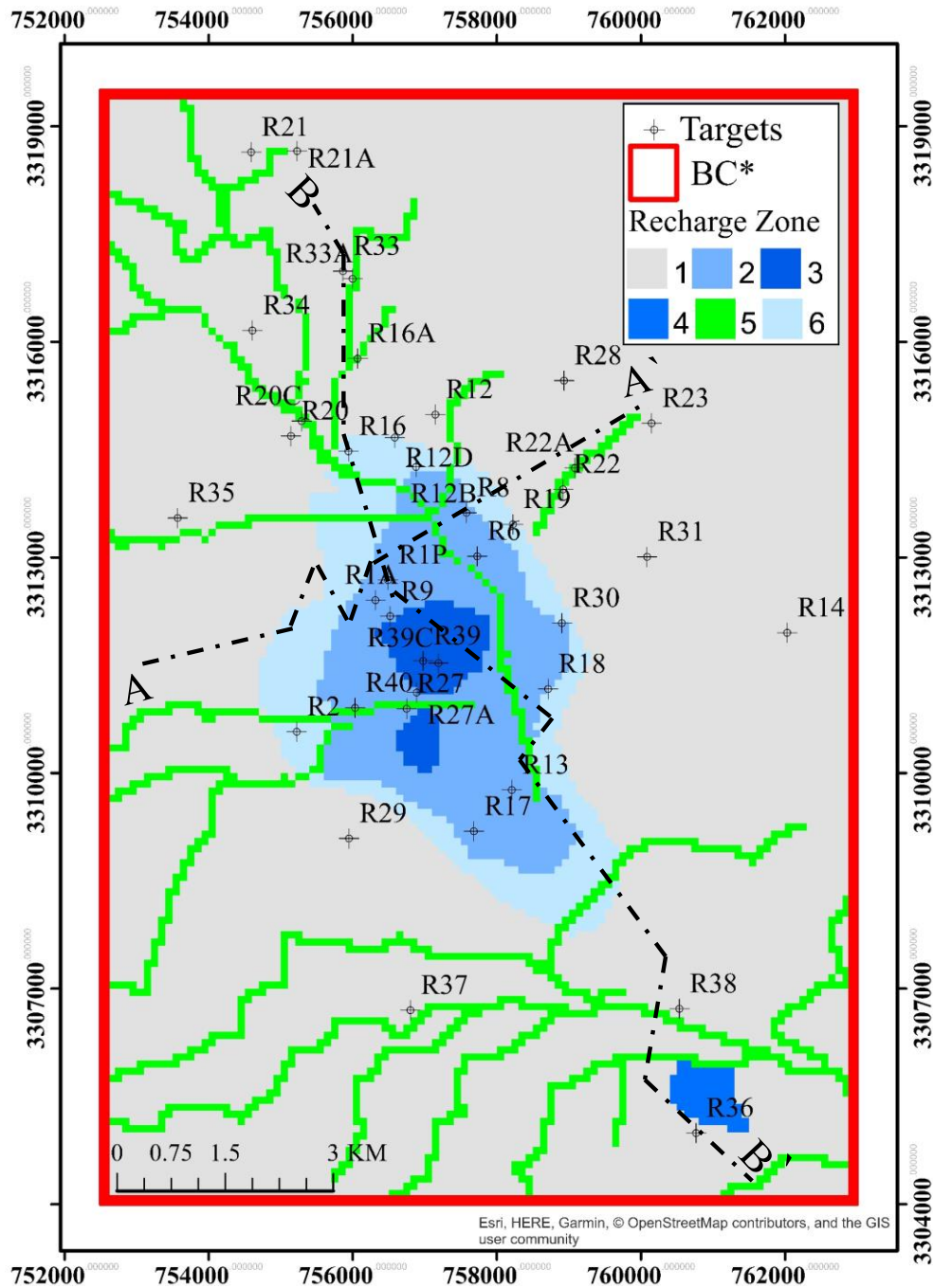


Figure 3.2. Model domain set up (*BC stand for Boundary Conditions where the south and west boundaries represent specified-head conditions and the north and east boundaries represent head-dependent flux conditions)

Table 3.3. Model layer details and hydraulic conductivity values (Senay, 1988)

Aquifer Units	Thickness (m)	Number of layers	K_h (m/day)	K_v (m/day)
Upper Aquifer-A	15	13	24.5	2.45
Aquitard	3	3	0.86	0.086
Upper Aquifer-B	10	10	24.5	2.45
Aquitard	4	2	0.86	0.086
Lower Aquifer	18	6	12.2	1.22

There is no well-defined large-scale environmental dispersivity estimate for the Rwadatain FGL because there are multiple recharge zones, as shown in Figure 3.2. Estimating or using a value of dispersivity for the FGL is an open topic of research and uncertain in several studies (Mukhopadhyay et al., 1994; Yihdego & Al-Weshah, 2017). Gelhar et al. (1992) found that there are no reliable 3D dispersivity values at scales larger than 300 m. Beyond that scale, almost all dispersivity estimates are from contaminant transport and environmental tracer studies. In such studies, solute input is typically poorly defined, and controlled input tracer experiments have not been conducted at larger scales because of the very long time periods required. Gelhar et al. (1992) suggested that values of dispersivity for uncontrolled environmental events (such as seawater intrusion) are commonly determined by fitting a solute transport model to historical data. In this study, dispersivity values were altered to achieve the best match, resulting in values of 50 m, 5 m, and 0.1 m in the longitudinal, transverse horizontal, and transverse vertical directions, respectively. The higher dispersivity values promote more mixing and result in a smaller freshwater lens and vice versa.

Six recharge zones were used (Figure 3.2). Zones 1, 2 and 6 represent regional diffuse recharge rates (estimated to be very low). Zones 3, 4 and 5 represent focused recharge beneath

the depression, playa, and wadis, respectively. Recharge zones were allocated based on depression topography, water age (Fadlelmawla et al., 2008), and spatial TDS data. Each zone was assigned a fixed percentage of the total annual recharge volume, as listed in Table 3.4.

Table 3.4. Model recharge zones

Recharge Zone	Zone Area (km ²)	Recharge Zone Percentage (%)
Zone 1	133.1	19.4
Zone 2	9.9	10.8
Zone 3	1.9	35.7
Zone 4	0.8	14.8
Zone 5	9.6	18.1
Zone 6	7.6	1.1

There are no natural hydrologic boundaries within nor near to the domain of our study. Hydrologically, the Rawdatain FGL is floating above brackish groundwater of a regional extended country-wide hosting aquifer. In such conditions, implementing specified-head boundary conditions that represents the natural balance between the formative and loss factors (i.e. head gradient, density gradient and buoyancy phenomena) would be the most feasible and reliable option. The boundary conditions were extended beyond the Rawdatain depression to cover the surrounding hosting aquifer (Figure 3.2). This would help to better simulate the regional flow regime and allow for natural mixing of recharge water with ambient brackish groundwater beneath the recharge zones, thus; minimize the effects of the boundary conditions on recharge zones.

The values of the specified heads and concentrations of the boundaries were initially assigned based on field measurements collected by Parsons Corporation (1964) prior to sustained pumping from Rawdatain field. These values were slightly adjusted until a basic head calibration was achieved. Specified-head conditions were set along the east boundary that spatially varying from 13 m above sea level (asl) from lowest southern cell to 10.25 m asl at the highest northern

cell, whereas 13 m asl was set along the south boundary. Head-dependent flux conditions were set along the north and east boundaries that spatially varying from 13 m asl at the south eastern corner and 10.25 m asl at the north western corner to 9.25 m asl at the north eastern corner. During preliminary simulations, we found that the head-dependent flux boundary condition more accurately handled the flux of solute leaving the model domain along the north end.

Bergstrom and Aten (1964) found that the general flow regime is from south west to north east and the head gradients were from about 0.0001 to 0.0008. The natural flow regime was successfully reproduced and the simulated head gradient (i) was 0.0002. Note, the simulated head gradient represents the effects of the boundary conditions only (i.e. no recharge was applied). However, as will be discussed later, the recharge rates and the location of recharge zones did have some further effect on groundwater head values and gradients. Later, the simulated head gradients with applied recharge will be comparable with the values reported by Bergstrom and Aten (1964). The boundary conditions were not further adjusted in the simulations presented herein. A sensitivity analysis was applied to explore the effects of different Specified-head boundary conditions for both development and stability simulations.

Each model simulation began with no freshwater present, i.e., an initial TDS concentration set to increase gradually from 4,000 mg/L at the top layer to 12,000 mg/L at the bottom layer. These values are representative of TDS values reported outside of and below the Rawdatain FGL. Vertical recharge was then applied to the top layer, and the simulation was run until the FGL approached a steady-state configuration and volume. The TDS concentration of the recharge water was assumed to be 200 mg/L, which was the best water quality found in the lens. Also, Fadlelmawla et al. (2008) found that the main geochemical processes controlling the

salinization of the recharge is mixing with regional brackish water, whereas the magnitude of salinization during infiltration, subsurface runoff and percolation to the water table is minimal.

3.3.4 Multi-Target Calibration Approach

To provide accurate estimates of recharge, the constructed SEAWAT model was tested against multiple data targets to limit what otherwise were a wide variety of non-unique possible parameter sets. This concept has been addressed extensively in the literature, including many examples regarding the importance of multi-target calibration (e.g., Kim et al. 1999; Saiers et al. 2004).

The pre-development data for Rawdatain FGL were collected in the early 1960s and consist of TDS at 47 locations (including various depths) and water table data at 42 locations (Parsons Corporation, 1964). Locations of the wells providing the groundwater head and TDS data are shown in Figure 3.2, and more details (such as, date of measurements) are presented in Table A&B in the appendix A. These data provide information on the lens's pre-development volume and depth at three different water quality levels (0-700 mg/L, 700-1000 mg/L, and 1000-2000 mg/L TDS), as well as insight into the 3D spatial variability of salinity. These data were used to guide and constrain the construction and calibration of the groundwater flow and salt transport model.

A strong focus was placed on calibrating to the 1962 estimates of freshwater volume because of the interest in using the Rawdatain FGL as a freshwater resource. The volume estimates were based on TDS data at the same point, yet this still provides two different types of calibration targets. As noted by Hill & Tiedeman (2006), the use of point data in calibrating transport models can be problematic because concentrations can vary by orders of magnitude over short distances. Furthermore, this variability is partly due to subsurface heterogeneities,

often at a scale that can never be known or modeled in sufficient detail. For these reasons, a close match of point data is not expected. Calibration to the total mass of a contaminant plume (freshwater lens, in this case) is more feasible, and perhaps even more informative, than attempts to calibrate to highly variable point concentration data (Feehley et al., 2000). Other examples of alternatives to using point concentration measurements are discussed by Julian et al. (2001), Barth and Hill (2005a,b), Anderman et al. (1996), and Bailey et al. (2014). Still, although calibrating to the volume (mass) of the freshwater lens is a primary goal, the point data do provide useful information about the shape and distribution of the lens. For this reason, the model's fit to the point TDS data was also monitored during calibration.

The freshwater thickness (i.e., depth) calibration targets were of course ultimately based on the original point TDS data, but some specific thickness targets of the freshwater lens were also based on diagrams created by Senay (1989). The thickness targets were helpful in eliminating several non-unique combinations of calibrated parameters.

3.3.5 Groundwater Age Constraint

Groundwater age data help to constrain the rate of recharge, the residence time of aquifer storage, and the time frame of contaminant fate and transport (McCallum et al. 2017). In the Rawdatain basin, Fadlelmawla et al. (2008) collected 24 samples for radioactive carbon isotope analysis (^3H and ^{14}C). The samples were collected within the 2000 mg/L TDS contour, and their average depths ranged between 3 to 39 m below the water table. The analysis of the samples indicated that the groundwater age ranges from less than 500 years to 2043 years. A more thorough quantitative comparison is difficult because age depends on both depth and location, and also on the sampling location with respect to the complex flow dynamics within the lens (Sanford, 2002). In this study, the age of the lens volume with TDS less than or equal to 2000

mg/L is used only to constrain the simulated period of lens development (i.e, groundwater age is not tracked during simulation). Multiple calibration targets were compared with the simulated results at 2000 years. This approach provides an independent factor that constrains the hydraulic conductivity, recharge rate, and dispersivity.

3.3.6 Scenarios

Twelve recharge rate scenarios (Table 3.5) were simulated, starting with no freshwater lens present and then running for 4000 years. The R9 to R12 recharge scenarios test the high range of average annual recharge values from previous studies shown in Table 3.1. Based on interpolation of extraction rate and water quality in comparison with natural recharge, Senay (1973 & 1977) and Mukhopadhyay (2016) concluded that the studies listed in Table 3.1 clearly overestimated recharge. Thus, the R1 to R8 recharge scenarios were implemented to test a lower range of annual recharge rates. The recharge scenario that best matches the data targets at 2000 years was used for the stability assessment. In the stability assessment, the shrinkage scenarios started from the lens condition at 2000 years and ran for more 2000 years, with reductions of 10, 20, 30, 40, 50, and 100% of the initial recharge rate to determine likely effects of future changes in land-use or climate.

Table 3.5. Annual volume recharge scenarios

Recharge Scenario	Annual Volume Recharge (m³/year)	Recharge Scenario	Annual Volume Recharge (m³/year)
R1	200,000	R7	600,000
R2	300,000	R8	800,000
R3	400,000	R9	1,000,000
R4	450,000	R10	1,200,000
R5	500,000	R11	2,000,000
R6	550,000	R12	5,000,000

A sensitivity analysis was carried out by varying hydraulic conductivity values in the best recharge scenario. A range of multipliers (0.1, 0.5, 1.5, 2, 3 and 4) was applied to the hydraulic

conductivity set K in Table 3.3 to test against the volumes and vertical thicknesses of stored groundwater of the three different water quality ranges. The anisotropy ratio values were always set to 10. Also, a sensitivity analysis was performed to assess the effects of different specified-head boundary conditions for both development and stability simulations. For the development period, four new sets of specified-head values were assigned by changing the specified-head values along the west and south boundaries and the specified-head values along the east and north boundaries as the following pairs: (+1, +0.82), (+3, +2.63), (-1, -0.81) and (-3, -2.62) m, respectively. Each of those pairs led to change the original head gradient (i) as following: $+5\%i$, $+10\%i$, $-5\%i$, and $-10\%i$, respectively. For the stability assessment, additional eight simulations were run to assess the effects of the change in the head gradients and the change in both recharge and head gradients, and then compared with the change in recharge only.

3.4. Results

3.4.1 Simulations of Lens Formation as a Function of Recharge

Figure 3.3 is a plot of the simulated freshwater lens volume over time, starting at the initial condition and continuing until a steady configuration was approached. Three different volume targets are shown: (a) 700 mg/L (32.6 million m³), b) 1000 mg/L (64.4 million m³), and (c) 2000 mg/L (149 million m³). Curves for the many simulated recharge rates (Table 3.5) are shown for 4000 years.

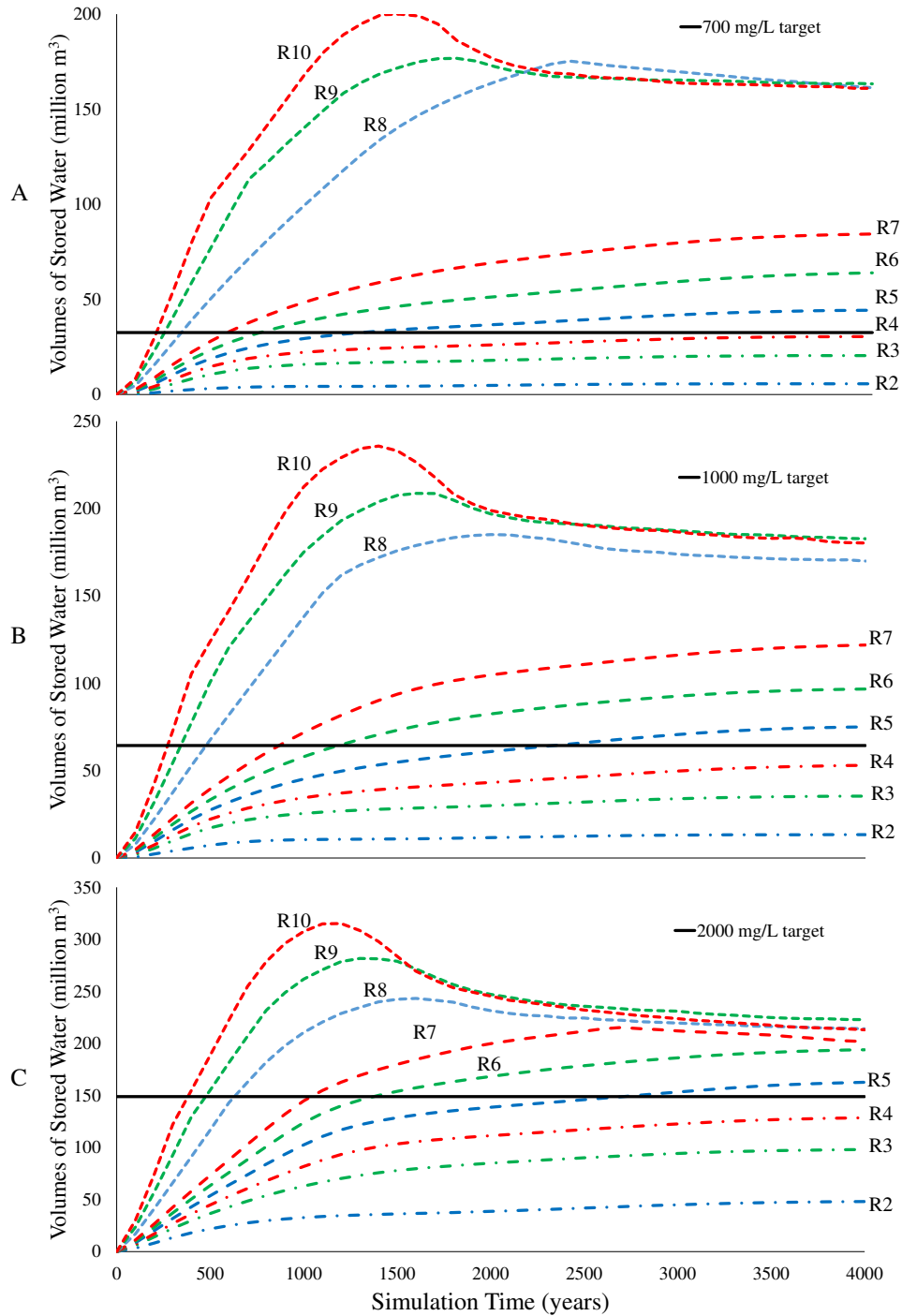


Figure 3.3. Scenarios of Rawdatain FGL development: A) 700 mg/L, B) 1000 mg/L, and C) 2000 mg/L water quality categories.

Figure 3.3A shows the development of the Rawdatain FGL against the first volume target of 700 mg/L. Recharge scenarios R2, R3 and R4 never exceeded the target volume, whereas R8, R9 and R10 met the target volume in less than 400 years and did not tend to reach a steady

volume. Scenarios R5, R6 and R7 reached the closest to the target volume, but R6 and R7 tended to meet the target faster and then continued to increase over time to a greater extent than R5. R5 met the target volume within 1400 years. Figures 3.3B and 3.3C show similar overall trends for the second and third volume targets. R5 met the second and third volume targets within 2200 and 2600 years, respectively. R1, R11 and R12 are not shown in the figures because the recharge fluxes in the scenarios were either too low or too high to develop the lens.

As evidenced from Figure 3.3, the lens volume is sensitive to the recharge rate, with the best fit found for an overall basin recharge rate of 500,000 m³/year (Scenario R5). In this model, increases and decreases in recharge on the order of 10% (i.e R6 and R4) clearly miss the volume targets by +/- (20% to 60%). Note that when starting from an initial no-freshwater condition, the simulated lens with R5 required from 1400 to 2600 years to reach its final volume in the model domain.

Figure 3.4 summarizes the data from the three plots of Figure 3.3 by including all three volume targets at one simulation time (2000 years). Again, the good fit for R5 is apparent, along with the relative sensitivities of the increases and decreases for R4 and R6. R5 performed the best among the scenarios, as it minimized the absolute errors between the simulated volumes and the three volume targets. The absolute errors were 12.9%, 5.3% and 6.9% for the three volume targets, respectively. The high absolute error for the first volume target could be because we compared the simulated volume with one field estimate from U.A.R., as shown in Table 3.2. Figure 3.4 also indicates that low recharge scenarios would not be able to create the lens, and the high recharge scenarios developed very large lenses.

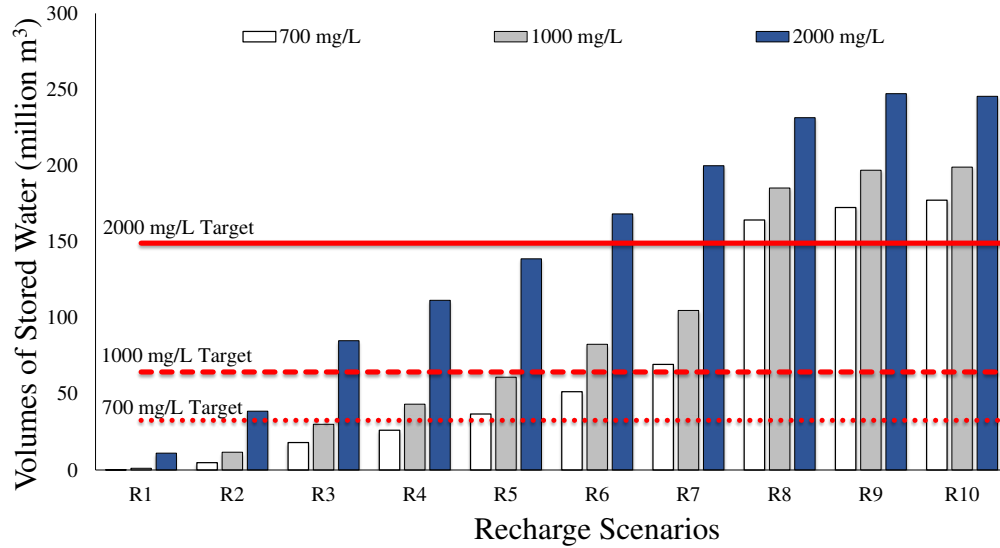


Figure 3.4. Volumes predicted for different recharge scenarios at 2000 years compared with target volumes (red lines).

A greater emphasis was placed on achieving a close calibration to lens volume targets than to TDS point data, for reasons explained above. Indeed, point concentration results show the expected degree of scatter for the concentrations, with results for scenarios R1, R5, and R10 shown in Figure 3.5. Nevertheless, this measure of calibration was also sensitive to recharge rates. As shown in Figure 3.5, the R5 rate (500,000 m³/year) achieved a reasonably good fit. In comparison, the low recharge value of 200,000 m³/year (R1) greatly over-predicts TDS, whereas the high recharge value of 1,200,000 m³/year (R10) greatly under-predicts TDS point concentration data. The range of the Scaled Root Mean Square Error (S-RMSE) of TDS was found to be between 0.167 and 0.447, as shown in Figure 3.6. In terms of the S-RMSE values, the best three recharge scenarios were R7, R6 and R5, with values of 0.167, 0.174 and 0.188, respectively.

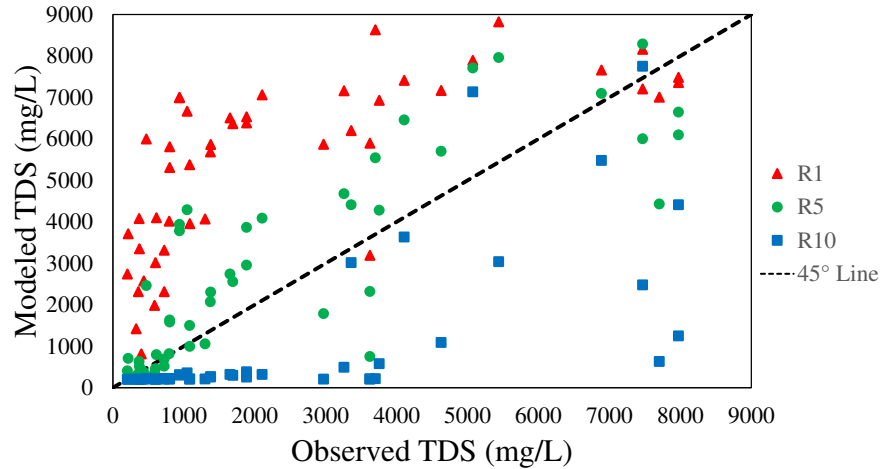


Figure 3.5. Observed vs. modeled TDS concentrations for the R1, R5, and R10 recharge scenarios.

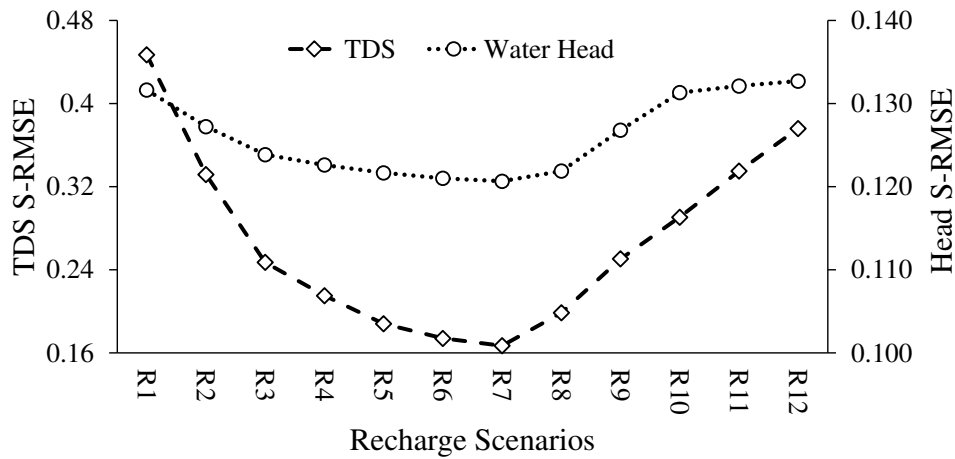


Figure 3.6. S-RMSE for TDS and head with different recharge scenarios

Calibrating the model to groundwater head is not a particularly robust or stringent method for solute transport models. Indeed, we found head calibration to have a lower sensitivity to recharge than other calibration targets. Still, the higher and lower recharge rates (0.2 and 1.2 million m³/year) did noticeably degrade the head calibration (Figure 3.7). As shown in Figure 3.6, the narrow range of S-RMSE values (0.121 and 0.132) for the groundwater head did not help to distinguish the performance of the different recharge scenarios, unlike the range of TDS S-RMSE values. These results demonstrate the usefulness of combining groundwater transport and flow models.

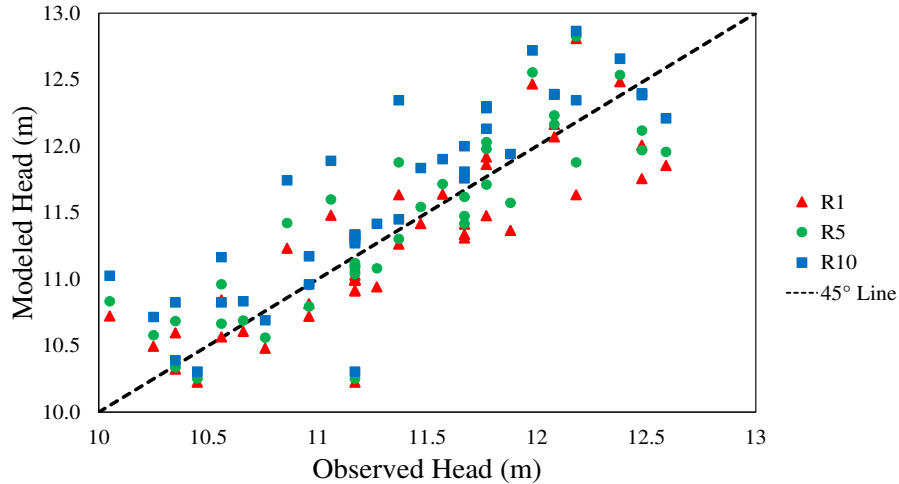


Figure 3.7. Observed vs. modeled head for the R1, R5, and R10 recharge scenarios.

The final calibration target was the maximum lens thickness, as presented by Senay (1989). The thickness of a lens can be an important factor for the feasibility of recovering (pumping) the freshwater without causing excessive mixing of the underlying brackish waters. Figure 3.8 is a plot of simulated maximum thickness for scenarios R1-R10. Once again, it is apparent that R5 has the best fit, and small changes in recharge (R4 and R6) result in a poor fit. Overall, scenario R5 performed the best, as it minimized the absolute errors between the simulated maximum lens thickness and the three thickness targets. The absolute errors were 10.5%, 3.9% and 2.6% for the three thickness targets, respectively. Also, Figure 3.8 indicates that low recharge scenarios developed very thin lenses, and the high recharge scenarios established very deep lenses. It is difficult to distinguish between the three thickness targets for R9 and R10 because the lens hit the model depth base at 50 m. These simulations suggested that water with 700 mg/L TDS exists at 50 m, which is more than twice the depth at which concentrations this low were measured in the field. In fact, lenses of that thickness did not exist with any of the three TDS targets, so the higher recharge scenarios (R11 and R12) were eliminated from further analysis.

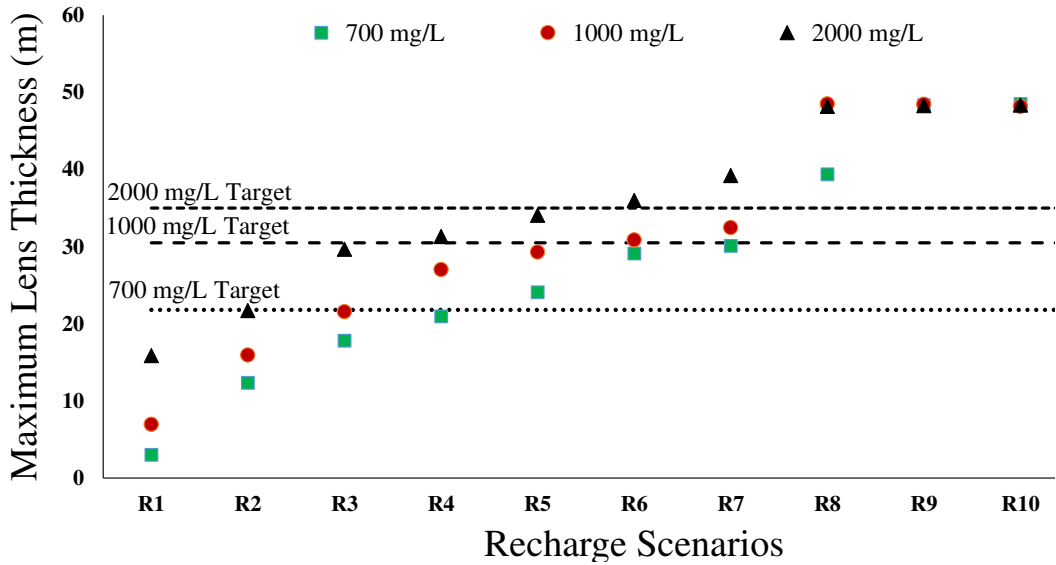


Figure 3.8. Maximum lens thickness predicted for different recharge scenarios at 2000 years compared with target values (black lines).

In addition to using freshwater thickness as a quantitative target, we also considered lens thickness and overall lens shape qualitatively. This criterion also helps to confirm the accuracy of the recharge zones, as it represents the shape of the lens under the recharge zones. Figure 3.9 depicts the longitudinal and transverse cross-sections of the lens presented by Senay (1977). Figure 3.9 (C, D) shows the corresponding cross-sections through the simulated lens from scenario R5, showing a favorable visual comparison with the observed cross-section of TDS.

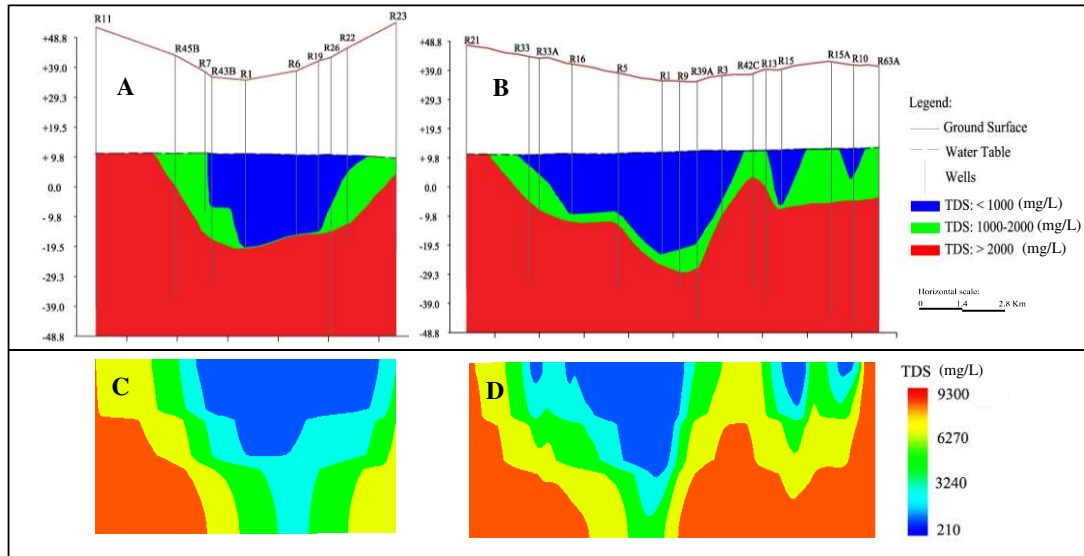


Figure 3.9. (A) & (B) Rawdatain cross-sections A-A' and B-B', respectively (modified after Senay, 1977). (C) & (D) Modeled cross sections A-A' and B-B', respectively (not to scale) using the R5 recharge scenario

3.4.2 Simulation of Lens Stability under Changes in Recharge

The Rawdatain FGL is a unique and potentially valuable natural resource. One concern about its reliability and security is the degree to which land-use changes or climate changes may affect the historical average recharge rate in the basin and thereby affect the lens. The best-fit recharge model (R5) was used to predict how future recharge reductions may affect the volume of the lens inside the model domain. These simulations do not consider the pumping that has taken place from 1962 to present. Rather, these simulations start with the formation model at time $t = 2000$ years (after a creation period) and implement a sudden recharge reduction for the remainder of the simulation. The simulations included reductions of 10, 20, 30, 40, 50, and 100% of the calibrated recharge rate ($500,000 \text{ m}^3/\text{year}$).

The results are plotted in Figure 3.10. The results confirm an expectation that was intuitive from the formation simulations, i.e. because recharge is small compared with the lens volume and because the lens required approximately 2000 years to form at such low recharge rates, a reduction in recharge would not have an immediate impact. In the worst case scenario,

assuming a 100% reduction in recharge (i.e., no recharge), the three different volumes would be depleted after approximately 300, 400 and 700 years, respectively. This shows that the zone of 700 mg/L TDS is more sensitive to reduction in recharge than the zone of 2000 mg/L TDS. The simulated lens required approximately 500 to 1000 years to reach a newly equilibrated volume after the change in recharge rate. With a 20% reduction in recharge and 1000 years, the new simulated volumes of the 700, 1000, and 2000 mg/L water quality zones would be reduced by 43%, 40%, and 26% from the original volumes, respectively. Within the next several decades or even a century, the effect of recharge reduction would have less impact on the lens volume. For instance, within 100 years and with a 20% reduction in recharge, the lens will shrink only by 8%, 6% and 3% for the three water quality volume targets, respectively. Within a century, the lens still had a significant volume even with a 100% reduction in recharge.

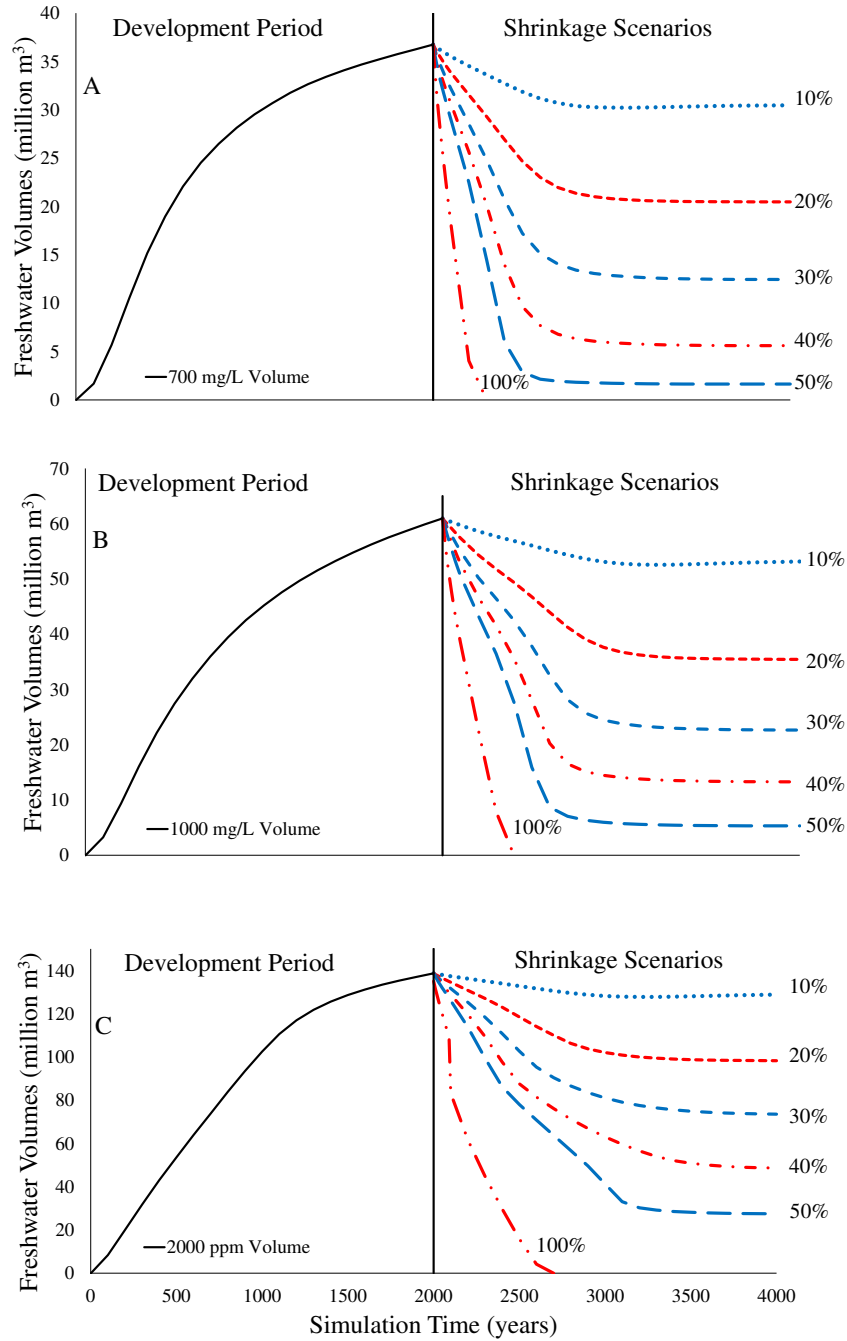


Figure 3.10. Development period and shrinkage scenarios for the A) 700 mg/L, B) 1000 mg/L, and C) 2000 mg/L water quality categories.

3.4.3 Sensitivity Analysis

The capability of the tested groundwater model was used to assess the sensitivity of the Rawdatain FGL to hydraulic conductivity and boundary conditions. A sensitivity analysis was

carried out by varying hydraulic conductivity under the R5 recharge scenario. The x-axis in Figure 3.11 represents different hydraulic conductivity sets. Hydraulic conductivity set K represents the values of horizontal and vertical hydraulic conductivity in Table 3.3, whereas the values 0.1, 0.5, 1.5, 2, 3 and 4 are multipliers. The anisotropy ratio values were always set to 10. Figure 3.11 shows results for the three water quality categories, showing that K has a strong influence on the volume and thickness of the lens. Results show that the set of K values provided by Senay (1988) (the “K” scenario in Figure 3.11) satisfies all three water quality categories, their corresponding maximum thicknesses, and the age of the stored groundwater. This indicates that the K set is reasonably representative of the entire aquifer domain. The lower values of K (0.1K, 0.5K) result in a large volume and a thick freshwater lens compared with the other sets, which presumably implies a fast freshwater development and therefore a younger age of stored water. In contrast, the higher values of the K set prevent the existence of the lens.

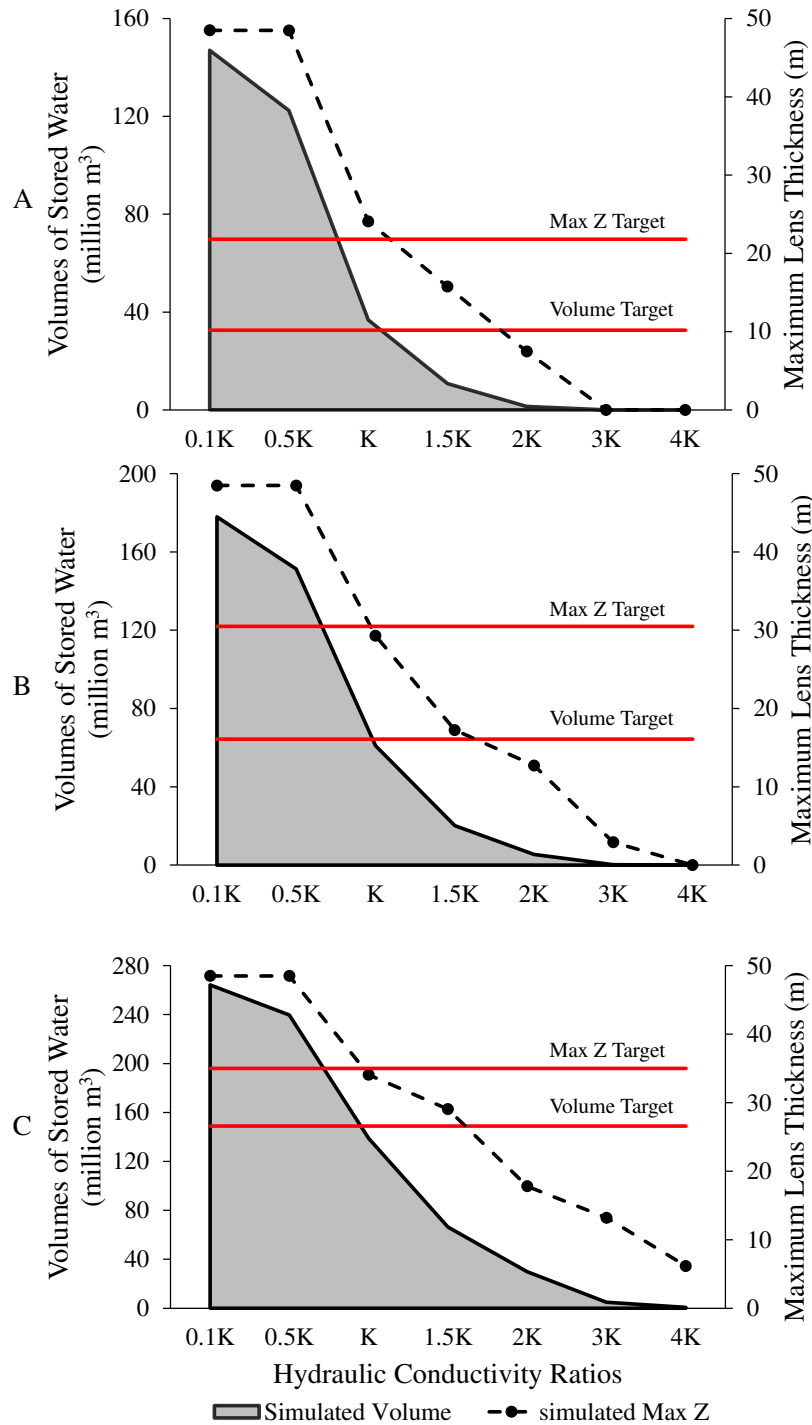


Figure 3.11. Sensitivity of lens volume and thickness to hydraulic conductivity with the R5 recharge scenario: A) 700 mg/L, B) 1000 mg/L, and C) 2000 mg/L water quality categories. (Max Z stands for maximum lens thickness) (Red lines represent the targets of the volumes of stored water at each water quality category and the corresponding lens thickness)

For development period, the base scenario in Table 3.6 represents the simulations resulted from using R5 and original head gradient (i). The model was re-run from the initial condition (i.e., no freshwater present) with the new four head gradients ($+5\%i$, $+10\%i$, $-5\%i$, and $-10\%i$) using the R5 for 2000 years. Then, the performance of the additional 4-runs were tested against the targets data and compared with the base scenario. An increase in the head gradient by 5% would lead to a slight decrease in simulated volumes of stored water by 6.3 to 7.9% and no significant change in simulated lens maximum thickness compared to the base scenario. The $+10\%i$ scenario indicates more flows from the ambient water towards the freshwater lens resulting in decrease in its volume. In the other hand, no significant effects on the simulated volumes and maximum thickness with the $-5\%i$ and $-10\%i$ scenarios.

Table 3.6. Sensitivity of lens development to boundary conditions

Comparison criteria	Targets	Base Scenario		Sensitivity Analysis Scenarios											
		<i>i</i>	Error (%)	+5% <i>i</i>	Error (%)	Change (%)	+10% <i>i</i>	Error (%)	Change (%)	-5% <i>i</i>	Error (%)	Change (%)	-10% <i>i</i>	Error (%)	Change (%)
Volume of Stored Water (10⁶m³)															
700 mg/L	32.6	36.8	+12.9	33.9	+4.0	-7.8	30.9	-4.9	-15.8	36.7	+12.8	-0.1	36.9	+13.2	+0.3
1000 mg/L	64.4	61.0	-5.3	56.2	-12.7	-7.9	51.3	-20.4	-15.9	60.9	-5.3	-0.1	61.1	-5.0	+0.3
2000 mg/L	149.0	138.7	-6.9	129.9	-12.8	-6.3	119.2	-20.0	-14.1	138.8	-6.9	+0.1	139.4	-6.4	+0.5
Lens Maximum Thickness (m)															
700 mg/L	21.80	24.08	+10.5	23.29	+6.9	-3.3	22.33	+2.4	-7.3	24.10	+10.6	+0.1	24.13	+10.7	+0.2
1000 mg/L	30.50	29.30	-3.9	29.24	-4.1	-0.2	29.15	-4.4	-0.5	29.30	-3.9	0.0	29.31	-3.9	0
2000 mg/L	35.00	34.08	-2.6	33.81	-3.4	-0.8	33.50	-4.3	-1.7	34.08	-2.6	0.0	34.09	-2.6	0
S-RMSE for TDS	-----	0.188	-----	0.201	-----	-----	0.215	-----	-----	0.190	-----	-----	0.190	-----	-----
S-RMSE for head	-----	0.122	-----	0.297	-----	-----	0.846	-----	-----	0.319	-----	-----	0.884	-----	-----
Mean Error for head (m)	-----	0.01	-----	-0.93	-----	-----	-2.89	-----	-----	1.02	-----	-----	3.02	-----	-----

The mean error (ME) for head (observed minus simulated) was added as a new comparison criterion to assess the magnitude of the errors. It can be clearly seen that the simulated heads are very sensitive to the boundary conditions. The MEs demonstrate that the freshwater lens is shifted up or down as a corresponding to the change in specified-head boundary. These analysis illustrate that the original head gradient (i) is a very well representative of the natural gradient across the Rawdatain depression. Indeed, without the natural mild head gradient, the Rawdatain FGL would have not formed.

Table 3.7 shows the simulations of the lens stability under change in the head gradients ($+5\%i$, $+10\%i$, $-5\%i$, and $-10\%i$) and change in both recharge and head gradients ($-10\%R5\&+5\%i$, $-10\%R5\&-5\%i$, $-50\%R5\&+5\%i$, $-50\%R5\&-5\%i$). These simulations start with the same initial conditions that reduction in recharge scenarios started with in section 3.4.2. The results of $-10\%R5$ and $-50\%R5$ scenarios in (Figure 3.10) are represented in (Table 3.7) for comparison purposes. In general, the simulated volumes of stored water are more sensitive to the reduction in recharge than an increase in the head gradients. The 5% increase in the head gradients associated with the $-10\%R5$ scenarios leads to a consistent increase in salinization of 45, 65, and 100% within 100 to 1000-years for the three water quality volume categories, respectively. In contrast, the 5% decrease in the head gradients reduces the salinization by 21, 22, and 42% within 100-years for the three water quality volume categories, respectively. The benefit of the decrease in gradients on the salinization reduction is monotonically decrease as the freshwater lens reaches a new steady state volume condition.

Table 3.7. Sensitivity of the lens stability to boundary conditions

Years	Change in Recharge		Change in Gradient				Change in Both Recharge and Gradient			
	-10% R5	-50% R5	+5%i	+10%i	-5%i	-10%i	-10%R5 & +5%i	-10%R5 & -5%i	-50%R5 & +5%i	-50%R5 & -5%i
<i>Change in Volume of Stored water 700 mg/L (%) (started from initial volume at 2000 years = 36.8 (10⁶ m³))</i>										
2100	-3.4	-21.2	-2.5	-5.4	-1.1	-1.4	-4.9	-2.6	-22.3	-21.3
2500	-13.3	-92.2	-8.8	-15.9	-3.1	-2.6	-18.7	-12.0	-94.1	-92.2
3000	-17.7	-95.3	-10.6	-19.1	-2.6	-1.9	-24.6	-16.1	-96.0	-95.3
<i>Change in Volume of Stored water 1000 mg/L (%) (started from initial volume at 2000 years = 61.0 (10⁶ m³))</i>										
2100	-2.0	-17.0	-1.4	-4.0	-0.2	-0.4	-3.3	-1.6	-18.1	-17.0
2500	-8.1	-73.9	-4.4	-10.4	0.4	0.8	-12.5	-7.2	-80.2	-73.7
3000	-13.4	-90.6	-6.6	-15.6	1.6	2.4	-20.8	-12.3	-92.0	-90.6
<i>Change in Volume of Stored water 2000 mg/L (%) (started from initial volume at 2000 years = 138.7 (10⁶ m³))</i>										
2100	-1.0	-9.1	-0.9	-2.6	0.2	0.6	-1.9	-0.6	-10.0	-8.9
2500	-4.2	-43.7	-3.2	-9.6	0.9	1.5	-8.6	-3.6	-46.0	-43.5
3000	-7.5	-70.2	-5.4	-12.6	2.1	2.8	-15.1	-6.9	-75.8	-70.0

3.5. Discussion

3.5.1 Lens Formation and Stability

Many aspects of the Rawdatain FGL have been documented and well-studied, but we believe that we have developed the first model of its formation and pre-development conditions, along with its macro-scale stability. We have provided a quantitative estimate of annual recharge for the lens (500,000 m³/year) that is consistent with Senay's (1973) conclusion that prior recharge estimates by Bergstrom and Aten (1964) and Kwarteng et al. (2000) were too high. Their estimates were tested in the R9 (1 million m³/year) and R11 (2 million m³/year) recharge scenarios, and it was clear that both overestimated recharge based on comparison with TDS, lens volume, and lens thickness. Studies that used the surface water zone to estimate the potential recharge also overestimated actual recharge (Table 3.1). That said, the prior estimates (Table 3.1) may have been correct for the time scale, spatial scale, and modern precipitation periods on which they were based, but our estimate is a long-term average rate. As such, we suggest that our rate is more appropriate for considering the hydrodynamics of the lens.

Unlike our study, none of these studies estimated the focused recharge under the main depression (playa) and wadis (ephemeral stream). Our study estimates the focused recharge at the center of the Rawdatain depression and playa locations (recharge zones 3 and 4) to be 96 mm/year. This value is similar in magnitude to a recorded recharge of 109 mm in well R-39 at the center of the depression corresponding to a water table rise of 910 mm ($S_y = 0.12$) after a rain storm on December 29, 1976 (Senay, 1977). Similar focused recharge estimates beneath playas in Texas, USA ranged from 60 to 120 mm/year (Scanlon & Goldsmith, 1997). The focused recharge beneath the wadis (zone 5) is 9.4 mm/year, which is similar to estimates of recharge from ephemeral streams at two different locations in Saudi Arabia, ranging from 6.1 to

20 mm (Subyani, 2004&2005). Recharge estimates outside of the playas and wadis (Zones 1, 2, and 6) are between 0.7 and 5.5 mm/year. These recharge values correlate well with recharge estimated for shallow aquifers in the Arabian Peninsula (Bazuhair & Wood, 1996; Al-Senafy et al., 2013).

With an annual recharge rate of 500,000 m³/year, the lens would require over 2000 years to initially form or to naturally reform if depleted. At the same time, this low recharge rate and the slow formation of the lens also means that the lens is relatively stable, in the near term, with respect to changes in natural recharge potentially caused by land-use changes or climate changes. Our simulations indicate that there would be minor changes in the overall lens volume within the timeframe of typical civil planning horizons (e.g., 50 years). These conclusions suggest that the lens could be a reliable emergency water reserve. They further suggest that there would be a need to artificial recharge the lens if continued or increased usage is planned. Finally, these simulations suggest that there is merit in recharging the lens in that the lens appears to be a stable reserve, at least at the macro-scale, assuming artificial recharge and pumping methods were conducted in a manner that would not trigger mixing with the underlying brackish waters.

3.5.2. A Tool for Future Work

Al-Senafy et al. (2013) recommended using a suitable numerical modeling package to study the dynamics of the groundwater flow and solute transport at Rawdatain FGL. They believed that this type of model will provide estimates of the volume and quality of recoverable groundwater based on reserve mining utilization scenarios. Several studies have drawn attention to Aquifer Storage & Recovery (ASR) in Kuwait (Senay, 1977; Mukhopadhyay et al., 1994, 2004; Al-Otaibi & Mukhopadhyay, 2005; Darwish & Al Awadhi, 2009). These studies

highlighted the need for maintaining a large volume of stored groundwater to meet the demand for water under emergency conditions.

With results from this study, we now have a well-founded and calibrated model that can be used to interpret how the intensive pumping of the 1963-1973 period damaged the lens in places and how pumping may be done more carefully in the future. This model can be used to further quantify the current volume of the lens and the portion that may be safely extracted in times of emergency, which in turn can be used to consider the potential to augment the lens via artificial recharge. The use of coupled numerical groundwater flow and transport models for ASR is the best method for assessing the effects of interactions between hydrogeologic and operational parameters on predictions of recovery efficiency (Lowry & Anderson, 2006). Artificial recharge could be conducted using Kuwait's seasonal excess freshwater capacity that comes from seawater desalination or from its highly treated wastewater sources. The use of highly treated wastewater for recharge may also provide a solution to the negative public reception toward immediately and directly using treated wastewaters.

3.6. Summary and Conclusions

Among the fresh groundwater lenses (FGLs) in the Arabian Peninsula, the Rawdatain FGL in Kuwait is an ideal and potentially unique candidate to use for evaluating the formative and potentially changing dynamics of groundwater lenses in arid regions. In this study, numerical modeling of the saturated zone was used to estimate long-term recharge for Rawdatain, including both diffuse recharge within the regional system and focused recharge along wadis. Groundwater age data and multiple calibration targets (groundwater TDS concentration, groundwater head, lens volume, lens thickness) were used to constrain the uncertainty in the applied recharge rate. This method was selected because of the wealth of data

available in the saturated zone and the capability of such models for evaluating conceptual models and model assumptions, assessing the sensitivity of recharge estimates to model parameters, and predicting the effect of future climate and land use changes on recharge rates.

Twelve recharge amount scenarios, encompassing a wide range of long-term average annual recharge values (200,000-5,000,000 m³/year), were tested against the multiple targets and compared with the groundwater age of the Rawdatain lens (500–2043 years). The model calibration suggests that the long-term average annual recharge is approximately 500,000 m³/year. The rates of both diffuse and focused recharge are in agreement with several similar studies. At this recharge rate, the lens formed very slowly and would require over 2000 years to reform if depleted.

The tested model was used to consider the macro-scale stability of the lens (lens volume) under changes in natural recharge potentially caused by land-use changes or climate changes. The simulations suggest that the lens volume would change slowly in the near term (e.g., the first 50 to 100 years) after a change in recharge. Within a 100-year time frame, a 50% reduction in annual recharge would reduce the lens volumes by 21%, 17% and 9% for the 700 mg/L, 1000 mg/L, and 2000 mg/L water quality categories, respectively. This conclusion is understandable given that the lens has a slow rate of formation and a volume that is much larger than the annual recharge volume.

The slow natural changes expected for the lens means it could be a reliable short-term water supply in a time of emergency. This also means that pumping needs to be carefully managed so as to not damage this natural resource. Finally, the simulated stability of the lens suggests that there is merit in considering artificial recharge of the lens to augment its ability to serve as a short-term emergency water supply.

This study successfully establishes a baseline for a focused rainfall recharge FGL in arid regions. The use of a 3D density-dependent groundwater flow model tested against multiple data targets and water age was capable of evaluating conceptual models and model assumptions, assessing the sensitivity of recharge estimates and boundary conditions to model parameters, and predicting the effect of future climate and land use changes on recharge rates. The output of this model provides a reliable assessment and results that enhance the understanding of the formation and stability of these lenses, and thus it will lead to better planning and management for these valuable water reserves in the region.

REFERENCES

- Al-Dousari, A., Milewski, A., Din, S. U., & Ahmed, M. (2010). Remote sensing inputs to SWAT model for groundwater recharge estimates in Kuwait. *Advances in Natural and Applied Sciences*, 4(1), 71-77.
- Al-Katheeri, E. S. (2008). Towards the establishment of water management in Abu Dhabi Emirate. *Water resources management*, 22(2), 205.
- Allan, J. A. (2001). *The Middle East water questions. Hydropolitics and the global economy*. London: I.B. Tauris.
- Almedeij, J. (2012). Modeling rainfall variability over urban areas: a case study for Kuwait. *The Scientific World Journal*, 2012.
- Al-Otaibi, M., & Mukhopadhyay, A. (2005). Options for managing water resources in Kuwait. *Arabian Journal for Science and Engineering*, 30(2C), 55.
- Al-Rashed, M. F., & Sherif, M. M. (2000). Water resources in the GCC countries: an overview. *Water resources management*, 14(1), 59-75.
- Al-Senafy, M., Fadlelmawla, A., Bhandary, H., Al-Khalid, A., Rashid, T., Al-Fahad, K., & Al-Salman, B. (2013). Assessment of Usable Groundwater Reserve in Northern Kuwait. *International Journal of Scientific & Engineering Research*, 4(6), 2427-2436.
- Alsumaiei, A. A., & Bailey, R. T. (2018). Quantifying threats to groundwater resources in the Republic of Maldives Part I: Future rainfall patterns and sea-level rise. *Hydrological Processes*, 32(9), 1137-1153.
- Anderman, E. R., Hill, M. C., & Poeter, E. P. (1996). Two-dimensional advective transport in ground-water flow parameter estimation. *Groundwater*, 34(6), 1001-1009.
- Atkinson, A. P., Cartwright, I., Gilfedder, B. S., Cendón, D. I., Unland, N. P., & Hofmann, H. (2014). Using 14 C and 3 H to understand groundwater flow and recharge in an aquifer window. *Hydrology and Earth System Sciences*, 18(12), 4951-4964.
- Bailey, R. T., Gates, T. K., and Ahmadi, M. (2014). Simulating reactive transport of selenium coupled with nitrogen in a regional-scale irrigated groundwater system. *J.Hydrol.*, 515, 29 – 46.
- Bailey, R. T., Wible, T. C., Arabi, M., Records, R. M., & Ditty, J. (2016). Assessing regional-scale spatio-temporal patterns of groundwater–surface water interactions using a coupled SWAT-MODFLOW model. *Hydrological processes*, 30(23), 4420-4433.

- Barth, G. R., & Hill, M. C. (2005b). Parameter and observation importance in modelling virus transport in saturated porous media—investigations in a homogenous system. *Journal of contaminant hydrology*, 80(3-4), 107-129.
- Barth, G., & Hill, M. C. (2005a). Numerical methods for improving sensitivity analysis and parameter estimation of virus transport simulated using sorptive–reactive processes. *Journal of contaminant hydrology*, 76(3-4), 251-277.
- Bazuhair, A. S., & Wood, W. W. (1996). Chloride mass-balance method for estimating ground water recharge in arid areas: examples from western Saudi Arabia. *Journal of Hydrology*, 186(1-4), 153-159.
- Bergstrom, R. E., & Aten, R. E. (1965). Natural recharge and localization of fresh ground water in Kuwait. *Journal of Hydrology*, 2(3), 213-231.
- Bureau De Recherche Geologiques et Mineres (BRGM). 1977. Al-Hassa development project: groundwater resources study and management program, unpublished report to Ministry of Agriculture and Water, Riyadh, 4 vols.
- Burns, E. R., Morgan, D. S., Rachael, S. P., Rachael, S., & Kahle, S. C. (2011). *Three-Dimensional Model of the geologic framework for the Columbia Plateau regional aquifer system, Idaho, Oregon, and Washington*. U. S. Geological Survey.
- Comte, J. C., Join, J. L., Banton, O., & Nicolini, E. (2014). Modelling the response of fresh groundwater to climate and vegetation changes in coral islands. *Hydrogeology journal*, 22(8), 1905-1920.
- Darwish, M. A., & Al Awadhi, F. M. (2009). The need for integrated water management in Kuwait. *Desalination and Water Treatment*, 11(1-3), 204-214.
- De Vries, J. J., & Simmers, I. (2002). Groundwater recharge: an overview of processes and challenges. *Hydrogeology Journal*, 10(1), 5-17.
- Din, S. U., Al Dousari, A., & Al Ghadban, A. N. (2007). Sustainable fresh water resources management in Northern Kuwait—a remote sensing view from Raudatain basin. *International journal of applied earth observation and geoinformation*, 9(1), 21-31.
- Ebrahim, M., Siwek, Z., & Al-Ruwaih, F. (1993). Study of groundwater quality variation at selected sites in Kuwait. *Kuwait Institute for Scientific Research, Final Report No. KISR.4187, Kuwait*.
- Fadlelmawla, A., Hadi, K., Zouari, K., & Kulkarni, K. M. (2008). Hydrogeochemical investigations of recharge and subsequent salinization processes at Al-Raudhatain depression in Kuwait. *Hydrological sciences journal*, 53(1), 204-223.
- FAO. 1979. Survey and evaluation of available data on shared water resources in the Gulf States and Arabian Peninsula, Three Volumes, FAO, Rome.

- Feehley, C. E., Zheng, C., & Molz, F. J. (2000). A dual-domain mass transfer approach for modeling solute transport in heterogeneous aquifers: Application to the Macrodispersion Experiment (MADE) site. *Water Resources Research*, 36(9), 2501-2515.
- Garabedian, S. P., LeBlanc, D. R., Gelhar, L. W., & Celia, M. A. (1991). Large-scale natural gradient tracer test in sand and gravel, Cape Cod, Massachusetts: 2. Analysis of spatial moments for a nonreactive tracer. *Water Resources Research*, 27(5), 911-924.
- Gee, G. W., & Hillel, D. (1988). Groundwater recharge in arid regions: review and critique of estimation methods. *Hydrological Processes*, 2(3), 255-266.
- Gelhar, L. W., Welty, C., & Rehfeldt, K. R. (1992). A critical review of data on field-scale dispersion in aquifers. *Water resources research*, 28(7), 1955-1974.
- Goswami, R. R., & Clement, T. P. (2007). Laboratory-scale investigation of saltwater intrusion dynamics. *Water Resources Research*, 43(4).
- Grealish, G., Omar, S., & Quinn, M. (1998). Affected area soil survey—assessing damage magnitude and recovery of the terrestrial eco-system—follow-up of natural and induced desert recovery. *Kuwait Institute for Scientific Research, Report No. KISR.FA015C, Kuwait*.
- Gulf Cooperation Council, GCC (2015). Development of United Water Sector Strategy and Implementation Plan for the Gulf Cooperation Council of Arab member States for the Year 2015-2035.
- Healy, R. W. (2010). *Estimating groundwater recharge*. Cambridge University Press.
- Hill, M. C., & Tiedeman, C. R. (2006). *Effective groundwater model calibration: with analysis of data, sensitivities, predictions, and uncertainty*. John Wiley & Sons.
- Holding, S., & Allen, D. M. (2015). From days to decades: numerical modelling of freshwater lens response to climate change stressors on small low-lying islands. *Hydrology and Earth System Sciences*, 19(2), 933-949.
- Huang, T., Pang, Z., Liu, J., Yin, L., & Edmunds, W. M. (2017). Groundwater recharge in an arid grassland as indicated by soil chloride profile and multiple tracers. *Hydrological processes*, 31(5), 1047-1057.
- Italconsult. (1969). Water and Agricultural Development Studies for Area IV. Eastern Province. Saudi Arabia: Riyadh, Saudi Arabia: Unpublished report to Ministry of Agriculture and Water.
- Jeong, J., & Park, E. (2017). A shallow water table fluctuation model in response to precipitation with consideration of unsaturated gravitational flow. *Water Resources Research*, 53(4), 3505-3512.

- Julian, H. E., Boggs, J. M., Zheng, C., & Feehley, C. E. (2001). Numerical simulation of a natural gradient tracer experiment for the natural attenuation study: Flow and physical transport. *Groundwater*, 39(4), 534-545.
- Kahle, S. C., Morgan, D. S., Welch, W. B., Ely, S. R., Vaccaro, J. J., & Orzol, L. L. (2011). *Hydrogeologic framework and hydrologic budget components of the Columbia Plateau Regional Aquifer System, Washington, Oregon, and Idaho*. U. S. Geological Survey.
- Kim, K., Anderson, M. P., & Bowser, C. J. (1999). Model calibration with multiple targets: A case study. *Groundwater*, 37(3), 345-351.
- Kim, N. W., Chung, I. M., Won, Y. S., & Arnold, J. G. (2008). Development and application of the integrated SWAT–MODFLOW model. *Journal of Hydrology*, 356(1-2), 1-16.
- KISR (2012) Assessment of usable groundwater reserve in Northern Kuwait. WM027C. Hydrology Department Water Resources Division, Kuwait Institute for Scientific Research.
- Kwarteng, A. Y., Viswanathan, M. N., Al-Senafy, M. N., & Rashid, T. (2000). Formation of fresh ground-water lenses in northern Kuwait. *Journal of arid environments*, 46(2), 137-155.
- Laattoe, T., Werner, A. D., Woods, J. A., & Cartwright, I. (2017). Terrestrial freshwater lenses: Unexplored subterranean oases. *Journal of hydrology*, 553, 501-507.
- Langevin, C., Thorne, D. J., Dausman, A., Sukop, M., & Guo, W. (2007). *User's Guide to SEAWAT: A Computer Program for Simulation of Three-Dimensional Variable-Density Ground-Water Flow*. United States Geological Survey.
- Le Grand ADSCO Ltd., Messrs, J.D., & Watson, D.M. 1959. A Survey of the Freshwater Resources of the Northern Qatar.
- LeBlanc, D. R., Garabedian, S. P., Hess, K. M., Gelhar, L. W., Quadri, R. D., Stollenwerk, K. G., & Wood, W. W. (1991). Large-scale natural gradient tracer test in sand and gravel, Cape Cod, Massachusetts: 1. Experimental design and observed tracer movement. *Water Resources Research*, 27(5), 895-910.
- Lerner, D. N., Issar, A. S., & Simmers, I. (1990). *Groundwater recharge: a guide to understanding and estimating natural recharge* (Vol. 8, pp. 99-228). Hannover: Heise.
- Li, Z., Chen, X., Liu, W., & Si, B. (2017). Determination of groundwater recharge mechanism in the deep loessial unsaturated zone by environmental tracers. *Science of the Total Environment*, 586, 827-835.
- Liu, Y., Yamanaka, T., Zhou, X., Tian, F., & Ma, W. (2014). Combined use of tracer approach and numerical simulation to estimate groundwater recharge in an alluvial aquifer system: A case study of Nasunogahara area, central Japan. *Journal of hydrology*, 519, 833-847.

- Lloyd, J. W. (1986). A review of aridity and groundwater. *Hydrological processes*, 1(1), 63-78.
- Lowry, C. S., & Anderson, M. P. (2006). An assessment of aquifer storage recovery using ground water flow models. *Groundwater*, 44(5), 661-667.
- Macumber, P. G. (2003). Lenses, plumes and wedges in the Sultanate of Oman: a challenge for groundwater management. In *Developments in Water Science* (Vol. 50, pp. 349-370). Elsevier.
- Macumber, P. G., Al Abri, R., & Al Akhzami, S. (1998). Hydrochemical facies in the groundwater of central and southern Oman. In *Quaternary Deserts and Climatic Change* (pp. 511-520). Balkema Rottendam.
- Macumber, P. G., Barghash, B. G. S., Kew, G. A., & Tennakoon, T. B. (1995). Hydrogeologic implications of a cyclonic rainfall event in central Oman. *Groundwater quality. Chapman and Hall, London*, 87-97.
- Mancosu, N., Snyder, R., Kyriakakis, G., & Spano, D. (2015). Water scarcity and future challenges for food production. *Water*, 7(3), 975-992.
- McCallum, J. L., Cook, P. G., Dogramaci, S., Purtschert, R., Simmons, C. T., & Burk, L. (2017). Identifying modern and historic recharge events from tracer-derived groundwater age distributions. *Water Resources Research*, 53(2), 1039-1056.
- McDonald, M. G., & Harbaugh, A. W. (1988). *A modular three-dimensional finite-difference ground-water flow model* (Vol. 6, p. A1). Reston, VA: US Geological Survey.
- MEW. 2015. Electricity and Water Statistical Year Book. Ministry of Electricity and Water, Kuwait.
- Milewski, A., Sultan, M., Al-Dousari, A., & Yan, E. (2014). Geologic and hydrologic settings for development of freshwater lenses in arid lands. *Hydrological processes*, 28(7), 3185-3194.
- Mukhopadhyay, A., Akber, A., Rashed, T., Kotwicki, V., Uddin, S., & Bushehri, A. (2016). Establishing a baseline to evaluate future impacts to groundwater resources in North Kuwait. *Environmental Earth Sciences*, 75(4), 324.
- Mukhopadhyay, A., Al-Awadi, E., Oskui, R., Hadi, K., Al-Ruwaih, F., Turner, M., & Akber, A. (2004). Laboratory investigations of compatibility of the Kuwait Group aquifer, Kuwait, with possible injection waters. *Journal of hydrology*, 285(1-4), 158-176.
- Mukhopadhyay, A., Al-Sulaimi, J., & Barrat, J. M. (1994). Numerical Modeling of Ground-Water Resource Management Options in Kuwait. *Groundwater*, 32(6), 917-928.
- Parsons Corporation. 1964. Groundwater Resources of Kuwait, vols I, II and III. Ministry of Electricity and Water, Kuwait.

- Qahman, K., & Larabi, A. (2006). Evaluation and numerical modeling of seawater intrusion in the Gaza aquifer (Palestine). *Hydrogeology Journal*, 14(5), 713-728.
- Raiber, M., Webb, J. A., Cendón, D. I., White, P. A., & Jacobsen, G. E. (2015). Environmental isotopes meet 3D geological modelling: conceptualising recharge and structurally-controlled aquifer connectivity in the basalt plains of south-western Victoria, Australia. *Journal of Hydrology*, 527, 262-280.
- Rizk, Z. S., & Alsharhan, A. S. (2003). Water resources in the United Arab Emirates. In *Developments in Water Science* (Vol. 50, pp. 245-264). Elsevier.
- Robinson, B. W., & Al Ruwaih, F. (1985). The stable-isotopic composition of water and sulfate from the raudhatain and Umm Al Aish freshwater fields, Kuwait. *Chemical Geology: Isotope Geoscience section*, 58(1-2), 129-136.
- Rushton. K. (1997). Recharge from permanent water bodies. In: Simmers I (ed) Recharge of phreatic aquifers in (semi)arid areas. AA Balkema, Rotterdam, pp 215–255.
- Saiers, J. E., Genereux, D. P., & Bolster, C. H. (2004). Influence of calibration methodology on ground water flow predictions. *Groundwater*, 42(1), 32-44.
- Sanford, W. (2002). Recharge and groundwater models: an overview. *Hydrogeology journal*, 10(1), 110-120.
- Scanlon, B. R., & Goldsmith, R. S. (1997). Field study of spatial variability in unsaturated flow beneath and adjacent to playas. *Water Resources Research*, 33(10), 2239-2252.
- Scanlon, B. R., Healy, R. W., & Cook, P. G. (2002). Choosing appropriate techniques for quantifying groundwater recharge. *Hydrogeology journal*, 10(1), 18-39.
- Schulze-Makuch, D. (2005). Longitudinal dispersivity data and implications for scaling behavior. *Groundwater*, 43(3), 443-456.
- Senay, Y. (1973). Geohydrology of Al-Rawdhatain Field. *Report to the Ministry of Electricity and Water, Kuwait*, 24-43.
- Senay, Y. (1977). Groundwater resources and artificial recharge in Rawdhatain water field. *Ministry of Electricity and Water, Kuwait*, 35.
- Senay, Y. (1989). Artificial recharge and reproduction of fresh water at Rawdhatain for emergency use. *Report to the Ministry of Electricity and Water, Kuwait*.
- Shiklomanov, I. A. (1990). Global water resources. *Nature and resources*, 26(3), 34-43.
- Shiklomanov, I. A. (1998). *World water resources: a new appraisal and assessment for the 21st century: a summary of the monograph World water resources*. UNESCO.

Simmers, I. (ed) (1997). Recharge of phreatic aquifers in (semi-)arid areas. AA Balkema, Rotterdam, 277 pp.

Simmons, C. T. (2005). Variable density groundwater flow: From current challenges to future possibilities. *Hydrogeology Journal*, 13(1), 116-119.

SMEC (Snowy Mountains Engineering Corporation). (2002). Characteristics of groundwater quality in Kuwait before August 1990. Report No. 4, GD1.1.

Subyani, A. M. (2004). Use of chloride-mass balance and environmental isotopes for evaluation of groundwater recharge in the alluvial aquifer, Wadi Tharad, western Saudi Arabia. *Environmental Geology*, 46(6-7), 741-749.

Subyani, A. M. (2005). Hydrochemical identification and salinity problem of ground-water in Wadi Yalamlam basin, Western Saudi Arabia. *Journal of Arid Environments*, 60(1), 53-66.

UAR (United Arabic Republic) Experts. 1964. Ministry of Electricity and Water, Kuwait.

Viswanathan, M. N., Al-Senafy, M. N., Mukhopadhyay, A., Kodittuwakku, K. A. W., & Al-Fahad, K. (1997). Assessment of the long-term pollution potential of the groundwater of Raudhatain and Umm Al-Aish Area. *Kuwait Institute for Scientific Research, Report No. KISR.5006, Kuwait.*

Wallace, C. D., & Bailey, R. T. (2017). Geohydrologic factors governing atoll island groundwater resources. *Journal of Hydrologic Engineering*, 22(6), 05017004.

Wang, B., Jin, M., Nimmo, J. R., Yang, L., & Wang, W. (2008). Estimating groundwater recharge in Hebei Plain, China under varying land use practices using tritium and bromide tracers. *Journal of Hydrology*, 356(1-2), 209-222.

World Bank. 2007. Making the Most of Scarcity: Accountability for Better Water Management Results in the Middle East and North Africa. MENA Development Report. Washington, DC. © World Bank. <https://openknowledge.worldbank.org/handle/10986/6845> License: CC BY 3.0 IGO.

Yihdego, Y., & Al-Weshah, R. A. (2017). Engineering and environmental remediation scenarios due to leakage from the Gulf War oil spill using 3-D numerical contaminant modellings. *Applied Water Science*, 7(7), 3707-3718.

Zheng, C., & Wang, P. P. (1999). *MT3DMS: a modular three-dimensional multispecies transport model for simulation of advection, dispersion, and chemical reactions of contaminants in groundwater systems; documentation and user's guide*. Alabama Univ University.

CHAPTER 4. DETERMINING VALUES OF LARGE-SCALE DISPERSIVITY FOR A FRESH GROUNDWATER LENS IN AN ARID REGION

Highlights

The phenomenon of fresh groundwater lenses (FGLs) overlying saline or brackish groundwater in subterranean oases in the Arabian Peninsula (AP) provides a potential source of fresh water in an extremely arid region. These FGLs in the AP are proposed as suitable locations for aquifer storage and recovery to serve as long-term storage for emergency uses. Because of this, it is important to simulate mixing between fresh water and seawater or brackish water, which requires characterization of the large-scale dispersivity of the FGL. In this study, a 3D density-dependent groundwater flow and solute transport model is tested against several data targets to estimate the dispersivity values, including groundwater head, spatially-variable total dissolved solids (TDS) concentration in groundwater, three lens volume targets, three lens thickness targets, and geometrical shape features of the lens along a cross-section. A total of 28 different sets of 3D dispersivity values, encompassing a wide range of feasible longitudinal dispersivity values for the Rawdatain FGL (1–500 m), were tested against the multiple targets and compared with the groundwater age of the Rawdatain FGL in Kuwait. The power of the multi-calibration targets approach aids in eliminating several non-unique calibration parameters and in decreasing the uncertainty of the calibrated parameters. Based on a multi-criteria score-based method, the D16 dispersivity set ranked best in performance among all of the targets, with the longitudinal, horizontal transverse, and vertical transverse dispersivity values estimated to be 50 m, 5 m and 0.1 m, respectively. A sensitivity analysis found that vertical transverse dispersivity values of greater than one meter prevent the formation of the Rawdatain FGL. The

methodology presented herein shows that it is feasible to estimate large-scale environmental dispersivity, and it can be applied to other FGLs to overcome the limitations and cons of in-situ large-scale dispersivity measurement.

4.1. Introduction

The formation of fresh groundwater lenses (FGLs) floating above denser, saline or brackish groundwater is a fascinating hydrologic phenomenon that creates groundwater supplies of great potential value for humans and ecosystems in several formation settings, such as coastal areas, atoll islands, riverine floodplains, and subterranean oases in arid regions. FGLs are in danger of salinization due to natural events (e.g., seawater intrusion due to sea level rise (Werner & Simmons, 2009), groundwater inundation (Rotzoll & Fletcher 2013), and tsunami events (Illangasekare et al., 2006) in coastal areas, drought conditions due to El Niño events (Bailey et al., 2009; Barkey and Bailey, 2017), and storm-induced overwash events (Chui & Terry, 2012; Bailey & Jenson, 2014) on atoll islands), or anthropogenic activities (e.g., losing river conditions induced by pumping (Berens et al., 2009) in riverine floodplains, and upconing of brackish water due to pumping (Kwarteng et al., 2000) in subterranean oases in arid regions).

Among the different formation settings of FGLs, the FGLs in subterranean oases in the Arabian Peninsula (AP) are a crucial source of fresh water for local populations. Freshwater supplies are extremely scarce across the AP, as there are no perennial rivers or lakes, and the climate and landforms make it difficult to harvest and store precipitation (Alrashid and Sherif 2000). Desalination becomes the most feasible alternative for meeting the current and future water supply requirements, although vulnerable to power interruptions and various other risks. More than 65% of the world's desalination capacity was concentrated in the Gulf Cooperation Council (GCC) in 2003 (Dawoud, 2005). Abdulrazzah (1995) reported an imbalance between the

available water resources and demand in the region as a result of rapid economic development. The lack of water availability in the AP has been shown to be an obstacle to sustainable development (Shiklomanov, 1990&1998), and drinking water security is a major concern in populated areas. Climate change is expected to result in an increase in the severity and frequency of droughts in the region (Döll et al., 2015; Feitelson & Tubi, 2017). In consequence, water wars and disputes are likely to be triggered between neighboring countries and to threaten political stability in the Middle East in future decades (Gleick, 1994; Amery, 2002&2015).

The functional significance of the FGLs has also been reported worldwide, such as in Israel (Vengosh & Rosenthal, 1994), Argentina (Jayawickreme et al., 2011), Australia (Jolly et al., 1993&1998; Cendón et al., 2010), Paraguay (Houben et al., 2014), Pakistan (Asghar et al., 2002), Botswana (Bauer et al., 2006&2008), the USA (Panday et al., 1993; James et al., 1996), and atoll islands (Bailey et al., 2009; Terry and Chui, 2012; Werner et al., 2017). Understanding the formation and hydrogeology of FGLs in arid and semi-arid climates has long been of scientific interest in the AP (e.g., Kwarteng et al., 2000; Macumber, 1995; Senay, 1973&1977; Omar et al., 1981; Young et al., 2004; and others), as well as globally (e.g., Cendón et al., 2010; Werner & Laattoe, 2016; Laattoe et al., 2017; Stofberg et al., 2017; Cartwright et al., 2019).

Methods for investigating FGLs have ranged from field data surveys, analytical solutions, and simple empirical relationships to three-dimensional density-dependent models (Holding & Allen, 2015; Werner et al., 2017; Wallace and Bailey, 2017). Field data surveys include direct sampling approaches (e.g., Bergstrom and Aten, 1964; Terry and Falkland, 2010), as well as indirect measurement techniques such as geophysical surveys (e.g., Stewart, 1988; Anthony, 1992) and remote sensing (e.g., Din et al., 2007; Milewski et al., 2014). Although the indirect techniques tend to be less expensive than the direct sampling methods, their results are non-

unique (i.e., the same set of observation can be explained by more than one model) (Falkland, 1993). However, field data have been used as a foundation for empirical, analytical and numerical models used to understand the formation and hydrogeology of FGLs. Although the empirical approaches bypass the need for large amounts of data and provide rough estimates of recharge in the FGLs (Oberdorfer and Buddemeier, 1988), Woodroffe and Falkland (2004) and Bailey et al. (2008&2010) discussed significant limitations of the empirical models because of their simplification of aquifer properties and recharge mechanisms. In particular, the analytical solutions used for FGLs rely on various assumptions that are inherent in the Ghyben-Herzberg approximation. They only consider simplified, steady-state conditions, and they exclude aquifer heterogeneity, as well as dispersive and transient effects, which results in the overestimation of FGL resources (Oberdorfer et al., 1990; Bailey et al., 2010).

Numerical solutions have been widely applied because they overcome the limitations of the analytical and empirical solutions, as they allow for transient density-dependent flow and transport involving dispersivity and aquifer heterogeneity. Examples of using numerical models for specific investigations include assessing the effect of change of river stage on the FGLs under riverine floodplains (Alaghmand et al., 2014), the effect of climate change (Alam and Falkland, 1997) and overwash (e.g., Bailey & Jenson, 2014) on FGLs in atoll islands, the impact of sea-level rise on FGLs in coastal areas (Masterson & Garabedian, 2007), and the effect of reduction of natural recharge (Alrashidi & Bailey, 2019a) on FGLs in subterranean oases in an arid region.

Numerical modeling of FGLs relies on several aspects, such as boundary conditions (e.g., flow fluxes and salt concentration), geometry (e.g., grid discretization), and aquifer properties (such as hydraulic conductivity, dispersivity, and porosity) (Eeman et al., 2011). The effects of

boundary conditions can be illustrated by numerical modelling of the effects of tidal activity on seawater intrusion in an unconfined aquifer by Ataie-Ashtiani et al. (1999), who found that the tidal fluctuations resulted in a thicker interface than would occur in the absence of tidal effects. Similar findings were reported for the FGLs in atoll islands, such as in a comparison of tidal and nontidal models in terms of the dynamics of FGLs (Underwood et al., 1992) and sea level rise (Alsumaiei & Bailey, 2018). On the other hand, a modelling effort by Karasaki et al. (2006) failed to predict a wide mixing zone when imposing a tidal boundary condition unless a large dispersion coefficient was used. To successfully simulate the FGLs, an appropriate grid discretization should be implemented based on the grid Peclet number (Pe) (Voss and Souza, 1987). Voss (1984) and Zhang et al. (2004) discussed choosing the appropriate transport solution techniques based on Pe to solve the advection-dispersion equation. Although heterogeneity in hydraulic conductivity contributes to mixing, Abarca et al. (2006) showed that moderate heterogeneity has relatively little effect on the width of the mixing zone.

Although many of these factors can be measured or assessed, dispersivity is particularly difficult to quantify (Eeman et al., 2011). The issue of how to characterize large-scale dispersivity in aquifers remains an open question in the literature (Garabedian et al., 1991; LeBlanc et al., 1991; Gelhar et al., 1992; Schulze-Makuch, 2005). It has been found through both theoretical and experimental studies that field-scale dispersivities are up to several orders of magnitude greater than lab-scale dispersivities for the same material. Most investigators agree that this difference in dispersivity is due to natural heterogeneities at the field scale, which produce irregular flow patterns (Gelhar et al., 1992). This leads to the problem in parameter estimation known as “scale-up”, meaning that quantities measured at the laboratory scale cannot be extrapolated to the field scale. This is because parameters such as diffusion, porosity, and

permeability used for field-scale simulations are not simple volume averages of the same quantities at smaller spatial scales. Thus, such simple scaling approaches are precluded by the nonlinearity of the relationships involved (Glimm et al., 1993). As a consequence, laboratory dispersivity measurements cannot be used to predict field-scale dispersivity, and investigation of field-scale transport must be performed at the field scale.

Many theoretical and experimental investigations of dispersion in aquifers have indicated that solute longitudinal dispersivities are scale-dependent, meaning that solute dispersion is dependent on the distance traveled by the particle (Gelher et al., 1992; Xu & Eckstein, 1995; Hunt & Skinner, 2010; Hunt et al., 2015). Hence, some empirical equations can be found in the literature relating longitudinal dispersivity to field transport distance (Arya et al., 1988; Neuman, 1990; Schulze-Makuch, 2005). However, scaling laws of this type are inconsistent with the findings of Zech et al. (2015), who analyzed field data from more than 70 field experiments and found that an increase in dispersivity with scale is not supported by the available data.

Characterization of the dispersivity at a particular field site is essential to any effort to simulate mixing between fresh water and seawater or brackish water, and it provides a reliable assessment and leads to better planning and management of FGLs. Underwood et al. (1992) found that an increased longitudinal dispersivity resulted in increased mixing and a decrease in the lateral extent of the numerically predicted FGL, or even prevented the FGL from forming. As another example, field observations from Enjebi Island (Marshall Islands) indicated that the mixing zone is so broad that the usable freshwater in the lens is negligible (Buddemeier and Oberdorfer, 2004). Eeman et al. (2011) examined several parameters (including longitudinal and transverse dispersivities) that dominate the mixing processes for physically feasible ranges of parameters by using dimensionless groups and scaled sensitivities. They found that the early

stages of lens formation are dominated by longitudinal dispersion, whereas diffusion and transversal dispersion dominate under steady state conditions.

4.2. Research Objective

The Rawdatain basin in Kuwait is a notable example of a FGL in the AP due to its size and because of the extensive subsurface data set (Parsons Corporation, 1964) collected before significant groundwater extraction began. The quality of this data set makes Rawdatain ideal for investigating the formation and dynamics of FGLs in arid regions. The Rawdatain basin, as well as other lenses in the AP, were proposed as suitable locations for aquifer storage and recovery (ASR) to serve as long-term storage for emergency uses (Senay, 1989; Rizk & Alsharhan, 2003; Al-Katheeri, 2008). Therefore, reliable dispersivity values are required to successfully assess the recovery efficiency (Lowry & Anderson, 2006; Ward et al., 2009).

There is no well-defined large-scale environmental dispersivity estimate for the Rawdatain basin because there are multiple recharge zones. Estimating or using a value of dispersivity for the basin was an open question and uncertain in several studies (Mukhopadhyay et al., 1994; Yihdego & Al-Weshah, 2017). Gelhar et al. (1992) found that there are no reliable three dimensional dispersivity values at scales greater than 300 m. Beyond that scale, almost all dispersivity estimates are from contaminant transport and environmental tracer studies. In such studies, solute input is typically poorly defined, and controlled input tracer experiments have not been conducted at larger scales because of the very long time periods required. Gelhar and coauthors (1992) suggested that values of dispersivity for uncontrolled environmental events (such as seawater intrusion) are commonly determined by fitting a solute transport model to historical data.

Because dispersivity is an important factor in variable density groundwater flow (Simmons, 2005), assessments of 3D large-scale environmental dispersivity are discussed in this paper. The objective of this study is to provide a realistic range of longitudinal (α_L), horizontal transverse (α_h), and vertical transverse (α_v) dispersivity values for the Rawdatain FGL, with a general methodology that can be used for other FGLs. The dispersivity estimates are based on multi-target calibration of a 3D density-dependent groundwater flow and solute transport model using the following pre-development period calibration targets: (1) groundwater head, (2) spatially-variable total dissolved solids (TDS) groundwater concentration, (3-5) three groundwater volume targets, and (6-8) three vertical thickness targets of stored groundwater of three different water quality TDS ranges (0–700, 700–1000, and 1000–2000 mg/L). Then, a multi-criteria score-based method with an equal weight for all the targets was applied to rank the best performance of the dispersivity sets. In addition to the eight quantitative targets, the overall lens shape and thickness were compared qualitatively with geometrical shape features of the lens along cross-sections.

4.3. Background

4.3.1. Study Area

The AP is located in southwest Asia, within one of the great desert belts of the world, as shown in Figure 4.1. The aridity index for the AP is classified as hyper-arid to arid according to the global distribution of climatic zones (UNESCO, 1979). The majority of the AP is characterized by high average temperature, erratic sparse rainfall, and high evapotranspiration rates (Alrashed & Sherif, 2000). In the central part of the AP, shade temperatures frequently exceed 48°C during the summer months. The annual average precipitation received by the region is very low, typically less than 150 mm/year and ranging from as low as 50 mm in the northern

and central parts to as high as 300 mm/year in the south (Alsharhan et al., 2001). The annual potential evaporation ranges from 2500 mm/year in the coastal areas to approximately 4500 mm in the central areas (Alsharhan et al., 2001).

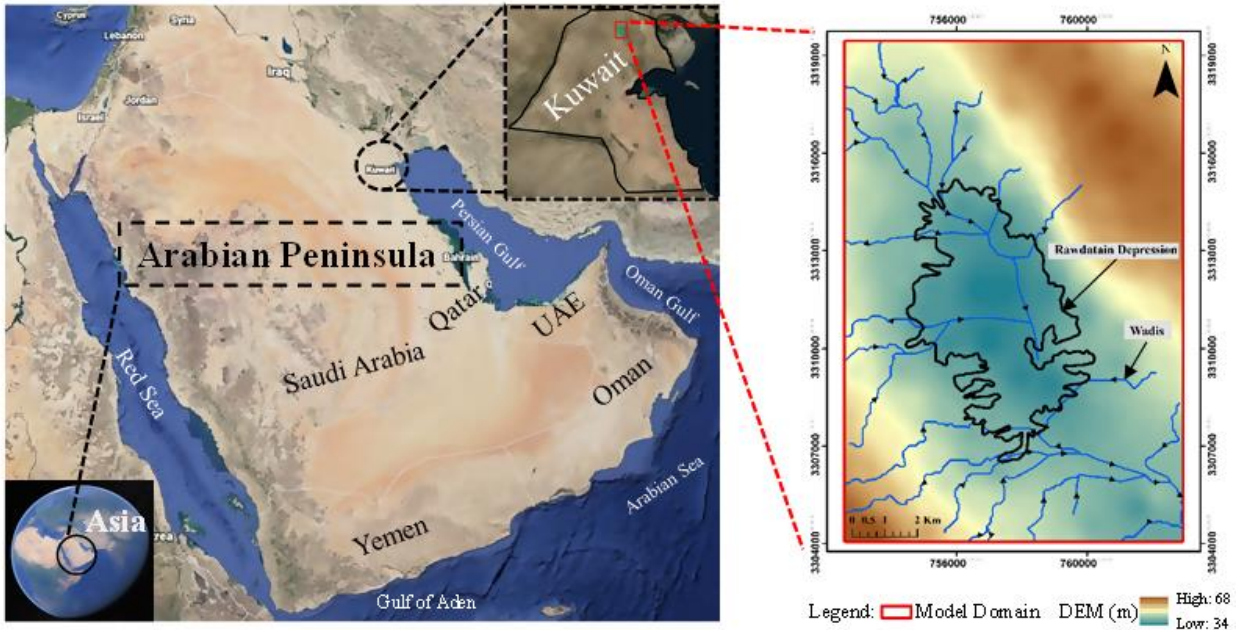


Figure 4.1. The Arabian Peninsula (left) and the model domain at the Rawdatain Basin in Kuwait (right)

Because of the arid climate, groundwater is the main source of freshwater supply in the AP. FAO (1979) classified the regional groundwater in the AP into two main aquifer systems: Systems A and B. System A represents the deep, non-renewable (fossil) groundwater aquifers, and System B represents the shallow, renewable groundwater aquifers. Authman (1983), BAAC (1980) and MAW (1984) subdivided the deep aquifers into more than 20 principal and secondary aquifers based on various parameters such as specific yield, aquifer thickness, areal extent, and the volume and quality of stored water. The groundwater reserves in the deep aquifers are estimated at 2330 billion cubic meters (BCM), with a wide range of total dissolved solids. The total annual recharge of these aquifers is approximately 0.1% of the total reserved volume, or 2692 million cubic meters per year (Abdulrazzah, 1994&1995). Significant withdrawals have

been reported from these aquifers (FAO, 1998). As a result, the water levels have declined dramatically (MAW, 1982 & 1984) and salinity increases have been noted (Fadlelmawla & Al-Otaibi, 2005; Zubari, 1999). All of the deep aquifers extend into two or more countries within the AP or even outside of the AP. This situation has led to conflicts over transboundary aquifers in the region (Puri & Aureli, 2005; Fallatah et al., 2017; Lee et al., 2018).

In contrast, System B represents discontinuous FGLs occurring over deeper brackish groundwater. These FGLs extend over the eastern part of the AP. Because recharge to these lenses depends on surface runoff from rainfall events that may vary considerably from year to year in timing and magnitude, these lenses have relatively small longevities and likelihood of formation (FAO, 1979). As of the mid-1950s, several studies have discussed the existence of these freshwater lenses, which are flooded and surrounded by brackish or saline water. Examples of the studies include Italconsult (1969) and BRGM (1977) in Saudi Arabia, Le Grand ADSCO et al. (1959) and FAO (1979) in Qatar, Rizk & Alsharhan (2003) and Al-Katheeri (2008) in United Arab Emirates (UAE), Macumber et al. (1995; 1998; 2003) and Young et al. (2004) in Oman, and Parsons Corporation (1964), Kwarteng et al. (2000), and Milewski et al. (2014) in Kuwait. Unlike the System A aquifers, the System B aquifers have small areal extents. As a result, the potential for transboundary conflicts is negligible because each known lens falls within the boundary of one political unit.

Several studies have discussed the practical importance of water production from the FGLs and their best potential use in the AP. FGLs have been exploited for domestic and municipal uses by Dhahran and Al-Khober cities and agricultural activities in the Eastern Province in SA (Abderrahman et al., 1995). The freshwater lenses have been used as potable water supplies in the Al-Wusta Region of Central Oman (Macumber et al., 1995) and as an

irrigation water source for several small farms near the Al-Ma'abar depression (Macumber, 1995). In the Liwa area in the UAE, freshwater lenses were also documented and proposed as appropriate locations for artificial aquifer storage and recovery (Rizk & Alsharhan, 2003; Al-Katheeri, 2008). The freshwater lenses in the Rawdatain and Umm Al-Aish depressions represent the only natural freshwater source in Kuwait (Kwarteng et al., 2000). Senay (1989) highlighted the need for considering artificial recharge for the freshwater lenses in Kuwait to meet the demand for water under emergency conditions. These lenses were pumped extensively for water supply during 1962–1974 (Kwarteng et al., 2000), and afterwards the production decreased due to an increase in salinity (Al-Ruwaih et al., 2000). Currently, the Rawdatain freshwater lens is used for commercial bottling of drinking water (Din et al., 2007), while the entire field is acting as a strategic reserve for use during an emergency (Mukhopadhyay et al., 2016).

4.3.2. Previous Studies

4.3.2.1. Dispersivity Data from Field Studies

Investigation of dispersivity values from field data was an interest as early as studies conducted by Arya et al. (1988), Neuman (1990), and Gelhar et al. (1992). Recently, Schulze-Makuch (2005) and Zech et al. (2015) reanalyzed the data provided by Gelhar et al. (1992) and added more recent field studies since then. They analyzed only the longitudinal dispersivity, unlike Gelhar et al. (1992) who documented more information for the transverse horizontal and vertical dispersivities, which makes the Gelhar et al. (1992) study more beneficial for constructing 3D flow-transport models. Because of that, we will focus on the studies from Gelhar et al. (1992), which have more than 1800 citations in the literature.

Gelhar et al (1992) conducted an extensive literature review for 74 publications that reported the dispersivity values from 59 fields in a tabular summary and included several figures for the scales of observations with the longitudinal, horizontal transverse, and vertical dispersivities (106, 24, and 10 values, respectively) . In their study, the dispersivity values were calculated or inferred from large-scale, uncontrolled subsurface solute transport events (with environmental or contamination tracers) or controlled tracer tests. The environmental tracers represent the natural, uncontrolled and unknown input history events over hundreds of meters (regional scales), such as tritium in groundwater from recharge, seawater intrusion, and mineral dissolution. The contamination tracers characterize human-induced and uncontrolled events, including leaks, spills, and infiltration from landfills, storage tanks, and infiltration basins into the groundwater. Pulse (instantaneous) or step (continuous) tracers represent the controlled events where the quantity and duration of solute input are known. They have also classified the dispersivity data based on their criteria of evaluating the data quality into three reliability classes: low, moderate and high. The details of the reliability criteria will not be restated here and can be found in the original study.

From a critical review of data on field-scale dispersion in aquifers, Gelhar et al. (1992) suggested that the longitudinal dispersivity values in fields generally range from the pore scale of 0.01 m to large scales of 10 km at observations scales of 0.75 m to 100 km, with no high-reliability points at scales greater than 300 m. The methods of data interpretation applied to determine the dispersivity values commonly include breakthrough curve analysis or the method of spatial moments for flow tests and numerical methods for contamination events. Based on the Gelhar classification for dispersivities, the dispersivity for the FGLs is considered as an environmental type. For the interests of our study, only eight environmental dispersivity values

were reported from simulation studies in Table (4.1A), showing that the range of the longitudinal dispersivity values is from 6.7 m to 40 km at observation scales of 100 m to 100 km. Only two of these values are classified as high-reliability data, corresponding to two data sets from Hoehn and Santschi (1987). Ten transverse vertical dispersivity values were reported from both simulations and experimental studies in Table (4.1B), showing that the range is between a few millimeters and 0.67 m. Unlike the longitudinal and transverse horizontal dispersivities, Gelhar et al. (1992) concluded that the transverse vertical dispersivity data do not indicate any noteworthy trend with the scale of the observations.

Table 4.1.A. Environmental longitudinal dispersivity data from field studies (Gelher et al., 1992)

Reference	Site Name (Country)	Aquifer Material/Aquifer Name	Tracer (Type)	Method of Data Interpretation (Model Name)	Scale of Observation (m)	Dispersivity $\alpha_L/\alpha_h/\alpha_v$ (m)	Study/Duration/ Hydraulic Conductivity (K) or Transmissivity(T)
Rabinowitz and Gross (1972)	Roswell Basin, New Mexico (USA)	fractured limestone	^3H (environmental)	One-dimensional uniform flow solution	32,000	20-23	Simulation/ -----/ T= 864 - 25060 m ² /d
Gupta et al (1975)	Sutter Basin, California (USA)	sandstone, shale, sand, and alluvial sediments	Cl^- (environmental)	three-dimensional numerical model	50,000	80-200/8-20	Simulation/ -----/ -----
Segol and Pinder (1976)	Cutler area, Florida (USA)	fractured limestone and calcareous sandstone/ Biscayne Bay	Cl^- (environmental)	two-dimensional numerical model	490	6.7/----/0.67	Simulation/ 1 week/ K _h , K _v = 390, 0.8 m/d
Wood (1981)	Aquia Formation, Maryland (USA)	sand	Na^+ (environmental)	One-dimensional uniform flow solution	100000	5600-40000	Simulation/ 10 ⁶ years/ T= 25-75 m ² /d
Egboka et al (1983)	Borden, Ontario (Canada)	glaciofluvial sand	^3H (environmental)	One-dimensional uniform flow solution	600	30-60	Simulation/ 27 years/ K= 4.32 m/d
Hoehn and Santschi (1987)	lower Glatt Valley (Switzerland)	layered gravel and silty sand	^3H (environmental)	two-dimensional temporal moments	100 110 500	6.7 10 58	Simulation/ 20 months/ K= 7.0 - 570 m/d

Table 4.1.B. Vertical dispersivity data from field studies (Gelher et al., 1992)

Reference	Site Name (Country)	Aquifer Material/Aquifer Name	Tracer (Type)	Method of Data Interpretation (Model Name)	Scale of Observation	Dispersivity $\alpha_L, \alpha_H, \alpha_V$ (m)	Study/Duration/ Hydraulic Conductivity (K) or Transmissivity(T)
Segol and Pinder (1976)	Cutler area, Florida (USA)	fractured limestone and calcareous sandstone/ Biscayne Bay	Cl ⁻ (environmental)	two-dimensional numerical model	490	6.7/----/0.67	Simulation/ 1 week/ K _h , K _v = 390, 0.8 m/d
New Zealand Ministry of Works and Development (1977)	1) Roys Hill (New Zealand)	gravel with cobbles/ Heretaunga	¹³¹ I, RhWt, ⁸² Br, Cl ⁻ , <i>E. Coli</i> (pulse)	three-dimensional uniform flow solution	54-59	1.4- 11.5/0.1- 3.3/0.04-0.1	Experiment/ -----/ T= 25000 m ² /d
	2) Flaxmere (New Zealand)	alluvium (gravels)/ Heretaunga	RhWt, ⁸² Br (<i>pulse</i>)		25	0.3-1.5/--- /0.06	Experiment/-----/ T= 32000 m ² /d
	3) Hastings City rubbish dump (New Zealand)	alluvium (gravels)/ Heretaunga	Cl ⁻ (contamination)		290	41/10/0.07	Experiment/ -----/ T= 12100-30240 m ² /d
Robson (1978)	Barstow, California (USA)	alluvial sediments/ Twin Lake	TDS (contamination)	two-dimensional numerical model	3200	61/----/0.2	Experiment/3.5 years/ K= 43.2 m/d
Sykes et al (1982)	Borden, Ontario (Canada)	sand	Cl ⁻ (pulse)	two-dimensional numerical model	700	7.6/----/0.31	Simulation/1 year/ K _h = 5.0 to 6.2 m/d
Sykes et al (1983)	Mobile, Alabama (USA)	sand, silt, and clay	heat (step)	three-dimensional numerical model	57.3	0.76/---- /0.15	Simulation/-----/ K _h , K _v = 43.2, 2.2 m/d
Garabedian (1987)	Cape Cod, Massachusetts (USA)	medium to coarse sand, some gravel overlying silty sand	Br ⁻ (pulse)	three-dimensional spatial moments	250	0.96/0.018/ 0.0015	Experiment/17 months/ K= 112 m/d
Moltyaner and Killey (1988a, b)	Chalk River, Ontario (Canada)	fluvial sand	¹³¹ I (pulse)	two-dimensional uniform flow solution	40	0.06-0.16 /----/ 0.0006- 0.002	Experiment/2 years/ -----
Rajaram and Gelhar (1991)	Borden, Ontario (Canada)	glaciofluvial sand	Br ⁻ , Cl ⁻ (pulse)	three-dimensional spatial moments	90	0.5/0.05/ 0.0022	Experiment/3 years/ K= 6.2 m/d

4.3.2.2. Dispersivity Data from FGLs Studies

The phenomenon of dispersive mixing between the natural recharge and the host aquifer water (brackish water in subterranean oases or saline water in atoll islands), or between the seawater and fresh water in coastal areas, is not well defined. A wide range of scales have been used in several studies as shown in Table (4.1C). The longitudinal dispersivity values proposed in numerical modeling studies for FGLs range from the scale of centimeters (Oberdorfer et al., 1990; Comte et al., 2010) to the scale of meters (Oude Essink et al., 2010; Delsman et al., 2014) or even to hundreds of meters (Cobaner et al., 2012; Ataie-Ashtiani et al., 2013). As a further example, Werner et al., (2017) reviewed 24 case studies of numerical modeling of FGLs in atoll islands and found that the longitudinal, transverse horizontal, and transverse vertical dispersivities ranged from 0.05 to 50 m, 0.001 to 1 m, and 0.01 to 1 m, respectively.

Because of limited field data, site-specific dispersivity models are difficult to derive (Fetter, 2000). Thus, some studies have implemented assumed dispersivity values during the simulations, without calibration. These assumptions were either based on previous studies for the same study area (e.g., Oude Essink et al., 2010; Alsumaiei & Bailey, 2018), based on the scaling approach where the dispersivity values were assumed to be a function of the observation scale (e.g., Delsman et al., 2014; Yihdego & Al-Weshah, 2017), or the dispersivity values were assumed at to be least equal to a quarter of the grid size to keep the grid Peclet number less than one (Anderson and Woessner, 2015) to minimize numerical dispersion (e.g., Wilson, 2005; Cobaner et al., 2012). Other studies have applied the dispersivity values as variables tested during the simulations using different calibration or comparison data, as shown in Table (4.1C).

Table 4.1.C. Dispersivity data from FGLs studies

Reference	Site Name (Country)	FGL Formation	Model (Dimensions)	Calibration or Comparison data	Timescale/ Hydraulic Conductivity (K) or Transmissivity(T)	Dispersivity $\alpha_L, \alpha_h, \alpha_v$ (m)	Calibrated	Sensitivity Analysis
Wilson (2005)	Coastline between Pamlico-Cape Fear, North Carolina (USA)	coastal areas	RST2D code (Raffensperger, 1996) (2-D)	topography-driven flow, seawater recirculation, and geothermal convection	millions of years/ varies as a function of depth	100/---/10 ^{a,b}	No	Yes
Comte et al. (2010)	Mba Island (NewCaledonia)	atoll islands	SEAWAT (3-D) SUTRA (2-D)	electrical resistivity tomography, groundwater head and salinity	K=10-900 m/d	0.7/0.02/0.1	Yes	No
Oude Essink et al. (2010)	Dutch delta region (Netherlands)	coastal areas	MOCDENS3D code (Vandenbohede, 2007) (3-D)	groundwater head	100 years/ K= 0.1- 40 m/d	10/1/1 ^c	No	No
Cobaner et al. (2012)	Goksu delta, Silifke (Turkey)	coastal areas	SEAWAT model (3-D)	groundwater head and TDS concentration	822 years/ K= 0.8- 648 m/d	100/10/10 ^a	No	Yes
Alaghmand et al. (2014)	Lower Murray River (Australia)	riverine floodplains	HGS model (Therrien et al., 2006) (3-D)	river stages, floodplain aquifer heads and solute concentrations.	2070 days/ K= 0.1, 35, and 40 m/d	3/0.3/0.3	Yes	No
Delsman et al. (2014)	south Amsterdam city (Netherlands)	coastal areas	SEAWAT model (2-D)	groundwater head, chloride concentration, and tracers	8500 years	1/0.1/0.01 ^{b,c}	No	Yes
Ataic-Ashtiani et al. (2014)	Kish island, Persian Gulf (Iran)	island in semiarid regions	Inverse modeling SUTRA (3-D)	points of pressure and concentration	K= 0.01-86 m/d	335/34/34	Yes	Yes
Bailey et al. (2014)	several atoll islands (Republic of Maldives)	atoll islands	SUTRA (2-D)	freshwater lens thickness	14 years/ K= 75-5000 m/d	6/---/0.05 ^c	No	No
Yihdego & Al-Weshah (2017)	Rawdatain and Umm-Aish (Kuwait)	subterranean oases	MODFLOW-SURFACT model (3-D)	groundwater head and TDS concentration	73 years/ T= 10-980 m ² /d	(40/4/0.4, 500/50/5, 1/0.1/0.01) ^{a,b}	No	Yes
Alsumaiei & Bailey (2018)	four atoll islands (Republic of Maldives)	atoll islands	SEAWAT model (3-D)	freshwater lens volume	54 years/ K= 75-5000 m/d	6/0.05/0.05 ^c	No	No
Alrashidi & Bailey (current study)	Rawdatain (Kuwait)	subterranean oases	SEAWAT model (3-D)	groundwater head, TDS concentration, and volume and thickness of lens	2000 years/ K= 12- 25 m/d	50/5/0.1	Yes	Yes

Implementing dispersivity values were based on: (a) a grid Peclet number, (b) a function of the observation scale, and (c) previous studies

The data on vertical transverse dispersivity are much more limited. The range of field-scale vertical dispersivity values has been reported as low as a few millimeters to one meter (Gelher et al., 1992). In numerical studies, it is common practice to relate the vertical and longitudinal dispersivities according to a constant ratio, ranging between 0.01 and 0.001 (Voss, 1984; Marsily, 1986; Gelher et al., 1992). Using such a ratio has led to the use of high values of vertical dispersivity in the numerical modeling of FGLs, such as 10 m (Wilson, 2005) or even up to 30 m (Ataie-Ashtiani et al., 2013). Underwood et al. (1992) showed that the component of the vertical transverse dispersivity controls the mixing zone width between seawater and fresh water. Neglecting the vertical transverse dispersivity would lead to a sharp interface (Maas, 2007) and a poor representation of the salinity distribution (Sakr, 1999). Vacher (2004) found that the vertical mixing within the transition zone separating fresh water and seawater in atoll FGLs affects the depths at which potable water is assessable. However, Eeman et al. (2011) investigated the thickness of the mixing-zone between a freshwater lens and upwelling saline water, and they found that vertical transverse dispersion may become less important than longitudinal dispersion if the lens thickness fluctuates significantly.

4.3.2.3. Dispersivity Data from Studies in Kuwait

Information on the dispersivity values in Kuwait aquifers is both uncertain and limited to a few experimental and numerical studies, as shown in Table (4.1D). Mukhopadhyay et al (1994) conducted an artificial groundwater recharge field experiment around Well SU-135A in the Kuwait Group Aquifer (KGA), and the injection/withdrawal data were analyzed numerically (FLOTRA model) to estimate the longitudinal dispersivity value. A high recovery efficiency indicated a low longitudinal dispersivity value (1 m) for the KGA around the well. Two more field experiments were conducted around Wells SU-10 and C-105 in the Dammam aquifer.

AlRukaibi & McKinney (2013) evaluated the efficiency of ASR with a multi-cycle concept in the Dammam Aquifer using MT3D to simulate TDS transport. A 10 m longitudinal dispersivity value was used to analyze the mixing between brackish water and injected water. Yihdego & Al-Weshah (2017) assessed the impact of saline sea water that was imported to extinguish the oil well fires during the Gulf war on the Rawdatain and Umm-Aish freshwater aquifers in 1990-1991. The MODFLOW-SURFACT model was used to simulate several scenarios for the areal extent of the TDS plume in the Rawdatain and Umm-Aish freshwater lenses. Different dispersivity values and transport solution techniques were used, and significant changes in TDS were noticed as a result of changing the longitudinal dispersivity between 1 and 500 m.

Table 4.1.D. Dispersivity data from studies in Kuwait

Reference	Site Name (Country)	Aquifer Material/Aquifer Name	Tracer (Type)	Method of Data Interpretation (Model Name)	Scale of Observation	Dispersivity $\alpha_L/\alpha_h/\alpha_v$ (m)	Study/Duration/ Transmissivity(T)
Mukhopadhyay et al (1994)	Sulaibiya, Well SU-135A (Kuwait)	sand and gravel/ Kuwait Group	tritium (pulse)	radial numerical model (FLOTRA)	0-100	1.0/---/---	Experiment/2 weeks/ T= 250-300 m ² /d
Mukhopadhyay et al (1994)	Sulaibiya, Well SU-10 (Kuwait)	limestone/ Dammam	Cl ⁻ , TDS, EC (pulse)	radial numerical model (FLOTRA)	0-100	10/---/---	Experiment/4 months/ T= 30-50 m ² /d
Mukhopadhyay et al (1994)	Shigaya, Well C-105 (Kuwait)	limestone/ Dammam	sodium fluorescein (pulse)	radial numerical model (FLOTRA)	0-100,7000	20-200/--- /---	Experiment/8 months/ T= 4000 or higher m ² /d
AlRukaibi & McKinney (2013)	Kabd Area (Kuwait)	limestone/ Dammam	TDS (contamination)	two-dimensional numerical model (MT3D)	200	10/---/---	Simulation/4 years/ T= 200-400 m ² /d
Yihdego & Al- Weshah (2017)	Rawdatain and Umm-Aish (Kuwait)	sand and gravel/ Kuwait Group	TDS (contamination)	three-dimensional numerical model (MODFLOW- SURFACT)	5000	40/4/0.4, 500/50/5, 1/0.1/0.01	Simulation/73 years/ T= 10-980 m ² /d

4.4. Methods

4.4.1. Dispersivity Value Sets

A total of 28 different sets of 3D dispersivity values are selected to be tested in this study, as shown in Table 4.2. These sets encompass all of the feasible longitudinal dispersivity values for the Rawdatain basin that could be suggested by the literature based on the scale of the observations or previous studies in the same aquifer. The lower range of the longitudinal dispersivity sets (D1 to D4: 1 to 3 m) represents the previous studies conducted in the same aquifer (KG) (Mukhopadhyay et al., 1994; Yihdego & Al-Weshah, 2017). The main ranges of longitudinal dispersivity sets (D5 to D25: 5 to 250 m) were selected based on the lens size and scale-based ranges suggested by Gelhar et al. (1992). In our case, there is no well-defined scale of our study area because there are multiple recharge zones, as shown in Figure 4.2A. However, based on the plume length, the scale could be as high as 1 to 3 km, and the corresponding longitudinal dispersivity values are between 5 and 250 m. The upper range (D26 to D28: 300 to 500 m) represents high dispersivity values that have been used for the FGLs in the Rawdatain basin in the AP (Yihdego & Al-Weshah, 2017) and Kish Island in the Persian Gulf (Ataie-Ashtiani et al., 2014). The ratio of horizontal transverse dispersivity to longitudinal dispersivity was assumed to be 0.1 for all sets.

Table 4.2. Dispersivity set IDs and values, grid Peclet numbers, and numerical methods

Range	Set IDs	Dispersivity (m)			Grid Peclet Number	Numerical Method
		Longitudinal	Horizontal Transverse	Vertical Transverse		
Lower Range	D1	1	0.1	0.001	100.0	TVD
	D2	1	0.1	0.01	100.0	TVD
	D3	3	0.3	0.003	33.3	TVD
	D4	3	0.3	0.03	33.3	TVD
Main Range	D5	5	0.5	0.005	20.0	TVD
	D6	5	0.5	0.05	20.0	TVD
	D7	10	1	0.01	10.0	TVD
	D8	10	1	0.1	10.0	TVD
	D9	20	2	0.02	5.0	TVD
	D10	20	2	0.2	5.0	TVD
	D11	25	2.5	0.025	4.0	TVD
	D12	25	2.5	0.25	4.0	TVD
	D13	30	3	0.03	3.3	FD
	D14	30	3	0.1	3.3	FD
	D15	50	5	0.05	2.0	FD
	D16	50	5	0.1	2.0	FD
	D17	60	6	0.06	1.7	FD
	D18	60	6	0.1	1.7	FD
	D19	100	10	0.1	1.0	FD
	D20	150	15	0.15	0.7	FD
D21	150	15	0.1	0.7	FD	
D22	200	20	0.2	0.5	FD	
D23	200	20	0.1	0.5	FD	
D24	250	25	0.25	0.4	FD	
D25	250	25	0.1	0.4	FD	
Upper Range	D26	300	30	0.1	0.3	FD
	D27	400	40	0.1	0.25	FD
	D28	500	50	0.1	0.2	FD

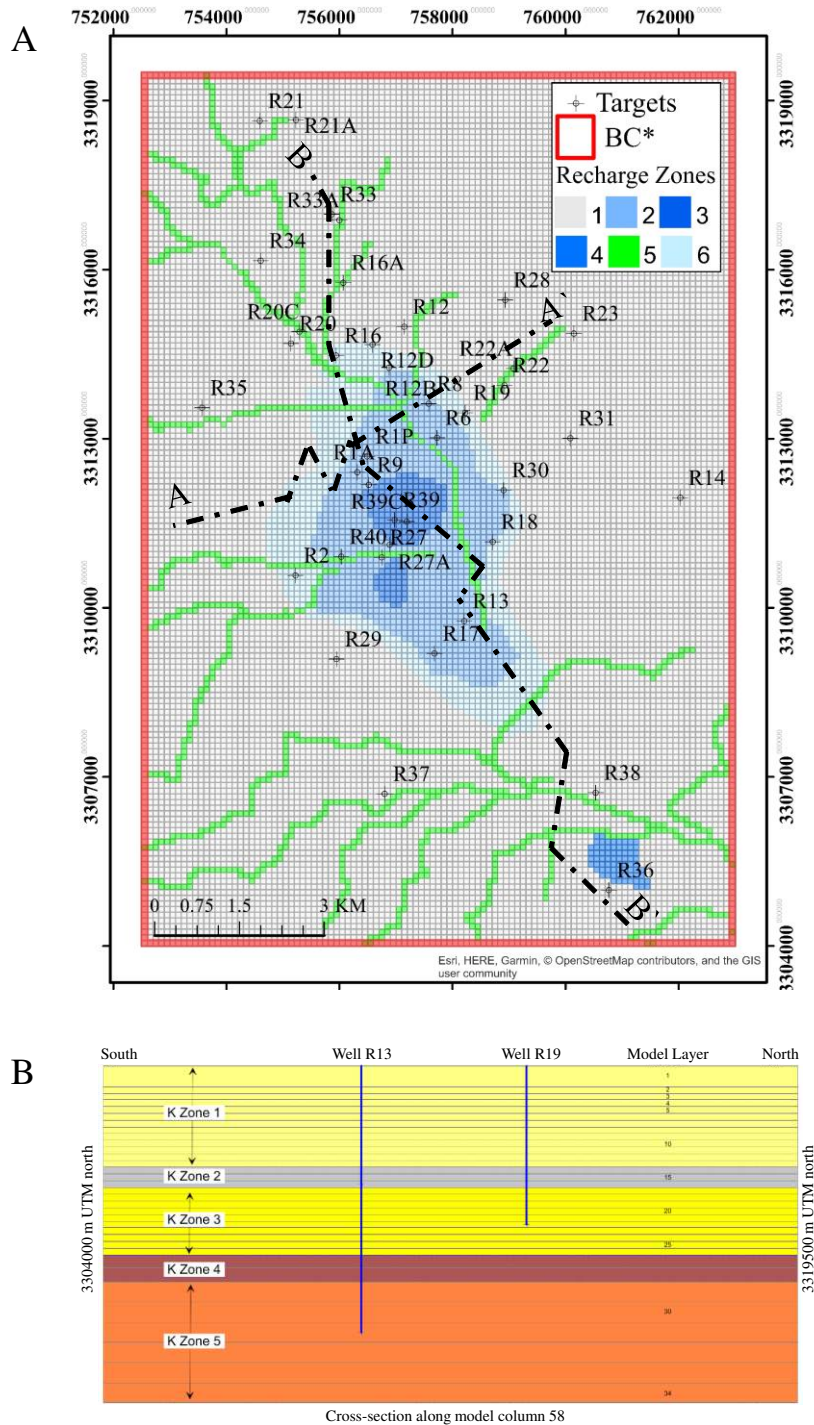


Figure 4.2. (A) Recharge zones, data target points, and boundary conditions (*BC where the south and west boundaries represent specified-head conditions and the north and east boundaries represent head-dependent flux conditions). (B) Vertical cross-section of model grid.

Because of limited information on the vertical transverse dispersivity and its influence on controlling the vertical mixing between fresh water and saline or brackish water, two ratios of the vertical transverse dispersivity were assessed for each longitudinal dispersivity value. For D1 to D12, the lower and upper ratios are 1/1000 and 1/100, respectively. For D13 to D28, the lower ratio is 1/1000 and the upper vertical transverse dispersivity is fixed at 0.1 m. Without assuming a fixed upper limit, the vertical transverse dispersivity will exceed the reliable values that are reported for similar aquifer material and hydraulic conductivities but different tracers and subsurface solute transport events (Robson, 1978; Sykes et al., 1982; Sykes et al., 1983), as shown in Table 4.1B. However, a sensitivity analysis was applied to explore the effects of using higher vertical transverse dispersivity values resulting from tying α_v to large-scale α_L .

4.4.2. Model Code

SEAWAT (Langevin et al. 2007), a 3D finite difference code developed by the U.S. Geological Survey, was used to simulate the formation and behavior of the Rawdatain lens. The code is capable of simulating transient density-dependent flow and advection and dispersion of solutes. This is accomplished using a combination of MODFLOW (McDonald & Harbaugh, 1988) for simulating groundwater flow and MT3DMS (Zheng & Wang, 1999) for simulating solute transport. MODFLOW and MT3DMS are run iteratively in order to update the head solution based on changes in fluid density caused by changing solute concentrations. Groundwater Vistas (Rumbaugh & Rumbaugh, 2011) was used to generate the model grid, prepare input files, and interpret the model outputs. Model Viewer (Hsieh & Winston, 2002) was used to display and visualize the results in 2D cross-sections. Many applications of SEAWAT have been published, such as the simulation of FGLs in coastal areas (Oude Essink et al., 2010;

Delsman et al., 2014), in atoll islands (Comte et al., 2010; Alsumaiei & Bailey, 2018), and in subterranean oases in arid regions (Alrashidi & Bailey, 2019a).

The MT3DMS code provides three major transport solution techniques for solving the advection-dispersion equation: the standard finite difference method (SFD), the Eulerian-Lagrangian methods, and the total variation diminishing method (TVD). In these three solution options, the dispersion, sink/source, and reaction terms are treated in the same way using the block-centered finite-difference method (explicit or implicit schemes), but they differ in the approach to solving the advection term. However, none of these techniques can produce highly satisfactory solutions under a wide range of hydrogeologic conditions. Zhang et al. (2004) reviewed some common transport solution techniques, discussing their strengths and limitations, and other studies have discussed the sensitivity of model results to the choice of technique (Mehl & Hill, 2001; Lowry & Anderson, 2006; Konikow, 2011). Voss (1987) reported that particular attention to the numerical methods is required for successfully simulating groundwater systems where the transition zone between fresh and salt water is narrow.

When simulating variable density-transport problems, it is important to adopt an adequate spatial discretization scheme. The appropriateness of the spatial discretization can be evaluated using a grid Peclet number (Pe), which is a measure of the local advective transport relative to the local hydrodynamic dispersion. In cases where the molecular diffusion is small relative to the mechanical dispersion, the grid Peclet number can be defined as $Pe = \Delta_L / \alpha_L$, where Δ_L is the grid element length parallel to flow and α_L is the longitudinal dispersivity (Voss and Souza, 1987).

As noted by several sources, the SFD with upstream or central-in-space weighting is reasonably accurate and can thus be used with confidence when the grid Pe is less than 4 (indicating a system dominated by dispersion). When advection dominates ($Pe \geq 4$), the

numerical techniques are plagued by oscillations, and use of the TVD method is recommended. In this study, SFD and TVD were implemented based on the Pe that resulted from testing the wide range of longitudinal dispersivities reported in Table 4.2.

4.4.3. Model Construction

4.4.3.1 Model Grid and Boundary Conditions

The model domain (Figures 4.1 and 4.2) covers the entire surface area (162.75 km²) to a depth of 50 m. The model has a uniform 100 m x 100 m cell size with 155 rows and 105 columns (the total number of active cells is 553,350). The grid is aligned with true north and is centered on the surface depression. The model utilizes 34 computational layers to represent three aquifer zones (Upper A, Upper B, and Lower) separated by two aquitard zones (Figure 4.2B). Fine layering in the upper layers was used to accurately represent the vertical salinity profile within the aquifer.

The boundary conditions constraining the general groundwater flow regime include spatially varying specified-head boundary conditions along the south and west model boundaries, as well as spatially varying head-dependent flux boundary conditions along the north and east boundaries (Figure 4.2A). During preliminary simulations, we found that the head-dependent flux boundary condition more accurately handled the flux of solute leaving the model domain along the north end. The boundary conditions were adjusted until a basic head calibration was achieved but were not further adjusted in the simulations presented herein. The lower boundary of the model was designated as a no-flow boundary.

4.4.3.2. Aquifer Parameters and Recharge Rates

The initial conditions for each model simulation included an absence of fresh water, such that the initial TDS concentration increased gradually from 4000 mg/L at the top layer to 12000

mg/L at the bottom layer. These are representative of measured TDS values outside of and below the freshwater lens. Next, vertical recharge was applied to the top layer, and then the simulation was run until the configuration shape and volume of the freshwater lens approached a steady state. Fadlilmawla et al. (2008) found that the magnitude of salinization during infiltration, subsurface runoff and percolation to the water table is minimal. Thus, the TDS concentration of the recharge water was assumed to be 200 mg/L, representing the lowest TDS value observed in the freshwater lens.

Each layer is assumed to be horizontally homogenous. The hydraulic conductivity values (K) were based on results from 14 pumping tests reported by the Parsons Corporation (1964) and Senay (1988). The anisotropy ratios were set to 10, and the authors estimated the specific yield and porosity to be 0.12 and 0.22, respectively. Alrashidi & Bailey (2019a), in estimating recharge rates for the same aquifer, carried out a sensitivity analysis by varying horizontal K values by a factor ranging from 0.1 to 4. Their results indicated that the K set is reasonably representative of the entire aquifer domain.

Long-term average annual recharge for each simulation is set to 500,000 m³/year based on the study by Alrashidi & Bailey (2019a). Six recharge zones are used (Figure 4.2A). Regional diffuse recharge rates are represented by Zones 1, 2 and 6, and focused recharge beneath the depression, playa, and wadis are represented by Zones 3, 4 and 5, respectively. Depression topography, water age (Fadlilmawla et al., 2008), and spatial TDS data were used as the basis for delineating the recharge zones. Based on a fixed percentage of the total annual recharge volume and each zone area, steady recharge rates were assigned as follows: 96 mm/year for Zones 3 and 4, 9.4 mm/year for Zone 5, 5.5 mm/year for Zone 2, and 0.7 mm/year for Zones 1 and 6.

4.4.4. Testing Processes

To provide accurate estimates of large-scale environmental dispersivity, the model was tested against multiple data targets to limit what otherwise would be a wide variety of non-unique possible parameter sets. This approach has been extensively discussed in the literature, and many examples illustrating the importance of multi-target calibration have been presented (e.g., Kim et al. 1999; Saiers et al. 2004).

The pre-development data for the Rawdatain basin include TDS at 47 locations at various depths and water table data at 42 locations (Parsons Corporation, 1964); the locations are shown in Figure 4.2A. These data provide insight into the 3D spatial variability of salinity, as well as information used to determine the lens's pre-development volume and depth at three different water quality levels (0–700 mg/L, 700–1000 mg/L, and 1000–2000 mg/L TDS) and to constrain the construction and calibration of the groundwater flow and salt transport model.

Because of the interest in using the Rawdatain basin as a freshwater resource, a strong focus was placed on calibrating the model to the 1962 estimates of freshwater volume. The volume estimates were based on the 3D spatial distribution of salinity, yet the volumes and TDS data points provide two different types of calibration targets. Hill & Tiedeman (2006) noted that the use of point data in calibrating transport models can be problematic because the concentrations can vary by orders of magnitude over short distances. This variability is partly due to subsurface heterogeneities that are often at a scale that can never be known or modeled in sufficient detail. Because of the high spatial variability of TDS values and subsurface heterogeneities, a close match with point data is not expected.

The freshwater thickness (i.e., depth) calibration targets were mainly based on the original point TDS data, but some specific thickness targets were also based on diagrams created

by Senay (1989) (shown in Figure 4.3). The thickness targets aided in the elimination of several non-unique combinations of calibrated parameters.

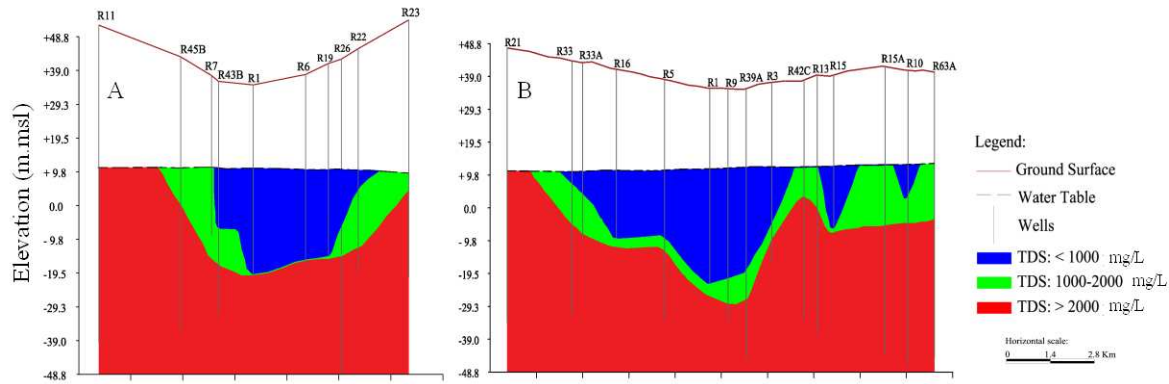


Figure 4.3. (A) & (B) Rawdata in cross-sections A-A' and B-B', respectively (modified after Senay, 1977).

Groundwater age data can be used to constrain the rate of recharge, the residence time of aquifer storage, and the time frame of contaminant fate and transport (McCallum et al. 2017). In the Rawdatain basin, Fadlemawla et al. (2008) collected 24 samples for radioactive carbon isotope analysis (^{14}C and ^3H) from within the 2000 mg/L TDS contour, with average depths ranging from 3 to 39 m below the water table. The analysis of these samples indicated groundwater ages ranging from less than 500 years to 2043 years. Because the groundwater age depends on both depth and location, as well as on the sampling location with respect to the complex flow dynamics within the lens, it is difficult to conduct a more thorough quantitative comparison (Sanford, 2002). In this study, the simulated period of lens development was constrained using the age of the lens volume with TDS less than or equal to 2000 mg/L (i.e., groundwater age was not tracked during the simulation of this period). As part of the calibration, multiple targets were compared with the simulated results at 2000 years, which constrains the hydraulic conductivity, recharge rate, and dispersivity of the system.

Finally, a multi-criteria score-based method was employed to evaluate the performance of each of the dispersivity sets based on the multiple data targets at 2000 years of simulation. To assess the performance, the absolute error was calculated for each simulation compared with seven data targets, and then the error was ranked for each model with an equal weight for all targets. This step helped determine the best dispersivity set that satisfies all of the data targets with an absolute error that should not exceed 10% for each data target.

4.5. Results and Discussion

4.5.1. Dispersivity Sets Simulation

Figure 4.4 is a plot of the simulated freshwater lens volume at 2000 years against the three volume targets for the 28 different sets of dispersivity values, on a scale of 0 to 300×10^6 m³. The lower dispersivity values promote less mixing and result in a larger freshwater lens with less distinction between the three volume targets, whereas the higher dispersivity values prevent extensive development of fresh water. For example, longitudinal dispersivity values less than 5 m result in simulated volumes of up to 86–587% and 149–242% more than the targeted volumes at 700 mg/L (32.6 million m³) and 1000 mg/L (64.4 million m³), respectively. In contrast, longitudinal dispersivity values of 200 m or more result in simulated volumes that are 20 to 70% less than the three targeted volumes. The best three dispersivity sets are D18, D14 and D17 for volumes targets below 700 mg/L, 1000 mg/L, and 2000 mg/L, respectively, with absolute errors of 8.7%, 1.2% and 3.4%.

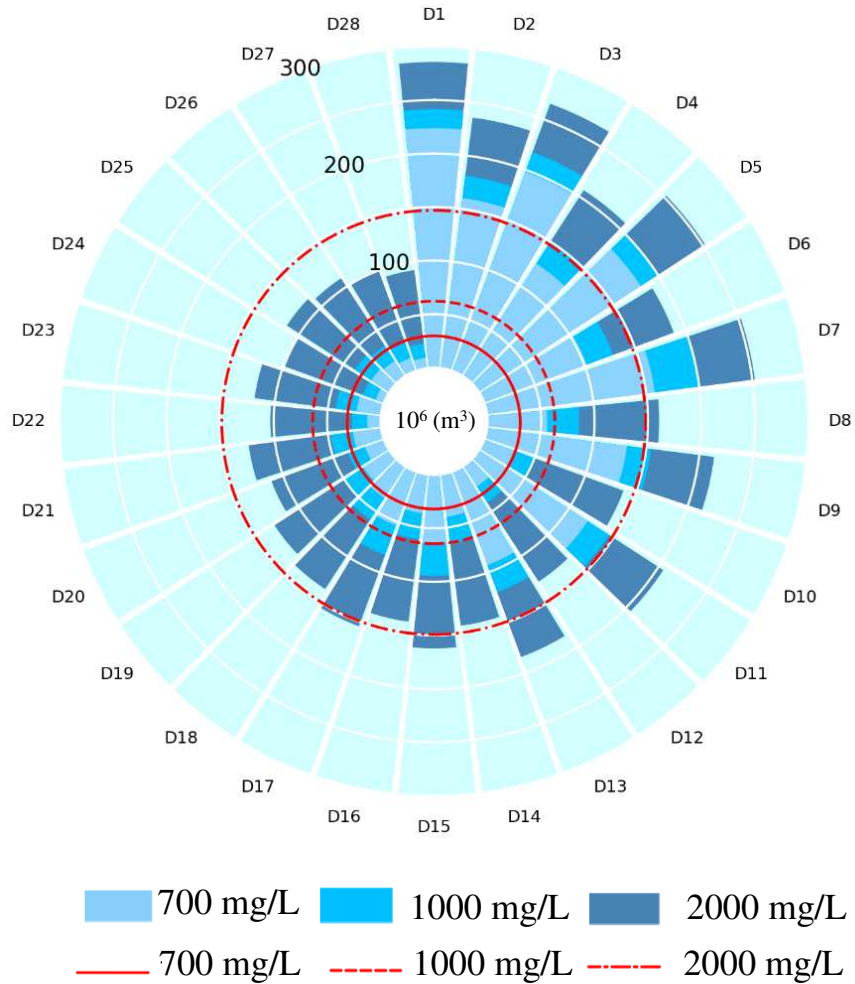


Figure 4.4. Volumes predicted for different dispersivity sets at 2000 years compared with target volumes (red lines).

The second calibration target was the maximum lens thickness, as presented by Senay (1989). The thickness of a lens can affect the feasibility of recovering (pumping) fresh water without causing excessive mixing with the underlying brackish waters. Figure 4.5 is a plot of the simulated maximum thickness at 2000 years tested for the 28 dispersivity sets. It is apparent that the higher dispersivity values provide an accurate match of the three lens thicknesses targets because they allow for more mixing, whereas the lower dispersivity values fail to do so. Figure 4.5 indicates that lower longitudinal (≤ 5 m) and vertical transverse (< 0.06 m) dispersivities developed a thick freshwater lens with 700 mg/L TDS (i.e. with low TDS). These dispersivity

values suggested that water with 700 mg/L TDS exists at depths between 28 to 32 m, which are up to 9 to 45% more than the targeted maximum thickness for the 700 mg/L (21.8 m) level quality. The best three dispersivity sets are D21, D9 and D5 for the three thickness targets, respectively, with absolute errors of 0.4%, 0.6% and 0.1%.

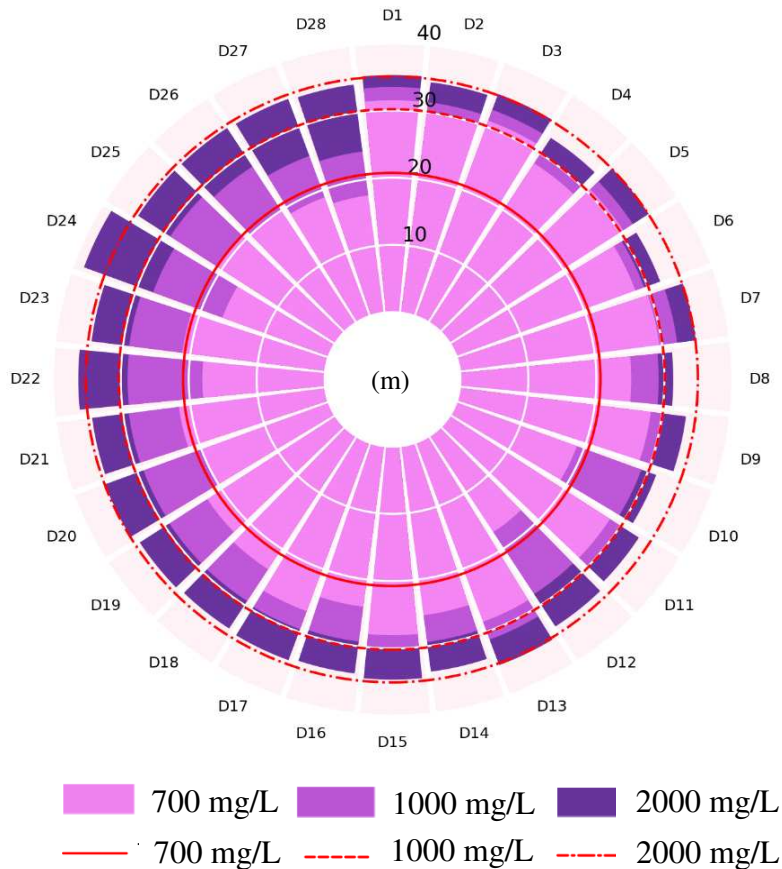


Figure 4.5. Maximum lens thickness predicted for different dispersivity sets at 2000 years compared with target values (red lines).

For reasons explained above, more emphasis was placed on achieving a close calibration to lens volume and maximum thickness targets than to TDS point data. Nevertheless, the Scaled Root Mean Square Error (S-RMSE) of TDS was found to be sensitive to dispersivity values, as shown in Figure 4.6. The general trend is that the high longitudinal dispersivity values (≥ 30 m) and their corresponding transverse dispersivities achieved a reasonably good fit between the measured and simulated TDS point data. In terms of the S-RMSE values, the best dispersivity

sets are D13 to D19, with values between 0.185 and 0.195. In comparison, the S-RMSE values of lower dispersivities (≤ 25 m) and their corresponding transverse dispersivities are more than 0.256.

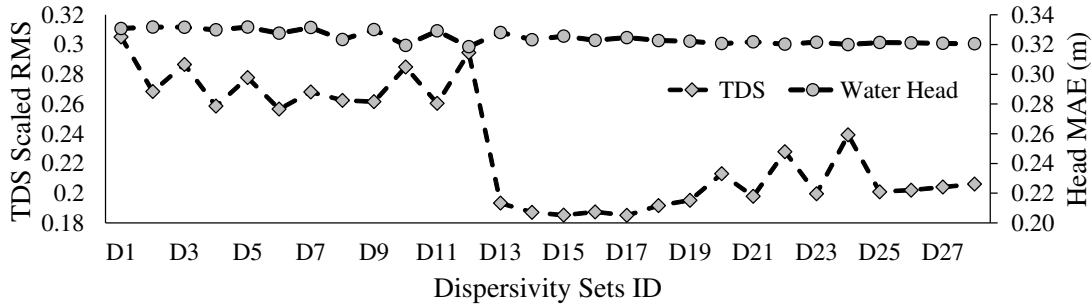


Figure 4.6. S-RMSE for TDS and MAE for head with different dispersivity sets

The calibration of solute transport models to groundwater head is not a particularly robust or stringent method. Indeed, we found groundwater head calibration to have a lower sensitivity to dispersivity values than to other calibration targets because the water density does not change very much during the simulation processes, as shown in Figure 4.6. The range of the Mean Absolute Error (MAE) of the groundwater heads was found to be between 0.31 and 0.33 m. The reason is that the initial TDS concentration is set to between 4,000 mg/L (1000.3 kg/m^3) and 12,000 mg/L (1007.3 kg/m^3), and the final simulated TDS range is between 200 mg/L (998.4 kg/m^3) and 8000 mg/L (1004.3 kg/m^3) within the groundwater head target's location (assuming that the water temperature is constant at 20°C). However, groundwater heads have been used effectively on FGL modeling in coastal areas and atoll islands because of the large difference between the fresh water and seawater densities: 1000 kg/m^3 and 1025 kg/m^3 , respectively (Oude Essink et al., 2010; Comte et al., 2010; Cobaner et al., (2012).

A multi-criteria score-based method was applied to assess the performance of each of the dispersivity sets based on the multiple data targets. The data targets included the volume and vertical thickness of stored groundwater of three different water quality TDS ranges (0–700

mg/L, 700–1,000 mg/L, 1000–2,000 mg/L), as well as total dissolved solids (TDS) concentrations in groundwater. The groundwater head data were excluded because of the result discussed above. To evaluate the performance, the absolute error was calculated for each simulation compared with seven data targets, and then the errors were ranked for each model with an equal weight for all of the targets. These results show that simulations are more sensitive to the volumes targets than to the other targets because the ranges of the absolute errors were 8.7–587.4%, 1.2–275.2% and 3.4–91.7% for the three volume targets, respectively. At the same time, the range of the S-RMSE values of the TDS point data was between 0.185 and 0.305. In fact, it is more feasible and perhaps even more informative to calibrate to the total mass of a contaminant plume (a freshwater lens in this case) than to attempt to calibrate to highly variable point concentration data (Feehley et al., 2000). Other alternatives to using point concentration measurements are discussed by Julian et al. (2001), Barth and Hill (2005a,b), Anderman et al. (1996), and Bailey et al. (2014). Nonetheless, although calibration to the point data is not a primary goal, the point data do provide useful information about the shape and distribution of the lens, and hence the model's fit to the point TDS data was monitored during calibration.

Results are shown in Table 4.3. The highest two ranked dispersivity sets were D16 and D18, with total scores of 49 and 50, respectively. Indeed, the D18 set satisfied all three volume and lens thickness targets with an absolute error of less than 9%. The D16 set achieved the same targets except for the targeted volume and lens thickness at 700 mg/L, where the absolute errors were 12.9% and 10.5%, respectively. These slightly high absolute errors for the two targets could be because we compared the simulated volume with one field estimate from the U.A.R.

The power of using the multi-target calibration approach can be seen in Table 4.3, which shows how one set of the dispersivity values can satisfy one or two targets but be significantly

inaccurate in a third target. For example, D17 ranked first in both the targeted volume at 2000 mg/L (absolute error 3.4%) and in the S-RMSE values of the TDS point data, but it ranked 14th (absolute error 64.5%) and 7th (absolute error 29.0%) for the targeted volumes at 700 mg/L and 1000 mg/L, respectively. The D9 and D5 sets had the best performance (ranked 1st) for the lens maximum thickness for 1000 and 2000 mg/L, respectively, whereas they ranked 23rd and 25th for the lens volume at the same quality.

Table 4.3. Multi-criteria score-based method results

Model ID	Target criteria																		Total Score	Final Rank			
	Volume of Stored water (million m ³)									Lens Maximum Thickness (m)											Spatial TDS		
	700 ppm	Abs Error (%)	Rank	1000 ppm	Abs Error (%)	Rank	2000 ppm	Abs Error (%)	Rank	700 ppm	Abs Error (%)	Rank	1000 ppm	Abs Error (%)	Rank	2000 ppm	Abs Error (%)	Rank			RMS	Scaled	Rank
D1	223.7	587.4	28	241.5	275.2	28	285.5	91.7	28	31.5	44.6	28	33.5	9.9	26	35.3	0.8	5	0.305	28	171	28	
D2	160.1	391.8	25	181.1	181.4	24	235.8	58.3	24	29.8	36.7	25	31.6	3.5	8	34.6	1.3	12	0.268	23	141	24	
D3	198.2	509.0	27	217.7	238.2	27	265.8	78.4	27	31.0	42.1	27	32.7	7.3	22	35.2	0.6	4	0.287	26	160	27	
D4	125.5	285.6	22	149.1	131.7	22	207.2	39.1	22	28.3	29.9	22	29.9	2.0	3	32.8	6.2	24	0.259	18	133	21	
D5	180.9	455.6	26	200.9	212.3	25	252.4	69.4	25	30.6	40.1	26	32.2	5.8	20	35.0	0.1	1	0.278	24	147	26	
D6	102.1	213.6	20	128.5	99.7	20	188.8	26.8	16	28.1	29.0	19	29.5	3.2	7	32.0	8.6	25	0.257	17	124	18	
D7	158.0	385.3	24	200.9	212.3	25	252.4	69.4	25	29.6	35.8	24	32.2	5.8	20	35.0	0.1	1	0.268	22	141	24	
D8	55.8	71.6	16	85.6	33.1	8	160.5	7.7	5	25.1	15.3	11	29.2	4.3	13	31.3	10.5	27	0.263	21	101	14	
D9	131.8	305.1	23	154.6	140.2	23	213.8	43.6	23	28.3	29.9	21	30.3	0.6	1	33.5	4.2	22	0.262	20	133	21	
D10	29.5	9.4	2	50.2	22.0	4	138.6	7.0	4	18.9	13.3	9	29.0	4.8	18	31.3	10.5	27	0.285	25	89	11	
D11	121.2	272.2	21	145.3	125.8	21	205.3	37.9	20	28.2	29.2	20	29.8	2.1	4	33.2	5.1	23	0.260	19	128	20	
D12	22.9	29.6	8	40.6	36.9	10	128.9	13.5	8	17.1	21.5	15	28.1	7.7	23	33.9	3.2	19	0.295	27	110	16	
D13	93.4	186.8	19	120.2	86.7	19	184.7	24.0	13	28.4	30.4	23	31.2	2.5	5	35.3	0.8	6	0.193	6	91	13	
D14	40.0	22.9	6	65.1	1.2	1	142.6	4.3	2	25.4	16.4	12	29.4	3.6	9	33.8	3.4	20	0.187	3	53	3	
D15	64.0	96.8	18	94.3	46.6	14	162.2	8.9	7	28.0	28.6	18	29.9	1.9	2	34.7	1.0	9	0.185	2	70	8	
D16	36.8	12.9	4	61.0	5.3	2	138.7	6.9	3	24.1	10.5	8	29.3	3.9	10	34.1	2.6	18	0.188	4	49	1	
D17	53.6	64.5	14	83.0	29.0	7	154.0	3.4	1	26.7	22.5	16	29.6	3.0	6	34.5	1.5	13	0.185	1	58	6	
D18	35.4	8.7	1	59.2	8.0	3	136.9	8.1	6	23.7	8.5	7	29.3	3.9	11	34.2	2.4	17	0.192	5	50	2	
D19	28.9	11.3	3	49.4	23.3	5	128.1	14.0	9	22.6	3.5	3	29.2	4.1	12	34.4	1.7	15	0.195	7	54	4	
D20	18.9	41.8	10	35.8	44.4	12	112.0	24.8	14	20.0	8.3	6	29.1	4.6	15	35.1	0.3	3	0.213	14	74	10	
D21	26.5	18.6	5	47.4	26.3	6	124.7	16.3	10	21.7	0.4	1	29.2	4.4	14	34.6	1.2	11	0.198	8	55	5	
D22	12.5	61.6	13	26.7	58.4	16	103.2	30.7	17	18.0	17.5	13	29.0	4.8	18	36.3	3.6	21	0.228	15	113	17	
D23	23.1	29.2	7	42.5	34.0	9	119.1	20.0	11	21.2	2.7	2	29.1	4.6	15	34.7	0.9	7	0.200	9	60	7	
D24	8.3	74.5	17	21.0	67.3	18	98.3	34.0	19	16.7	23.5	17	27.6	9.5	25	38.4	9.7	26	0.239	16	138	23	
D25	20.1	38.3	9	38.2	40.6	11	114.1	23.4	12	20.6	5.3	4	29.0	4.8	17	34.7	0.9	7	0.201	10	70	8	
D26	17.5	46.2	11	34.5	46.4	13	109.3	26.6	15	20.1	8.0	5	27.8	8.8	24	34.6	1.1	10	0.202	11	89	11	
D27	13.1	59.6	12	28.3	56.1	15	100.6	32.5	18	18.9	13.4	10	25.4	16.6	27	34.5	1.5	14	0.204	12	108	15	
D28	9.7	70.1	15	23.1	64.1	17	92.3	38.0	21	17.6	19.3	14	24.2	20.6	28	34.2	2.2	16	0.206	13	124	18	

In addition to using quantitative targets, we also considered lens thickness and overall lens shape qualitatively. This criterion also helps to confirm the accuracy of the freshwater plumes, as it represents the shape of the lens under the recharge zones (Alrashidi & Bailey, 2019a). Figure 4.7 shows the corresponding cross-sections through the simulated lens through time for dispersivity sets D1 (ranked 28th), D8 (ranked 14th), and D16 (ranked 1st). The D1 cross-section represents a large lens with low TDS at the top layers and then a sharp increase in TDS with depth due to less mixing between the recharge and brackish groundwater. The D8 and D16 sets show a favorable visual comparison with the longitudinal and transverse cross-sections of the lens presented by Senay (1977), as shown in (Figure 4.3). However, the D16 set is better than D8 in terms of the TDS range. In addition to lens shape, the D16 set shows a range of TDS between 210 and 9300 mg/L, which is close to the field range of 200 to 8000 mg/L (Alsanafy, 2010). Therefore, the D16 ($\alpha_L = 50$ m: $\alpha_h = 5$ m: $\alpha_v = 0.1$ m) dispersivity set can be used when applying the model to water management scenarios.

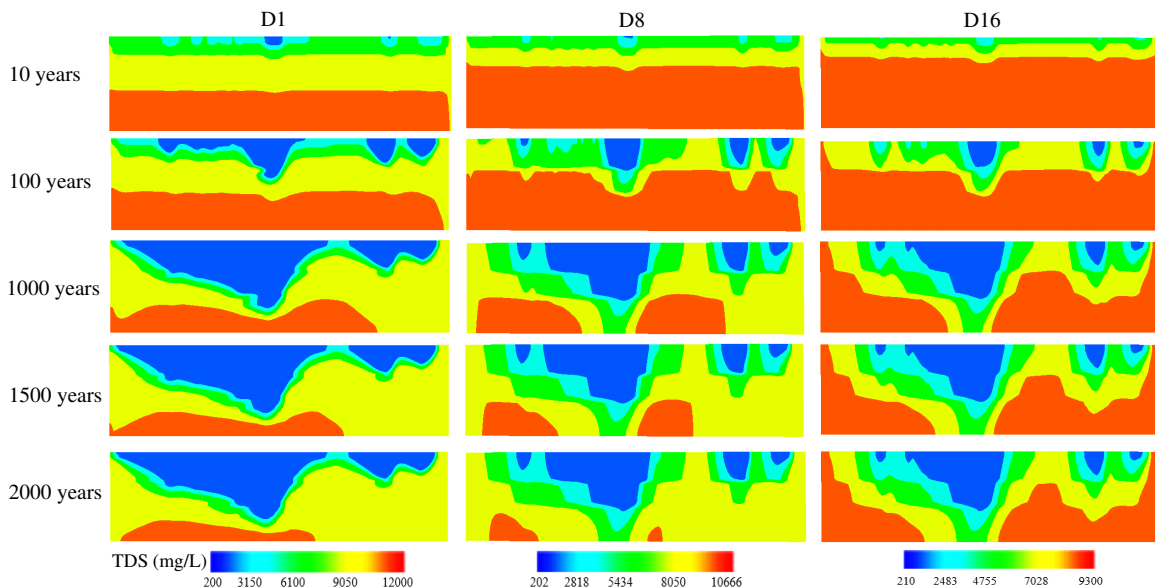


Figure 4.7. Modeled cross sections B-B' (not to scale) for the D1, D8, and D16 dispersivity sets

4.5.2. Sensitivity Analysis

The model was used to assess the sensitivity of freshwater lens volumes at three quantity categories to the vertical transverse dispersivity, as shown in Figure 4.8. The sensitivity analysis was carried out by two sets of dispersivity values: D and D'. The D set represents the fixed vertical transverse dispersivity at 0.1 m, whereas the D' set represents the vertical transverse dispersivity tied to the longitudinal dispersivity by a factor of 1/100 (i.e., α_v equals 0.2 to 2.5 m as a function of α_L in the x-axis). The ratio of horizontal transverse dispersivity to longitudinal dispersivity is kept equal to 0.1. The results of this analysis indicate that α_v has a more significant influence on the simulated freshwater volumes than α_L . The higher α_v values for D' promote more vertical mixing and result in a greater decline in simulated stored water compared with the D set, ranging between 29 and 99%, 27 and 81%, and 8 and 89% for the three water quality categories, respectively. The results also indicate that the freshwater at the quality equal to or less than 700 mg/L (Figure 4.8A) is more sensitive to α_v than the other TDS ranges (Figure 4.8B&C) because there is a more than 90% reduction in the simulated volumes with α_v values greater than or equal to 1.5 m. When using $1 \text{ m} \leq \alpha_v \leq 2.5 \text{ m}$, the absolute errors of the simulated volumes at the three quality categories with respect to the volume targets were (89–100%), (64–89%), and (79–91%) respectively. This is in agreement with the Gelhar et al. (1992) study, which suggested that no α_v values greater than one meter could be found from field investigations.

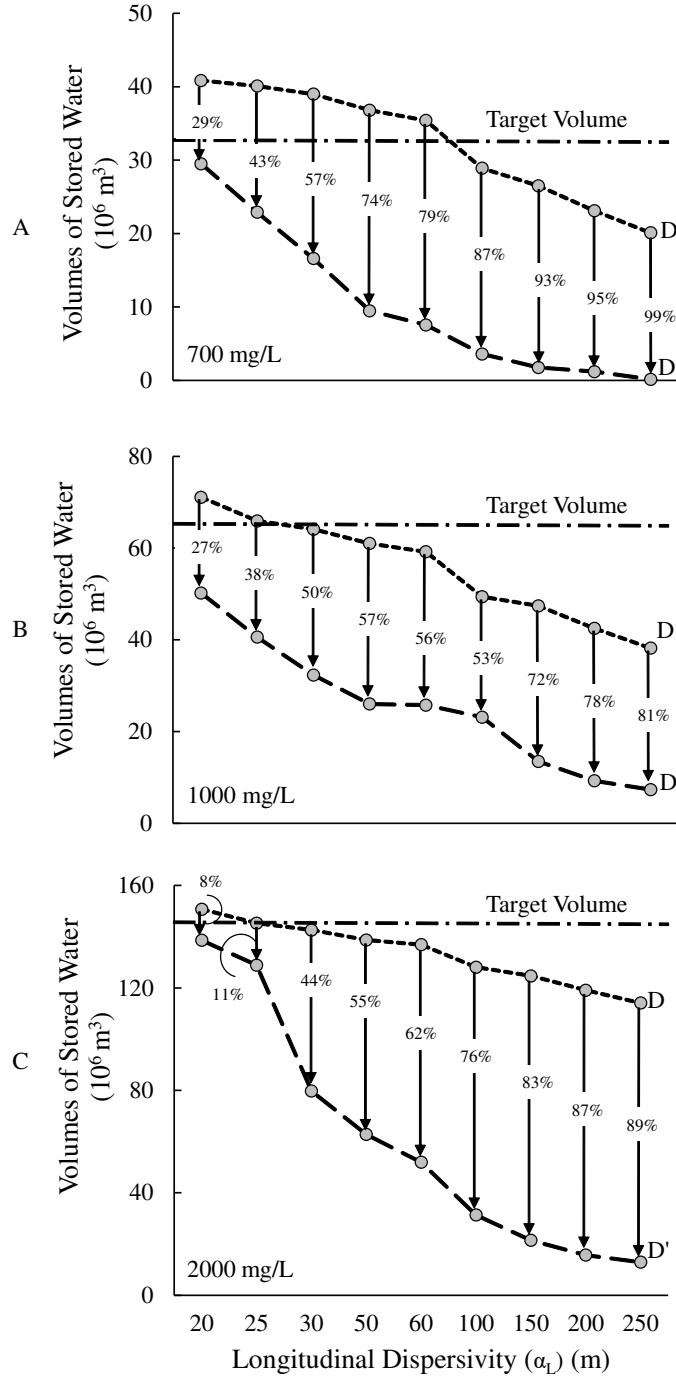


Figure 4.8. Sensitivity of lens volume to vertical transverse dispersivity: A) 700 mg/L, B) 1000 mg/L, and C) 2000 mg/L water quality categories. (D represents fixed α_v and equal to 0.1 m, whereas D' represents variable α_v as a function of $1/100\alpha_L$) (Vertical lines show the reduction percentage of simulated volumes of stored water from using D' compared with D)

4.6. Summary and Conclusions

Fresh groundwater lenses (FGLs) have functional significance known worldwide in several formation settings, such as coastal areas, atoll islands, riverine floodplains, and subterranean oases in arid regions. Recently, the formation of these FGLs has received particular attention and extensive research, as they create groundwater supplies of great potential value for humans and ecosystems, and they are in danger of salinization due to natural events and anthropogenic activities. Numerical modeling solutions have been widely applied to investigating FGLs because they allow for transient density-dependent flow and transport involving dispersivity and aquifer heterogeneity.

However, characterization of the large-scale dispersivity for a FGL is essential to any effort to simulate mixing between fresh water and seawater or brackish water. From several studies, information on the large-scale dispersivity for FGLs is both uncertain and limited to approaches based on the scaling approach, grid Peclet number, or on previous studies of the same study area without calibration. These approaches to implementation have requirements beyond the limited field data and are hindered by the difficulty of measuring the large-scale dispersivity in situ because it needs long-term monitoring (years) over large spatial scales in order to capture the natural environmental processes of the mixing. Therefore, a realistic and feasible method to assess the uncontrolled environmental events of the FGLs is to fit a groundwater flow and solute transport model to historical data.

The availability of an extensive pre-development subsurface dataset collected in the Rawdatain basin in Kuwait makes the Rawdatain FGL an ideal case among the FGLs in the Arabian Peninsula (AP) for determining values of large-scale dispersivity. The main objective was to provide a realistic range of longitudinal (α_L), horizontal transverse (α_h), and vertical

transverse (α_v) dispersivity values for the Rawdatain FGL. In this study, a 3D density-dependent groundwater flow and solute transport model was tested against the following data targets to estimate the dispersivity values: groundwater head, spatially-variable total dissolved solids (TDS) concentration in groundwater, three lens volume targets, three lens thickness targets, and geometrical shape features of the lens along a cross-section.

A total of 28 different sets of 3D dispersivity values, encompassing a wide range of feasible longitudinal dispersivity values for the Rawdatain FGL (1–500 m), were tested against the multiple targets and compared with the groundwater age of the Rawdatain lens. D18, D14 and D17 were the best dispersivity sets in terms of performance, based on the three volume targets of 700 mg/L, 1000 mg/L, and 2000 mg/L, respectively, with absolute errors of 8.7%, 1.2% and 3.4%. Based on the three thickness targets, the best three dispersivity sets were D21, D9 and D5, respectively, with absolute errors of 0.4%, 0.6% and 0.1%. In terms of the Scaled Root Mean Square Error (S-RMSE) of TDS point data, the range of S-RMSE for all of the dispersivity sets ranged from 0.185 to 0.305, where the best dispersivity sets were D13 to D19, with values between 0.185 and 0.195. In contrast, there was no best performance of the dispersivity sets that could be distinguished in terms of the Mean Absolute Error (MAE) of the groundwater heads. The MAE range for all dispersivity sets was between 0.31 and 0.33 m, indicating a lower sensitivity to dispersivity values than to other calibration targets.

Finally, a multi-criteria score-based method was performed to rank the best performance of the dispersivity sets among all of the targets with an equal weight. The highest ranked dispersivity was D16, with a total score of 49. Indeed, the D16 set satisfied the three volume targets with absolute errors of 12.9%, 5.3% and 6.9%, respectively, and it satisfied the three lens thickness targets with absolute errors of 10.5%, 3.9%, and 2.6%, respectively. In addition, the

D16 set achieved a good fit between the measured and simulated TDS point data, with an S-RMSE of TDS equal to 0.188. Regarding the qualitative assessment of the overall lens shape, the D16 set displayed a favorable visual comparison with the longitudinal and transverse cross-sections and a close match to the field range of TDS. Hence, the D16 dispersivity set ($\alpha_L = 50$ m: $\alpha_h = 5$ m: $\alpha_v = 0.1$ m) represents the best large-scale environmental dispersivity values for the Rawdatain FGL.

The method presented herein demonstrates the capability of estimating 3D large-scale environmental dispersivity by using a density dependent groundwater flow and solute transport model tested against multiple calibration targets. This method would not have been successful without implementing the multi-calibration targets approach, which was helpful in eliminating several non-unique calibration parameters and in decreasing the uncertainty of the calibrated parameters. This methodology can be applied to other FGLs to overcome the limitations and cons of in-situ large-scale dispersivity measurement. Identifying reliable and presentable 3D environmental dispersivity values for a FGL will be very valuable to water managers for analyzing future water security in the AP and establishing appropriate water supply plans. In particular, the mixing rate would affect any use of these FGLs as long-term storage for emergency uses.

REFERENCES

- Abarca, E., Pool, M., Carrera, J., & Dentz, M. (2006, December). Can Seawater Intrusion Modeling be Simplified?. In AGU Fall Meeting Abstracts.
- Abderrahman, W. A., Rasheeduddin, M., Al-Harazin, I. M., Esuflebbe, M., & Eqnaibi, B. S. (1995). Impacts of management practices on groundwater conditions in the eastern province, Saudi Arabia. *Hydrogeology Journal*, 3(4), 32-41.
- Abdulrazzak, M. J. (1994). Review and assessment of water resources in Gulf Cooperation Council countries. *International Journal of Water Resources Development*, 10(1), 23-37.
- Abdulrazzak, M. J. (1995). Water supplies versus demand in countries of Arabian Peninsula. *Journal of Water Resources Planning and Management*, 121(3), 227-234.
- Alaghmand, S., Beecham, S., Jolly, I. D., Holland, K. L., Woods, J. A., & Hassanli, A. (2014). Modelling the impacts of river stage manipulation on a complex river-floodplain system in a semi-arid region. *Environmental modelling & software*, 59, 109-126.
- Alaghmand, S., Beecham, S., Woods, J. A., Holland, K. L., Jolly, I. D., Hassanli, A., & Nouri, H. (2015). Injection of fresh river water into a saline floodplain aquifer as a salt interception measure in a semi-arid environment. *Ecological engineering*, 75, 308-322.
- Alam, K., & Falkland, A. (1997). Vulnerability to climate change of the Bonriki freshwater lens, Tarawa. Report No HWR97/11, ECOWISE Environmental, ACTEW Corporation, prepared for Ministry of Environment and Social Development, Republic of Kiribati.
- Al-Katheeri, E. S. (2008). Towards the establishment of water management in Abu Dhabi Emirate. *Water resources management*, 22(2), 205.
- Alrashed, M. F., & Sherif, M. M. (2000). Water resources in the GCC countries: an overview. *Water resources management*, 14(1), 59-75.
- Alrashidi, M. S., & Bailey, R. T. (2019a). Estimating groundwater recharge for a fresh groundwater lens in an arid region: formative and stability assessment. *Hydrological Processes*, (Revised).
- AlRukaibi, D., & McKinney, D. C. (2013). Conceptual Designing and Numerical Simulation of the ASR Technique Operations-Case Study Kuwait. In *World Environmental and Water Resources Congress 2013: Showcasing the Future* (pp. 2601-2613).
- Al-Ruwaih, F., Shehata, M., & Al-Awadi, E. (2000). Groundwater utilization and management in the State of Kuwait. *Water international*, 25(3), 378-389.

- Alsharhan, A. S., Rizk, Z. A., Nairn, A. E. M., Bakhit, D. W., & Alhajari, S. A. (Eds.). (2001). *Hydrogeology of an arid region: the Arabian Gulf and adjoining areas*. Elsevier.
- Alsumaiei, A. A., & Bailey, R. T. (2018). Quantifying threats to groundwater resources in the Republic of Maldives Part I: Future rainfall patterns and sea-level rise. *Hydrological Processes*, 32(9), 1137-1153.
- Amery, H. A. (2002). Water wars in the Middle East: a looming threat. *Geographical Journal*, 168(4), 313-323.
- Amery, H. A. (2015). *Arab water security: Threats and opportunities in the Gulf States*. Cambridge University Press.
- Anderman, E. R., Hill, M. C., & Poeter, E. P. (1996). Two-dimensional advective transport in ground-water flow parameter estimation. *Groundwater*, 34(6), 1001-1009.
- Anderson, M. P., Woessner, W. W., & Hunt, R. J. (2015). *Applied groundwater modeling: simulation of flow and advective transport*. Academic press.
- Anthony, S. S. (1992). Electromagnetic methods for mapping freshwater lenses on Micronesian atoll islands. *Journal of Hydrology*, 137(1-4), 99-111.
- Arya, A., Hewett, T. A., Larson, R. G., & Lake, L. W. (1988). Dispersion and reservoir heterogeneity. *SPE Reservoir Engineering*, 3(01), 139-148.
- Asghar, M. N., Prathapar, S. A., & Shafique, M. S. (2002). Extracting relatively-fresh groundwater from aquifers underlain by salty groundwater. *Agricultural Water Management*, 52(2), 119-137.
- Ataie-Ashtiani, B., Rajabi, M. M., & Ketabchi, H. (2013). Inverse modelling for freshwater lens in small islands: Kish Island, Persian Gulf. *Hydrological Processes*, 27(19), 2759-2773.
- Authman, M. N. (1983). *Water and development processes in Saudi Arabia*, Tihama Press, Jeddah, Saudi Arabia.
- BAAC (British Arabian Advisory Company). 1980. *Water demand and re-use*. Ministry of Agriculture and Water, Riyadh, Saudi Arabia. 246 pp.
- Bailey, R. T., & Jenson, J. W. (2014). Effects of marine overwash for atoll aquifers: environmental and human factors. *Groundwater*, 52(5), 694-704.
- Bailey, R. T., Jenson, J. W., & Olsen, A. E. (2009). Numerical modeling of atoll island hydrogeology. *Groundwater*, 47(2), 184-196.
- Bailey, R. T., Jenson, J. W., & Olsen, A. E. (2010). Estimating the ground water resources of atoll islands. *Water*, 2(1), 1-27.

- Bailey, R. T., Jenson, J. W., Rubinstein, D., & Olsen, A. E. (2008). Groundwater resources of atoll islands: Observations, modeling, and management. Water and Environmental Research Institute of the Western Pacific, University of Guam.
- Bailey, R. T., Khalil, A., & Chatikavanij, V. (2014). Estimating transient freshwater lens dynamics for atoll islands of the Maldives. *Journal of hydrology*, 515, 247-256.
- Barkey, B., & Bailey, R. (2017). Estimating the impact of drought on groundwater resources of the Marshall Islands. *Water*, 9(1), 41.
- Barth, G. R., & Hill, M. C. (2005b). Parameter and observation importance in modelling virus transport in saturated porous media—investigations in a homogenous system. *Journal of contaminant hydrology*, 80(3-4), 107-129.
- Barth, G., & Hill, M. C. (2005a). Numerical methods for improving sensitivity analysis and parameter estimation of virus transport simulated using sorptive–reactive processes. *Journal of contaminant hydrology*, 76(3-4), 251-277.
- Bauer, P., Held, R. J., Zimmermann, S., Linn, F., & Kinzelbach, W. (2006). Coupled flow and salinity transport modelling in semi-arid environments: The Shashe River Valley, Botswana. *Journal of Hydrology*, 316(1-4), 163-183.
- Bauer-Gottwein, P., Rasmussen, N. F., Feificova, D., & Trapp, S. (2008). Phytotoxicity of salt and plant salt uptake: Modeling ecohydrological feedback mechanisms. *Water Resources Research*, 44(4).
- Berens, V., White, M., Souter, N., 2009. Bookpurnong Living Murray Pilot Project: A trial of three floodplain water management techniques to improve vegetation condition, Rep. no. 2009/21, 1-2 Department of Water, Land and Biodiversity Conservation, Adelaide, Australia. https://www.waterconnect.sa.gov.au/Content/Publications/DEW/dwlbc_report_2009_21.pdf
- Bergstrom, R. E., & Aten, R. E. (1965). Natural recharge and localization of fresh ground water in Kuwait. *Journal of Hydrology*, 2(3), 213-231.
- Buddemeier, R. W., & Oberdorfer, J. A. (2004). Hydrogeology of Enewetak atoll. In *Developments in Sedimentology* (Vol. 54, pp. 667-692). Elsevier.
- Bureau De Recherche Geologiques et Mineres (BRGM). 1977. Al-Hassa development project: groundwater resources study and management program, unpublished report to Ministry of Agriculture and Water, Riyadh, 4 vols.
- Cartwright, I., Werner, A. D., & Woods, J. A. (2019). Using geochemistry to discern the patterns and timescales of groundwater recharge and mixing on floodplains in semi-arid regions. *Journal of Hydrology*.
- Cendón, D. I., Larsen, J. R., Jones, B. G., Nanson, G. C., Rickleman, D., Hankin, S. I., ... & Maroulis, J. (2010). Freshwater recharge into a shallow saline groundwater system, Cooper Creek floodplain, Queensland, Australia. *Journal of Hydrology*, 392(3-4), 150-163.

- Chui, T. F. M., & Terry, J. P. (2012). Modeling fresh water lens damage and recovery on atolls after storm-wave washover. *Groundwater*, 50(3), 412-420.
- Cobaner, M., Yurtal, R., Dogan, A., & Motz, L. H. (2012). Three dimensional simulation of seawater intrusion in coastal aquifers: A case study in the Goksu Deltaic Plain. *Journal of hydrology*, 464, 262-280.
- Comte, J. C., Banton, O., Join, J. L., & Cabioch, G. (2010). Evaluation of effective groundwater recharge of freshwater lens in small islands by the combined modeling of geoelectrical data and water heads. *Water Resources Research*, 46(6).
- Dawoud, M. A. (2005). The role of desalination in augmentation of water supply in GCC countries. *Desalination*, 186(1-3), 187-198.
- Delsman, J. R., Hu-A-Ng, K. R. M., Vos, P. C., De Louw, P. G., Oude Essink, G. H., Stuyfzand, P. J., & Bierkens, M. F. (2014). Paleo-modeling of coastal saltwater intrusion during the Holocene: an application to the Netherlands. *Hydrology and Earth System Sciences*, 18(10), 3891-3905.
- Din, S. U., Al Dousari, A., & Al Ghadban, A. N. (2007). Sustainable fresh water resources management in Northern Kuwait—a remote sensing view from Raudatain basin. *International journal of applied earth observation and geoinformation*, 9(1), 21-31.
- Döll, P., Jiménez-Cisneros, B., Oki, T., Arnell, N. W., Benito, G., Cogley, J. G., & Nishijima, A. (2015). Integrating risks of climate change into water management. *Hydrological Sciences Journal*, 60(1), 4-13.
- Eeman, S., Leijnse, A., Raats, P. A. C., & Van der Zee, S. E. A. T. M. (2011). Analysis of the thickness of a fresh water lens and of the transition zone between this lens and upwelling saline water. *Advances in Water Resources*, 34(2), 291-302.
- Egboka, B. C. E., Cherry, J. A., Farvolden, R. N., & Frind, E. O. (1983). Migration of contaminants in groundwater at a landfill: A case study: 3. Tritium as an indicator of dispersion and recharge. *Journal of Hydrology*, 63(1-2), 51-80.
- Fadlelmawla, A., & Al-Otaibi, M. (2005). Analysis of the water resources status in Kuwait. *Water resources management*, 19(5), 555-570.
- Fadlelmawla, A., Hadi, K., Zouari, K., & Kulkarni, K. M. (2008). Hydrogeochemical investigations of recharge and subsequent salinization processes at Al-Raudhatain depression in Kuwait. *Hydrological sciences journal*, 53(1), 204-223.
- Falkland, A.C., 1993. Water resources assessment, development and management of small coral islands. In: *Proceedings of the Regional Workshop on Small Island Hydrology*, 16th–19th February 1993, Batam Island, Indonesia, 26 p.

Fallatah, O. A., Ahmed, M., Save, H., & Akanda, A. S. (2017). Quantifying temporal variations in water resources of a vulnerable middle eastern transboundary aquifer system. *Hydrological Processes*, 31(23), 4081-4091.

FAO (Food and Agriculture Organization), 1998. Proceedings of the Second Expert Consultation on National Water Policy Reform in the Near East, Cairo, Egypt, 24–25 November 1997.

FAO. 1979. Survey and evaluation of available data on shared water resources in the Gulf States and Arabian Peninsula, Three Volumes, FAO, Rome.

Feehley, C. E., Zheng, C., & Molz, F. J. (2000). A dual-domain mass transfer approach for modeling solute transport in heterogeneous aquifers: Application to the Macrodispersion Experiment (MADE) site. *Water Resources Research*, 36(9), 2501-2515.

Feitelson, E., & Tubi, A. (2017). A main driver or an intermediate variable? Climate change, water and security in the Middle East. *Global Environmental Change*, 44, 39-48.

Fetter, C. W. (2000), *Applied Hydrogeology*, Prentice Hall, Upper Saddle River, N. J.

Garabedian, S. P. (1987). *Large-scale dispersive transport in aquifers: Field experiments and reactive transport theory* (Doctoral dissertation, Massachusetts Institute of Technology).

Garabedian, S. P., LeBlanc, D. R., Gelhar, L. W., & Celia, M. A. (1991). Large-scale natural gradient tracer test in sand and gravel, Cape Cod, Massachusetts: 2. Analysis of spatial moments for a nonreactive tracer. *Water Resources Research*, 27(5), 911-924.

Gelhar, L. W., Welty, C., & Rehfeldt, K. R. (1992). A critical review of data on field-scale dispersion in aquifers. *Water resources research*, 28(7), 1955-1974.

Gleick, P. H. (1994). Water, war & peace in the Middle East. *Environment: science and policy for sustainable development*, 36(3), 6-42.

Glimm, J., Lindquist, W. B., Pereira, F., & Zhang, Q. (1993). A theory of macrodispersion for the scale-up problem. *Transport in Porous Media*, 13(1), 97-122.

Gupta, S. K., Tanji, K. K., & Luthin, J. N. (1975). A three-dimensional finite element ground water model. UCAL-WRC-C-152, Calif. Water Resour. Cent., Univ. of Calif., Davis, 1975. (Available as NTIS PB 248-925 from Natl. Tech. Inf. Serv., Springfield, Va.)

Hill, M. C., & Tiedeman, C. R. (2006). *Effective groundwater model calibration: with analysis of data, sensitivities, predictions, and uncertainty*. John Wiley & Sons.

Hoehn, E., & Santschi, P. H. (1987). Interpretation of tracer displacement during infiltration of river water to groundwater. *Water Resources Research*, 23(4), 633-640.

Holding, S., & Allen, D. M. (2015). From days to decades: numerical modelling of freshwater lens response to climate change stressors on small low-lying islands. *Hydrology and Earth System Sciences*, 19(2), 933-949.

- Houben, G., Noell, U., Vassolo, S., Grissemann, C., Geyh, M., Stadler, S., ... & Vera, S. (2014). The freshwater lens of Benjamín Aceval, Chaco, Paraguay: a terrestrial analogue of an oceanic island lens. *Hydrogeology journal*, 22(8), 1935-1952.
- Hsieh, P. A., & Winston, R. B. (2002). User's guide to Model Viewer, a program for three-dimensional visualization of ground-water model results (No. 2002-106).
- Hunt, A. G., & Skinner, T. E. (2010). Predicting dispersion in porous media. *Complexity*, 16(1), 43-55.
- Hunt, A. G., Ghanbarian, B., Skinner, T. E., & Ewing, R. P. (2015). Scaling of geochemical reaction rates via advective solute transport. *Chaos: An Interdisciplinary Journal of Nonlinear Science*, 25(7), 075403.
- Illangasekare, T., Tyler, S. W., Clement, T. P., Villholth, K. G., Perera, A. P. G. R. L., Obeysekera, J., ... & Kaluarachchi, J. J. (2006). Impacts of the 2004 tsunami on groundwater resources in Sri Lanka. *Water Resources Research*, 42(5).
- Italconsult. 1969. Water and Agricultural Development Studies for Area IV. Eastern Province. Saudi Arabia: Riyadh, Saudi Arabia: Unpublished report to Ministry of Agriculture and Water.
- James, W. P., Chakka, K. B., & Mascianglioli, P. A. (1996). CONTROL OF NATURAL BRINE SPRINGS IN BRAZOS RWER BASIN PART I: RECOVERY SYSTEM 1. *JAWRA Journal of the American Water Resources Association*, 32(3), 475-484.
- Jayawickreme, D. H., Santoni, C. S., Kim, J. H., Jobbágy, E. G., & Jackson, R. B. (2011). Changes in hydrology and salinity accompanying a century of agricultural conversion in Argentina. *Ecological Applications*, 21(7), 2367-2379.
- Jolly, I. D., Narayan, K. A., Armstrong, D., & Walker, G. R. (1998). The impact of flooding on modelling salt transport processes to streams. *Environmental Modelling & Software*, 13(1), 87-104.
- Jolly, I. D., Walker, G. R., & Thorburn, P. J. (1993). Salt accumulation in semi-arid floodplain soils with implications for forest health. *Journal of Hydrology*, 150(2-4), 589-614.
- Julian, H. E., Boggs, J. M., Zheng, C., & Feehley, C. E. (2001). Numerical simulation of a natural gradient tracer experiment for the natural attenuation study: Flow and physical transport. *Groundwater*, 39(4), 534-545.
- Kim, K., Anderson, M. P., & Bowser, C. J. (1999). Model calibration with multiple targets: A case study. *Groundwater*, 37(3), 345-351.
- Konikow, L. F. (2011). The secret to successful solute-transport modeling. *Groundwater*, 49(2), 144-159.
- Kwarteng, A. Y., Viswanathan, M. N., Al-Senafy, M. N., & Rashid, T. (2000). Formation of fresh ground-water lenses in northern Kuwait. *Journal of arid environments*, 46(2), 137-155.

- Laattoe, T., Werner, A. D., Woods, J. A., & Cartwright, I. (2017). Terrestrial freshwater lenses: Unexplored subterranean oases. *Journal of hydrology*, 553, 501-507.
- Langevin, C., Thorne, D. J., Dausman, A., Sukop, M., & Guo, W. (2007). *User's Guide to SEAWAT: A Computer Program for Simulation of Three-Dimensional Variable-Density Ground-Water Flow*. United States Geological Survey.
- Le Grand ADSCO Ltd., Messrs, J.D., & Watson, D.M. 1959. *A Survey of the Freshwater Resources of the Northern Qatar*.
- LeBlanc, D. R., Garabedian, S. P., Hess, K. M., Gelhar, L. W., Quadri, R. D., Stollenwerk, K. G., & Wood, W. W. (1991). Large-scale natural gradient tracer test in sand and gravel, Cape Cod, Massachusetts: 1. Experimental design and observed tracer movement. *Water Resources Research*, 27(5), 895-910.
- Lee, E., Jayakumar, R., Shrestha, S., & Han, Z. (2018). Assessment of transboundary aquifer resources in Asia: Status and progress towards sustainable groundwater management. *Journal of Hydrology: Regional Studies*.
- Lowry, C. S., & Anderson, M. P. (2006). An assessment of aquifer storage recovery using ground water flow models. *Groundwater*, 44(5), 661-667.
- Maas, K. (2007). Influence of climate change on a Ghijben–Herzberg lens. *Journal of hydrology*, 347(1-2), 223-228.
- Macumber, P. G. (2003). Lenses, plumes and wedges in the Sultanate of Oman: a challenge for groundwater management. In *Developments in Water Science* (Vol. 50, pp. 349-370). Elsevier.
- Macumber, P. G., Al Abri, R., & Al Akhzami, S. (1998). Hydrochemical facies in the groundwater of central and southern Oman. In *Quaternary Deserts and Climatic Change* (pp. 511-520). Balkema Rottendam.
- Macumber, P. G., Barghash, B. G. S., Kew, G. A., & Tennakoon, T. B. (1995). Hydrogeologic implications of a cyclonic rainfall event in central Oman. *Groundwater quality*. Chapman and Hall, London, 87-97.
- Macumber, P. G., Barghash, B. G. S., Kew, G. A., & Tennakoon, T. B. (1995). Hydrogeologic implications of a cyclonic rainfall event in central Oman. *Groundwater quality*. Chapman and Hall, London, 87-97.
- Marsily, G. D. (1986). *Quantitative hydrogeology: groundwater hydrology for engineers* (No. 551.49 M3).
- Masterson, J. P., & Garabedian, S. P. (2007). Effects of sea-level rise on ground water flow in a coastal aquifer system. *Groundwater*, 45(2), 209-217.
- MAW (Ministry of Agriculture and Water), 1982. *Census of agriculture according to farm size, 1981–82*. MAW, Riyadh.

- MAW (Ministry of Agriculture and Water), 1984. Water Atlas of Saudi Arabia. Riyadh, MAW.
- McCallum, J. L., Cook, P. G., Dogramaci, S., Purtschert, R., Simmons, C. T., & Burk, L. (2017). Identifying modern and historic recharge events from tracer-derived groundwater age distributions. *Water Resources Research*, 53(2), 1039-1056.
- McDonald, M. G., & Harbaugh, A. W. (1988). A modular three-dimensional finite-difference ground-water flow model (Vol. 6, p. A1). Reston, VA: US Geological Survey.
- Mehl, S., & Hill, M. C. (2001). A comparison of solute-transport solution techniques and their effect on sensitivity analysis and inverse modeling results. *Groundwater*, 39(2), 300-307.
- Milewski, A., Sultan, M., Al-Dousari, A., & Yan, E. (2014). Geologic and hydrologic settings for development of freshwater lenses in arid lands. *Hydrological processes*, 28(7), 3185-3194.
- Moltaner, G. L., & Killey, R. W. D. (1988a). Twin Lake tracer tests: Longitudinal dispersion. *Water Resources Research*, 24(10), 1613-1627.
- Moltaner, G. L., & Killey, R. W. D. (1988b). Twin Lake tracer tests: Transverse dispersion. *Water Resources Research*, 24(10), 1628-1637
- Mukhopadhyay, A., Akber, A., Rashed, T., Kotwicki, V., Uddin, S., & Bushehri, A. (2016). Establishing a baseline to evaluate future impacts to groundwater resources in North Kuwait. *Environmental Earth Sciences*, 75(4), 324.
- Mukhopadhyay, A., Al-Sulaimi, J., & Barrat, J. M. (1994). Numerical Modeling of Ground-Water Resource Management Options in Kuwait. *Groundwater*, 32(6), 917-928.
- Neuman, S. P. (1990). Universal scaling of hydraulic conductivities and dispersivities in geologic media. *Water resources research*, 26(8), 1749-1758.
- New Zealand Ministry of Works and Development, Water and Soil Division (1977). Movement of contaminants into and through the Heretaunga Plains aquifer, report, Wellington.
- Oberdorfer, J. A., & Buddemeier, R. W. (1988). Climate change: effects on reef island resources (No. UCRL-98880; CONF-880873-3). Lawrence Livermore National Lab., CA (USA); San Jose State Univ., CA (USA). Dept. of Geology.
- Oberdorfer, J. A., Hogan, P. J., & Buddemeier, R. W. (1990). Atoll island hydrogeology: flow and freshwater occurrence in a tidally dominated system. *Journal of Hydrology*, 120(1-4), 327-340.
- Omar, S. A., Al-Yaqubi, A., & Senay, Y. (1981). Geology and groundwater hydrology of the State of Kuwait. *Journal of the Gulf and Arabian Peninsula Studies*, 1, 5-67.
- Oude Essink, G. H. P., Van Baaren, E. S., & De Louw, P. G. (2010). Effects of climate change on coastal groundwater systems: A modeling study in the Netherlands. *Water Resources Research*, 46(10).

- Panday, S., Huyakorn, P. S., Robertson, J. B., & McGurk, B. (1993). A density-dependent flow and transport analysis of the effects of groundwater development in a freshwater lens of limited areal extent: the Geneva area (Florida, USA) case study. *Journal of contaminant hydrology*, 12(4), 329-354.
- Parsons Corporation. 1964. Groundwater Resources of Kuwait, vols I, II and III. Ministry of Electricity and Water, Kuwait.
- Puri, S., & Aureli, A. (2005). Transboundary aquifers: a global program to assess, evaluate, and develop policy. *Groundwater*, 43(5), 661-668.
- Rabinowitz, D. D., & Gross, G. W. (1972). Environmental tritium as a hydrometeorologic tool in the Roswell Basin, New Mexico, Tech. Completion Rep. OWRR: A-O37-NMEX, NM Water Resour. Res. Inst., Las Cruces.
- Raffensperger, J. P. (1996). Numerical simulation of sedimentary basin-scale hydrochemical processes. In *Advances in porous media* (Vol. 3, pp. 185-305). Elsevier.
- Rajaram, H., & Gelhar, L. W. (1991). Three-dimensional spatial moments analysis of the Borden tracer test. *Water Resources Research*, 27(6), 1239-1251.
- Rizk, Z. S., & Alsharhan, A. S. (2003). Water resources in the United Arab Emirates. In *Developments in Water Science* (Vol. 50, pp. 245-264). Elsevier.
- Robson, S. G. (1978). Application of digital profile modeling techniques to ground-water solute transport at Barstow, California (No. 2050). Dept. of the Interior, Geological Survey: for sale by the Supt. of Docs., US Govt. Print. Off.
- Rotzoll, K., & Fletcher, C. H. (2013). Assessment of groundwater inundation as a consequence of sea-level rise. *Nature Climate Change*, 3(5), 477.
- Rumbaugh, J. O., & Rumbaugh, D. B. (2011). Guide to Using Groundwater Vistas, Version 6, Environmental Simulations. Inc., Reinholds, Pennsylvania, USA.
- Saiers, J. E., Genereux, D. P., & Bolster, C. H. (2004). Influence of calibration methodology on ground water flow predictions. *Groundwater*, 42(1), 32-44.
- Sakr, S. A. (1999). Validity of a sharp-interface model in a confined coastal aquifer. *Hydrogeology Journal*, 7(2), 155-160.
- Sanford, W. (2002). Recharge and groundwater models: an overview. *Hydrogeology journal*, 10(1), 110-120.
- Schulze-Makuch, D. (2005). Longitudinal dispersivity data and implications for scaling behavior. *Groundwater*, 43(3), 443-456.
- Segol, G., & Pinder, G. F. (1976). Transient simulation of saltwater intrusion in southeastern Florida. *Water Resources Research*, 12(1), 65-70.

- Senay, Y. (1973). Geohydrology of Al-Rawdhatain Field. Report to the Ministry of Electricity and Water, Kuwait, 24-43.
- Senay, Y. (1977). Groundwater resources and artificial recharge in Rawdhatain water field. Ministry of Electricity and Water, Kuwait, 35.
- Senay, Y. (1989). Artificial recharge and reproduction of fresh water at Rawdhatain for emergency use. Report to the Ministry of Electricity and Water, Kuwait.
- Shiklomanov, I. A. (1990). Global water resources. *Nature and resources*, 26(3), 34-43.
- Shiklomanov, I. A. (1998). World water resources: a new appraisal and assessment for the 21st century: a summary of the monograph World water resources. UNESCO.
- Simmons, C. T. (2005). Variable density groundwater flow: From current challenges to future possibilities. *Hydrogeology Journal*, 13(1), 116-119.
- Stewart, M. (1988). Electromagnetic mapping of fresh-water lenses on small oceanic islands. *Groundwater*, 26(2), 187-191.
- Stofberg, S. F., Essink, G. H. O., Pauw, P. S., De Louw, P. G., Leijnse, A., & van der Zee, S. E. (2017). Fresh Water Lens Persistence and Root Zone Salinization Hazard Under Temperate Climate. *Water resources management*, 31(2), 689-702.
- Sykes, J. F., Pahwa, S. B., Lantz, R. B., & Ward, D. S. (1982). Numerical simulation of flow and contaminant migration at an extensively monitored landfill. *Water Resources Research*, 18(6), 1687-1704.
- Sykes, J. F., Pahwa, S. B., Ward, D. S., & Lantz, R. B. (1983). The validation of SWENT, a geosphere transport model. In *Proceedings* (Vol. 2, pp. 8-13).
- Terry, J. P., & Chui, T. F. M. (2012). Evaluating the fate of freshwater lenses on atoll islands after eustatic sea-level rise and cyclone-driven inundation: a modelling approach. *Global and Planetary Change*, 88, 76-84.
- Terry, J. P., & Falkland, A. C. (2010). Responses of atoll freshwater lenses to storm-surge overwash in the Northern Cook Islands. *Hydrogeology Journal*, 18(3), 749-759.
- Underwood, M. R., Peterson, F. L., & Voss, C. I. (1992). Groundwater lens dynamics of atoll islands. *Water Resources Research*, 28(11), 2889-2902.
- UNESCO. (1979). Map of the world distribution of arid regions. *Man and Biosphere Tech Notes*, no. 7, UNESCO: Paris; 54.
- Vacher, H. L. (2004). Introduction: Varieties of carbonate islands and a historical perspective. In *Developments in Sedimentology* (Vol. 54, pp. 1-33). Elsevier.

- Vandenbohede, A. (2007). Visual MOCDENS3D: visualisation and processing software for MOCDENS3D, a 3D density dependent groundwater flow and solute transport model. User Manual. Research Unit Groundwater Modelling, Ghent University.
- Vengosh, A., & Rosenthal, E. (1994). Saline groundwater in Israel: its bearing on the water crisis in the country. *Journal of Hydrology*, 156(1-4), 389-430.
- Voss, C. I. (1984). A finite-element simulation model for saturated-unsaturated, fluid-density-dependent ground-water flow with energy transport or chemically-reactive single-species solute transport. *Water resources investigations report*, 84(4369), 409.
- Voss, C. I., & Souza, W. R. (1987). Variable density flow and solute transport simulation of regional aquifers containing a narrow freshwater-saltwater transition zone. *Water Resources Research*, 23(10), 1851-1866.
- Wallace, C. D., & Bailey, R. T. (2017). Geohydrologic factors governing atoll island groundwater resources. *Journal of Hydrologic Engineering*, 22(6), 05017004.
- Ward, J. D., Simmons, C. T., Dillon, P. J., & Pavelic, P. (2009). Integrated assessment of lateral flow, density effects and dispersion in aquifer storage and recovery. *Journal of Hydrology*, 370(1-4), 83-99.
- Werner, A. D., & Laattoe, T. (2016). Terrestrial freshwater lenses in stable riverine settings: Occurrence and controlling factors. *Water Resources Research*, 52(5), 3654-3662.
- Werner, A. D., & Simmons, C. T. (2009). Impact of sea-level rise on sea water intrusion in coastal aquifers. *Groundwater*, 47(2), 197-204.
- Werner, A. D., Sharp, H. K., Galvis, S. C., Post, V. E., & Sinclair, P. (2017). Hydrogeology and management of freshwater lenses on atoll islands: Review of current knowledge and research needs. *Journal of Hydrology*, 551, 819-844.
- Wilson, A. M. (2005). Fresh and saline groundwater discharge to the ocean: A regional perspective. *Water Resources Research*, 41(2).
- Wood, W. W. (1981). A geochemical method of determining dispersivity in regional groundwater systems. *Journal of Hydrology*, 54(1-3), 209-224.
- Woodroffe, C.D., Falkland, A.C., 2004. Chapter 31: geology and hydrogeology of the Cocos (Keeling) Islands. In: Vacher, H.L., Quinn, T.M. (Eds.), *Geology and Hydrogeology of Carbonate Islands, Developments in Sedimentology 54*. Elsevier, Amsterdam, pp. 885–908. 0-444-51644-1. ([https://doi.org/10.1016/S0070-4571\(04\)80053-0](https://doi.org/10.1016/S0070-4571(04)80053-0))
- Xu, M., & Eckstein, Y. (1995). Use of weighted least-squares method in evaluation of the relationship between dispersivity and field scale. *Groundwater*, 33(6), 905-908.
- Yihdego, Y., & Al-Weshah, R. A. (2017). Assessment and prediction of saline sea water transport in groundwater using 3-D numerical modelling. *Environmental Processes*, 4(1), 49-73.

Young, M. E., Macumber, P. G., Watts, M. D., & Al-Toqy, N. (2004). Electromagnetic detection of deep freshwater lenses in a hyper-arid limestone terrain. *Journal of Applied Geophysics*, 57(1), 43-61.

Zech, A., Attinger, S., Cvetkovic, V., Dagan, G., Dietrich, P., Fiori, A., & Teutsch, G. (2015). Is unique scaling of aquifer macrodispersivity supported by field data?. *Water resources research*, 51(9), 7662-7679.

Zhang, Q., Volker, R. E., & Lockington, D. A. (2004). Numerical investigation of seawater intrusion at Gooburrum, Bundaberg, Queensland, Australia. *Hydrogeology Journal*, 12(6), 674-687.

Zheng, C., & Wang, P. P. (1999). MT3DMS: a modular three-dimensional multispecies transport model for simulation of advection, dispersion, and chemical reactions of contaminants in groundwater systems; documentation and user's guide. Alabama University.

Zubari, W. K. (1999). The Dammam aquifer in Bahrain—Hydrochemical characterization and alternatives for management of groundwater quality. *Hydrogeology Journal*, 7(2), 197-208.

CHAPTER 5. ASSESSMENT OF THE NATURAL AND ANTHROPOGENIC IMPACTS ON A FRESH GROUNDWATER LENS IN A SUBTERRANEAN OASIS IN KUWAIT

Highlights

The sole natural source of fresh water available in Kuwait is the Rawdatain Fresh groundwater lens (FGL), and it stands as a secured strategic reserve for emergency uses. Understanding the natural formation, assessing the effect of historical and future anthropogenic activities and evaluating artificial recharge for lens recovery storage (LSR) is essential to better planning and management for this valuable resource. In this study, a 3D transient density dependent baseline model was established for the predevelopment period (2000 years) using a pulse recharge mechanism (PRM), including an assessment of recharge event frequency and a range of large-scale environmental dispersivity values as natural formative and destructive factors, respectively. Based on model testing against multiple data targets and water age, the 50 m longitudinal dispersivity set and a frequency of pulse recharge ($1 \times 10^6 \text{ m}^3$) of once every two years were selected to represent the natural dynamic of the Rawdatain FGL. The initial volumes for the three quality categories in 1963 were $28 \times 10^6 \text{ m}^3$ (700 mg/L), $69 \times 10^6 \text{ m}^3$ (1000 mg/L) and $142 \times 10^6 \text{ m}^3$ (2000 mg/L) before any significant pumping. Due to pumping (1963-2018), the volumes of the stored water decreased by 28%, 17% and 12% for the three water quality categories. For future annual pumping extractions (2019-2100), a rate of $0.16 \times 10^6 \text{ m}^3$ per year is appropriate for saving significant storage for emergency uses if needed, whereas higher pumping rates accelerate salinization. A future increase of 20% in natural recharge will not lead to significant recovery, and continued decline of the lens is expected even with no pumping. The artificial injection scenarios revealed that up to 100% LSR could be attained within 6 to 9 years,

depending on the amounts of injected water and the locations of injection wells. This study provides a first attempt to model the past, present and future of a FGL, and the methodology presented herein is suitable for similar FGLs in arid regions.

5.1. Introduction

As a country where surface water resources such as rivers or lakes do not exist, Kuwait has very limited natural water resources. The only naturally occurring body of water in Kuwait is the Arabian Gulf (AG), which is undrinkable due to its high salinity and exceeds 40,000 mg/L near the Kingdom of Bahrain (Burashid & Hussian, 2004). The AG, which extends from Shatt Al-Arab to the Strait of Hormuz, has an area of 240,000 square kilometers (Al Barwani & Purnama, 2008) and a mean depth of 36 m (Reynolds, 1993). The shallowness and high evaporation rate of the AG, as well as the low river discharges entering the sea, are the main factors contributing to its high surface salinity. In Kuwait, approximately 90% of the potable water production comes from the unconventional resource of seawater desalination from the AG, even if it is vulnerable to power interruptions and various other risks. However, Kuwait has recently started a program to reuse treated municipal wastewater to supplement its available freshwater resources. In Kuwait, municipal wastewater is treated at four main plants located in the Um-Al-Haiman, Riqqa, Jahra and Sulaibiya areas (Al-Anzi et al., 2011). Treated wastewater is generally used for the irrigation of gardens, highways, landscaping and limited farming activities.

Kuwait was classified within the most critical areas worldwide in terms of challenges of balancing between water scarcity, population growth, and food production (Mancosu et al., 2015). As consequences, water wars and disputes are likely to be triggered between neighboring countries and to threaten political stability in the Middle East in future decades (Gleick, 1994;

Amery, 2002&2015). Climate change is expected to result in an increase in the severity and frequency of droughts in the region (Döll et al., 2015; Feitelson & Tubi, 2017). Although a reliance on seawater desalination has been in place for many decades and most likely will continue into the foreseeable future, complete dependence on a highly industrialized source for fresh water has major drawbacks such as the lack of a secured strategic water reserve. As such, the very limited fresh and brackish groundwater resources in the region must be maintained responsibly.

Two regional groundwater aquifer systems, the Kuwait Group and Dammam aquifers, make up the only conventional water resources in Kuwait. These aquifers produce brackish water, with TDS contents of 2,500-7,500 mg/L, which is mainly used as raw water for desalination and also for irrigation, watering of gardens, and blending with distilled water to raise TDS. These waters become more saline as they flow from recharge zones in Saudi Arabia and southern Iraq to the discharge zone along the coast of the Arabian Gulf (Alsharhan et al., 2001). The occurrence of fresh groundwater is restricted to discontinuous fresh groundwater lenses (FGLs) in the northern parts of Kuwait, where it occurs in the form of freshwater lenses floating atop brackish water in the aquifer sediments. The potentiality of these lenses is relatively small and depends on surface runoff recharge from rainfall events, and thus it may vary considerably from one year to another.

The FGLs in Kuwait have been the subject of comprehensive investigations from the 1960s to the present because they are the only source of fresh water in Kuwait. Early in the 1960s, the Parsons Corporation named two large FGLs in the northern part (the Rawdatain and Umm Al-Aish basins) and several small lenses in the Al-Qashaniya, Mutla and Al-Abdali areas (Parsons Corporation, 1964). The volumes of stored water with less than 2000 mg/L TDS in

these lenses in the Rawdatain and Umm Al-Aish areas were approximately 136 and 72 million m³, respectively. In 1964, the Parsons studies were reevaluated by experts from the United Arab Republic (U.A.R) at the invitation of the Ministry of Electricity and Water in Kuwait. These two studies have provided much data associated with these lenses. The Umm-Aish FGL was affected by hydrocarbon pollution after the 1991 Gulf War (Mukhopadhyay et al., 2008). Because of that, the Rawdatain FGL has been of interest to many studies, such as Bergstrom and Aten (1964), Robinson & Al-Ruwaih (1985), Al-Sulaimi et al. (1997), Din et al. (2007), Kwarteng et al. (2000), Al-Dousari et al. (2010), Al-Senafy et al. (2013), Mukhopadhyay et al. (2016), Al-Weshah & Yihdego (2016), and Yihdego & Al-Weshah (2017).

Several studies highlighted the need for maintaining a large volume of stored groundwater in the Rawdatain FGL to meet the demand for water under emergency conditions (Senay, 1977; Al-Otaibi & Mukhopadhyay, 2005; Darwish & Al Awadhi, 2009). Al-Senafy et al. (2013) recommended using a suitable numerical modeling package to study the dynamics of groundwater flow and solute transport in the Rawdatain basin. They believed that this type of model could provide estimates of the volume and quality of recoverable groundwater based on reserve mining utilization scenarios. Alrashidi & Bailey (2019a) have successfully established a baseline model that represents the natural development and stability of the Rawdatain FGL using a 3D density-dependent groundwater flow model with constant recharge mechanism (CRM) tested against multiple data targets and water age. They found that the long-term average recharge (500,000 m³/year) is very minimal compared with the Rawdatain freshwater lens volume. Additionally, the best ranges of the environmental dispersivity values for the Rawdatain FGL that characterize the natural mixing between the main formative factor (i.e., recharge rate) and the major pre-development loss factor (i.e., regional brackish water) were 30-60 m, 3-5 m,

and 0.1 m in the longitudinal, transverse horizontal, and transverse vertical directions, respectively.

The objective of this study is to assess the Rawdatain freshwater lens in Kuwait and its effective management and conservation, as it constitutes a strategic natural source in the country. The main aims of this study are to assess the effect of historical pumping patterns on freshwater lens volumes, which consists of a high-pumping period (1963-1978) and a low-pumping period (1981-2018), followed by the evaluation of future scenarios of pumping rates, natural recharge rates, and artificial recharge rates on lens dynamics through the year 2100. The methodology and model can be used for other freshwater lenses in Kuwait and the Arabian Gulf countries, which are characterized by similar prevalent climatic and environmental conditions.

5.2. Background

5.2.1 The State of Kuwait

The state of Kuwait is one of the smallest countries in the Middle East, and one of the Gulf Cooperation Council (GCC) countries. It is located in the northwestern portion of the Arabian Peninsula, where it covers an area of 17,818 km² and has a total coastline of 195 km. Its geographic coordinates are between latitudes 28.4° and 30.2° N and longitudes 46.4° and 48.5° E. It shares borders with Iraq to the north and northwest and the Kingdom of Saudi Arabia to the south and southwest, and the Arabian Gulf bounds Kuwait to the east. Kuwait is divided into six governorates and has nine islands. The total population of Kuwait was 4,777,433 in mid-2019, of which only 1,414,297 were Kuwaitis and the rest were foreign, according to the official website of the Public Authority for Civil Information. The population growth rate has fluctuated rapidly due to the large population percentage of foreigners. Kuwait depends mainly on crude oil reserves of approximately 104 billion barrels - approximately 8% of the world reserves. People

in Kuwait have access to improved water sources and sanitation facilities (99% and 100%, respectively) (source: World Bank, World Development Indicators, 2015).

Like most parts of the Arabian Shield, Kuwait is characterized by a desert-type environment with scanty rainfall, and a dry, hot climate. Summer is very hot, especially in July and August, with a mean temperature of 37.4°C and a mean maximum temperature of 45°C. The average total yearly potential precipitation recorded between 1962 and 2014 was 115 mm. The maximum and minimum annual potential precipitation for the same period was 260 mm in 1975 to 1976, and 28 mm in 1963 to 1964, respectively. Although detectable rainfall usually begins in November and ends in April, Almedej (2012) described rare occasions in which rainfall occurred in October and May. From the number of years of rainfall data available, there appears to be no conspicuous pattern of highs and lows. In sharp contrast, extreme rainfall events, such as the one that occurred in Kuwait City on 11 November 1997, can cause excessive rainfall (greater than 100 mm) in just hours, resulting in large surface runoff and property damage (Al-Rashed and Sherif 2000). The average daily potential evaporation varies from as low as 3.2 mm/day in January to as high as 21.0 mm/day in July, with an annual total of approximately 4040 mm.

5.2.2 The Rawdatain Freshwater Lens

The Rawdatain FGL is located in the topographically closed Rawdatain depression, which is approximately 60 km north-northwest of Kuwait City, as shown in Figure 5.1. The Rawdatain basin has a unique drainage system, which includes 12 wadis that drain into the depression. The drainage system lies approximately between latitudes 29° 40'N and 29° 59'N and longitudes 47° 20'E and 47° 44'E. The lithology shows that the Rawdatain FGL is hosted within the unconfined Dibdibba Formation, which consists mainly of sand and gravel and is only

present in the north of Kuwait (Al-Senafy & Al-Fahad, 2000). The Kuwait Group, which ranges in thickness from 150 to 400 m, mainly consists of clastic sediments with minor amounts of gypsum and calcareous limestone. It is divided into three formations: the Dibdibba (Pleistocene), Lower Fars (Lower-Middle Miocene), and Ghar (Oligocene-Lower Miocene) Formations, from youngest to oldest. The Kuwait Group system overlies the Dammam aquifer (Eocene), which is exploited in the southwestern and central parts of Kuwait where it produces brackish water with salinity ranging from 2500 to 5000 mg/L (Mukhopadhyay, 1995).



Figure 5.1. State of Kuwait and the Rawdatain model domain

The Rawdatain FGL, as mapped to date, is roughly 10 km long and 5 km wide, with an average thickness of approximately 25 m and a maximum thickness of 35 m. The average freshwater volume based on pre-development data (Parsons Corporation 1964, UAR 1964) has been estimated at 33 million m³ of groundwater below 700 mg/L TDS, 64 million m³ below 1000 207 mg/L, and 149 million m³ below 2000 mg/L. Since the start of freshwater production (i.e. pumping) in 1964, the groundwater quality in the lens has changed significantly, such that the quality of freshwater produced from the lens has deteriorated with pumping time due to increased mixing between the freshwater of the lens and the underling brackish water body (Kwarteng et al., 2000; Mukhopadhyay et al., 2016). This will be discussed more in Section 5.3.2.

5.2.3 Comparison with Other Freshwater Lenses

The phenomenon of subsurface freshwater lenses overlying saline or brackish groundwater is more common worldwide in places such as Israel (Vengosh & Rosenthal, 1994), Argentina (Jayawickreme et al., 2011), Australia (Jolly et al., 1993&1998; Cendón et al., 2010), Paraguay (Houben et al., 2014), Pakistan (Asghar et al., 2002), Botswana (Bauer et al., 2006&2008), and the USA (Panday et al., 1993; James et al., 1996). The FGLs in coastal areas and small atoll islands have received particular attention and extensive research in recent years because they are more in danger of salinization due to natural events than FGLs in subterranean oases in arid regions. Examples of the natural events in coastal areas include seawater intrusion due to sea level rise (Werner & Simmons, 2009), groundwater inundation (Rotzoll & Fletcher 2013), and tsunami events (Illangasekare et al., 2000), whereas events on atoll islands include drought conditions due to El Niño events (Bailey et al., 2009), and marine overwash events (Bailey & Jenson, 2014). In contrast, the FGLs in subterranean oases in arid regions are typically

far from coastal areas and less sensitive to reduction in annual recharge rates. However, they are more sensitive to anthropogenic activities because the annual replenishment from natural recharge is minimal compared to their storage volumes and pumping rates.

The formation setting of the Rawdatain FGL and other lenses in the subterranean oases in arid regions is different than the fresh groundwater lenses in the coastal and atoll islands settings in terms of geology, recharge mechanisms and boundary conditions. For instance, there is a sharp change in the hydraulic conductivity between the formations hosting the freshwater lens and seawater, such as the Holocene and Pleistocene aquifers in the atoll islands and terrestrial and marine formations in coastal areas, respectively. In contrast, the Rawdatain FGL floats above and is surrounded by the regional brackish or saline water within the same aquifer formation. Another factor is the density difference between the freshwater lens and the surrounding water. For instance, the Rawdatain lens is surrounded by brackish water with TDS values up to 5,000 to 8000 mg/L, whereas the seawater concentration in the coastal and atoll islands is up to 35,000 mg/L (i.e. the concentration of ocean water). The lower density difference between the fresh and brackish waters may lead to the Rawdatain freshwater lens being more susceptible to mixing.

In terms of recharge, the volumes of FGLs on atoll islands respond significantly and instantaneously to changes in precipitation due to the thin vadose zone (Alsumaiei & Bailey, 2018), where the average annual precipitation ranges from 1700 to 2350 mm/year. In contrast, a 50% reduction in annual recharge does not lead to a significant decline in the volume of the Rawdatain freshwater lens within a 100-year time frame (Alrashidi & Bailey, 2019a). Moreover, the recharge occurrence for the Rawdatain FGL depends on infrequent intensive rainfall events, and is classified as focused recharge beneath the playa and wadis. Regarding the boundary conditions, the sea level at coastlines and island perimeters represent a constant head condition

for the coastal areas and atoll islands, respectively. Furthermore, the effects of tidal activity on the dynamics of the freshwater lenses in those settings can be illustrated by numerical modeling using transient boundary conditions such as tidal fluctuations (Underwood et al., 1992; Ataie-Ashtiani et al., 1999) and sea level rise (Alsumaiei & Bailey, 2018). In contrast, there are no natural hydrologic boundaries within or near the Rawdatain freshwater lens. Thus, these different features should be assessed while establishing the first attempt to model the formation, stability and anthropogenic impacts of fresh groundwater lenses in subterranean oases in arid regions.

5.3. Methods

In Alrashidi & Bailey (2019a, 2019b), the original baseline model for the Rawdatain aquifer was developed using a constant recharge mechanism (CRM) to assess the formation and stability conditions of the lens, estimate long-term diffuse and focused groundwater recharge, and provide a realistic range of longitudinal (α_L), horizontal transverse (α_h), and vertical transverse (α_v) dispersivity values. In this study, a pulse recharge mechanism (PRM) is applied to assess the effects of natural, infrequent recharge events and anthropogenic pumping on the dynamics of the freshwater lens during both historical (1963-2018) and future (2019-2100) time periods. Lens storage recovery scenarios also will be explored. The model grid, boundary conditions, and other aquifer parameters are the same as in the baseline modeling studies (Alrashidi and Bailey, 2019a,b).

5.3.1 Pulse Recharge Mechanism (PRM)

The recharge for the Rawdatain FGL depends on surface runoff from infrequent cyclonic rainfall events that may vary considerably from year to year in terms of timing and magnitude. Table 5.1 shows the likelihood of potential runoff (excess precipitation) that may have occurred during 1962-2014 with different curve numbers. Senay (1977) found that the water table in Well

R-39 at the center of the depression of the Rawdatain FGL continued to rise for 10 days after a single rainstorm on December 29, 1976, and then the water table remained static afterward.

Alrashidi & Bailey (2019a) estimated the long-term average annual recharge for the Rawdatain FGL to be 500,000 m³/year, distributed into six recharge zones that represent both regional diffuse recharge and focused recharge beneath the depression, playa, and wadis. Instead of dividing the annual volume recharge over 365 days (i.e., the CRM scenario) as in the baseline model, in this study the annual recharge volume was divided into 10 days of recharge (i.e., the PRM scenario). Table 5.2 shows the annual volume recharge and annual recharge rate for each recharge zone, as well as a comparison between the CRM and PRM based on the duration and frequency. Three PRM scenarios are tested: once every 1 year (500,000 m³/year), once every 2 years (1,000,000 m³/year), and once every 4 years (2,000,000 m³/year), as shown in Table 5.2. For each PRM scenario, five longitudinal dispersivity values were also tested: 10, 30, 50, 60 and 100 m. The ratio of horizontal transverse dispersivity to longitudinal dispersivity was assumed to be 0.1 for all sets, and the vertical transverse dispersivity is fixed at 0.1 m

Table 5.1. Occurrence of potential runoff associated with different curve numbers from 1962 to 2014

Occurrence of Potential Runoff					Occurrence of Potential Runoff				
Year	(Excess Precipitation) (R) (mm/day)*				Year	(Excess Precipitation) (R) (mm/day)*			
	P > 26.2	P > 23.9	P > 21.8	P > 19.8		P > 26.2	P > 23.9	P > 21.7	P > 19.8
	(CN=66)	(CN=68)	(CN=70)	(CN=72)		(CN=66)	(CN=68)	(CN=70)	(CN=72)
1962	—	—	22.6	—	1988	—	—	—	—
1963	—	—	—	—	1989	—	—	—	—
1964	—	—	—	—	1990/1	NA	NA	NA	NA
1965	—	—	—	20.0	1992	—	—	—	—
1966	—	—	—	—	1993	45.1	26.0	21.9	—
1967	26.9	24.2, 25	—	—	1994	37.0	—	—	—
1968	—	—	—	—	1995	—	24.0	—	19.9
1969	—	—	—	—	1996	36.4,30.2	23.0	—	—
1970	—	—	—	20.1	1997	65.0	—	—	—
1971	32.3	—	—	—	1998	—	—	—	—
1972	—	—	21.9	20.2,20.6	1999	60.2	—	—	—
1973	—	—	—	—	2000	—	—	—	—
1974	—	25.4	—	—	2001	38.0	—	—	19.9
1975	38.2	—	—	—	2002	31.1	—	—	—
1976	38.4,48.4	—	—	20.4	2003	37.7,43.5	—	—	—
1977	—	—	22.6	—	2004	31.4,31	—	22.4,22.0	20.2,20.0
1978	—	24.4	—	—	2005	45.6,30.5	—	22.3	20.0
1979	27.6	—	—	—	2006	28.3	—	23.3	—
1980	—	24.0	23.8	—	2007	—	—	—	—
1981	—	—	—	—	2008	—	—	—	—
1982	32.4	—	—	—	2009	42.7	—	23.6	—
1983	—	—	—	—	2010	—	—	—	—
1984	—	—	—	—	2011	—	—	—	20.9
1985	—	—	23.6	—	2012	—	—	—	21.2
1986	—	—	—	—	2013	31.1,33.8	25.6	—	—
1987	—	—	—	—	2014	—	—	23.3	—

* Potential Runoff (R) = total precipitation (P) – initial abstraction (I_a)
 where I_a = 0.2S_{max} ; S_{max} is the potential maximum retention
 S_{max} (mm) = 25400/CN – 254; CN is curve number

Table 5.2. Model recharge zones and annual volume recharge scenarios

Recharge Zone	Annual Volume Recharge (m ³ /year)	Zone Area (km ²)	Annual Recharge (mm)	Recharge Scenarios					
				Constant Recharge		Pulse Recharge Frequency			
				Duration (day)	Recharge (mm)	Duration (day)	1-year Recharge (mm)	2-year Recharge (mm)	4-year Recharge (mm)
1	91500	133	0.7	365	0.002	10	0.069	0.137	0.275
2	54000	9.9	5.5	365	0.015	10	0.545	1.091	2.182
3	182000	1.9	95.8	365	0.262	10	9.579	19.158	38.316
4	76500	0.8	95.6	365	0.262	10	9.563	19.125	38.250
5	90500	9.6	9.4	365	0.026	10	0.943	1.885	3.771
6	5500	7.6	0.7	365	0.002	10	0.072	0.145	0.289

5.3.2 Historical Abstraction (1963-2018)

There are 26 production wells for the Rawdatain FGL, as shown in Figure 5.2. A total of 14 wells started pumping in 1963, and the remaining wells started one year later in 1964, as shown in Figures 5.3A and 5.3B, respectively. More details are provided in Table 5.3. Two historical abstraction regimes were considered, referred to as the periods of 1963-1978 and 1979-2018. The Rawdatain FGL was pumped extensively for water supply during the former period, with a total annual production between 1 and 4 million m³, as shown in Figure 5.4A. Afterwards, the production decreased in the later period due to an increase in groundwater salinity, in which the annual production rate has been limited to approximately 0.2 million m³ in recent years (MEW, 2015), as shown in Figure 5.4B. The Rawdatain freshwater lens is currently used for commercial bottling of drinking water (Din et al., 2007), whereas the entire field is standing as a strategic storage for use during an emergency (Mukhopadhyay et al., 2016). The new baseline model is used to assess the impact of the historical abstraction and to estimate the current lens volume. The total annual production volumes are divided by the number of active wells for each year, as shown in Table 5.4.

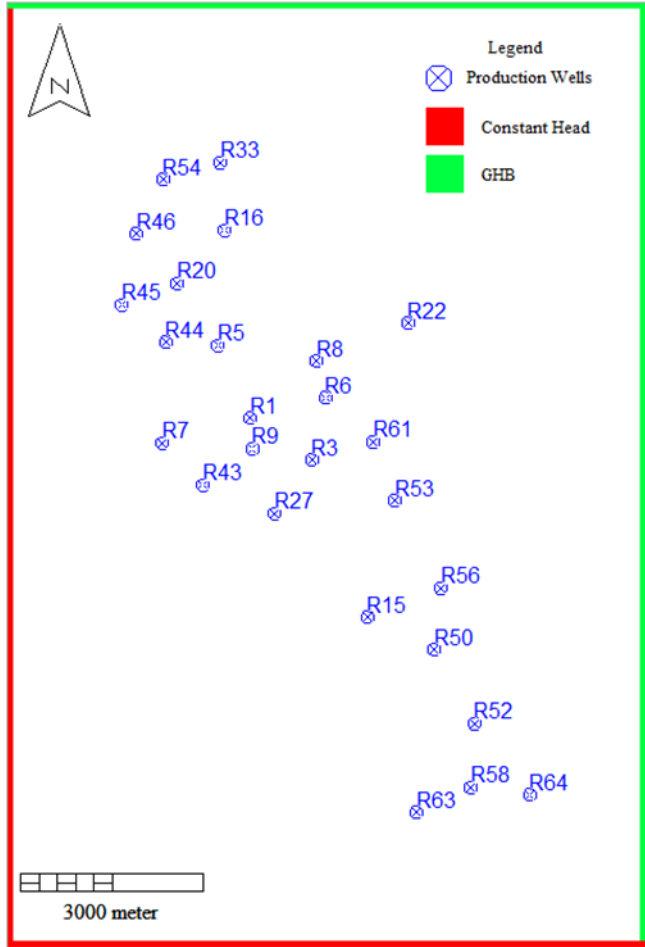


Figure 5.2. Model domain, boundary conditions, and production wells (GHB stand for general head boundary)

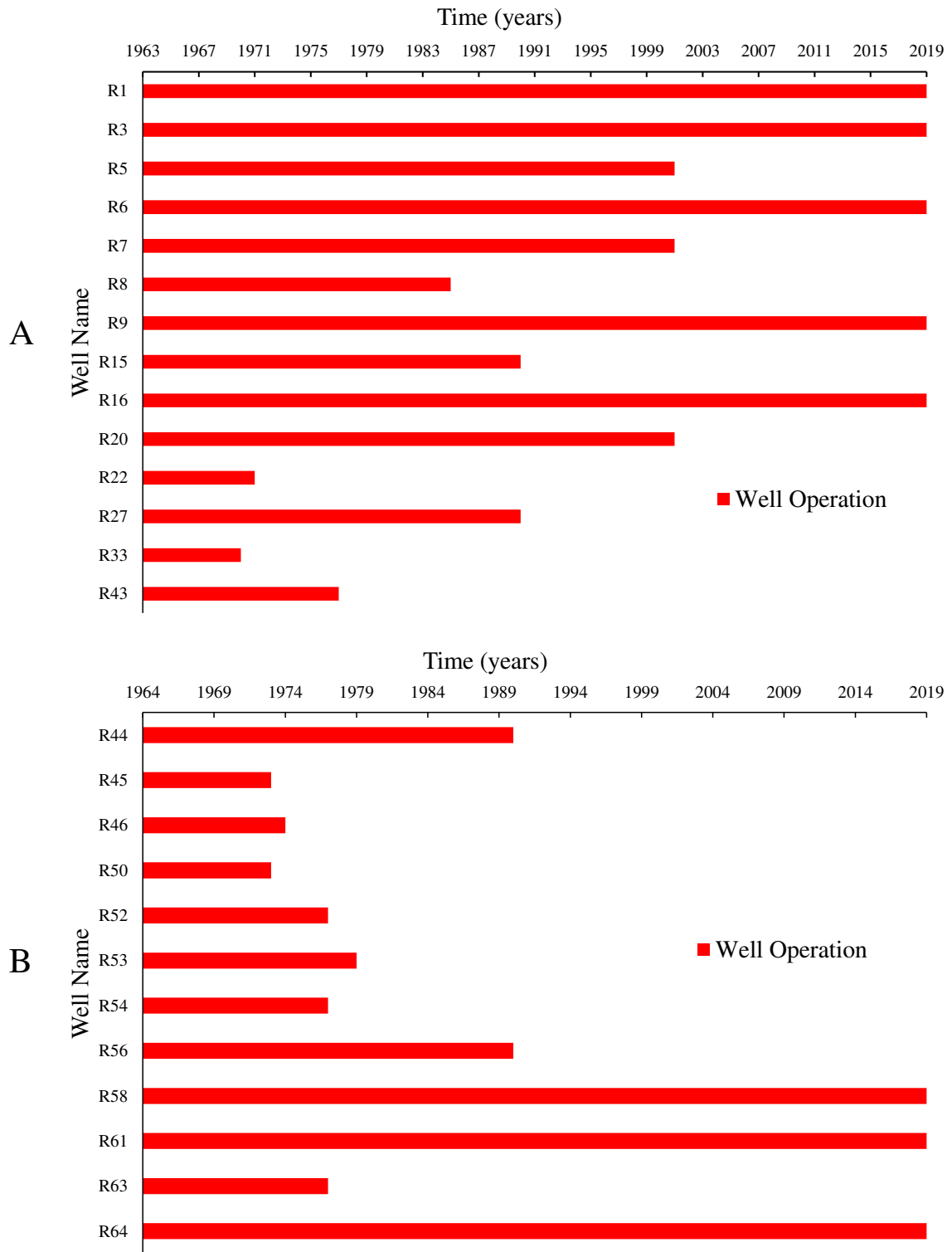


Figure 5.3. Wells operations: A) wells started from 1963. B) Wells started from 1964.

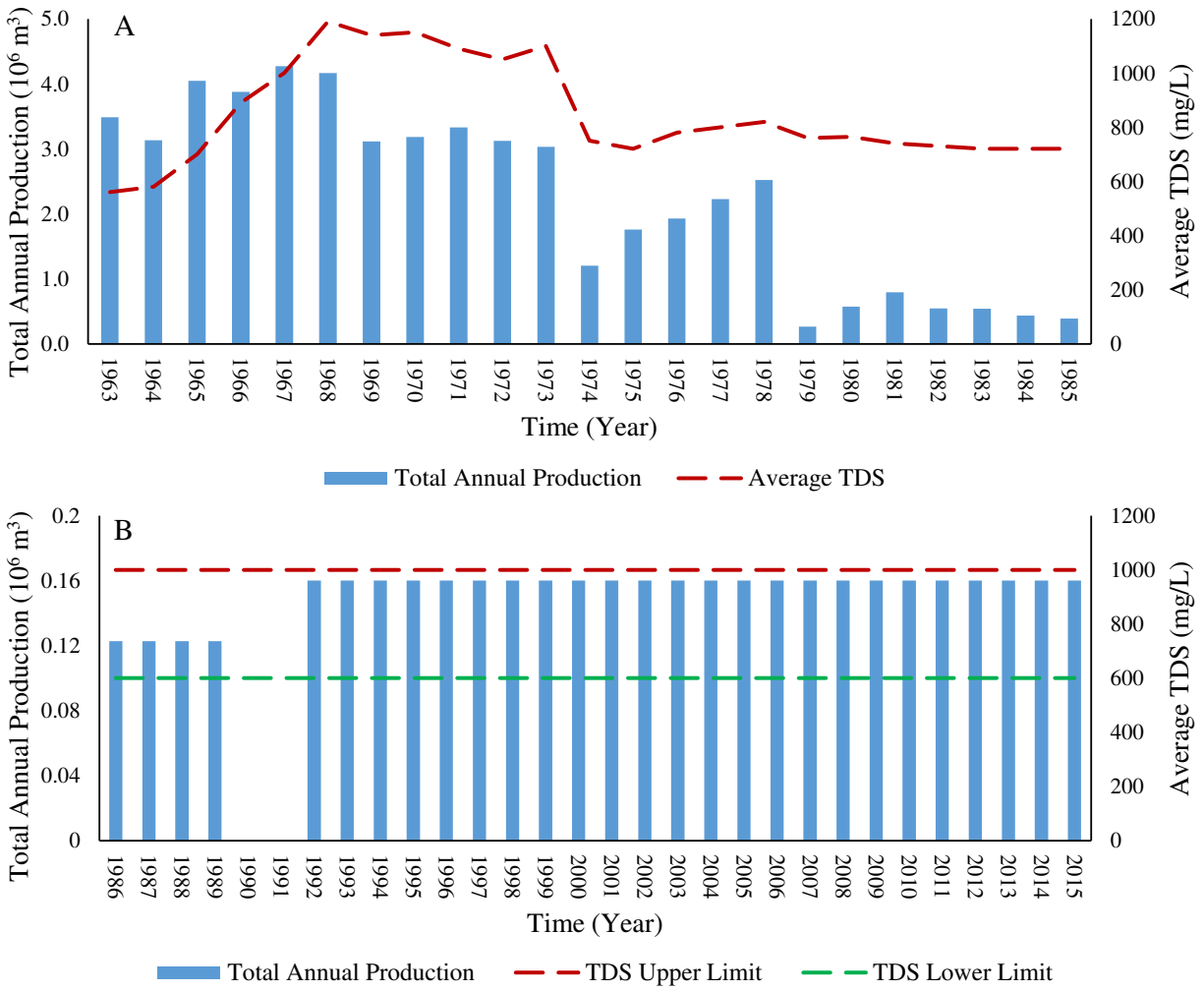


Figure 5.4. Total annual production and average TDS from 1963 to 1985 (A) and from 1986 to 2015 (B) for the Rawdatain basin.

Table 5.3. Well data (Parsons Corporation, 1964)

Well Name	Well ID	East (m)	North (m)	Total Depth (m)	Casing Depth (m) (bgl) ^a	Screen Top (m) (bgl) ^a	Screen Bottom (m) (bgl) ^a	Screen Length (m)
R1	K6490-Q2686	756490	3312686	56.38	56.4	33.5	54.9	18.2
R3	K7500-Q2000	757500	3312000	47.24	46.9	32.0	44.8	8.5
R5	K5960-Q3883	755960	3313882	73.15	73.2	48.8	73.2	24.3
R6	K7729-Q3018	757728	3313017	54.86	54.9	31.4	53.3	17.3
R7	K5048-Q2280	755047	3312279	45.71	45.7	36.6	44.2	7.6
R8	K7581-Q3624	757580	3313623	107.89	45.7	36.9	44.5	7.6
R9	K6520-Q2183	756520	3312183	70.10	66.1	34.7	66.1	17.3
R15	K8411-P9420	758411	3309420	42.67	42.7	35.1	41.1	6.1
R16	K6068-Q5769	756068	3315769	53.33	53.3	36.6	50.3	13.7
R20	K5292-Q4899	755292	3314899	50.29	50.3	39.6	48.8	9.1
R22	K9082-Q4247	759082	3314247	59.43	59.4	42.7	57.9	9.1
R27	K6890-Q1121	756890	3311121	45.71	45.7	32.0	44.2	12.2
R33	K5999-Q6878	755999	3316878	51.81	51.8	39.6	48.8	9.1
R43	K5712-Q1593	755712	3311593	53.03	53.0	38.7	51.8	14.0
R44	K5101-Q3932	755101	3313932	42.67	42.7	37.2	41.8	4.5
R45	K4382-Q4547	754382	3314547	42.06	42.1	36.3	40.8	4.5
R46	K4621-Q5709	754621	3315709	44.50	44.5	39.0	43.6	4.5
R50	K9513-P8892	759513	3308892	45.71	45.7	39.9	44.5	4.5
R52	K0170-P7678	760170	3307678	56.99	57.0	49.7	55.8	6.1
R53	K8866-Q1337	758866	3311337	60.95	47.2	39.6	46.3	6.7
R54	K5056-Q6600	755056	3316600	44.80	44.2	38.7	43.3	4.5
R56	K9620-P9901	759620	3309901	60.95	56.4	41.1	55.2	14.0
R58	L0114-P6631	760114	3306631	59.13	58.5	43.6	57.3	10.6
R61	K8510-Q2294	758510	3312294	49.98	50.0	40.5	48.8	6.1
R63	K9219-P6219	759219	3306219	44.50	44.5	37.9	43.6	5.6
R64	L1076-P6506	761076	3306506	70.10	70.1	42.7	68.9	20.1

5.3.3 Future Pumping Scenarios (2019-2100)

Six hypothetical future pumping scenarios were considered to evaluate the impact of a wide range of total annual volume extractions, as shown in Table 5.5. The S0 scenario represents the no pumping condition, S1 and S2 represent the historical low pumping period of 1979-2018, S3, S4 and S5 represent the historical high pumping period of 1963-1978, and S6 represents an extreme pumping scenario. The groundwater head and groundwater salinity concentration for each grid cell at the end of 2018 served as initial conditions for the simulations, and the simulation period is from 2019 to 2100. The maximum pumping capacity of the wells in the Rawdatain water field is 908 m³/day (350 gallon/min). As all pumping are no longer active, the criterion for assigning the number and names of wells for the simulations involves choosing the most recent active wells and not exceeding the maximum pumping capacity. The daily pumping rate of each well was calculated by dividing the total annual production volumes by the number of active wells for each scenario. Both the quantity and quality of the stored water (subsurface) and quality of pumped water (water supply) were evaluated for each scenario.

Table 5.5. Extraction scenarios

Scenarios	Total Annual Volume Extraction (m ³ /year)	Number of Operated Wells	Operated Wells	Daily Pumping Rate (m ³ /day)
S0	0	0	-----	0
S1	160,000	8		56
S2	500,000	8	R1, R3, R6, R9, R16, R58, R61, R64:	171
S3	1,000,000	8		343
S4	3,000,000	15	Above plus: R5, R7, R15, R20, R27,	546
S5	4,000,000	15	R44, R56	730
S6	8,000,000	26	Above plus: R8, R22, R33, R43, R45, R46, R50, R52, R53, R54, R63	537

Impact of climate change on the water resources remains uncertain and becomes an interest of comprehensive and extensive studies of the entire region of the Middle East. Lelieveld

et al. (2012) stated that the region is likely to be significantly affected by the climate change, as a result of a decline in precipitation and an increase in the intensity and frequency of drought periods. However, Chenoweth et al. (2011) found that there will be an increase in precipitation in Kuwait by 2040-2099. In contrast, a reduction in precipitation in Kuwait was predicted in 21st century (Evans, 2009; Terink et al., 2013). In the future scenarios, the long-term annual average recharge R (500,000 m³/year) was used for all of the future scenarios, and a sensitivity analysis was performed to consider the effect of increasing or decreasing annual recharge by $\pm 20\%$ to 600,000 m³/year and 400,000 m³/year, respectively, to account for possible changes in climate.

5.3.4 Lens Storage Recovery (LSR)

The use of coupled numerical groundwater flow and transport models for Aquifer Storage Recovery is the best method for assessing the effects of interactions between hydrogeologic and operational parameters on predictions of recovery efficiency (Lowry & Anderson, 2006). Here, the new baseline model was used to assess the Rawdatain Lens Storage Recovery (LSR) for ten years (2018-2028). Three artificial injection scenarios were conducted using different proposed annual injected volumes and number of wells, as shown in Table 5.6. The criterion for assigning the number and names of wells is the same as above.

Table 5.6. Injection scenarios

Scenarios	Total Annual Volume Injection (m ³ /year)	Number of Operated Wells	Operated Wells	Daily Injection Rate (m ³ /day)
I1	1,000,000	8	R1, R3, R6, R9, R16, R58, R61, R64	342
I2	3,000,000	15	Above plus: R5, R7, R15, R20, R27, R44, R56	548
I3	5,000,000	26	Above plus: R8, R22, R33, R43, R45, R46, R50, R52, R53, R54, R63	527

5.4. Results and Discussion

5.4.1 Aquifer Properties for Baseline Model

Figure 5.5, 5.6 and 5.7 are plots of the simulated Rawdatain FGL volumes, starting from no lens present and running for 4000 years, against the three volume targets for the three PRM scenarios associated with five different dispersivity sets. The three different volume targets are 700 mg/L (32.6 million m³), 1000 mg/L (64.4 million m³), and 2000 mg/L (149 million m³). Curves for all of the simulated volumes show that the PRM scenarios reached relatively flat steady state volumes compared with the CRM scenarios. This supported the choice of using of the PRM (formative factor) to represent the natural hydrological processes of the mixing between the recharge water and the ambient brackish water. The PRM scenarios with 10 m longitudinal dispersivity set tended to overestimate all of the volume categories, whereas the PRM scenario with the 100 m dispersivity set tended to underestimate all of the volume categories. In a general comparison between the three PRM scenarios based on the recharge frequency only, there were similar trends in the Rawdatain FGL formation. These results indicate that the Rawdatain FGL formation is not sensitive to the recharge event frequencies if the long-term average recharge is kept the same, which is in agreement with the slow development of the lens (approximately 2000 years) (Alrashidi & Bailey, 2019a).

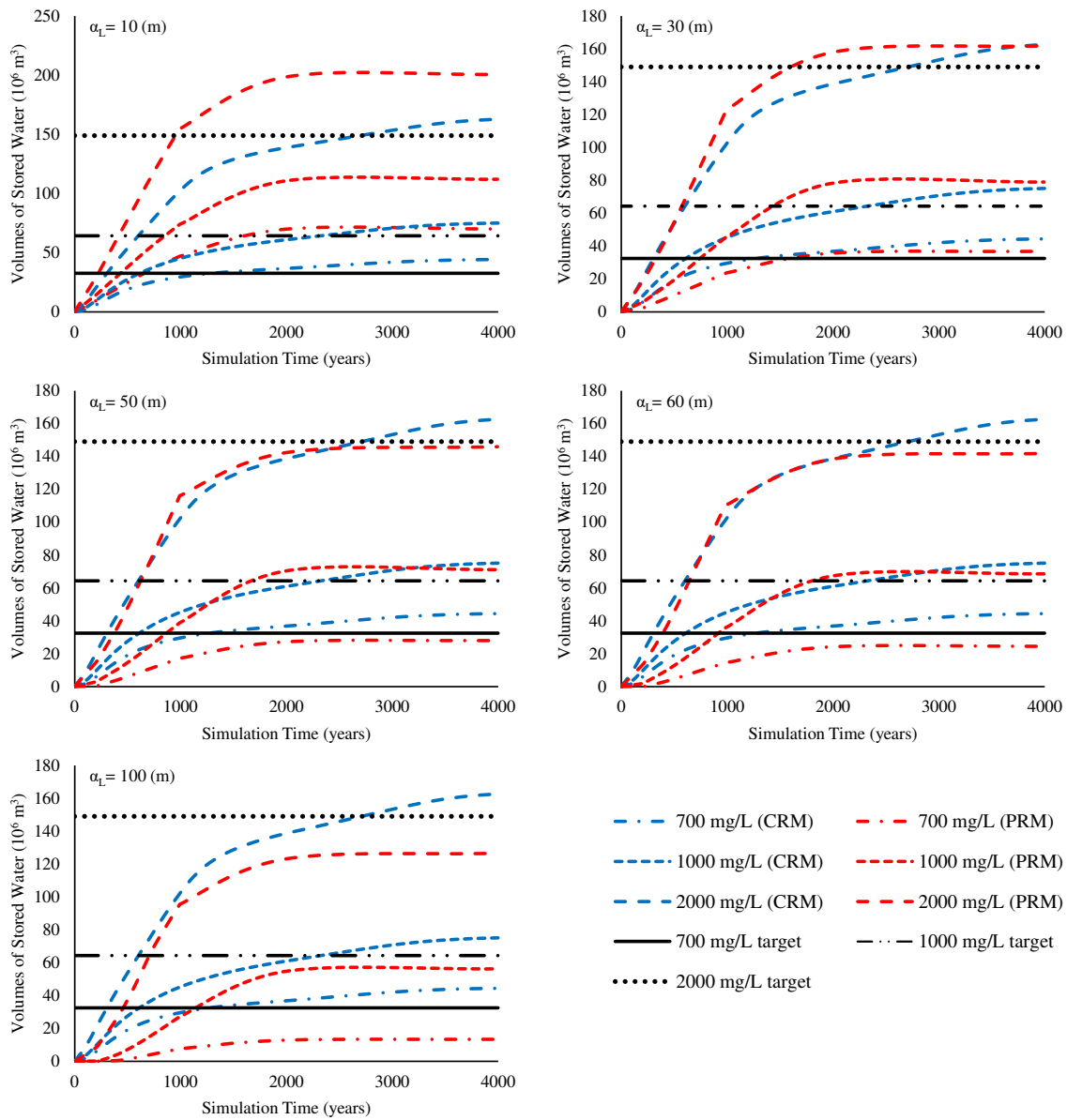


Figure 5.5. Pulse recharge scenario with one pulse per year and different longitudinal dispersivity values.

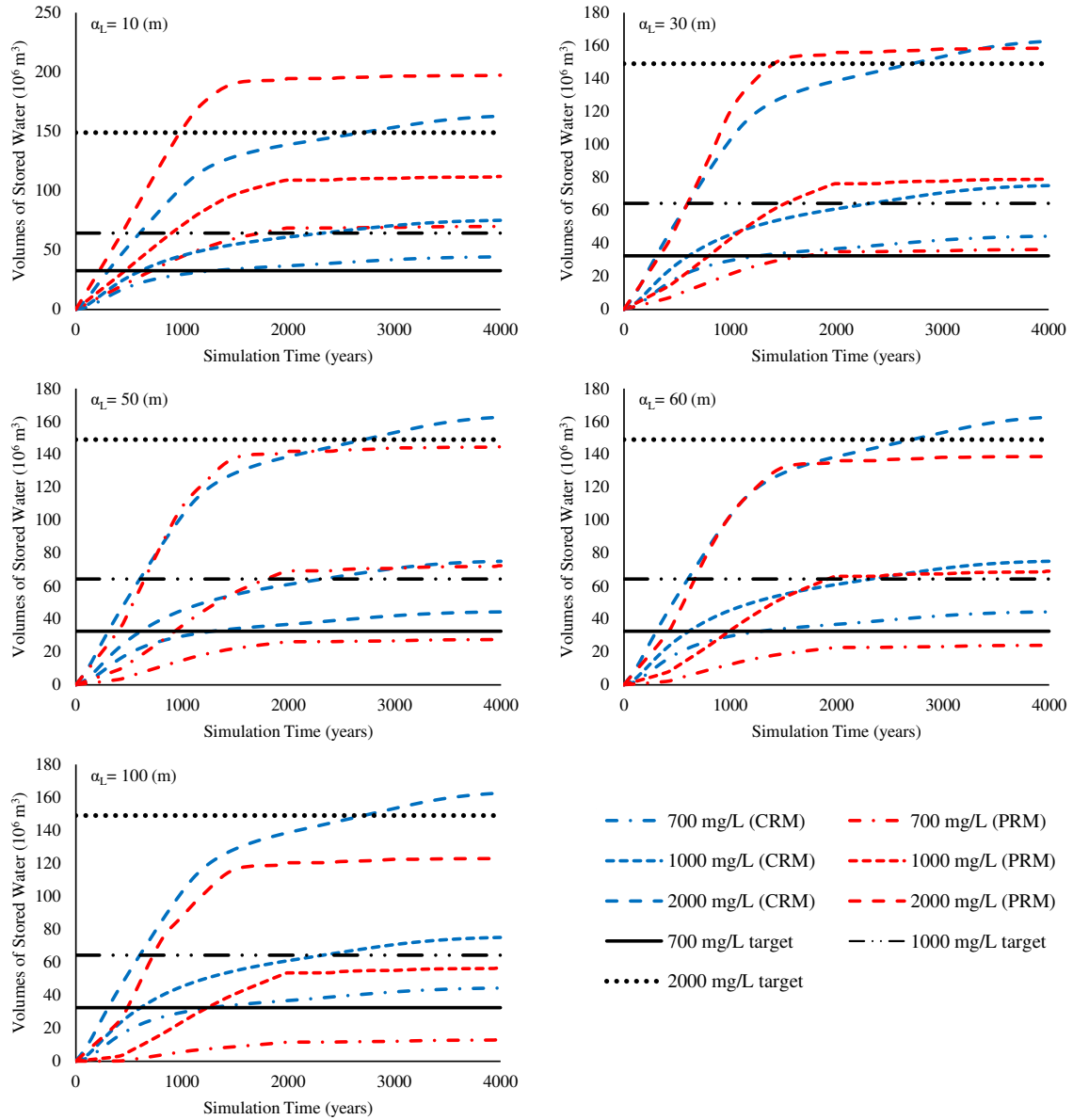


Figure 5.6. Pulse recharge scenario with one pulse every two years and different longitudinal dispersivity values

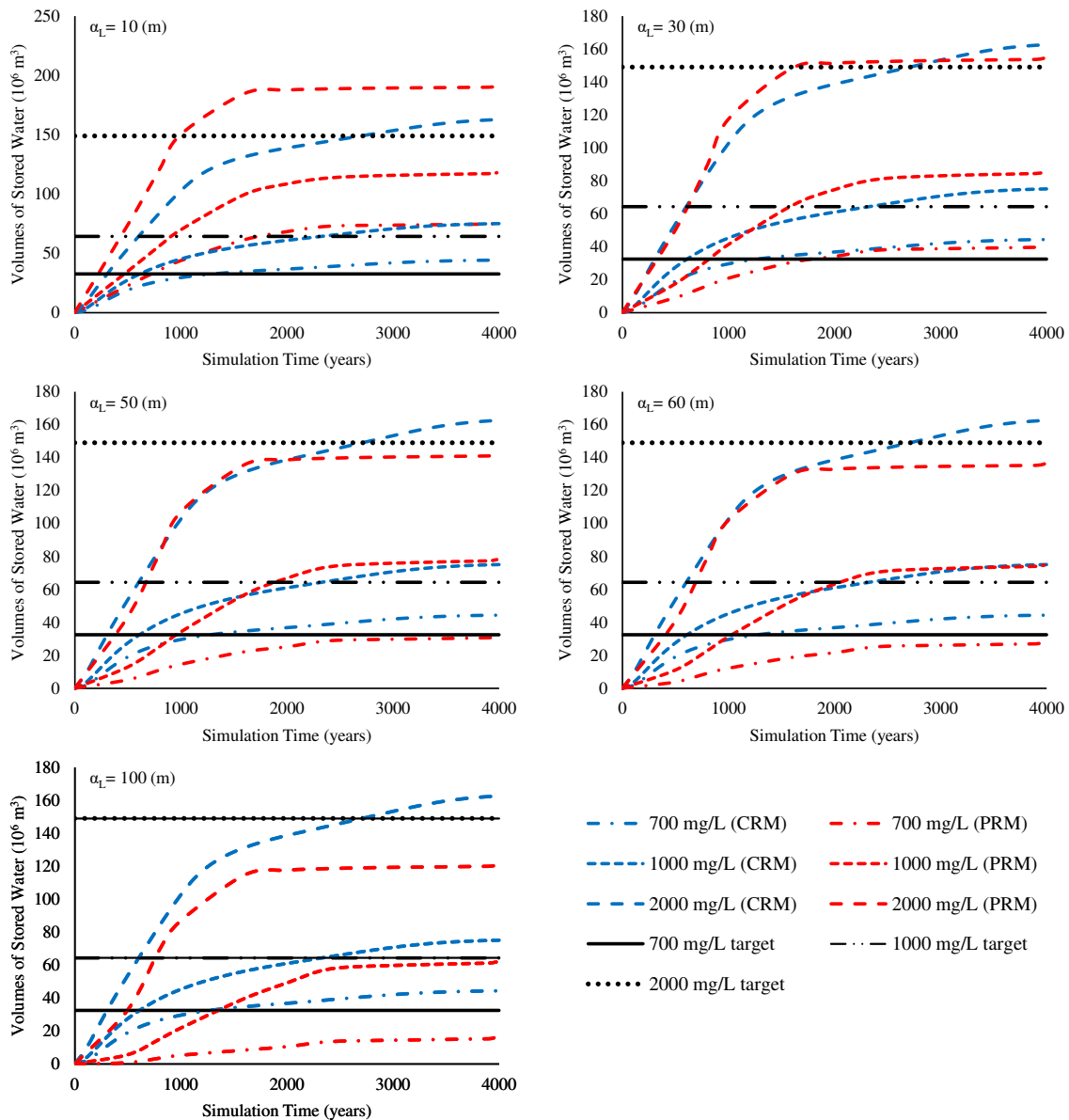


Figure 5.7. Pulse recharge scenario with one pulse every four years and different longitudinal dispersivity values.

Table 5.7 summarizes the performance of the CRM and PRM scenarios against the three volume targets at 2000 years. In general, the performance of the PRM scenarios improved with using less frequent recharge events for the 10 m longitudinal dispersivity set for all three targets, whereas the performance of the PRM scenario with the 100 m dispersivity set worsened with less frequent recharge events. In terms of the dispersivity set values, the 10 m longitudinal

dispersivity set resulted in volumes up to 115%, 69% and 31% more than the 700, 1000, and 2000 mg/L targeted volumes, respectively. In contrast, the 100 m longitudinal dispersivity set underestimated the simulated volumes by 56%, 58% and 68%, respectively.

Table 5.7. Results of the simulated volumes of stored water using constant recharge and pulse recharge scenarios with different longitudinal dispersivity values at 2000 years.

Comparison criteria	Targets	Constant Recharge		Pulse Recharge									
		$\alpha_L=50$ (m)	Error (%)	$\alpha_L=10$ (m)	Error (%)	$\alpha_L=30$ (m)	Error (%)	$\alpha_L=50$ (m)	Error (%)	$\alpha_L=60$ (m)	Error (%)	$\alpha_L=100$ (m)	Error (%)
Volume of Stored Water (10^6 m^3)		<i>Once Every Year</i>											
<i>700 mg/L</i>	33	37	13	70	115	37	13	29	-11	25	-22	14	-56
<i>1000 mg/L</i>	64	61	-5	111	72	78	22	70	9	67	4	55	-15
<i>2000 mg/L</i>	149	139	-7	198	33	158	6	142	-4	138	-7	123	-17
Volume of Stored Water (10^6 m^3)		<i>Once Every Two Years</i>											
<i>700 mg/L</i>	33	37	13	69	111	36	11	28	-12	25	-24	14	-58
<i>1000 mg/L</i>	64	61	-5	109	69	76	19	69	8	66	2	54	-17
<i>2000 mg/L</i>	149	139	-7	194	31	155	4	142	-5	136	-9	120	-19
Volume of Stored Water (10^6 m^3)		<i>Once Every Four Years</i>											
<i>700 mg/L</i>	33	37	13	68	110	34	5	28	-13	25	-25	10	-68
<i>1000 mg/L</i>	64	61	-5	109	69	75	16	67	4	63	-2	49	-24
<i>2000 mg/L</i>	149	139	-7	188	26	151	2	139	-7	133	-11	118	-21

Overall, the 30 m, 50 m and 60 m longitudinal dispersivity sets had the best performance, which is in agreement with the best ranges of the environmental dispersivity values using CRM (Alrashidi and Bailey, 2019b). However, the 30 m longitudinal dispersivity set overestimated the 1000 mg/L volume target by 22%, 19% and 16% for the three PRM scenarios, and the 60 m longitudinal dispersivity set underestimated the 700 mg/L volume target by 22%, 24% and 25%. The 50 m longitudinal dispersivity set with all PRM scenarios performed the best, obtaining an error percentage less than 10% for the 1000 mg/L and 2000 mg/L volume targets. The slightly high errors (-11%, -12% and -13%) for the 700 mg/L volume target are acceptable because we compared the simulated volume with one field estimate from the U.A.R. Therefore, the 50 m longitudinal dispersivity set with the once every two year PRM was selected to be the new baseline model for assessing water extraction and management under the historical and future scenarios.

5.4.2 Historical Period (1963-2018)

The volumes of stored water at the three volume categories that represent the predevelopment period in 1963 were $28 \times 10^6 \text{ m}^3$ (700 mg/L), $69 \times 10^6 \text{ m}^3$ (1000 mg/L) and $142 \times 10^6 \text{ m}^3$ (2000 mg/L), and they were used as the initial conditions for the model used to assess the impact of historical groundwater abstraction from 1963-2018. Figure 5.8 shows the simulated volumes of stored water and the changes in volume during the pumping period 1963-2018 for the three water quality categories. The results showed a significant reduction in the stored water during the period of extensive pumping in 1963 to 1978. These reductions within 11 years represented 79%, 82% and 83% of the total reduction during the 54 years of pumping (1963-2018). Afterwards, the changes in volume stabilized with a very low rate of reduction as a consequence of the low pumping rates in the 1979-2018 period. Figure 5.9 demonstrates the

pumping-induced depletion of the lens plotted versus the total abstraction volume. A total of 83% of the pumping volume occurred during the period 1963-1978 when the lens was considered as a water supply source, resulted in a significant shrinkage in the lens volume. Later, only an additional $9 \times 10^6 \text{ m}^3$ was pumped between 1978 and 2018, when the majority of the Rawdatain water field closed and was considered as a strategic reserve for emergency use. These results illustrate that the change in pumping rate saved the Rawdatain FGL, and it continues to store a significant volume of water.

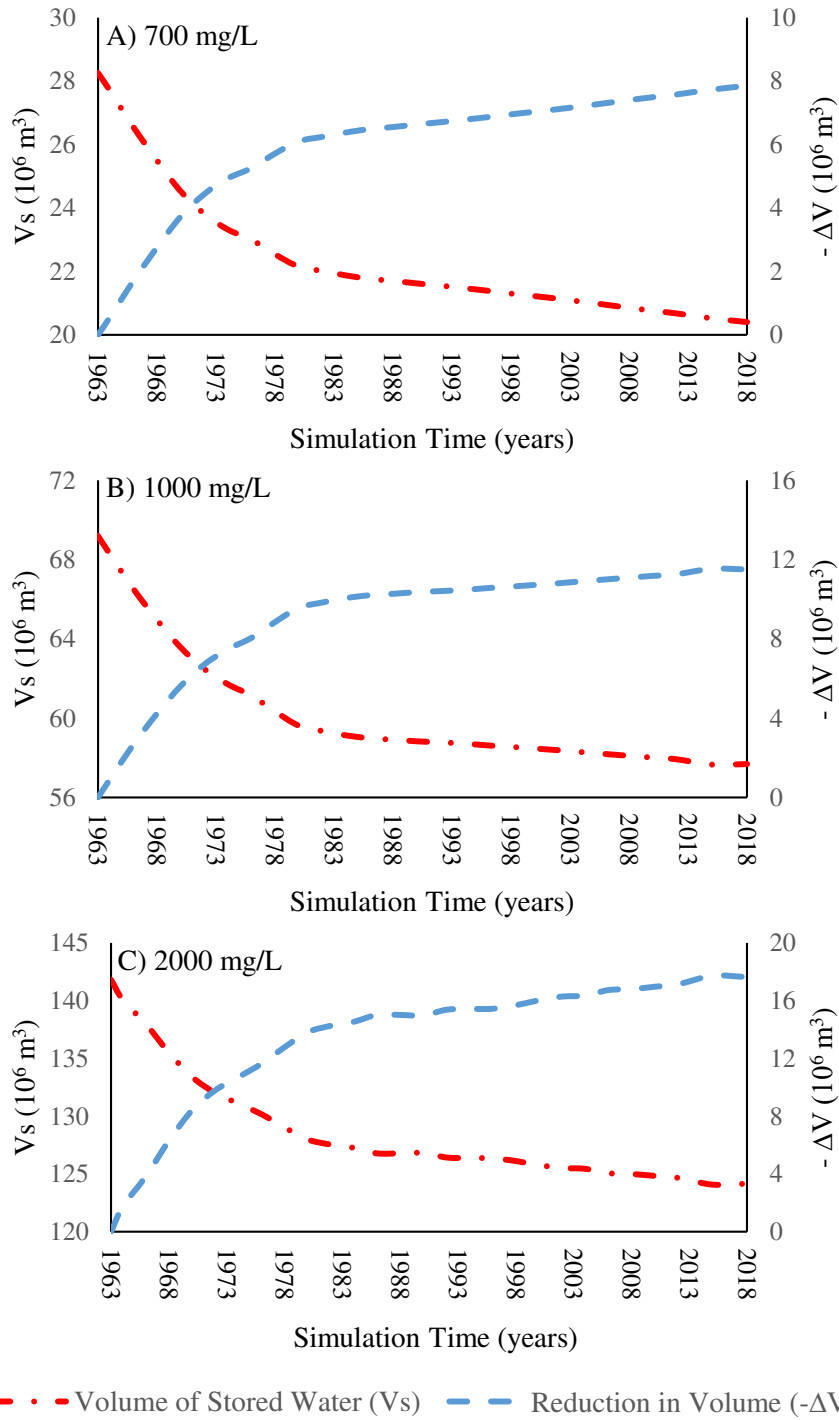


Figure 5.8. Simulated volumes of stored water and the reduction in volumes during the pumping period 1963-2018: A) 700 mg/L, B) 1000 mg/L, and C) 2000 mg/L water quality categories.

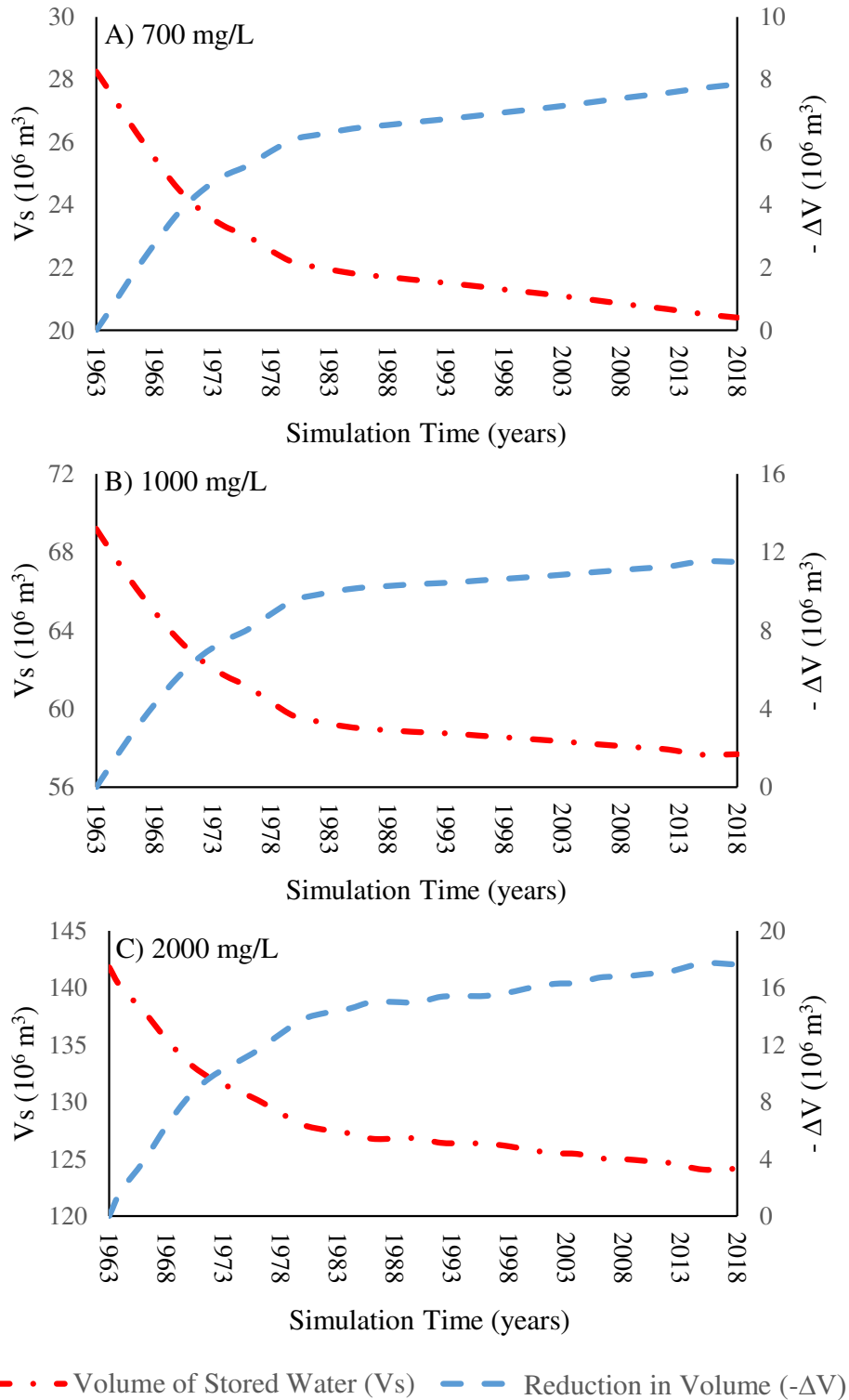


Figure 5.9. Simulated volumes of stored water and the reduction in volumes vs. total abstraction volume: A) 700 mg/L, B) 1000 mg/L, and C) 2000 mg/L water quality categories.

5.4.3 Future Period (2019-2100)

The results for the assumed future pumping scenarios (2019-2100) combined with the historical conditions are shown in Figure 5.10 and Table 5.8. It can be clearly seen that the 700 mg/L water quality category is more sensitive than the other categories. The no-pumping scenario (S0) will not prevent the reduction in the volumes of the stored water. However, the percentages of the reductions were negligible: 5%, 2% and 2% for the three water quality categories. This is because the 54 years of historical pumping caused brackish water to rise and an increase in the mixing rates, which affects the natural stability of the lens. If the current low pumping (S1, 160000 m³/year) is kept the same, the changes in the stored water would be small (17%, -6% and -5%) because the pumping rate is less than one third of the long-term average recharge rate (500000 m³/year). Moreover, this scenario would lead to sustainable pumped water quality between 850 and 1000 mg/L, and the fluctuation in TDS shown in Figure 5.11 indicates that S1 emphasizes the effect of the PRM. Thus, S1 would be safe and acceptable as a long-term pumping scenario and will not impact the storage of the lens significantly.

Table 5.8. Prediction of volumes of stored water with different pumping and recharge scenarios from 2019 to 2100

Volume Targets	Pumping Analysis - Simulated Stored Volumes (10^6 m^3) (reduction in stored volumes (%))										
	Initial Condition (1963)	Historical (1963 to 2018)		Initial Condition (2018)	Future Scenarios (2019 to 2100)						
		(1963-1978)	(1979-2018)		S0	S1	S2	S3	S4	S5	S6
700 mg/L	28.3	22.1 (22)	20.4 (28)	20.4	19.4 (5)	16.9 (17)	11.7 (43)	6.5 (68)	1.8 (91)	0.8 (96)	0.4 (98)
1000 mg/L	69.2	59.6 (14)	57.7 (17)	57.7	56.4 (2)	54.4 (6)	40.1 (31)	22.4 (61)	12.8 (78)	8.3 (86)	3.8 (93)
2000 mg/L	141.8	127.2 (10)	124.2 (12)	124.2	122 (2)	118 (5)	95.3 (23)	63.6 (49)	41.4 (67)	26.6 (79)	10.1 (92)

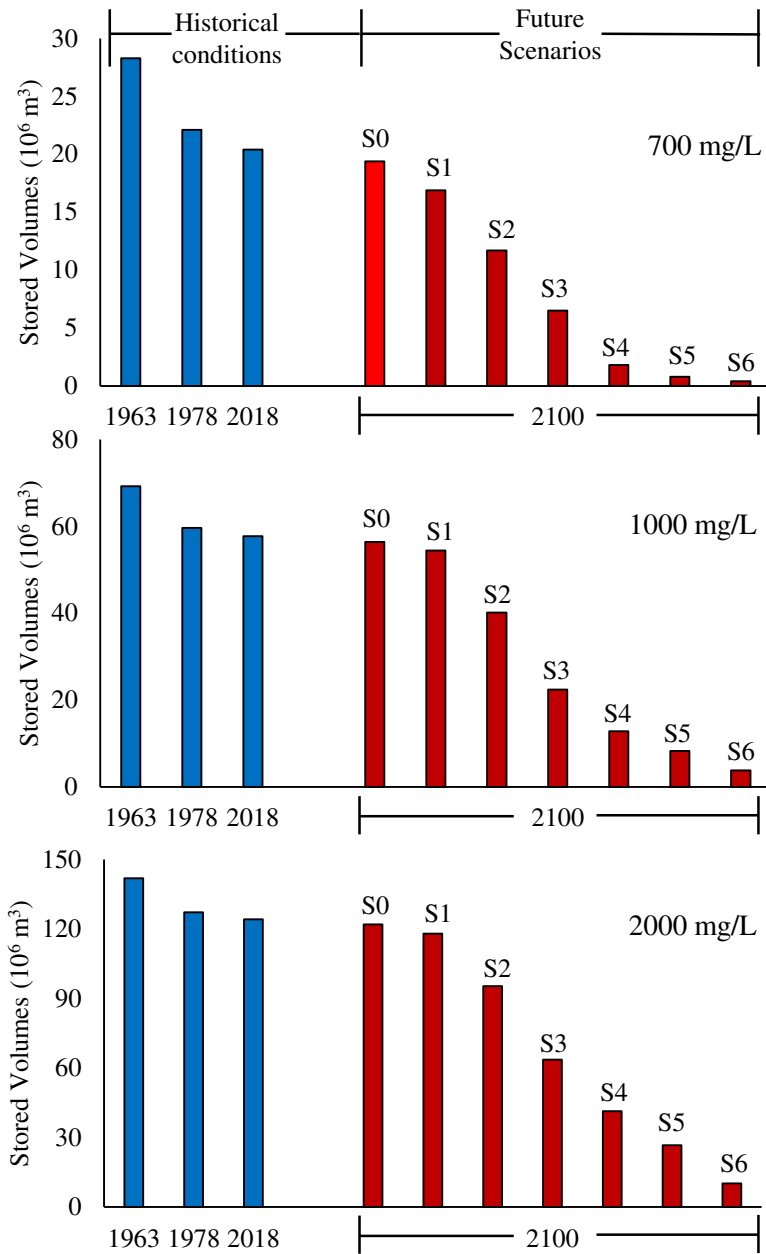


Figure 5.10. Simulated volumes of stored water for historical conditions (initial condition in 1963; intensive pumping period 1963-1978; low pumping rate period 1979-2018) and future scenarios (S0 to S6 for 2019-2100): A) 700 mg/L, B) 1000 mg/L, and C) 2000 mg/L water quality categories.

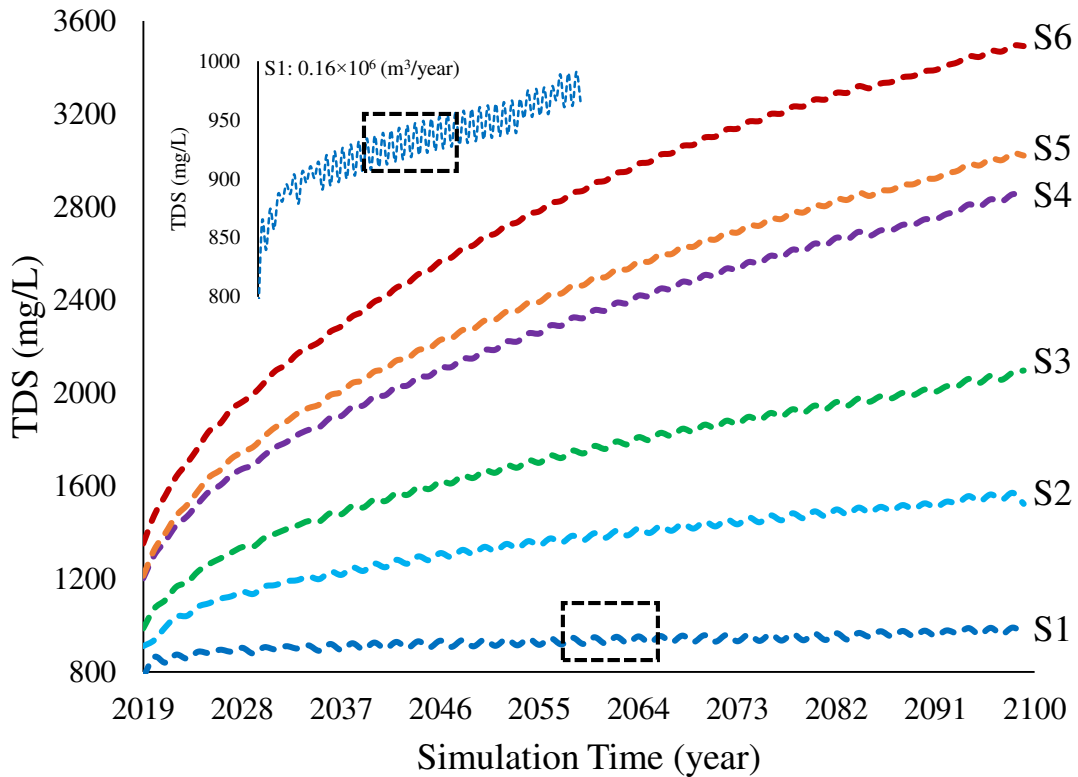


Figure 5.11. Simulated TDS of the pumped water for a range of annual volume extraction scenarios for 2019-2100.

S2 resulted in a remarkable decline in the 700 mg/L water quality category up to 43% and moderate decay (31% and 23%) in the other categories. The quality of the produced water exceeded 1200 mg/L after 20 years and continued to increase up to 1600 mg/L, and it became less sensitive to natural recharge events. Thus, the pumping rate of 500000 ($\text{m}^3\text{/year}$) is only a sustainable option for a short-term use. S3 introduced more negative impacts than S2 because it worsened the rate of degeneration for all of the water quality categories by 49% to 68%. The produced water was insensitive to recharge, and the TDS quickly became elevated. S4, S5 and S6 caused a deterioration of the Rawdatain FGL, indicating that the high pumping rates used in 1963 would not be suitable for the current condition. The lens did not recover during the 1979-2018 period because the recharge was very minimal compared with the volume of stored water.

The capability of the tested groundwater model was used to assess the sensitivity of the S0, S1 and S2 pumping future scenarios to a change in the natural recharge amount. A sensitivity analysis was carried out by varying the recharge by $\pm 20R$, where R is the long-term average recharge (500000 m³/year). The y-axis in Figure 5.12 represents the percentage change in stored water compared with the initial condition in 2018. There are three main findings: (1) within the same extraction scenarios, the range of the change of stored water narrowed from the 700 mg/L to the 2000 mg/L water quality categories, (2) among the extraction scenarios, the model sensitivity to the changes in recharge decreased as the annual extraction increased. The former finding is in agreement with the results of the produced water TDS in Figure 5.11, where the fluctuation of the TDS was very distinguishable with S1 and then reduced with S2 and became indistinguishable with the high pumping scenarios, and (3) An increase of 20% in the recharge will not lead to a significant recovery of the lens even with the no-pumping alternative.

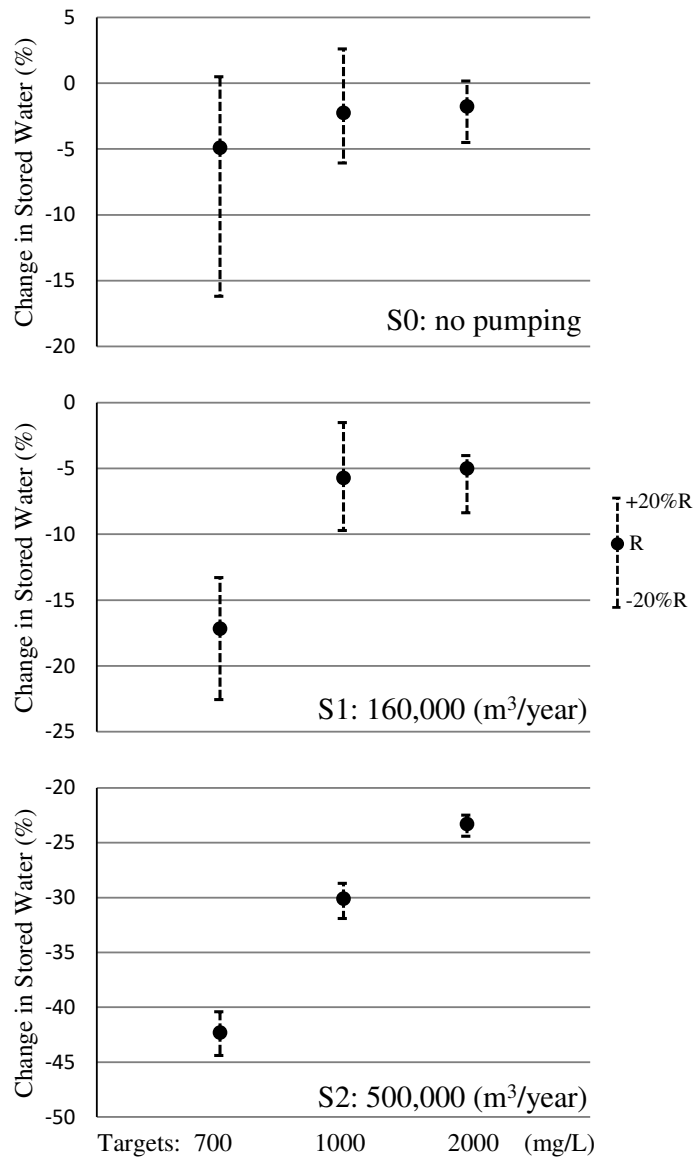


Figure 5.12. Sensitivity of change in stored water volumes with three annual volume extraction scenarios (S0, S1 and S2) associated with three long-term annual recharge scenarios (R = 500,000 m³/year, +20%R = 600,000 m³/year and -20%R = 400,000 m³/year) at the year 2100.

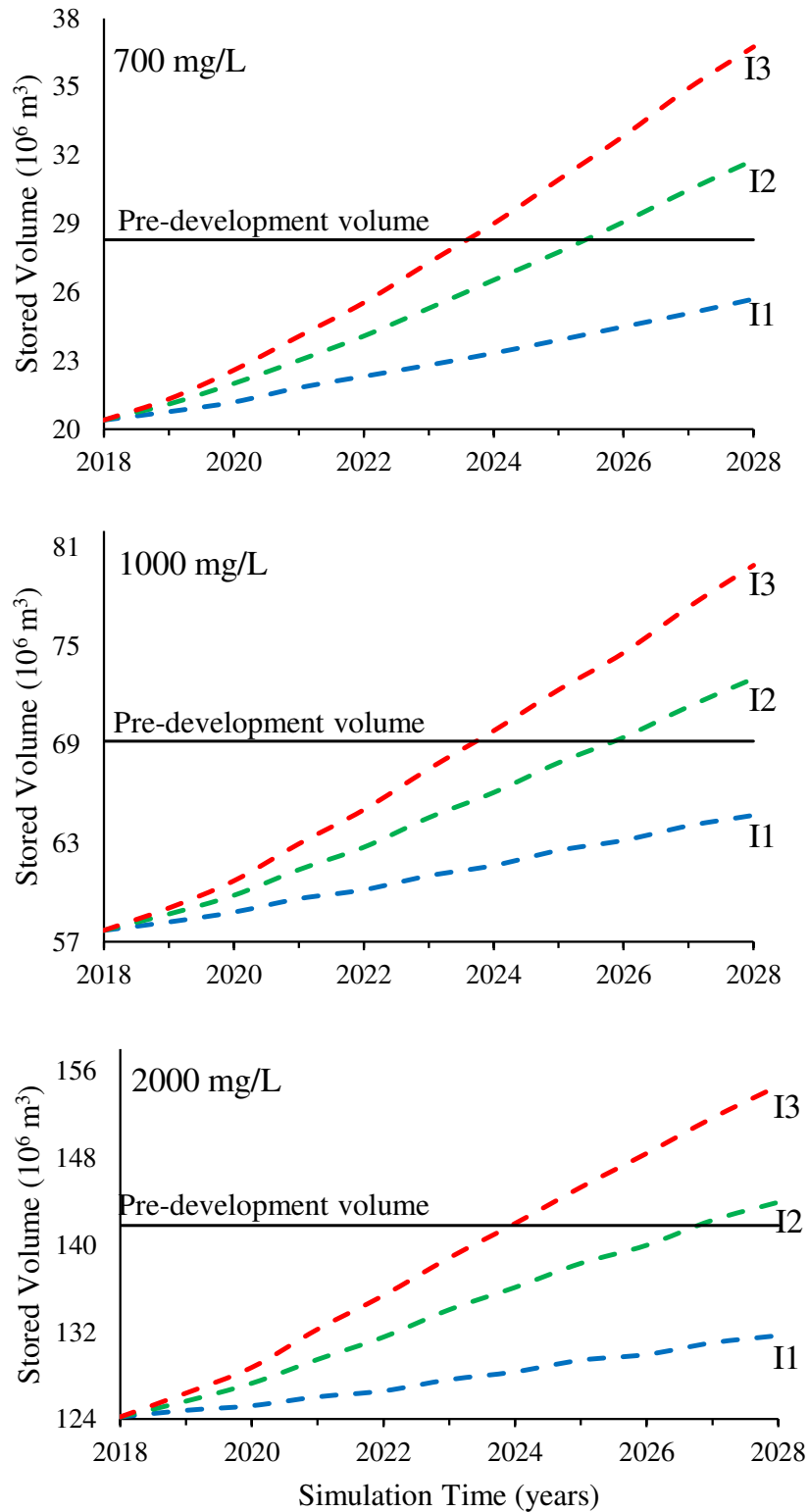


Figure 5.13. Simulated volumes of stored water for three annual volume injection scenarios (I1, I2 and I3) for the period 2019-2028: A) 700 mg/L, B) 1000 mg/L, and C) 2000 mg/L water quality categories. (Horizontal solid lines represent the pre-development volumes in 1963)

Because the decline of the Rawdatain FGL is expected to continue even with no pumping activities, and because of the very slow response to any increase in natural recharge rates, an artificial recharge solution should be implemented to accelerate the stored water recovery. The results of a brief modeling of three injection scenarios was conducted to evaluate the Lens Storage Recovery for the Rawdatain, as shown in Figure 5.13. Within 10 years, a recovery of 67%, 61% and 43% of the storage lost since original initial volumes in 1963 could be achieved by implementing the I1 alternative for all of the water quality categories, respectively. The I2 could reach the 100% storage recovery within 7.5, 8 and 9 years for all of the water quality categories, respectively. The I3 attained the 100% storage recovery within 6 years and add additional storage volumes of up to 80% by the end of the injection period. The volume of the injected water in I1 represents 33% and 20% of the injected water in I2 and I3. However, I1 achieved a reasonable storage recovery because of choosing appropriate locations for the injection. Indeed, the eight wells used for the I1 scenario are the same as the wells that are still operating and producing the best water quality. Thus, choosing suitable locations and amounts of injection would lead to a successful LSR.

5.5. Summary and Conclusion

Freshwater resources are extremely scarce in Kuwait because the harsh climate and landforms prevent the existence of surface water bodies and make it difficult to harvest and store precipitation. The majority of the potable water supply comes from the unconventional resources of seawater desalination and treated wastewater. Limited fresh and brackish groundwater are the main conventional source of usable of water supply. Indeed, the occurrence of fresh groundwater is restricted to two main FGLs, namely the Umm-Aish and Rawdatain. The former was contaminated by hydrocarbon pollution, and the latter is currently the only potential sizable

freshwater storage in the country. Thus, understanding the natural formation and current and future stability of the Rawdatain FGL is essential and will be very valuable to water managers analyzing future water security for the country and establishing appropriate water supply plans.

In this chapter, a new baseline model was established for the Rawdatain FGL predevelopment period using a pulse recharge mechanism (PRM) to simulate the effects of the infrequent rainfall events and anthropogenic impacts simultaneously. Three frequencies of PRM scenarios, one pulse every 1 year ($500,000 \text{ m}^3/\text{year}$), one pulse every 2 years ($1,000,000 \text{ m}^3/\text{year}$), and one pulse every 4 years ($2,000,000 \text{ m}^3/\text{year}$), with five longitudinal dispersivity values (between 10 m and 100 m) were evaluated against three volume targets: 700 mg/L (32.6 million m^3), 1000 mg/L (64.4 million m^3), and 2000 mg/L (149 million m^3). The results indicated that the Rawdatain FGL formation is more sensitive to the dispersivity set than to the recharge event frequencies. The model associated with the 50 m longitudinal dispersivity set and one pulse recharge every two years had the best performance among the three volume targets, and thus it was selected to be the new baseline model representing the condition of the Rawdatain FGL in 1963.

The new baseline model was used to assess the impact of historical groundwater abstraction from 1963 to 2018, starting from the initial volume conditions $28 \times 10^6 \text{ m}^3$, $69 \times 10^6 \text{ m}^3$ and $142 \times 10^6 \text{ m}^3$ for the three quality categories, respectively. The majority of the reduction in the lens storage occurred in the extensive pumping period between 1963 and 1978, resulting in a decline in the volumes of the three quality categories by 22%, 14% and 10%, respectively. Subsequently, the annual pumping rates were lowered dramatically from up to $4 \times 10^6 \text{ m}^3$ to less than $1 \times 10^6 \text{ m}^3$ during 1979-1985, and then no higher than $0.16 \times 10^6 \text{ m}^3$ from 1986 to 2018. As a consequence, the changes in the volumes stabilized with no significant reduction. By 2018, the

amounts of stored water in the Rawdatain FGL were estimated to be $20 \times 10^6 \text{ m}^3$, $57 \times 10^6 \text{ m}^3$ and $124 \times 10^6 \text{ m}^3$ for the three quality categories, respectively.

Six future pumping scenarios were assessed from 2019 to 2100, starting from the initial condition in 2018. The results revealed that the size of the Rawdatain FGL will not recover with the no-pumping scenario (S0). The lowest pumping scenario ($S1 = 0.16 \times 10^6 \text{ m}^3/\text{year}$) had no major effect on the stored volumes, whereas the second lowest pumping scenario ($S2 = 0.5 \times 10^6 \text{ m}^3/\text{year}$) caused a notable decay in the water quality category with the lowest TDS. Moreover, the produced water quality was sustained between 850 and 1000 mg/L until 2100 with S1, and it exceeded 1200 mg/L with S2 by 2040. Therefore, S1 is an appropriate scenario for keeping a significant storage available for an emergency use if needed, and S2 is a practical selection for short-term use. The rate of degeneration accelerated as the pumping rates increased with the S3 to S6 scenarios, reaching a damaging deterioration of the Rawdatain FGL by 2100, predominantly in the 700 mg/L water quality category. There was a fluctuation in the quality of the produced water in S1 and S2, indicating that the TDS of the produced water was more sensitive to the low-pumping scenarios and becomes less sensitive as the pumping rate exceeds the annual recharge.

A sensitivity analysis of the no-pumping and low-pumping scenarios to a change in the long-term recharge by $\pm 20\%$ showed that the 700 mg/L water quality category is more sensitive than the other water quality categories, and the model became less sensitive as the annual extraction increased. Indeed, an increase of 20% in the recharge will not lead to a significant recovery of the lens by 2100 even with the no-pumping alternative. Thus, three artificial recharge alternatives were applied to accelerate the Rawdatain lens storage recovery (LSR). A 100% storage recovery to the initial predevelopment volumes of 1963 was simulated by implementing

the I2 scenario in 2027. The I1 scenario could not reach a full recovery within 10 years, whereas the I3 achieved a full recovery within 6 years. Hence, the LSR approaches indicated that the recovery percentage depends not only on the amounts of injected water but also on choosing suitable locations for injection wells.

This study provides a first attempt to model the natural creation of a FGL in a subterranean oasis in an arid region. The baseline model was developed through transient 3D density-dependent simulations that allow simulation of the natural mixing between the pulse recharge events and the environmental dispersivity for 4000 years of simulation time until the FGL reaches equilibrium. A unique example of a calibration approach was implemented by using multiple data targets and water age, which led to the elimination of several non-unique calibration parameters and reduced the uncertainty of the calibrated parameters. The model was capable of evaluating the effects of the historical and assumed future abstractions and assessing the benefits of LSR. The methodology presented herein can be applied to other FGLs with similar climatic and environmental circumstances.

REFERENCES

- Al Barwani, H. H., & Purnama, A. (2008). Evaluating the effect of producing desalinated seawater on hypersaline Arabian Gulf. *European Journal of Scientific Research*, 22(2), 279-285.
- Al-Anzi, B., Abusam, A., & Shahalam, A. (2011). Wastewater Reuse in Kuwait and Its Impact on Amounts of Pollutants Discharged into the Sea. *Journal of Environmental and Analytical Toxicology* 2011, S, 3.
- Al-Dousari, A., Milewski, A., Din, S. U., & Ahmed, M. (2010). Remote sensing inputs to SWAT model for groundwater recharge estimates in Kuwait. *Advances in Natural and Applied Sciences*, 4(1), 71-77.
- Almedejj, J. (2012). Modeling rainfall variability over urban areas: a case study for Kuwait. *The Scientific World Journal*, 2012.
- Al-Otaibi, M., & Mukhopadhyay, A. (2005). Options for managing water resources in Kuwait. *Arabian Journal for Science and Engineering*, 30(2C), 55.
- Al-Rashed, M. F., & Sherif, M. M. (2000). Water resources in the GCC countries: an overview. *Water resources management*, 14(1), 59-75.
- Alrashidi, M. S., & Bailey, R. T. (2019a). Estimating groundwater recharge for a fresh groundwater lens in an arid region: formative and stability assessment. *Hydrological Processes*, (Revised).
- Alrashidi, M. S., & Bailey, R. T. (2019b). Determining values of large-scale dispersivity for a fresh groundwater lens in an arid region. *Journal of Hydrology*, (Submitted).
- Al-Senafy, M., & Al-Fahad, K. (2000). Petrography of calcretes and their effects on the hydrology of Kuwait Group aquifer. Paper presented at the Proceedings of the First International Conference on Geotechnical Geo-Environmental Engineering and Management in Arid Lands.
- Al-Senafy, M., Fadlelmawla, A., Bhandary, H., Al-Khalid, A., Rashid, T., Al-Fahad, K., & Al-Salman, B. (2013). Assessment of Usable Groundwater Reserve in Northern Kuwait. *International Journal of Scientific & Engineering Research*, 4(6), 2427-2436.
- Alsharhan, A. S., Rizk, Z. A., Nairn, A. E. M., Bakhit, D. W., & Alhajari, S. A. (Eds.). (2001). *Hydrogeology of an arid region: the Arabian Gulf and adjoining areas*. Elsevier.
- Al-Sulaimi, J., Khalaf, F. J., & Mukhopadhyay, A. (1997). Geomorphological analysis of paleo drainage systems and their environmental implications in the desert of Kuwait. *Environmental geology*, 29(1-2), 94-111.

- Alsumaiei, A. A., & Bailey, R. T. (2018). Quantifying threats to groundwater resources in the Republic of Maldives Part I: Future rainfall patterns and sea-level rise. *Hydrological Processes*, 32(9), 1137-1153.
- Al-Weshah, R. A., & Yihdego, Y. (2016). Flow modelling of strategically vital freshwater aquifers in Kuwait. *Environmental Earth Sciences*, 75(19), 1315.
- Amery, H. A. (2002). Water wars in the Middle East: a looming threat. *Geographical Journal*, 168(4), 313-323.
- Amery, H. A. (2015). *Arab water security: Threats and opportunities in the Gulf States*. Cambridge University Press.
- Asghar, M. N., Prathapar, S. A., & Shafique, M. S. (2002). Extracting relatively-fresh groundwater from aquifers underlain by salty groundwater. *Agricultural Water Management*, 52(2), 119-137.
- Ataie-Ashtiani, B., Rajabi, M. M., & Ketabchi, H. (2013). Inverse modelling for freshwater lens in small islands: Kish Island, Persian Gulf. *Hydrological Processes*, 27(19), 2759-2773.
- Bailey, R. T., & Jenson, J. W. (2014). Effects of marine overwash for atoll aquifers: environmental and human factors. *Groundwater*, 52(5), 694-704.
- Bailey, R. T., Jenson, J. W., & Olsen, A. E. (2009). Numerical modeling of atoll island hydrogeology. *Groundwater*, 47(2), 184-196.
- Bauer, P., Held, R. J., Zimmermann, S., Linn, F., & Kinzelbach, W. (2006). Coupled flow and salinity transport modelling in semi-arid environments: The Shashe River Valley, Botswana. *Journal of Hydrology*, 316(1-4), 163-183.
- Bauer-Gottwein, P., Rasmussen, N. F., Feificova, D., & Trapp, S. (2008). Phytotoxicity of salt and plant salt uptake: Modeling ecohydrological feedback mechanisms. *Water Resources Research*, 44(4).
- Bergstrom, R. E., & Aten, R. E. (1965). Natural recharge and localization of fresh ground water in Kuwait. *Journal of Hydrology*, 2(3), 213-231.
- Burashid, K., & Hussain, A. R. (2004). Seawater RO plant operation and maintenance experience: Addur desalination plant operation assessment. *Desalination*, 165, 11-22.
- Cendón, D. I., Larsen, J. R., Jones, B. G., Nanson, G. C., Rickleman, D., Hankin, S. I., ... & Maroulis, J. (2010). Freshwater recharge into a shallow saline groundwater system, Cooper Creek floodplain, Queensland, Australia. *Journal of Hydrology*, 392(3-4), 150-163.
- Chenoweth, J., Hadjinicolaou, P., Bruggeman, A., Lelieveld, J., Levin, Z., Lange, M. A., & Hadjikakou, M. (2011). Impact of climate change on the water resources of the eastern Mediterranean and Middle East region: Modeled 21st century changes and implications. *Water Resources Research*, 47(6).

- Darwish, M. A., & Al Awadhi, F. M. (2009). The need for integrated water management in Kuwait. *Desalination and Water Treatment*, 11(1-3), 204-214.
- Din, S. U., Al Dousari, A., & Al Ghadban, A. N. (2007). Sustainable fresh water resources management in Northern Kuwait—a remote sensing view from Raudatain basin. *International journal of applied earth observation and geoinformation*, 9(1), 21-31.
- Döll, P., Jiménez-Cisneros, B., Oki, T., Arnell, N. W., Benito, G., Cogley, J. G., ... & Nishijima, A. (2015). Integrating risks of climate change into water management. *Hydrological Sciences Journal*, 60(1), 4-13.
- Evans, J. P. (2009). 21st century climate change in the Middle East. *Climatic Change*, 92(3-4), 417-432.
- Feitelson, E., & Tubi, A. (2017). A main driver or an intermediate variable? Climate change, water and security in the Middle East. *Global Environmental Change*, 44, 39-48.
- Gleick, P. H. (1994). Water, war & peace in the Middle East. *Environment: science and policy for sustainable development*, 36(3), 6-42.
- Houben, G., Noell, U., Vassolo, S., Grisseman, C., Geyh, M., Stadler, S., ... & Vera, S. (2014). The freshwater lens of Benjamín Aceval, Chaco, Paraguay: a terrestrial analogue of an oceanic island lens. *Hydrogeology journal*, 22(8), 1935-1952.
- Illangasekare, T., Tyler, S. W., Clement, T. P., Villholth, K. G., Perera, A. P. G. R. L., Obeysekera, J., ... & Kaluarachchi, J. J. (2006). Impacts of the 2004 tsunami on groundwater resources in Sri Lanka. *Water Resources Research*, 42(5).
- James, W. P., Chakka, K. B., & Mascianglioli, P. A. (1996). CONTROL OF NATURAL BRINE SPRINGS IN BRAZOS RWER BASIN PART I: RECOVERY SYSTEM 1. *JAWRA Journal of the American Water Resources Association*, 32(3), 475-484.
- Jayawickreme, D. H., Santoni, C. S., Kim, J. H., Jobbágy, E. G., & Jackson, R. B. (2011). Changes in hydrology and salinity accompanying a century of agricultural conversion in Argentina. *Ecological Applications*, 21(7), 2367-2379.
- Jolly, I. D., Narayan, K. A., Armstrong, D., & Walker, G. R. (1998). The impact of flooding on modelling salt transport processes to streams. *Environmental Modelling & Software*, 13(1), 87-104.
- Jolly, I. D., Walker, G. R., & Thorburn, P. J. (1993). Salt accumulation in semi-arid floodplain soils with implications for forest health. *Journal of Hydrology*, 150(2-4), 589-614.
- Kwarteng, A. Y., Viswanathan, M. N., Al-Senafy, M. N., & Rashid, T. (2000). Formation of fresh ground-water lenses in northern Kuwait. *Journal of arid environments*, 46(2), 137-155.

- Lelieveld, J., Hadjinicolaou, P., Kostopoulou, E., Chenoweth, J., El Maayar, M., Giannakopoulos, C., & Xoplaki, E. (2012). Climate change and impacts in the Eastern Mediterranean and the Middle East. *Climatic change*, 114(3-4), 667-687.
- Lowry, C. S., & Anderson, M. P. (2006). An assessment of aquifer storage recovery using ground water flow models. *Groundwater*, 44(5), 661-667.
- Mancosu, N., Snyder, R., Kyriakakis, G., & Spano, D. (2015). Water scarcity and future challenges for food production. *Water*, 7(3), 975-992.
- MEW. 2015. Electricity and Water Statistical Year Book. Ministry of Electricity and Water, Kuwait.
- Mukhopadhyay, A. (1995). Distribution of transmissivity in the Dammam limestone formation, Kuwait. *Groundwater*, 33(5), 801-805.
- Mukhopadhyay, A., Akber, A., Rashed, T., Kotwicki, V., Uddin, S., & Bushehri, A. (2016). Establishing a baseline to evaluate future impacts to groundwater resources in North Kuwait. *Environmental Earth Sciences*, 75(4), 324.
- Mukhopadhyay, A., Al-Awadi, E., Quinn, M., Akber, A., Al-Senafy, M., & Rashid, T. (2008). Ground water contamination in Kuwait resulting from the 1991 Gulf War: a preliminary assessment. *Groundwater Monitoring & Remediation*, 28(2), 81-93.
- Panday, S., Huyakorn, P. S., Robertson, J. B., & McGurk, B. (1993). A density-dependent flow and transport analysis of the effects of groundwater development in a freshwater lens of limited areal extent: the Geneva area (Florida, USA) case study. *Journal of contaminant hydrology*, 12(4), 329-354.
- Parsons Corporation. 1964. Groundwater Resources of Kuwait, vols I, II and III. Ministry of Electricity and Water, Kuwait.
- Reynolds, R. M. (1993). Physical oceanography of the Gulf, Strait of Hormuz, and the Gulf of Oman—Results from the Mt Mitchell expedition. *Marine Pollution Bulletin*, 27, 35-59.
- Robinson, B. W., & Al Ruwaih, F. (1985). The stable-isotopic composition of water and sulfate from the raudhatain and Umm Al Aish freshwater fields, Kuwait. *Chemical Geology: Isotope Geoscience section*, 58(1-2), 129-136.
- Rotzoll, K., & Fletcher, C. H. (2013). Assessment of groundwater inundation as a consequence of sea-level rise. *Nature Climate Change*, 3(5), 477.
- Senay, Y. (1977). Groundwater resources and artificial recharge in Rawdhatain water field. Ministry of Electricity and Water, Kuwait, 35.
- Senay, Y. (1977). Groundwater resources and artificial recharge in Rawdhatain water field. Ministry of Electricity and Water, Kuwait, 35.

Terink, W., Immerzeel, W. W., & Droogers, P. (2013). Climate change projections of precipitation and reference evapotranspiration for the Middle East and Northern Africa until 2050. *International journal of climatology*, 33(14), 3055-3072.

UAR (United Arab Republic) Experts. 1964. Ministry of Electricity and Water, Kuwait.

Underwood, M. R., Peterson, F. L., & Voss, C. I. (1992). Groundwater lens dynamics of atoll islands. *Water Resources Research*, 28(11), 2889-2902.

Vengosh, A., & Rosenthal, E. (1994). Saline groundwater in Israel: its bearing on the water crisis in the country. *Journal of Hydrology*, 156(1-4), 389-430.

Werner, A. D., & Simmons, C. T. (2009). Impact of sea-level rise on sea water intrusion in coastal aquifers. *Groundwater*, 47(2), 197-204.

Yihdego, Y., & Al-Weshah, R. A. (2017). Assessment and prediction of saline sea water transport in groundwater using 3-D numerical modelling. *Environmental Processes*, 4(1), 49-73.

CHAPTER 6. SUMMARY, CONCLUSIONS, AND FUTURE WORK

In this chapter, the problem statement and research objectives are summarized, the main findings and outputs for each task are concluded, and possible areas for future research are listed.

6.1 Summary for Problem Statement and Research Objectives

The FGLs in subterranean oases in the AP are considered as a critical source of freshwater storage because the harsh climate and landforms prevent the existence of surface water bodies and make it difficult to harvest and store precipitation. These FGLs are in danger of salinization due to heavy anthropogenic activities. The recharge mechanism of FGLs in subterranean oases is classified as a focused recharge and depends on surface runoff from infrequent cyclonic rainfall events that may vary considerably from year to year in terms of timing and magnitude. Hence, the natural recharge quantity and frequency are both scarce and uncertain. Moreover, there is no reliable three dimensional large-scale environmental dispersivity value at the scale of these lenses, this being an open question and recognized uncertainty in several studies. These FGLs are also proposed as suitable locations for aquifer storage and recovery to serve as long-term storage for emergency uses. Because of this, it is important to simulate mixing between fresh water and seawater or brackish water, which requires characterization of the large-scale dispersivity of the FGL.

The Rawdatain FGL was selected among the FGLs because of its size and the availability of extensive subsurface data for the pre-development period. The first main objective of this study was to provide accurate long-term estimates of recharge for the Rawdatain FGL and to investigate the timing of lens depletion under scenarios of decreased recharge. The second aim was to provide a realistic range of longitudinal (α_L), horizontal transverse (α_h), and vertical

transverse (α_v) dispersivity values for the Rawdatain FGL. The last purpose was to assess the current and future conditions of the Rawdatain FGL and its effective management and conservation, as it constitutes a strategic natural resource in the country, by an evaluation of the effect of historical and future anthropogenic activities and natural recharge versus artificial recharge alternatives for lens recovery storage (LSR). The methodology presented herein provides a general approach that can be applied to other FGLs with similar climatic and environmental circumstances.

6.2 Conclusion for Estimating Groundwater Recharge for a Freshwater Lens in an Arid Region: Formative and Stability Assessment

The recharge rate estimates were based on multi-target calibration of a three-dimensional (3D) density dependent groundwater flow and solute transport model using a constant recharge mechanism (CRM). The groundwater age and the following pre-development period calibration targets were used with twelve recharge amount scenarios (R1 to R12): (1) volumes and thicknesses of stored groundwater at three different water quality categories (TDS of 0-700 mg/L, 700-1,000 mg/L, 1,000-2,000 mg/L), (2) spatially variable TDS concentration, (3) spatially-variable groundwater head, and (4) the geometrical shape of the lens along aquifer cross sections.

The R5 (0.5 million m³/year) recharge scenario satisfied the three volume targets with absolute errors of 12.9%, 5.3% and 6.9%, respectively, and it satisfied the three lens thickness targets with absolute errors of 10.5%, 3.9%, and 2.6%, respectively. When starting from an initial no-freshwater condition, the simulated lens with R5 required from 1400 to 2600 years to reach its final volume in the model, which is in agreement with the groundwater age of the Rawdatain FGL. For R5, the Scaled Root Mean Square Error (S-RMSE) of TDS and the

groundwater head were 0.188 and 0.125, respectively. A qualitative comparison with the overall lens shape reveals that R5 compares well with the observed cross-section of TDS. Therefore, the long-term average annual recharge of 0.5 million m³/year can be used when applying the model to water management scenarios.

These results demonstrated that the annual natural replenishment of the Rawdatain FGL is minimal compared with its size, which is in agreement with the slow formation and groundwater age of the Rawdatain FGL. Hence, if this lens is depleted, it will require over 2000 years to reform again. A macro-scale stability assessment under changes in natural recharge due to climate or land-use changes suggested that the lens storage would respond slowly to these changes within a 100-year time frame. For instance, a 50% reduction in annual recharge would reduce the lens volumes by 21%, 17% and 9% for the three water quality categories.

A sensitivity analysis was carried out to assess the effects of the hydraulic conductivity values and boundary conditions on the Rawdatain FGL storage during the development period. The results proved that the hydraulic conductivity set K from field pumping tests was an appropriate set representing the entire aquifer domain. Applying higher values of the K set resulted in prevention of the existence of the lens, whereas the use of lower values of K led to faster lens development. Regarding the boundary conditions, an increase of 10% in the head gradient across the Rawdatain basin would lead to an upward shift in the lens and increased salinization, whereas a decrease in the head gradient had no significant effects. Moreover, the simulated storage became more sensitive to the changes in head gradients when it was accompanied with changes in natural recharge, with the latter being more dominant.

6.3 Conclusion for Determining Values of Large-Scale Dispersivity for a Fresh Groundwater Lens in an Arid Region

A multi-criteria score-based method was performed to rank the best performance of 28 dispersivity sets (D1 to D28) among all of the targets with an equal weight to find a reliable range of longitudinal (α_L), horizontal transverse (α_h), and vertical transverse (α_v) dispersivity values for the Rawdatain FGL. These dispersivity sets include a wide range of feasible longitudinal dispersivity values for the Rawdatain FGL (1–500 m), on a scale of 0 to 300×10^6 m³. The performance of the dispersivity sets against the data targets was varied. For instance, D18, D14 and D17 were the best in terms of the volume targets, D21, D9 and D5 were the best in terms of the thickness targets, D13 to D19 were the best in terms of the S-RMSE of TDS point data, and there was no significant distinction in terms of the Mean Absolute Error (MAE) of the groundwater heads. Overall, D16, D18 and D14 had the highest rank based on their satisfaction of all targets, with total scores of 49, 50 and 53, respectively. Hence, the D16 dispersivity set ($\alpha_L = 50$ m: $\alpha_h = 5$ m: $\alpha_v = 0.1$ m) represents the best large-scale environmental dispersivity values for the Rawdatain FGL and can be used for analyzing the natural mixing between the ambient brackish water and fresh water.

An additional benefit of the multi-calibration targets approach is that it excluded several non-unique calibration parameters and lowered the uncertainty of the calibrated parameters. For example, one set of the dispersivity values can fulfill one or two targets but be significantly inaccurate in a third target. In addition, the model was used to assess the effect of vertical transverse dispersivity on the stored water volumes at the three quantity categories. The results indicated that vertical transverse dispersivity values of greater than one meter prevent the formation of the Rawdatain FGL.

6.4 Conclusion for Assessment of the Natural and Anthropogenic Impacts on a Fresh Groundwater Lens in a Subterranean Oasis in Kuwait

A new baseline model for the predevelopment period was established using a pulse recharge mechanism (PRM) for the Rawdatain FGL to simulate the effects of infrequent rainfall events and anthropogenic impacts simultaneously. Three frequencies of PRM scenarios (one pulse every 1 year, one pulse every 2 years, and one pulse every 4 years) and five longitudinal dispersivity values (10, 30, 50, 60 and 100 m) were tested to provide realistic aquifer properties for the new baseline. Generally, the results demonstrated that the PRM is better than the CRM as a formative factor for the natural hydrological processes during the FGL formation because the simulated volumes show that the PRM scenarios reached relatively flat steady state volumes compared with the CRM scenarios. Also, the model was found to be sensitive to the longitudinal dispersivity values and not sensitive to the recharge event frequencies. Overall, the model associated with the 50 m longitudinal dispersivity set and one pulse recharge every two years had the best performance, and it was selected as the new baseline for the Rawdatain FGL prior to its official opening for water production.

The new baseline was used to assess the impact of historical groundwater abstraction from 1963 to 2018, determine the effect of six future pumping scenarios from 2019 to 2100, and evaluate three artificial recharge alternatives from 2019 to 2028. The initial volume conditions in 1963 were $28 \times 10^6 \text{ m}^3$, $69 \times 10^6 \text{ m}^3$ and $142 \times 10^6 \text{ m}^3$, and these volumes decreased to $20 \times 10^6 \text{ m}^3$, $57 \times 10^6 \text{ m}^3$ and $124 \times 10^6 \text{ m}^3$, respectively, for the three quality categories as a result of the pumping activities from 1963 to 2018. However, most of the decline in the lens storage occurred during the heavy extraction period between 1963 and 1978. Regarding future pumping, S1 ($0.16 \times 10^6 \text{ m}^3/\text{year}$) was found to be a suitable scenario because it had no major effect on the

stored volume and the produced water quality was sustained between 850 and 1000 mg/L. Therefore, significant storage will be available for emergency use if needed. S2 (0.5×10^6 m³/year) resulted in a remarkable decline in the 700 mg/L water quality category up to 43% and a moderate decay (31% and 23%) in the other categories, and the TDS of the produced water exceeded 1200 mg/L after 20 years. These findings suggested that S2 is only a sustainable option for short-term use. Pumping scenarios with an annual volume extraction greater than one million cubic meters caused a notable deterioration of the Rawdatain FGL.

A sensitivity analysis was applied to assess the sensitivity of the S0, S1 and S2 pumping future scenarios to a change in the long-term recharge R5 scenario by $\pm 20\%$. The results illustrated that the best water quality category is more sensitive than the other two categories, and the model became less sensitive as the rate of annual extraction increased. Also, an increase of 20% in the recharge will not lead to a noteworthy recovery of the lens by 2100 even with the no-pumping alternative. Thus, the only feasible solution to enhance the Rawdatain FGL storage is artificial recharge. By implementing artificial recharge scenario I1, a significant recovery percentage up to 67%, 61% and 43% for the three quality categories could be reached within 10 years. I2 and I3 achieved a 100% storage recovery within shorter time frames: 9 and 6 years, respectively. The overall outcome, an effective LSR for the Rawdatain FGL, depends on selecting appropriate well locations and an appropriate amount of injected water.

6.5 Future Work

Possible areas of future research are grouped into short-term and long-term categories:

- **Short-term category**

A short-term future goal is to modify the LSR of the Rawdatain FGL with new locations and types of well injection and injection cycles. Instead of using the existing wells, the new injection well locations will be located within the best-quality TDS layers to minimize the mixing between the brackish water and injected fresh water. This step will help with reaching a high recovery percentage within a shorter period of time and with a lower amount of injected water. Furthermore, skimming and scavenger well systems will be implemented to reduce the up-coning of the underline brackish water during pumping. The skimming well system is a low-discharge cluster of wells extracting groundwater from relatively shallow depths without significantly lowering the pressure head in the vicinity of the well, whereas the scavenger well system installs a production well within the freshwater zone and a scavenger well within the brackish water zone in a single-bore hole or side-by-side bore holes to prevent the fresh–brackish interface from rising to reach the effective pumping zone. The performance of these systems will be determined based on the quality of the produced water from the Rawdatain FGL and then compared with the current traditional well system. Last, a determination the number of injection cycles and their repetition is essential to keeping a significant storage available for emergency use if needed.

- **Long-term category**

Although the methodology presented in this dissertation was implemented for only one FGL in the AP, it can be extrapolated to other FGLs that share the same hydrogeological settings. For instance, the model capability can be assessed by modeling the second largest

freshwater lens in Kuwait (Umm-Al-Aish). However, this future research cannot be conducted without more detailed data that are required by the multiple data targets approach. More data collection efforts are needed to make further contributions to the field of FGL hydrology in subterranean oases in arid regions. Enhancing the water manager's knowledge of the FGLs in the AP would help to establish an optimum short/long-term utilization strategy at each state scale.

APPENDIX A

Table A. TDS data (Parsons Corporation, 1964)

Well Name	Well ID	East (m)	North (m)	Date	Elevation (m)(amsl) ^a	Total depth (m)(bgl) ^b	Top screen (m)(bgl) ^b	Bottom screen (m)(bgl) ^b	TDS (mg/L)
R-01A-OW	K6316-Q2408	756316	3312406	20-May-62	35.1	57.0	33.5	54.9	370
R-01-PW	K6490-Q2686	756490	3312686	5-May-62	35.3	56.4	33.5	54.9	375
R-02A-TW	K5224-Q0577	755223	3310576	20-Dec-61	38.4	42.7	36.6	41.1	4628
R-06-TW	K7729-Q3018	757728	3313017	31-Dec-61	37.0	54.9	31.4	53.3	328
R-08-OW	K7581-Q3624	757580	3313623	14-Feb-61	39.3	107.9	36.9	44.5	588
R-09-PW	K6520-Q2183	756520	3312183	4-Feb-61	35.1	70.1	34.7	66.1	600
R-12B-TW	K6879-Q4262	756879	3314261	27-May-62	38.6	67.1	60.0	66.1	3700
R-12D-OW	K6585-Q4670	756585	3314670	10-Jul-62	40.6	56.4	37.5	55.8	795
R-12-TW	K7148-Q4990	757148	3314988	27-May-62	41.2	54.9	50.6	54.0	2970
R-13A-TW	K8217-P9775	758216	3309773	18-Apr-62	38.9	50.3	38.1	50.3	7470
R-13-TW	K8209-P9767	758209	3309765	18-Apr-62	38.7	76.2	59.4	71.6	7470
R-14-OW	L2031-Q1955	762030	3311953	4-Feb-61	54.9	55.8	43.5	53.3	3360
R-16A-PW	K6068-Q5769	756068	3315769	18-Apr-62	41.2	53.3	36.6	50.3	800
R-16-OW	K5941-Q4479	755941	3314478	2-Apr-62	41.2	50.3	38.1	50.3	800
R-17-TW	K7683-P9192	757682	3309191	9-Feb-62	38.4	54.9	32.6	46.9	4108
R-18-OW	K8712-Q1171	758712	3311170	27-Jan-62	38.0	50.3	32.0	41.1	1048
R-19-TW	K8226-Q3463	758225	3313462	23-Jan-62	41.6	57.0	50.3	56.4	1082
R-20B-TW	K5198-Q4677	755197	3314675	12-May-62	39.2	50.3	36.6	48.8	940
R-20C-PW	K5292-Q4899	755292	3314899	2-Jun-62	39.2	50.3	39.6	48.8	940
R-20-TW	K5144-Q4692	755143	3314691	4-Feb-62	39.8	50.3	39.6	47.2	2104
R-21A-TW	K4600-Q8649	754599	3318648	4-Feb-62	47.2	43.6	38.1	43.0	3756
R-21-TW	K4592-Q8641	754591	3318640	5-Feb-62	47.2	82.3	41.1	51.2	7704
R-22A-PW	K9082-Q4247	759082	3314247	15-Jul-62	46.0	59.4	42.7	57.9	1085
R-22-TW	K8921-Q3950	758920	3313949	30-Jan-62	46.0	64.9	45.7	57.9	1300
R-23A-TW	L0144-Q4870	760143	3314869	15-Feb-62	55.6	50.9	44.2	50.3	1692
R-23-TW	L0149-Q4871	760149	3314869	13-Feb-62	55.6	76.2	53.3	61.9	1652
R-27A-PW	K6890-Q1121	756890	3311121	27-May-62	35.8	45.7	32.0	44.2	725
R-27-TW	K6749-Q0897	756748	3310896	21-Apr-62	35.8	45.7	32.0	44.2	615
R-28A-TW	K8919-Q5460	758919	3315459	4-Apr-62	51.8	57.9	45.7	57.9	3625
R-28-TW	K8935-Q5463	758934	3315462	4-Apr-62	52.0	76.2	64.0	73.2	3625
R-29-TW	K5949-P9093	755948	3309091	25-Apr-62	40.3	54.9	30.5	42.7	7975
R-30A-TW	K8916-Q2092	758915	3312091	10-Apr-62	40.1	62.5	36.6	61.0	1885
R-30-TW	K8906-Q2089	758905	3312087	10-Apr-62	40.1	76.2	64.0	76.2	5440
R-31-TW	L0086-Q3010	760086	3313009	21-Apr-62	47.9	76.2	41.1	53.3	3260
R-33A-PW	K5999-Q6878	755999	3316878	20-Jul-62	42.8	51.8	39.6	48.8	1375
R-33-TW	K5866-Q6985	755865	3316984	24-Apr-62	43.7	75.9	38.1	47.2	1380
R-34-TW	K4608-Q6161	754608	3316160	27-Apr-62	42.6	61.0	36.6	48.8	1885
R-35-TW	K3572-Q3552	753571	3313550	2-May-62	41.5	60.3	42.7	57.9	7975
R-36-TW	L0767-P4993	760766	3304992	5-May-62	40.0	76.2	30.5	36.6	5075
R-37-TW	K6802-P6702	756801	3306701	24-Jul-62	42.7	38.1	29.0	37.5	6890
R-38-OW	L0536-P6722	760535	3306720	28-Jul-62	39.8	38.1	27.4	33.2	725
R-39A-OW	K6975-Q1584	756974	3311584	19-Sep-62	35.9	82.3	35.1	42.7	205
R-39B-OW	K6971-Q1606	756970	3311605	1-Oct-62	35.2	59.4	27.2	31.9	435
R-39C-RW	K6979-Q1559	756978	3311558	10-Oct-62	36.0	32.0	25.3	29.9	400
R-39D-OW	K6585-Q4668	756585	3314668	12-Oct-62	36.3	32.0	24.4	29.0	215
R-39-RW	K6979-Q1561	756978	3311560	17-Oct-62	35.9	48.8	33.5	45.7	360
R-40-OW	K6034-Q0910	756033	3310908	13-Oct-62	35.0	45.7	29.0	44.2	470

(a = above mean sea level; b = below ground surface level)

Table B. Head data (Parsons Corporation, 1964)

Well Name	Well ID	East (m)	North (m)	Date	Elevation (m)(amsl) ^a	Water depth (m) (bgl) ^b	Total depth (m)(bgl) ^b	Water head (m) (amsl) ^a
R-01A-OW	K6316-Q2408	756316	3312406	26-May-62	35.1	23.6	57.0	11.5
R-01-PW	K6490-Q2686	756490	3312686	4-Apr-62	35.3	23.6	56.4	11.7
R-06-TW	K7729-Q3018	757728	3313017	30-Dec-61	37.0	27.3	54.9	10.7
R-07A-PW	K5048-Q2280	755047	3312279	12-Jun-62	37.9	27.0	45.7	10.9
R-07-PW	K5155-Q2545	755155	3312545	3-Jan-62	37.9	26.5	45.7	11.3
R-09-PW	K6520-Q2183	756520	3312183	2-Jun-62	35.1	23.5	70.1	11.6
R-12B-TW	K6879-Q4262	756879	3314261	1-Jun-62	38.6	27.6	67.1	11.0
R-12D-OW	K6585-Q4670	756585	3314670	14-Jul-62	40.6	29.6	56.4	11.0
R-12-TW	K7148-Q4990	757148	3314988	11-Jan-62	41.2	30.5	54.9	10.8
R-13A-TW	K8217-P9775	758216	3309773	30-Apr-62	38.9	27.3	50.3	11.6
R-13-TW	K8209-P9767	758209	3309765	13-Apr-62	38.7	26.3	76.2	12.4
R-15A-PW	K8411-P9420	758411	3309420	1-Jul-62	38.7	27.2	42.7	11.6
R-16A-PW	K6068-Q5769	756068	3315769	1-Apr-62	41.2	31.3	53.3	9.9
R-17-TW	K7683-P9192	757682	3309191	16-Jan-62	38.4	26.1	54.9	12.3
R-20A-OW	K4551-Q4730	754550	3314728	30-Jan-62	39.2	28.2	35.1	11.0
R-20B-TW	K5198-Q4677	755197	3314675	7-May-62	39.2	28.2	50.3	11.0
R-20-TW	K5144-Q4692	755143	3314691	25-Jan-62	39.8	28.9	50.3	11.0
R-21A-TW	K4600-Q8649	754599	3318648	3-Feb-62	47.2	36.9	43.6	10.3
R-21-TW	K4592-Q8641	754591	3318640	31-Jan-62	47.2	36.2	82.3	11.0
R-22A-PW	K9082-Q4247	759082	3314247	11-Jul-62	46.0	35.5	59.4	10.4
R-22-TW	K8921-Q3950	758920	3313949	22-Jan-62	46.0	35.0	64.9	11.0
R-23-TW	L0149-Q4871	760149	3314869	9-Feb-62	55.6	45.1	76.2	10.4
R-25-TW	K3541-Q8545	753540	3318545	5-Feb-62	46.0	35.8	50.6	10.2
R-26-TW	K9542-P8087	759542	3308086	26-Feb-62	40.2	28.3	91.4	11.9
R-27A-PW	K6890-Q1121	756890	3311121	30-Apr-62	35.8	23.4	45.7	12.3
R-27-TW	K6749-Q0897	756748	3310896	18-Apr-62	35.8	23.5	45.7	12.3
R-28A-TW	K8919-Q5460	758919	3315459	31-May-62	51.8	41.6	57.9	10.2
R-28-TW	K8935-Q5463	758934	3315462	29-Mar-62	52.0	41.6	76.2	10.4
R-29-TW	K5949-P9093	755948	3309091	1-Apr-62	40.3	28.4	54.9	11.9
R-30A-TW	K8916-Q2092	758915	3312091	3-Apr-62	40.1	28.6	62.5	11.5
R-30-TW	K8906-Q2089	758905	3312087	3-Apr-62	40.1	28.6	76.2	11.5
R-31-TW	L0086-Q3010	760086	3313009	7-Apr-62	47.9	36.9	76.2	11.0
R-32-TW	L0076-Q0398	760075	3310396	17-Apr-62	40.6	29.2	76.2	11.4
R-33A-PW	K5999-Q6878	755999	3316878	23-Jul-62	42.8	32.7	51.8	10.1
R-33-TW	K5866-Q6985	755865	3316984	20-Apr-62	43.7	33.2	75.9	10.6
R-34-TW	K4608-Q6161	754608	3316160	22-Apr-62	42.6	31.8	61.0	10.8
R-35-TW	K3572-Q3552	753571	3313550	27-Apr-62	41.5	30.3	60.3	11.2
R-36-TW	L0767-P4993	760766	3304992	1-May-62	40.0	27.9	76.2	12.0
R-37-TW	K6802-P6702	756801	3306701	22-Jul-62	42.7	30.5	38.1	12.2
R-38-OW	L0536-P6722	760535	3306720	26-Jul-62	39.8	28.0	38.1	11.8
R-39A-OW	K6975-Q1584	756974	3311584	25-Sep-62	35.9	23.9	82.3	12.0
R-39-RW	K6979-Q1561	756978	3311560	7-Sep-62	35.9	24.8	48.8	11.2

(a = above mean sea level; b = below ground surface level)